Role of cancer associated fibroblasts in macrophage recruitment in head and neck cancer

By

Priyanka Prajapati

A thesis submitted in partial fulfilment of the requirements for the degree of Doctor of Philosophy

The University of Sheffield

Faculty of Medicine, Dentistry and Health

School of Clinical Dentistry

December 2017

Acknowledgements

Most importantly, I would like to thank my supervisor, Dan Lambert for the constant advice, support and motivation throughout the last four years. Ph.D.s are daunting, even more so in a foreign land, and this wouldn't have been possible without your support and guidance. You have helped create a positive outlook towards research, and peaked my interest in a research based career.

I would also like to thank Craig Murdoch, my second supervisor on his valuable input towards my Ph.D. project.

I can't thank my parents enough for sending me so far away, supporting me in every way possible, and being patient through weeks without skype calls and delayed travel plans.

I would also like to extend my thanks to Tasnuva and Genevieve for helping me set the right foundation. I also very much appreciate all the help from Brenka and Jason with various lab techniques and equipments.

A big thank you to Lucie, Hanan, Diana, Sofia, Javier, and all the other colleagues and friends for making my life in Sheffield more colourful.

I cannot express enough gratitude to Nick, who encouraged and took care of me, and kept me going through the writing process.

Abstract

Background: Cancer associated fibroblasts (CAFs) are known to stimulate crosstalk between stroma and cancer via paracrine signalling and promote cancer progression through matrix remodelling, angiogenesis and immunosuppression. CAFs arise from many sources and display different markers and characteristics in the tumour stroma; their presence in head and neck cancers is associated with poor prognosis. This study examines the differences in secretome of myofibroblasts and senescent fibroblasts in the context of their ability to recruit and polarise macrophages, with the aim of establishing which phenotype recruits more macrophages, which chemokine/receptor is primarily employed and which way are the macrophages polarised.

Methods: Normal oral fibroblasts (NOFs) were transdifferentiated to myofibroblasts (MF) using TGF-β1, or senesced using cisplatin. MF phenotype was confirmed by expression of α-smooth muscle actin (α-SMA), fibronectin with extra domain A (FNEDA), and collagen type 1 alpha 1 (COL1A1) using RT-qPCR, western blot and immunofluorescence. Senescence was confirmed by senescence associated β-galactosidase assay, RT-qPCR for $p16^{INK4A}$ and $p21^{CIP1/WAF-1}$. Primary monocytes were allowed to migrate towards conditioned medium (CM) from MFs, senescent fibroblasts (SFs) and patient CAFs in a Boyden chamber assay. The involvement of chemokine receptors were scrutinised using CCR2 antagonist and pertussis toxin. Macrophages were also polarised in the same CM, as assessed by qPCR. Levels of The secretome of MFs, SFs and patient-derived CAF was examined using ELISA, cytokine array and mass spectrometry.

Results: CCL2 secretion correlated with monocyte migration through CCL2/CCR2 axis towards CM from SF, MF and most patient CAFs. SFs secreted more IL-6 and CCL2 than MFs, in which secretion declined with longer duration of TGF-β1 treatment. Cytokine array detected more cytokines secreted by MF than SF, while MS revealed more collagen interacting proteins secreted by SF, while both secreted several types of collagen. MF, SF and patient CAF CM also polarised macrophages towards M2 phenotype, increasing CD206 mRNA compared to normal firboblasts CM. While CM from unpolarised (M0) macrophages induced highest expression of α-SMA expression

Conclusion: SF recruits more monocytes through CCL2/CCR2 axis and secreted more collagen interacting proteins than MF. However, both seem to polarisation macrophages towards M2 phenotype. Collectively the data identify differences and similarities in the secretome of MF and SF, and one or both can be potentially targeted to manipulate immune cell populations in tumour stroma to improve prognosis.

Contents

List of figures

List of tables

List of abbreviations

α-SMA – alpha smooth muscle actin

ADAM – A disintegrin and metalloprotease

ADAMST1 – A disintegrin and metalloprotease with thrombospondin motif

Bcl-XL B-cell lymphoma – extra large

BMDC – bone marrow derived cells

BMP – bone morphogenic protein

CAF – cancer associated fibroblast

CCL – chemokine ligand

CCR – chemokine receptor

CD – cluster of differentiation

CK2 – casein kinase 2

COL – collagen

COX – cyclooxygenase

CM – conditioned media

CXCL – (C-X-C) motif ligand

CXCR – (C-X-C) motif receptor

DNA – deoxyribonucleic acid

ECM – extracellular matrix

EGFR – epidermal growth factor receptor

EMT – epithelial to mesenchymal transition

EMMPRIN – extracellular matrix metalloproteinase inducer

End-MT – endothelial to mesenchymal transition

ERK – extracellular signal-regulated kinase

FAK – focal adhesion kinase

FAP – fibroblast activated protein

FGF – fibroblast growth factor

FNEDA – fibronectin with extra domain A

FSP – fibroblast specific protein

GLUT – glucose transporter

GM-CSF – granulocyte macrophage colony stimulating factor

GRP – glucose related protein

GS-OSCC – genetically stable oral squamous cell carcinoma

GU-OSCC – genetically unstable oral squamous cell carcinoma

HGF – hepatocyte growth factor

HIF – hypoxia inducible factor

HNC – head and neck cancer

HNSCC – head and neck squamous cell carcinoma

IgG – immunoglobulin G

IFN-γ – interferon gamma

IL – interleukin

JAK – janus tyrosine kinase

LPS – lipopolysaccharide

M-CSF – macrophage colony stimulating factor

MAPK – mitogen activated protein kinase

MEK – MAPK kinase

miRNA - miR – micro RNA

MMP – matrix metalloproteinase

mRNA – messenger ribonucleic acid

NF-κB – nuclear factor kappa B

NK cell – natural killer cell

NOS – nitric oxide synthase

PDGF – platelet derived growth factor

PI3K – phosphatidylinositide 3-kinase

RARRES – retinoic acid receptor responder protein

RNA – ribonucleic acid

ROS – reactive oxygen species

SDF – stromal derived factor

SPARC – secreted protein acidic and rich in cysteine

STAT – signal transducer and activator of transcription

T_{reg} – T regulatory cell

TAM – tumour associated macrophage

TGF-β – transforming growth factor beta

Th – T helper

TLR – toll like receptor

TME – tumour microenvironment

TNF – tumour necrosis factor

VEGF – vascular endothelial growth factor

X-gal – 5-Bromo-4-chloro-indolyl-D-galactopyranoside

Chapter 1

1. Review of literature

1.1 Introduction to Cancer

Cancer has become a major cause of morbidity and mortality around the world irrespective of region or race. World Health Organisation outlines in World Cancer Report 2014 that nearly 14 million new cases and 8 million cancer related deaths occurred in 2012 (McGuire, 2016). The report also highlights high incidence rates of all cancers combined in high income countries of North America, Western Europe (along with Australia, Japan, New Zealand, and Republic of Korea) compared to Central and South America, Eastern Europe, Africa, and South Asia (McGuire, 2016). However, cancer related mortality is higher in developing countries (McGuire, 2016).

1.2 Head and neck cancer

While lung, prostate, and breast cancers have the highest incidence, head and neck cancer (HNC) is the fifth common cancer worldwide. It is the most common malignant disease in Central Asia (Marcu and Yeoh, 2009). Squamous cell carcinoma predominates, making up over 95% of all HNC cases, while the rest (4-

5%) are mainly melanoma or salivary gland adenocarcinoma (Vikram et al., 1984). HNC includes cancers of the larynx, pharynx (nasopharynx, oropharynx, and hypopharynx), nasal cavity, paranasal sinuses, oral cavity, tongue, and salivary glands (fig.1.1). The main risk factors for HNC are excessive exposure to alcohol, tobacco (including chewing tobacco) and human papilloma virus infection (Mathers, 2006, Boyle, 2008). However, genetic predisposition can increase risk of HNC in non-consumers of alcohol, and tobacco, and so can poor oral hygiene (Rosenquist, 2005). In developing countries such as the Indian sub-continent, and South East Asian countries chewing of areca nut has been linked to cancer (Sankaranarayanan et al., 1998).

Oral cancer is sub-type of HNC, and manifests itself on the lip or the oral cavity, as described previously. Oral cancer is often referred to as oral squamous cell carcinoma as 90% of the cancers occurring in the oral cavity arise histologically from squamous cells (Lingen et al., 2008). The frequency of occurrence of oral cancer is in South East Asia (India, Pakistan, Sri Lanka, and Taiwan), France, Eastern Europe (Hungary, Slovenia, and Slovakia), and Latin America and Carribean

(Warnakulasuriya, 2009). Similar to other parts of head and neck, majority of cases of oral cancer are caused by chewing/smoking of tobacco, alcohol consumption, chewing of areca nut, poor nutrition (especially from poor socio-economic status), HPV infections, and poor oral hygiene (Johnson et al., 2011, Secretan et al., 2009, Conway et al., 2008, Doll and Peto, 1981, Syrjänen et al., 2011, Guha et al., 2007). With such a vast epidemiological spread and poor treatment options, this thesis dwells further in to biology of oral cancer to propose future treatment targets.

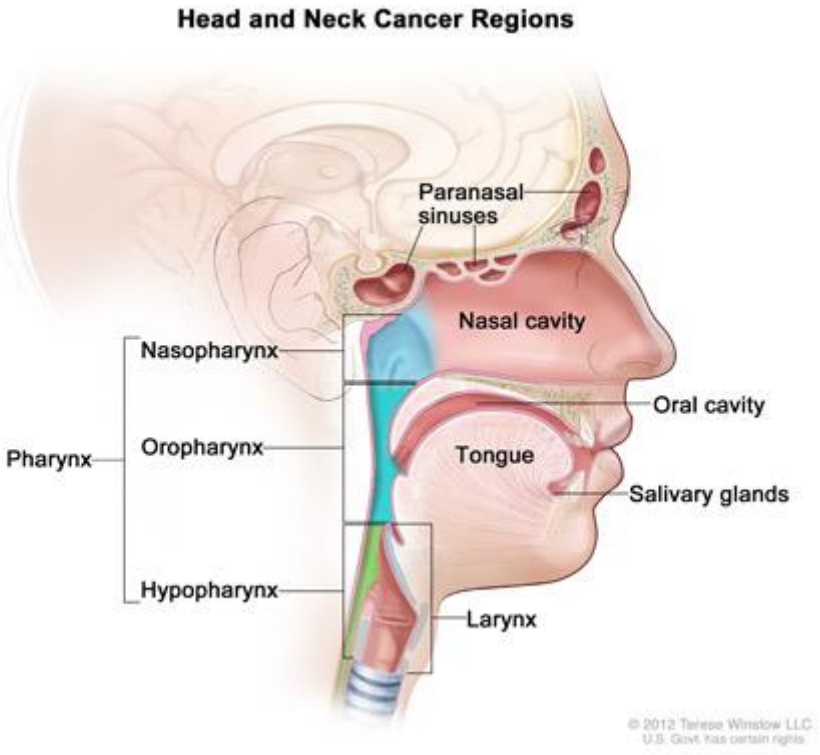

Figure 1.1 Regions common to cancers of the head and neck. (For the National Cancer Institute © 2012 Terese Winslow LLC, U.S. Govt. has certain rights, permission granted for use in this thesis)

Survival rates for HNC, including oral cancer are still quite poor at only 50% overall with no significant improvement for several decades, particularly for advanced disease (Döbróssy, 2005, Haddad and Shin, 2008). Disease outcome is improved if diagnosed early, with survival rates as high as 75% at five years, however patients frequently present with metastasis to lungs, bone, mediastinal lymph node, and adrenal gland (Chin et al., 2005, Wiegand et al., 2015).

Current treatment options for HNC include surgery, frequently involving removal of cervical lymph nodes to remove local metastases, combined with radiotherapy as well as chemotherapy. Therefore, there is a clear need to develop novel treatment strategies for HNC.

1.2.1 Therapies in HNC

Some of the new emerging therapies include the use of viruses; Gendicine is a non-replicating adeno-virus engineered to contain a human wild-type p53 expression cassette propelled by Rous sarcoma virus promoter. Intra-tumoral injections of Gendicine restores expression of p53, which is often down-regulated or mutated, in cancer cells to induce cell cycle arrest, and apoptosis

in humans (Hughes et al., 2015a). In phase III clinical trials, Gendicine demonstrated a response rate of 96% when used in conjunction with radiotherapy, compared to 80% when radiotherapy was used alone (Peng, 2005). Although Gendicine has been approved for use in China, it failed to get approval in the U.S.A and Europe (Pearson et al.) H101 is an oncolytic virus modified to only replicate in cancer cells; in phase III with cisplatin and 5-flurouracil, it has achieved 78.8% response rate compared to 39.6% with chemotherapy alone (Xia et al., 2004).

Another upcoming therapy makes use of epidermal growth factor receptor (EGFR) inhibitors. EGFR is implicated in several cancers like pancreatic, breast, lung, HNCs (Shostak and Chariot, 2015). However, EGFR inhibitors are often seen to provoke drug resistance, with second generation of EGFR inhibitors showing some advancement in breast, pancreatic, lung, and HNC (Lee et al., 2014a). EGFR inhibitors have shown to induce autophagy, which promotes recycling of organelles and cellular components providing nutrients to cancer cells; therefore autophagy inhibitor may prove to be cytotoxic to

cancer cells in this case. However, if autophagy inducers are administered, it could lead to autophagic cell death; hence tilting the scale either way – inhibiting or up-regulating autophagy may prove to be therapeutic (Cui et al., 2014).

Current therapies targeting EGFR include a chimeric IgG1 mAb called Cetuximab, approved in 2006 to treat locally or regionally advanced head and neck squamous cell carcinoma (HNSCC) in combination with radiation therapy (Santuray et al., 2018). Phase III clinical trials combining Cetuximab and radiation therapy showed significant improvement in median overall survival from 14.9 months for radiation alone to 24.9 months (Bonner et al., 2006). After another study, Cetuximab was approved as first line of treatment in combination with platinum based therapy in local or metastatic HNSCC as median overall survival improved from 7.4 to 10.1 months, however it was also approved to be used as single agent treatment in platinum based therapy resistant HNSCC where it reported a response rate of 13% (Vermorken et al., 2008).

Unfortunately, resistance towards Cetuximab is increasing, and other EGFR inhibitors like Pantinumab and Zalutumumab are in trials (Santuray et al., 2018).

Our body's natural immune system is capable of recognising neoplastic cell antigens, along with other costimulatory and inhibitory molecules, in order to eliminate those cells. However, cancer cells manipulate immune check points in the body to evade anti-tumour immunity (Pardoll, 2012). Immune check points are numerous inbuilt pathways to prevent auto-immune reactions, and modulate duration and magnitude of required immune reactions (Pardoll, 2012). Some of the well-known immune check points are cytotoxic T lymphocyte associated protein-4 (CTLA-4), and programmed cell death protein-1 (PD-1). PD-1 plays a role at a later stage of immune response in the infected tissue, where it binds with its ligand – PD-1 ligand (PDL-1) to regulate the activity of effector T cells to limit additional tissue damage (Santuray et al., 2018, Pardoll, 2012). Currently, Pembrolizumab, a monoclonal antibody (mAb) directed against PD-1, and was first authorised to be used to treat

metastatic melanoma. In August 2016, it was approved to be used in recurrent or metastatic HNSCC with or after platinum chemotherapy (Santuray et al., 2018). In tumour with 50% or more the cells expressing PDL-1, the overall survival improved from 7.9 months to 11.6 months with use of Pembrolizumab (Cohen, 2017). In another study, patients with unmanageable metastatic/recurrent HNSCC after both platinum and cetuximab, showed an overall response of 16% (Bauml et al., 2017).

Nivolumab is another mAb approved to treat metastatic/recurrent HNSCC with or after platinum chemotherapy. Compared to standard therapy (methotrexate, cetuximab, or docetaxel), Nivolumab increased 1 year survival rate from 16% to 36% (Ferris et al., 2016).

Although Pembrolizumab and Nivolumab show response rates below 20%, they show better overall survival than standard of care, and are being trialled with other drug combinations to increase their response rate (Santuray et al., 2018).

Meanwhile, CTLA-4 is normally expressed on regulatory T (T_{reg}) cells, but is upregulated in conventional T cells in tumour microenvironment (Pardoll, 2012, Syn et al., 2017). CTLA-4 is sequestered in intracellular vesicles, and not surfaced until the T cell receptors (TCR) are activated, where its expression increases with stronger TCR activation, and also binds with CD80 and CD86 on antigen presenting cells to dampen immune response (Santuray et al., 2018, Pardoll, 2012).

In HNSCC patients with tumours with surplus infiltration of CTLA-4 expressing T_{reg} cells, could be the reason behind dysfunction of effector cells (Albers et al., 2005). Furthermore, a study with cetuximab treated HNSCC patients with higher frequency of circulating CTLA-1 has poorer clinical outcome (Jie et al., 2015).

Currently there are no CTLA-4 inhibitors in clinic but Ipilimumab, a mAb against CTLA-4, has been approved to treat metastatic melanoma, is being trialled as single agent as well as in combination with Nivolumab to treat HNSCC (Larkin et al., 2015).

Alternatively, nanoparticles (versatile particles of 1-100 nm in diameter) are also being exploited to use as cancer therapy. Nanoparticles easily accumulate in tumour tissues due to leaky vasculature and inefficient lymphatic drainage, where they can extravasate though blood vessels and capillaries to deposit therapeutic agents and target cancer cells more efficiently (Wu and Zhou, 2015). Since nanoparticles are foreign bodies and will be attacked and cleared by the immune system, they're coated with biodegradable polyethylene glycol to reduce being phagocytosed.

Nanoparticles can be used to deliver anti-sense oligonucleotides, and small interfering RNA aimed at degradation of targeted mRNA to prevent expression of proteins like GLUT-1, EGFR, survivin, protein kinase CK2, ribonuclease reductase M2 amongst many to halt cancer growth (Wu and Zhou, 2015).

1.3 Inflammation and cancer

1.3.1 Acute inflammation

Acute inflammation is initiated as a mechanism to resolve infections and injurious stimuli. Inflammation is a complex reaction involving the resident

macrophages, dendritic cells, circulating leukocytes and neutrophils, connective tissue cells, and extracellular fibrous proteins and glycoproteins recruited to the site of infection/injury (Beck, 2013). The process of inflammation can damage the surrounding cells of the tissue if continued for too long, hence resolution of inflammation is an important aspect of maintaining homeostasis. The initial step towards resolution involves terminating pro-inflammatory mediators, and their catabolism, followed by clearance of immune cells present at the site of infection/injury. The leukocytes can either return back into systemic circulation or undergo apoptosis/necrosis resulting in phagocytosis/efferocytosis by macrophages (Gilroy and De Maeyer, 2015). Dying cells display surface markers that are recognised by macrophages which then phagocytose them. In the process these macrophage release anti-inflammatory molecules, such as IL-10 and TGF-β1 (Huynh et al., 2002). It's also been observed that when monocytes are exposed to glucocorticoids, they differentiate into highly phagocytic macrophages with elevated cell surface CD163 (Giles et al., 2001, Philippidis et al., 2004). Most macrophages then return back to the lymphatic

system while the remaining few undergo apoptosis themselves (Gilroy et al., 2003).

1.3.2 Chronic Inflammation and cancer

When either the inflammatory response is not short lived, or resolution of inflammation is inadequate, it can lead to chronic inflammation. Other reasons for chronic inflammation can be exposure to a toxic agent, for example tobacco or silica in lungs (Cohen and Pope, 1995), auto-immune disorders such as inflammatory bowel disease which can lead to colon cancer (Francescone et al., 2015), and obesity predisposing to liver cancer (Calle and Kaaks, 2004). However, infection plays the greatest role in chronic inflammation and related cancers with up to 20% of cancers worldwide associated with microbial infection, such as *Helicobacter pylori* causing gastric cancer or mucosa associated lymphoid tissue lymphoma (Kuper et al., 2000, De Falco et al., 2015). Prolonged inflammation also results in accumulation of metabolic products such as reactive oxygen species and reactive nitrogen species which potentially damage DNA by activating oncogenes and/or

inactivating tumour suppressor gene or mismatch repair mechanisms as depicted in fig. 1.2 (Ohnishi et al., 2013, Beck, 2013).

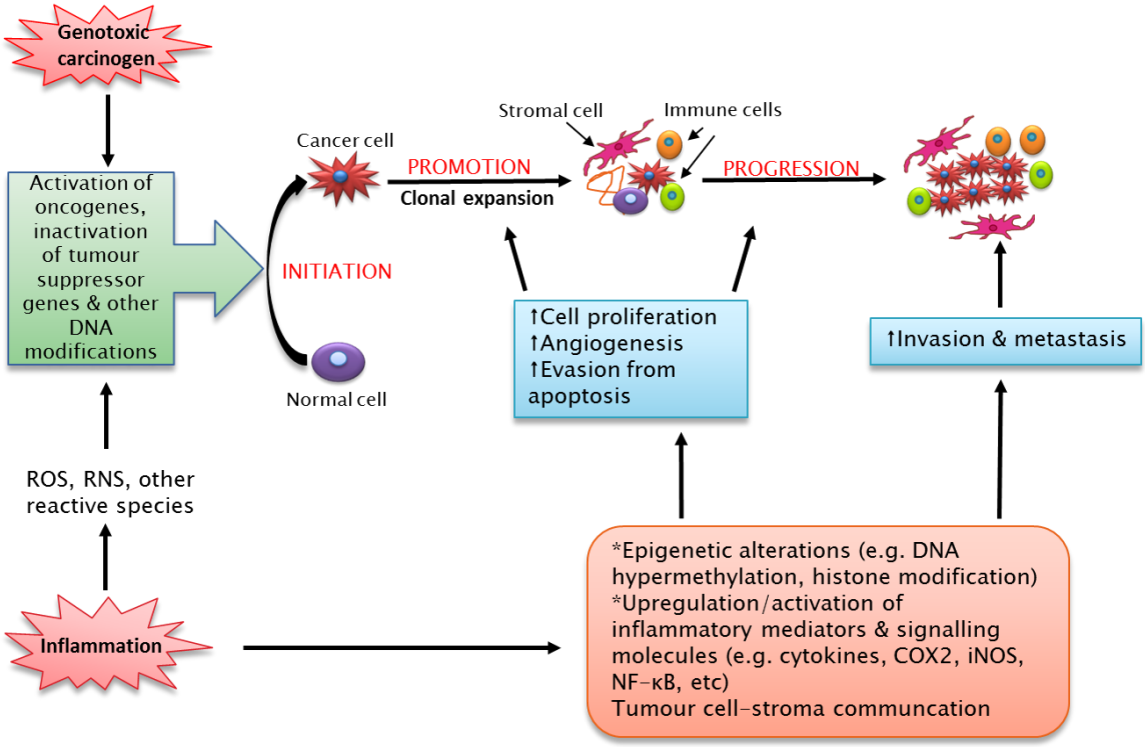

Figure 1.2: Relationship between inflammation and various stages of cancer development & progression. Inflammatory factors such as ROS, RNS, COX2, other cytokines when secreted chronically can alter DNA expression leading to activation of oncogenes, and deactivation of tumour suppressor genes, allowing uncontrolled proliferation of transformed cells. The same inflammatory factors can further fuel cancer progression and metastasis.

1.3.3 Role of COX2 in inflammation and cancer

One of the many inflammatory molecules implicated in promoting cancer is cyclooxygenase 2 (COX-2), which mediates immune responses by catalysing the production of prostaglandins and prostanoids and plays a vital role in angiogenesis, cell proliferation, inhibition of apoptosis, and cell motility. Moreover, COX-2 is found at sites of inflammation released by epithelial, mesenchymal and inflammatory cells in response to cytokines, environmental factors and infective agents (O'Byrne and Dalgleish, 2001). Consequently, COX-2 induces production of Th2 cytokines, IL-4 and IL-10, which are known to be immuno-suppressive and in turn suppress production of Th1 cytokines. Therefore, the site of inflammation may promote mutagenic changes in cells and provides an immuno-suppressive environment for these cells to evade host's immune surveillance and pass the mutations down to the next generation of cells while developing more mutations leading to neoplasia and eventually to a malignant tumour development (Kundu, 2008).

According to (Wu et al., 2014), COX-2 upregulated urokinase type plasminogen activator and its receptor which are involved in degrading extra-cellular matrix to promote metastasis in osteosarcoma.

COX-2 was also found to be upregulated and secreted by senescent fibroblasts, and regulates microRNA-335 which, further enhances secretion of IL-6, CCL2, and MMP-2 creating a pro-inflammatory secretome, which stimulated migration of H357 cells (HNC cell line) in an *in vitro* model (Kabir et al., 2016)

1.3.4 Role of IL-6 in inflammation and cancer

Another prominent molecule in inflammation is IL-6, which is a multifaceted cytokine. During inflammation, it is secreted by monocytes, macrophages, neutrophils, endothelial cells, fibroblasts, T-cells, and smooth muscle cells (Rose-John, 2012). IL-6 has a similar protein structure to IL-11, IL-27, IL-31, ciliary neurotrophic factor, cardiotrophin-1, cardiotrophin like cytokine, leukemia inhibitory factor, and oncostatin M, and these are all part of the IL-6 cytokine family. The IL-6 cytokine family, with exception of IL-31, activates the

JAK/STAT3 pathway, MAPK/ERK pathway, and PI3K pathway through their unique signalling receptors and glycoprotein 30 which increases transcription and translation of many downstream proteins promoting cell survival, proliferation, differentiation (Poncet et al., 2011, Hov et al., 2009, Guo et al., 2012, Yao et al., 2014), migration (Ara and Declerck, 2010, Walter et al., 2009, Foran et al., 2010), invasion (Walter et al., 2009, Lin et al., 2007, Huang et al., 2011, Sullivan et al., 2009, Yadav et al., 2011), angiogenesis (Middleton et al., 2014, Xu et al., 2005, Shinriki et al., 2011), metabolism, and inflammation (Tanaka et al., 2014).

In HNC patients, IL-6 has found to be elevated in blood samples, and distinctly predict tumour metastasis, recurrence and survival (Duffy et al., 2008, Riedel et al., 2005, Chen et al., 1999). IL- 6 is also known to promote malignant growth of SCC through complex cytokine and protease network (Lederle et al., 2011). IL-6 has also been associated with HNC progression where serum levels of IL-6 in stage IV were significantly different from stage I/II/III (Mojtahedi et al., 2011). It is also a powerful inducer of EMT via

JAK/STAT3/SNAIL, confirmed by up-regulation of vimentin, and down-regulation of E-cadherin; addition of recombinant IL-6 to tumour cell culture produced similar results (Yadav et al., 2011, Scherzad et al., 2015). Through persistent activation of STAT3 pathway by IL-6, target genes responsible for proliferation, migration, invasion, survival, cancer stem cell expansion, EMT and chemo-resistance expressed (Su et al., 2011, Yadav et al., 2011, Stanam et al., 2015). Evidence has shown that targeting IL-6/STAT3 pathway by inhibiting IL-6 receptor by an antibody led to decrease in mRNA of serpin B3/B4 (known to promote cell survival in HNC), enhancing tumour cell apoptosis (Ahmed and Darnell, 2009). IL-6 is also capable of altering CpG promoter, responsible for DNA methylation, and repress tumour suppressor genes like GATA5, PAX6, and CHFR (Gasche et al., 2011). With such diverse roles of IL-6 in HNC, its production by two CAF phenotypes are examined in this thesis further.

1.3.5 Role of CCL2 in inflammation and cancer

CCL2 is produced by several cells, such as, fibroblasts, endothelial cells, mesangial, smooth muscle, astrocytic and glial cells, with monocyte/macrophage as the major source of the chemokine (Deshmane et al., 2009). It is one of the many prevalent cytokines found at the site of inflammation, where it recruits monocytes through the CCL2/CCR2 axis, which then differentiate into macrophages to phagocytose invading pathogens, and to clear prevailing immune cells at the end of an acute inflammatory phase. It is also serves as a chemoattractant for memory T lymphocytes and natural killer (NK) cells (Deshmane et al., 2009). However, CCL2 has been found in tumours and their environment, and levels of CCL2 correlate with the presence of tumour associated macrophages and poor prognosis in prostate and breast cancer (Zhang et al., 2010, Ueno et al., 2000). A gene study from human monocytes as well as murine bone marrow derived macrophages has shown CCL2 is also able to selectively polarise these macrophages to a M2 phenotype in the presence of M-CSF with

upregulated expression of CD206, and increased secretion of IL-10 (Sierra-Filardi et al., 2014). Qian *et al* reported that monocytes recruited by tumour derived CCL2, stimulated extravasation of tumour cells via monocyte-derived endothelial growth factor (Qian et al., 2011). CCL2 is also able to bind to CCR4, recruiting T regulatory cells, building an immuno-suppressed environment in tumours (Lim et al., 2016). CCR2 expressing cancer cells respond to CCL2 through MEK-p42/44MAPK, and increasing the secretion of MMP9 resulting in increased cell motility and cell survival (Fang et al., 2012, Tang and Tsai, 2012). CCL2 has also been shown to assist mammary cancer cell proliferation and cell survival (Hembruff et al., 2010, Lim et al., 2016). CCL2 has also been associated with metastasis and cancer stem cells (Lu and Kang, 2009, Loberg et al., 2007, Tsuyada et al., 2012b, Kudo-Saito et al., 2013). It has also been observed *in vitro* that mesenchymal stem cell derived osteoblasts secrete high levels of CCL2, aiding migration of breast cancer cells, suggesting a role in bone metastasis in breast cancer by CCL2 (Molloy et al., 2009). Another study showed that human bone marrow endothelial cells also secrete high levels of CCL2 compared to dermal and cardiac endothelial

cells and attract prostate cancer cells using CCL2 *in vitro* (Loberg et al., 2006). Serum levels of CCL2 have been found to high in patients with prostate cancer with bone metastasis; when CCL2 production in prostate cancer cells was knockdown, it hampered osteoclast formation and upon transplantation in SCID mice tibia, reported reduced tumour growth (Lu et al., 2009) A study showed that blockade of CCL2, enhanced the chemosensitivity of ovarian cancer cells to paclitaxel, and carboplatin (Moisan et al., 2014).

CCL2 has been implicated in the cancers of HNC as well. In oral squamous cell carcinoma (OSCC), significantly lower serum levels of CCL2 was observed compared to healthy participants, and the ratio of CCL2/CCL3 correlated with disease progression, suggesting these can serve as potential biomarkers in OSCC (Ding et al., 2014b). CCL2 has also demonstrated to induce EMT and increased motility in head and neck cancer cells *in vitro* via activation of AKT pathway (Lee et al., 2015, Ji et al., 2014). Another *in vitro* study reported HNSCC cells educated macrophage to M2-like phenotype via CCL2, which in turn secreted EGF, enhancing invasion properties of HNSCC

cells by invadopodia which degraded ECM and allowing metastasis (Gao et al., 2016). Apart from HNC cells, cancer associated fibroblasts also secrete CCL2 when in vicinity of cancer cells *in vivo* or co-cultured *in vitro*, further enhancing production of endogenous reactive oxygen species which caused oxidative stress in HNC cells and fuelled production of cell cycle progression proteins promoting proliferation, migration and invasion (Li et al., 2014b). Recent evidence also shows that CCR4, found on T_{reg} cells are attracted to the tumour microenvironment by CCL2, and impeding CCL2/CCR4 pathway reduced this recruitment, allowing effector T cells to evoke anti-tumour immunity (Sun et al., 2016).

With such an array of data implicating CCL2 in HNC, this study looks at cancer associated fibroblasts as a source, and macrophage recruitment by the resulting CCL2.

1.3.6 Role of IL-8 in inflammation and cancer

Another molecule secreted during inflammation is IL-8 (CXCL8). It has also been linked with chronic inflammation and cancer. Initially it is responsible for

neutrophil recruitment and degranulation to destroy invading pathogens (Waugh and Wilson, 2008). However, in cancer it has been observed to be secreted by cancer cells themselves, mesenchymal cells, and macrophages (Singh et al., 2013). Breast cancer patients display higher serum levels of IL-8 which is correlated with early metastasis, and its involvement in metastasis could be mediated by COX2 (Benoy et al., 2004, Singh et al., 2006).

The above highlights only a few factors that illustrate the marriage between inflammation and cancer. This thesis goes on to highlight more factors, and some will be described in detail.

1.4 Importance of the tumour microenvironment

Tumours are not a homogenous group of cells causing disease, but rather a heterogeneous population of non-malignant cells, immune cells, expanding network of blood vessels, extra cellular matrix, and signalling molecules coordinating together and disrupting normal physiological processes as seen in fig. 1.3 (Quail and Joyce, 2013, Junttila and de Sauvage, 2013). The importance of the tumour microenvironment has been the focus of intense research in recent years with emphasis on fibroblasts, leukocytes, natural killer cells, T_{reg} cells, myeloid-derived suppressor cells, which co-evolve with cancer cells to contribute numerous signals in a paracrine fashion having pleiotropic effects on tumour progression, immune-evasion and metastasis (Curry et al., 2014). The tumour manipulates these cells in to changing the ECM around it for easier invasion, stifle attacks by cytotoxic T cell, macrophages, and NK cells, create a metabolically supportive environment, and allow formation of new blood and lymph vessels (Curry et al., 2014). By understanding the stroma around a tumour, and added benefit of stromal cells being more genetically stable compared cancer cells, one or more stromal component can

be targeted for a more accurate prognosis and treatment options. The importance of different aspects, including cells of the tumour microenvironment are described in sections after this.

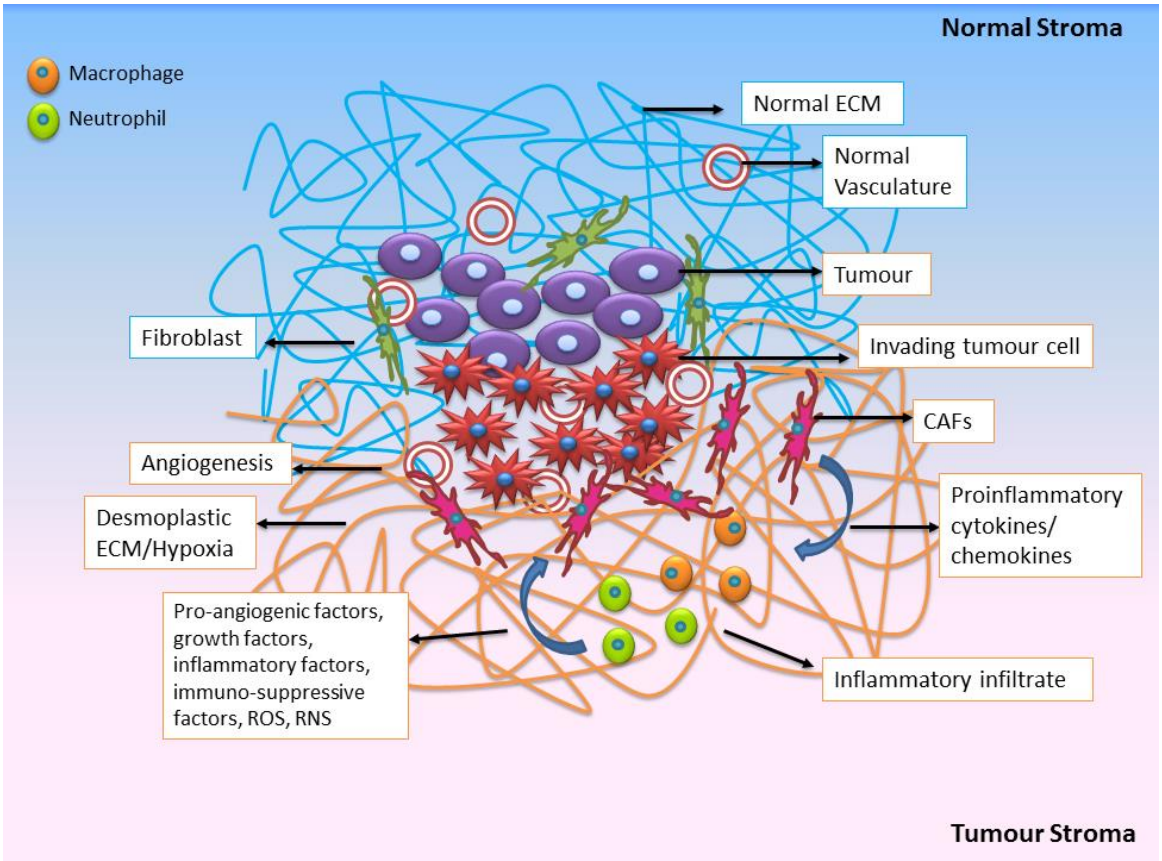

Figure 1.3: Diagrammatic representation of tumour microenvironment: A comparison of normal stroma vs tumour stroma where the extracellular matrix is stiffer and organised differently, epithelial cells are transformed to a malignant state, number of fibroblasts and immune cells increases with pro-tumorigenic phenotypes, and vasculature consisting of leaky irregular blood vessels. There are also various soluble signalling molecules being secreted by tumour cells and stromal cells, through which crosstalk occurs.

1.4.1 Extracellular matrix in TME

Patients usually visit the doctor upon feeling a lump suggesting the rigidity of the cancerous mass is more than its surrounding tissue. With this in mind, and increasing evidence, rigidity of TME can be considered another hallmark of cancer (Jonietz, 2012).

Radiological examination such as chest x-rays and mammography show that cancerous lesions are denser than surrounding tissue, which is a result of an increased deposition of extracellular matrix components like collagen and fibronectin, and can serve as an independent prognostic tool (Martin and Boyd, 2008, Aerts et al., 2014).

Evidence also suggests that mechanical properties of ECM alter cells' ability to invade. Provenzano *et al* showed that murine mammary epithelial cells displayed more invasive behaviour in stiffer matrix (~44 kPa) compared to softer matrix of (~25 kPa) (Provenzano et al., 2009). While Paszek *et al* demonstrated human mammary epithelial cells organised themselves in to organotypic acinar structures on soft gels (170 Pa), but this morphology is

disrupted and the cells lose their polarity on gels of increasing stiffness (up to ~1200 Pa) (Paszek et al., 2005). Chaudhuri *et al* reported similar findings where mammary epithelial cells cultured on stiffer substrates lost their polarisation, ability to arrest growth, and invaded the matrix (Chaudhuri et al., 2014). However mechanical forces do not transform cell phenotype permanently, and the resulting changes can be reversed with a less rigid ECM (Chaudhuri et al., 2014).

Evidence also suggests a correlation of cancer aggressiveness and invasiveness with stiffening of ECM. Acerbi *et al* reported notable deposition of collagen I and ECM remodelling in more aggressive forms of breast cancer such as human EGFR2 and Basal-like, in which the ECM were stiffer than Luminal A and B types; and at the invasive front of the tumour (Acerbi et al., 2015).

Further analysis of the stiffer invasive front of tumours revealed an infiltration of CD45, CD68 and CD163 positive macrophages, which further secrete TGF-β and stimulate production of ECM components such as collagen from the

stromal cells and activate lysyl oxidase causing cross-linking of collagen (Acerbi et al., 2015, Shanley et al., 1997). Collagen cross-linking caused by lysyl oxidase further induces activation of FAK (focal adhesion kinase)/Src pathways giving cancer cells a more proliferative and invasive phenotype (Baker et al., 2013).

Having observed the importance of ECM in tumour microenvironment; it is important to shed some light on the major source of these ECM components – fibroblasts. In the vicinity of cancer cells they're commonly known as cancer associated fibroblasts (CAFs). These CAFs possess the ability to produce, deposit and reorganise ECM proteins like collagen (Tuxhorn et al., 2002, Yang et al., 2011). One such study by Gaggioli *et al* demonstrated using reflectance imaging which captures a series of images with the object lit at variable angles, and transmission electron microscopy, that CAFs paved a path, using protease and force mediated matrix remodelling dependent on integrins α3 & α5 and regulation of Rho mediated myosin light chains, for cancer cells to follow on to invade (Gaggioli et al., 2007).

1.4.2 Angiogenesis in TME

With cancer cells proliferating quickly and forming a mass, they have an increased requirement for oxygen, nutrients, and waste removal, which is difficult to come by without sufficient blood vessels serving the growing tumour. This calls for an urgent need for angiogenesis, and vascular endothelial growth factor (VEGF) plays a pivotal role in the process of meeting these needs (Ferrara and Davis-Smyth, 1997, Shibuya and Claesson-Welsh, 2006). VEGF-A, a sub-type of VEGF family which plays a crucial role in formation of blood vessels, is implicated in development and several cancers (Matsumoto and Ema, 2014). Current evidence suggests that not only cancer cells, but also stromal cells such as CAFs and macrophages secrete VEGF, platelet derived growth factor, fibroblast growth factor, insulin-like growth factor, angiopoietins, TGF-β1, MMP-9 and several other chemokines to promote angiogenesis through endothelial cell invasion and blood vessel formation (Hlatky et al., 1994, Sakurai and Kudo, 2011, Murdoch et al., 2008, Albini et al., 2005). This, therefore, makes CAFs and macrophages good

targets to attempt to inhibit angiogenesis in tumours as a form of cancer therapy.

1.4.3 Immune cells in TME

It has been long observed that the tumour microenvironment is a home to several types of immune cell, and these immune cells are exploited by cancer cells to promote cancer progression by providing an immunosuppressed environment, stimulating angiogenesis, and metastasis (Gajewski et al., 2013). T cell populations have been found at invasive tumour fronts and draining into lymphoid organs (Restifo et al., 2012). Amongst the T cell population in TME, there are $CD8^+$ memory T cells and $CD4^+$ T helper 1 cells which provide an anti-tumour effect by secreting IFN-γ, and improve prognosis (Fridman et al., 2012). On the other hand, regulatory T cells ($CD4^+CD25^+Foxp3^+$) and Th17 cells are shown to promote tumour growth, mainly by suppressing activation of effector immune cells which present self-antigen, and by secreting TGF- β1 (Chen et al., 2003, Curiel et al., 2004, Kim et al., 2007, Littman and Rudensky, 2010).

Other immune cells in the TME include but are not limited to; myeloid-derived suppressor cells, which promote angiogenesis, disrupt natural killer (NK) cell cytotoxicity; also minimise antigen presentation by dendritic cells, and T cell activation against cancer cells (Bochet et al., 2013). Another commonly found immune cell in the TME is the neutrophil. Neutrophils are capable of acquiring different phentotypes under the influence of respective cytokine environment. Tumour associated neutrophils promote genetic instability through production of reactive oxygen species (ROS), tumour cell proliferation via neutrophil elastase, angiogenesis through VEGF-A, MMP-9 and hepatocyte growth factor and tumour invasion through cytokines as demonstrated in *in vivo* mice models of mesothelioma (Fridlender et al., 2012, Curry et al., 2014).

1.4.4 Tumour associated macrophages (TAMs)

Circulating monocytes are recruited to the site of injury and/or infection, where they differentiate in to 'M0' or unpolarised macrophages in tissue. Their primary role at this stage is to phagocytose damaged cells, invading bodies, microbes, and present resulting antigens to activate T cells resulting

inflammation (Navegantes et al., 2017). While a second subset of macrophage at the site of inflammation later aims to reduce inflammation while remodelling tissue to heal wounds (Mills, 2012). They are also found in and around tumours and this presence is often associated with poor prognosis in most cancers including head and neck (Gajewski et al., 2013, Bingle et al., 2002, Chen et al., 2005, Ryder et al., 2008, Zhu et al., 2008), with exceptions of certain cancers like non-small cell lung cancer where high density of macrophages are reported to improve prognosis (Kim et al., 2008). This conflicting role of TAM could be due to macrophages undergoing polarisation exhibiting different secretory phenotypes and markers in response to the cytokine environment in their surroundings. Figure 1.4 depicts differential activation of macrophages.

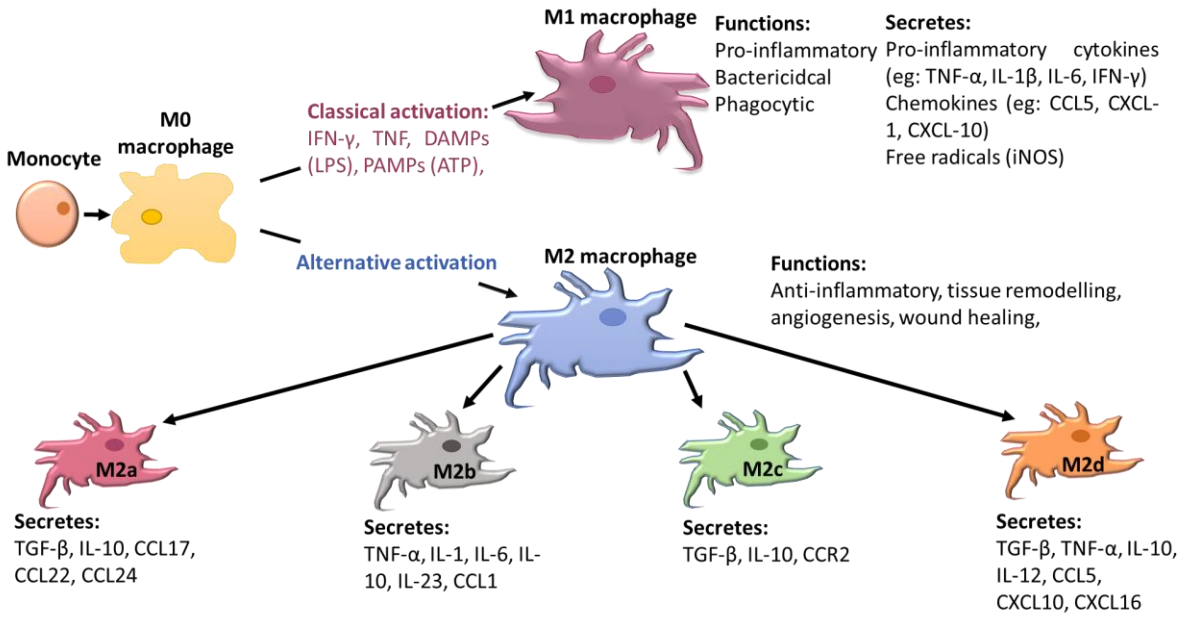

Figure 1.4. Macrophage activation and polarisation in response to their cytokine environment: Depending on the cytokine environment, macrophages can polarise towards inflammatory M1 or anti-inflammatory M2, which further sub-divides in to M2a, M2b, M2c, and M2d, secreting their own sets of cytokines. M1 activated macrophages respond to injury/infection to phagocytose cellular debris, and microbes, while presenting antigens to T cells, and are tumoricidal in nature. M2 activated macrophage participate in resolving infection, and wound healing, and are known to be pro-tumorigenic. However, in TME, TAMs can express markers everywhere on the spectrum of M1 to M2, dependent on the cytokine in their environment.

At present, macrophages are known to be activated via two pathways, namely classical and alternative pathway. Classically activated macrophages are termed M1 polarised macrophages which are immune stimulatory, are activated by IFN-γ, LPS, GM-CSF, TNF-α and TLR engagement (Navegantes et al., 2017). M1 macrophages secrete pro-inflammatory factors, such as IL-12, IL-6, IL-1β, TNF-α, and NO species, promote local tissue destruction, inflammation, nitrosative stress, and are tumoricidal (Mantovani and Sica, 2010, Qian and Pollard, 2010, Mantovani and Locati, 2013, Wang et al., 2012, Biswas and Mantovani, 2010). M1 macrophages express cell surface markers, such as CD40, CD68, CD80, CD86, MHC II, IL-1R, TLR2, TLR4, and SOCS3 in response to the cytokines in their environment (Poh and Ernst, 2018).

On the other hand, when macrophages are alternatively activated, they're polarised to M2 phenotype, and sub-classified in to M2a (activated by IL-4 & IL-13), M2b (activated by immune complexes with IL-1β and LPS), M2c (activated by IL-10, glucocorticoids, and TGF-β), and M2d (activated by IL-6, LIF and adenosines) (Rőszer, 2015, Poh and Ernst, 2018), play a role in tissue remodelling, angiogenesis, and immune-suppression via production of cytokines such IL-10, IL-12, TGF-β and

recruitment of regulatory T cells (Treg) (Kim et al., 2008, Biswas and Mantovani, 2010).

In terms of identification, M2 polarised macrophages tend to exhibit a range of markers due to existence of various sub-types: M2a – CD163, CD206, MHC II, SR, M2b – CD86, MHC II, MerTK, M2c – CD163, TLR1/8, M2d - VEGF; that being said, macrophages are very plastic and sit anywhere on the spectrum between M1 and M2 with a higher expression of any or combination of these markers depending on their location within the tumour and TME (Poh and Ernst, 2018).

In cancer, role of macrophages still remains unclear, partly due to their plasticity to polarise depending on the cytokine environment which varies across the span of a tumour. In colorectal cancer study, macrophages have been found to be classically activated, expressing M1 marker CD68 upon co-culturing with colorectal tumour cells, where the tumour cells showed upregulation of apoptosis associated genes and down-regulation of proliferation associated genes, compared to tumour cells cultured alone (Ong et al., 2012). The macrophages in the same study also expressed T cell co-stimulatory molecules like CD80 and CD86, elaborating further on the possibility of recruiting tumoricidal effector T cells to the TME (Ong et al.,

2012). Migratory inhibitory factor (MIF) is able to induce production of TNF-α and IL-1β in macrophages producing cytotoxic effects on melanoma cell lines (Pozzi and Weiser, 1992). In another *in vivo* mouse study, IL-18 was found to be secreted from macrophages which activated NK cells leading to anti-tumours effects fibrosarcoma models; IL-18 also induced the production of other cytokines, IL-1, IL-6, IL-8, and TNF-α (Netea et al., 2000, Osaki et al., 1999).

Having said that, several macrophage depletion studies have reported decreased tumour growth and metastasis, suggesting presence of macrophages in and around tumours as a double edged sword. Knocking out macrophage colony stimulating factor (M-CSF) gene, resulted in delayed mammary tumour growth and metastasis, while transgenic expression of M-CSF stimulated tumour progression and metastasis to lung (Lin et al., 2001). In another study, presence of $CD68^{+}$ macrophages correlated positively with tumour grade and live metastasis of human pancreatic neuroendocrine tumours (PNETs); M-CSF knockdown in mice with PNETs reported reduced homing of macrophages to tumour site (Pyonteck et al., 2012). Recently, Perrotta, *et al* found that nitric oxide produced by both human and mice M2 polarised ($CD206^{+}$) TAMs impart chemoresistance towards cisplatin to gliomas (Perrotta et al.,

2018). Another mouse model of breast cancer, revealed how M2 $CD206^{+}TIE2^{hi}CXCR4^{hi}$ macrophages assemble around blood vessels in breast tumours after chemotherapy, and promote re-vascularisation and relapse via secretion of VEGF-A (Hughes et al., 2015b). In the same study, the ligand for CXCR4, CXCL12 was found to be upregulated at perivascular sites after chemotherapy, promoting migration of TAMs (Hughes et al., 2015b). Muthana *et al* demonstrated that TAMs can be used as a carrier to deliver oncolytic virus to hypoxic tumour sites after chemotherapy or radiation therapy, slowing down tumour re-growth and metastasis after treatment (Muthana et al., 2013).

With such variable roles and potential of TAMs, their recruitment and possible polarisation by cancer associated fibroblasts was examined in this thesis.

1.5 Cancer associated fibroblasts (CAFs)

Cancer associated fibroblasts, as the name suggests, are present in close proximity to cancer cells, fuelling their initiation, progression and metastasis. Lim *et al* reported that fibroblasts from normal oral mucosa, epithelial dysplastic tissue, OSCC

(genetically stable and unstable) have different genetic profiles, suggesting differential gene regulation in normal environment and TME (Lim et al., 2011b).

It has been speculated that cancer associated fibroblasts (CAFs) may be composed of heterogeneous populations of which two sub-types identified are myofibroblasts and senescent fibroblasts (Routray et al., 2014a, Davalos et al., 2010a). The reason for this evident heterogeneity stems from topographical differences, the local paracrine milieu and their origins (Fig. 1.5).

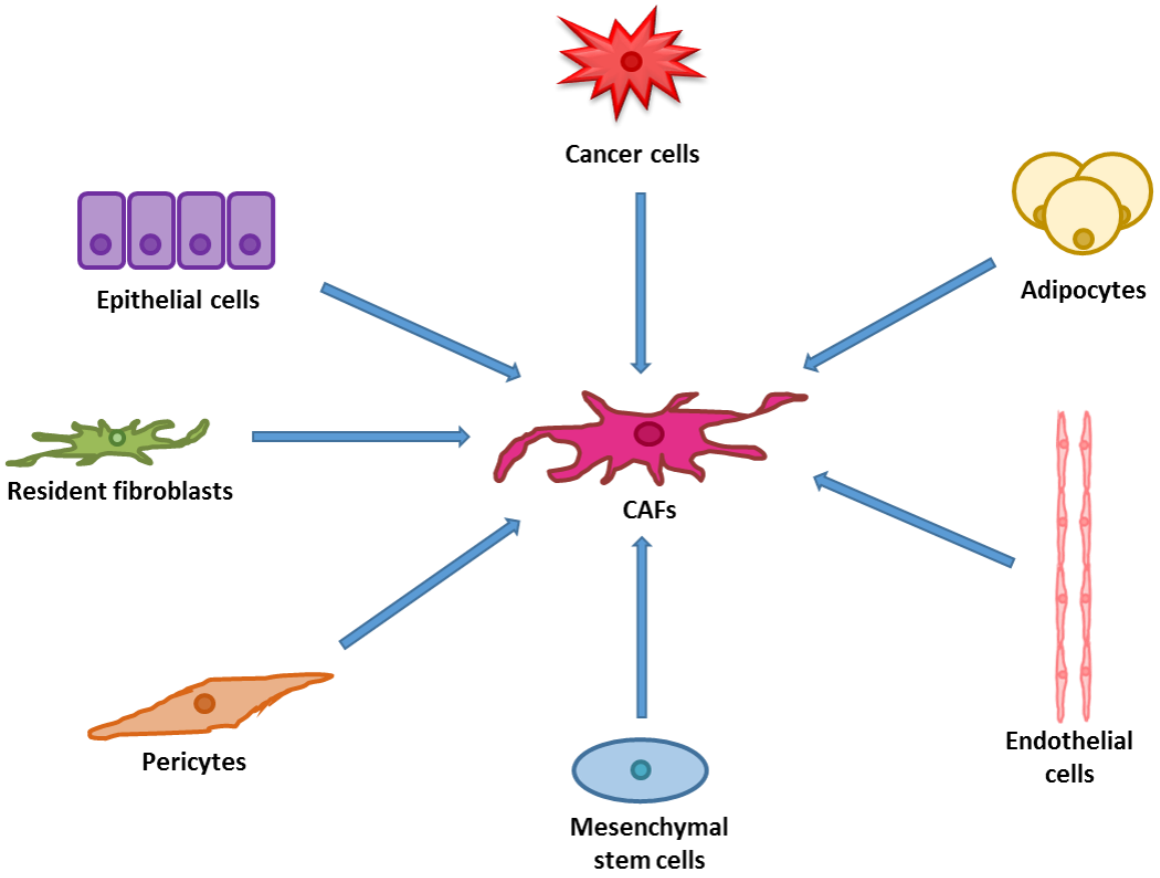

Figure 1.5: **Suggested origins of cancer associated fibroblasts:** Numerous studies have reported that CAFs express markers from the tissue they originally migrated from to transform in to CAFs in response to signalling molecules from the tumour cells and their neighbouring cells. So far, evidence suggests resident fibroblasts, pericytes, mesenchymal stem cells, adipocytes, endothelial cells, epithelial/cancer cells are capable of transforming in to CAFs.

1.5.1 Origin of cancer associated fibroblasts:

1.5.1.1 Resident fibroblast: One of the most convincing sources of CAFs is the local tissue resident fibroblasts which are activated in response to stimulants secreted by the tumour cells (Augsten, 2014b). TGF-β1 and SDF-1 from breast carcinoma cells activate and transdifferentiate fibroblasts in to tumour promoting myofibroblasts, forming an autocrine loop and maintaining the activated phenotype (Kojima et al., 2010). Reactive oxygen species (ROS) from cancer cells lead to an accumulation of the transcription factor hypoxia inducible factor (HIF)-1α and SDF-1, which again transdifferentiate normal fibroblasts in to CAFs (Toullec et al., 2010). Xu *et al* showed that recombinant extracellular matrix metalloproteinase inducer, EMMPRIN/CD147, through both, co-culture or conditioned medium from breast cancer *in vitro*, transformed quiescent fibroblasts into α-SMA expressing cancer associated fibroblasts (Xu et al., 2013). MicroRNAs, an abundant class of small non-coding RNA, regulate gene expression post transcription, thereby influencing the phenotype of cells. A study found CAFs from ovarian

cancer had downregulated miRNA-31 and miRNA-214, while miRNA-155 was upregulated; upon similar manipulation of these miRNAs levels in normal fibroblasts led to conversion in to a CAF like phenotype (Mitra et al., 2012). Another miRNA, miR-145 has been observed to be up-regulated in TGF-β1 transdifferentiated myofibroblasts in oral, dermal and lung fibroblasts imparting contractility and α-SMA expression (Melling, 2015, Yang et al., 2013b). Melling also described how excessive over-expression of microRNA-145 could prevent and partially reverse myofibroblast transdifferentiation (Melling, 2015). Senescent fibroblasts, a sub-type of CAF, have up-regulated microRNA-335, modulating an inflammatory secretome supporting tumour progression (Kabir et al., 2016). How these microRNAs were deregulated is still unclear, however their deregulation was sufficient to transform resident fibroblasts to CAFs. Other DNA damaging agents, such as: tobacco, areca nut, chemotherapy, radiation therapy, and old age impart CAF like phenotype by inducing senescence in resident fibroblasts (Kabir et al.,

2016, Schmitz et al., 2015, Rehman et al., 2016, Coppe et al., 2008, Yang et al., 2013a, Nyunoya et al., 2006).

1.5.1.2 Bone marrow derived stem cells: Signalling mediators produced and secreted by tumour cells can induce effects locally as well as on a systemic level resulting in recruiting cells such as bone marrow derived mesenchymal stem cells from distant locations to the tumour site. This phenomenon has been observed in studies where bone marrow from β-galactosidase transgenic mice was transplanted in to severe combined immune-deficient mice with a subcutaneous xenograft of a pancreatic cell line; analysis of the tumour xenografts 14 and 28 days post-transplant showed the presence of myofibroblasts in and around the tumour which stained positively using X-gal (Ishii et al., 2003). Another study transplanted green fluorescent protein (GFP) positive male mouse-derived bone marrow in to female GFP negative mice with pancreatic insulinoma. Tumour sections from female mice were then stained for GFP, α-smooth muscle actin, vimentin, and Y chromosome which confirmed that the CAFs were derived from the

transplanted bone marrow (Direkze et al., 2004). Recently it was discovered that GRP78, otherwise known as endoplasmic reticulum chaperone, is over expressed by colon cancer cells and aids transformation of murine and human bone marrow MSCs to CAFs by inducing expression of α-SMA through TGF-β1 receptor and phosphorylation of Smad2/3 (Peng et al., 2013). A study revealed that breast cancer cells expressing osteopontin are able to induce expression of TGF- β1 in mesenchymal stem cells via myeloid zinc finger 1 to form an autocrine loop and adopt a CAF like phenotype. The newly acquired CAF phenotype was confirmed by expression of α -SMA, vimentin, tenascin C and fibroblast specific protein (FSP) 1 (Weber et al., 2015).

1.5.1.3 Epithelial to mesenchymal transition (EMT): is the process through which epithelial cells lose their tight cell-cell junctions to transition in to mesenchymal cells with loose cell junctions and stem cells properties. TGF-β is one of the factors secreted by the tumour cells responsible

for EMT (Routray et al., 2014a, Radisky et al., 2007b, Rhyu et al., 2005). Furthermore, matrix metalloproteinases (MMPs), especially MMP-3, are known to induce EMT in cells via reactive oxygen species (ROS) dependent gene alteration and activation of pathways like Snail resulting in more CAFs (Radisky et al., 2007b, Radisky et al., 2005). Nightingale *et al* (2004) reported that oncostatin M released from T cells and monocytes transdifferentiated epithelial cells in to myofibroblasts via JAK/Stat signalling pathway; confirmed by upregulation of α-SMA, collagen I, fibronectin EDA and down-regulation of E-cadherin and cytokeratin 19 (Nightingale et al., 2004). However, some studies suggest that CAFs do not arise from cancer cells through EMT, such as in the case of when human HEp-2 laryngeal cancer cell line cells were xenografted into mouse model, and the arising CAFs were karotyped and found to be of mouse origin, and not human laryngeal origin, suggesting that the CAFs that arose, originated from a different source (Wang et al., 2015b). Another similar studied transplanted human cancer cells in mice and resulting stroma

failed to be recognised by human specific vimentin antibody (Dvorankova et al., 2015). Although controversy around the evidence for a role for EMT in generating CAF exists, the possibility that EMT is one of the many routes to generate CAFs in TME cannot be ignored. Perhaps, certain factors facilitate EMT in some cancers, more than others.

1.5.1.4 Endothelial cells of the heart and lung undergo endothelial to mesenchymal transition (End-MT) in response to TGF-β1 (Zeisberg et al., 2007, Rhyu et al., 2005). Zeisberg *et al* (Zeisberg et al., 2007) treated endothelial cells with TGF-β1 and showed emergence of fibroblast specific protein-1 and downregulation of CD31; a marker found specifically on endothelial cells (Thiery and Sleeman, 2006, Zeisberg et al., 2007, Bierie and Moses, 2006). This suggests endothelial cells are also a potential source of CAF.

1.5.1.5 Adipocyte derived CAFs: There have been suggestions of adipocytes contributing to the CAF population, and it was recently described by Bochet *et al* that breast cancer cells coerce mature adipocytes in to

becoming CAF like cells in a Wnt dependent manner. These adipocyte derived fibroblasts lost their lipid content, expressed FSP-1 but not α-SMA and generated increased amounts of ECM (Bochet et al., 2013). Despite varied origins of CAFs, they still promote tumour progression through their unique secretory factors (Fig. 1.6) as described in section 1.5.2.

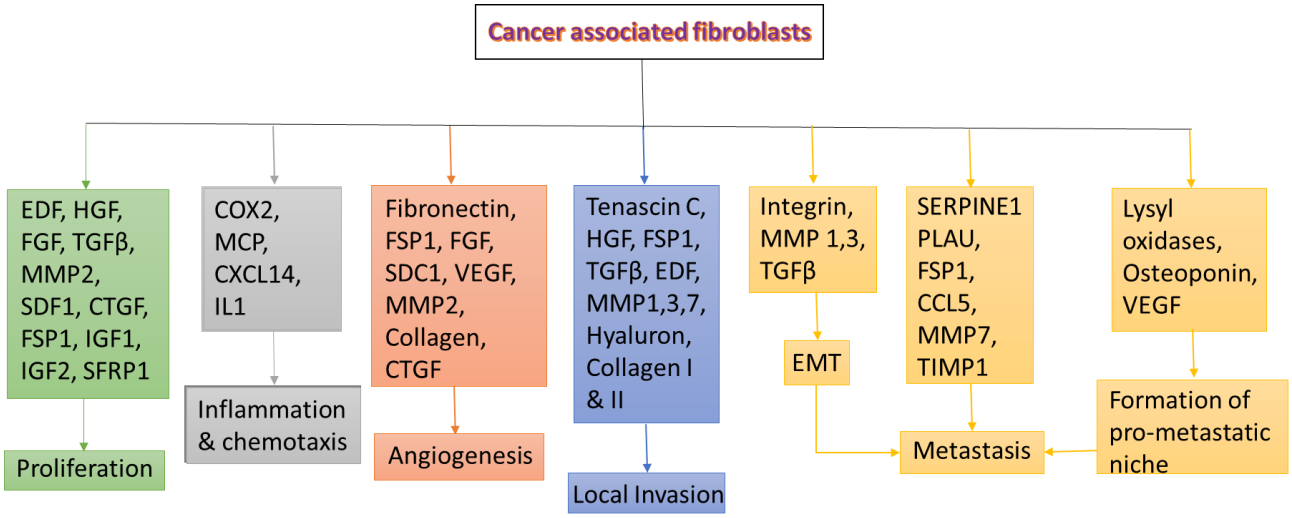

Figure 1.6: Gamut of factors secreted by CAFs and their effect on malignant cells and their environment. This diagram represents the multi-faceted roles that CAFs play in tumour proliferation, maintenance of inflammation and immune cell recruitment, angiogenesis, invasion and metastasis.

1.5.2 Tumour stimulatory effects of CAFs:

1.5.2.1 Cell proliferation – There is abundance of literature confirming cell proliferative effects of CAFs on cancer cells. Secretory factors from CD90, vimentin and α-SMA positive CAFs activated PI3k/Akt and MAPK/Erk pathways leading to proliferation; confirmed by phosophorylation of Akt and Erk, compared to secretory factors from normal fibroblasts (Subramaniam et al., 2013). Increased expression of TNF-α by CAFs activated EGFR, Akt, and Erk to again promote breast cancer cell proliferation (Gao et al., 2013). CAFs are known to secrete SDF-1, which was observed to facilitate lung cancer cell line proliferation and imparted chemoresistance against cisplatin via interaction with CXCR4 mediated activation of NFκB and Bcl-xL (Li et al., 2016a). Similarly, hepatocyte growth factor (HGF) secreted by CAFs promoted cell proliferation in both hepatocellular carcinoma and HNC (Jia et al., 2013, Kumar et al., 2015). CAFs were again seen to induce cell proliferation in oral tongue SCC, and HNSCC in pre-clinical models (Li et al., 2015, Wheeler et al., 2014). Keratinocyte growth

factor (KGF) secreted by CAFs induced proliferation in lingual carcinoma cell line (OSCC) (Lin et al., 2011), further providing evidence that CAFs promote tumour proliferation .

1.5.2.2 Migration and invasion – a major difference between benign tumours and malignant tumours is the potential to metastasise of the latter, which is also what makes them lethal and difficult to treat. CAFs produce and secrete a wide array of factors which stimulate dissociation of malignant cells from the primary tumour, invasion through tumour stroma and basement membrane which is made up of modified extracellular matrix (Cai et al., 2012, Matsumoto and Nakamura, 2006). Various studies demonstrated the ability of individual factors to stimulate tumour cell invasion; Matsumoto and Nakamura (Matsumoto and Nakamura, 2006); demonstrated that activation of c-Met by HGF leads to dissociation of malignant cells from the tumour due to production of metalloproteases and it also activates oncogenic pathways namely rat sarcoma, signal transducer and activator of transcription 3 (STAT3), and phosphatidylinositide 3-

kinase (PI3K) while Cai, *et al* 2012 (Cai et al., 2012) demonstrated the role of HGF in invasion of ovarian cancer cells into the omentum.

Glycoprotein stanniocalcin-1 (STC1) is a secreted, hypoxia regulated protein that was found to activate PDGF receptors expressed on CAFs to promote migration and invasion of colorectal cancer in matrigel *in vitro*; while *in vivo* STC-1 deficient mouse model reported reduced intravsation of colorectal cells, and fewer and smaller metastasis (Peña et al., 2013). Bone morphogenic protein 4 (BMP4) stimulation of fibroblasts leads to expression of pro-inflammatory factors (IL-6, CXCL1, CXCL12, CXCL16, CCL9, VEGF) and proteases (MMP2, MMP3), ECM components (versican, collagen, fibulin), and increased invasion of breast cancer cells in transwell setting by stimulation of both mouse fibroblast and human fibroblasts by BMP4, which inhibited using BMP4 receptor antagonist (Owens et al., 2013).

A disintegrin and metalloproteinase with thrombospondin motifs 1 (ADAMTS1) is known to degrade ECM components such as

aggrecan, versican, nidogen – 1 and 2, and decrease cell adheshion, promote cell migration and metastasis (Canals et al., 2006, Kuno et al., 2000, Rocks et al., 2008, Sandy et al., 2001). When breast cancer cells were co-cultured with normal human fibroblasts for 4 days, showed an increase in ADAMTS1 secretion, and the same was confirmed in patients by finding a correlation between lymph node metastasis and ADAMTS1 mRNA expression in patient CAFs (Tyan et al., 2012).

Plenty of evidence exists in HNC confirming the role of CAFs in cancer metastasis. Often MMP2/9 are secreted by CAFs in HNC which facilitate ECM modulation and promote cell motility and invasion (Koontongkaew et al., 2012). IL-33, HGF, FGF8b, SDF-1, and Activin secreted by CAFs have been implicated in HNC metastasis (Chen et al., 2013, Kumar et al., 2015, Lewis et al., 2004, Lui et al., 2011, Li et al., 2016b, Taylor et al., 2015). Endothelin-1 (ET-1) has shown to activate ADAM-17 mediated release of EGFR ligands from mouse embryonic fibroblasts (Blobel, 2005). With this in mind,

Hinsley *et al* confirmed that ET-1 enhanced migration of squamous cell carcinoma, SCC4 and H357 (HNC cell lines) in presence of oral fibroblasts, which abolished upon blocking ET-1 receptor, ET_AR and ET_BR, as well as by blocking ADAM, or using EGFR antagonist (Hinsley et al., 2012). Chemerin, secreted by CAF increased the expression and activity of MMP1/2/3 encouraging metastasis of squamous oesophageal cancer cells (Kumar et al., 2016).

1.5.2.3 Epithelial to mesenchymal transtition (EMT) – occurs when the cell loses its polarity, ability to adhere to neighbouring cells, and de-differentiates into a more primitive cell type or becomes multi-potent/stem cell like. This provides the cell potential to migrate, a signature feature of cancer dictating its aggressiveness. Giannoni *et al* (Giannoni et al., 2010) reported CAFs from prostate cancer stroma were responsible for EMT in the respective cancer cells due to low-level secretion of IL-6 and high level secretions of MMP-2 and MMP-9. Tsuyada *et al*, 2012 (Tsuyada et al., 2012a) showed that CCL2 produced and secreted by CAFs in breast cancer stroma enhanced

cancer stem cell production. Another study showed that CAFs increased the migration ability of ovarian cancer cells by increasing expression of enhancer of zeste homologue which has been implicated in promoting tumorigenesis (Xu, 2014). In one particular study, co-culture of CAFs and SCC9 cells (HNC cancer cell line) upregulated EMT markers like vimentin and fibronectin, while down-regulating E-cadherin (Zhou et al., 2014). It was observed that oral tongue squamous cell carcinoma cells in close proximity of CAFs have down-regulated E-cadherin, and the ECM around contained Cadherin-11, syndecan-1, SPARC, and FSP-1, further supporting EMT (Vered et al., 2010). Fibroblast growth factor 1 (FGF1) secreted by CAFs induced EMT in tongue squamous cell carcinoma via the FGFR with reduction in E-cadherin and increase in expression of vimentin (Jiao et al., 2015). Exposure to conditioned medium from irradiated fibroblasts induced expression of vimentin and loss of E-cadherin in esophageal squamous cell carcinoma (ESCC) suggesting ESCC cells having undergone EMT (Bao et al., 2015).

1.6 Types of cancer associated fibroblasts

As mentioned previously, the sources of CAFs vary, also depending on the type of tumour; different sub-populations of CAFs must exist within the tumour milieu. However, due to lack of CAF specific markers it has so far been a challenge to distinguish between the heterogeneous populations. Although CAFs can be distinguished from their normal counterparts based on markers such as: α-smooth muscle actin (α-SMA), FSP-1, fibroblast-activated protein (FAP), NG2 chondroitin sulphate proteoglycan (NG2), platelet-derived growth factor receptor α (PDGFR α), or podoplanin (Calon et al., 2014), there remains much to learn about different CAF phenotypes present in tumours.

1.6.1 Myofibroblasts

The most common type of activated fibroblast found is the myofibroblast expressing α-SMA as a significant and primary marker. Cancer associated myofibroblasts are similar to the activated fibroblasts/myofibroblasts associated with wound healing and fibrosis (Zigrino et al., 2005). The most common and prominent factor facilitating fibroblast activation is TGF-β, which

is found abundantly in the tumour stroma; produced by tumour cells themselves, and by other immune like macrophages and dendritic cells (Kellermann et al., 2008, Calon et al., 2014, Evans et al., 2003a).

Another type of CAF was reported by Gionnani *et al* in 2010, which was activated by IL-6, without expression of α-SMA but identified by expression of FAP and secretion of extra-cellular matrix. These CAFs, through secreted factors induced EMT markers confirmed by up-regulation of Snail, Twist, vimentin, and Met, while down-regulating E-cadherin, and up-regulated invasiveness by secreting MMP2 and MMP9 (Giannoni et al., 2010).

1.6.2 Senescent fibroblasts

Cellular senescence presents itself in response to DNA damage due to physical or chemical insults acquired during therapeutic interventions (chemotherapy or radiation therapy), or endogenous processes like mitogenic signals or oxidative stress and prevent the damage from being passed onto the next generation of cells and arrest malignant transformation. Some cells, however, especially fibroblasts, develop a senescence associated secretory

phenotype or SASP which allows them to secrete a wide range of proteases, growth factors, cytokines and chemokines, and insoluble ECM components (Freund et al., 2010, Hassona et al., 2013b). Since these cells are metabolically active; they persistently secrete molecules able to alter their surrounding microenvironment to one that is beneficial to tumours and allows them to progress and metastasise (Parkinson et al., 2016).

Senescent fibroblasts have been observed in several carcinomas; often recognised by the expression of α-SMA and staining positively in senescence associate β-galactosidase assay, along with an upregulation of p16 and p21 (Kabir et al., 2016, Mellone et al., 2017). They promote increased cancer cell proliferation in melanoma, breast cancer, prostate cancer with secretions of connective tissue growth factor (CTGF), SDF-1α, GRO-α, and IL-8 (Coppé et al., 2010a). The SASP of fibroblasts also enhances angiogenesis and immune-suppression by secreting VEGF, and granulocyte macrophage – colony stimulating factor (GM-CSF), IL-6 stimulating endothelial cells and myeloid suppressor cells respectively (Coppé et al., 2010a, Kabir et al., 2016).

SASP of the fibroblasts also stimulates cell migration and invasion through HGF, and MMP-2 (Hassona et al., 2014, Coppé et al., 2010b).

Senescent fibroblasts are also known to secrete high levels of chemokines and cytokines to attract and activate various immune cells to the tumour microenvironment: CCL-2, 8, 13 attracting primarily monocytes, NK cells, dendritic cells, T cells, stem cells, and macrophage inflammatory protein (MIP) – 3α and 1α recruiting lymphocytes, while attracting granulocytes causing neutrophilic inflammation and inducing fibroblasts to further secrete IL-1, IL-6 and TNF- α (Baba et al., 1997, Davalos et al., 2010a, Irving et al., 1990, Ohgo et al., 2015). Sica, *et al* 2006 (Sica et al., 2006b) described that tumour associated macrophages are recruited, activated and polarised (distinctly towards M2 phenotype) in the tumour site where the chemokines (CCL2) and other factors such as M-CSF, IL-4, are found to be secreted by senescent fibroblasts, giving rise to the possibility of senescent fibroblasts recruiting and polarising macrophages (Davalos et al., 2010a, Irving et al., 1990). This gamut of immune and stromal cells maintain inflammation, help in immune

evasion, and down-regulate the immune reaction allowing tumour cells to thrive. Senescent fibroblasts undergo catabolic metabolism due oxidative stress and coupled with anabolic cancer cells providing a nutrient rich environment for them via secretions of ketone bodies, lactate, glutamine, fatty acids, and other amino acids (Martinez-Outschoorn et al., 2014).

A notable observation made by Hassona *et al* is that senescent fibroblasts were genetically stable in the stroma of genetically unstable oral squamous cell carcinoma, which makes them a better and more reliable target for prognostic and therapeutic purpose as they lack the potential to develop resistance towards therapies through genetic mutations (Hassona et al., 2013b). They also observed that senescent fibroblasts are first activated to a myofibroblastic phenotype before reaching senescence (Hassona et al., 2013b). Another study observed similar phenomenon where activated fibroblasts or myofibroblasts from oral submucous fibrosis senesced due to oxidative damage to the DNA caused by ROS, possibly resulting from damaged mitochondria in presence of areca nut or tobacco chewing (Pitiyage

et al., 2011). Krizhanovsky *et al* revealed that hepatic stellate cells (myofibroblasts) senesce to resolve fibrosis in the liver by NK cells, however the mechanism causing senescence is yet to be determined; mice were treated with fibrosis inducing chemical, CCl_4, confirmed by positive immunochistochemistry (IHC) staining of fibrotic tissue with desmin and α-SMA, and senescence confirmed by positive IHC staining for senescence associated β-galactosidase assay, p16, p21 and p53 (Krizhanovsky et al., 2008a). In the same study, senescent hepatic stellate cells also showed up-regulated MICA, and ULBP2, which are activation ligands for NK cell receptor NKGD2 (Krizhanovsky et al., 2008b, Sagiv et al., 2016). Similarly, a study showed cysteine-rich angiogenic protein 61; a matricellular protein induced senescence in wound healing fibroblasts limiting fibrosis in cutaneous wound healing (Jun and Lau, 2010). All of these studies suggest that myofibroblasts could be senesced and this phenomenon could be targeted to gain control over the cross talk occurring between these fibroblasts and immune cells preventing the recruitment of the latter and checking inflammation, tumour progression and metastasis.

With review of literature providing evidence that CAFs, produce pro-inflammatory factors including chemoattractants, and that the presence of macrophages in tumours impacts prognosis of HNC, the following study was conducted to examine recruitment of macrophages by CAFs.

1.7 Main hypothesis and aims

With evidence present in literature that different sub-populations of CAFs (myofibroblasts and senescent fibroblasts) exist, and produce pro-inflammatory factors capable of recruiting macrophages, presence of which leads to poor prognosis in HNC, it was hypothesised that the two sub-populations of CAFs, namely myofibroblasts and senescent fibroblasts possess different capacities to recruit macrophages in HNC.

The aims of the study are:

- To establish previously described phenotypical characteristics of myofibroblasts and senescent fibroblasts in normal oral fibroblasts.
- Examine differential macrophage recruitment capabilities by both phenotypes and by patient derived CAFs.

- To confirm that the primary chemokine/receptor used by monocytes for migration is the CCL2/CCR2 axis.
- To characterise and differentiate between the secretomes of myofibroblasts, senescent fibroblasts, and a patient CAF.
- Investigate the effects of factors secreted by these phenotypes on macrophage polarisation.
- To examine correlation between presence of CAFs and macrophages in tumour sections.
- To study the effect of macrophage polarisation on fibroblast activation via secretory factors.

Chapter 2.

2. Materials and methods

2.1. Equipments:

All the laboratory equipment used in the project is listed in appendix 1.

2.2. Buffers and solutions:

Buffers and solutions prepared in-house are listed with their ingredients in appendix 2.

2.3. Primers:

Both SYBR green primers (table 1) used with SYBR green master mix (Thermo Fisher, UK) and Taqman primers/probes (table 2) used with Taqman Universal master mix II (Thermo Fisher, UK) were used in this research project.

Table 1: SYBR green primers:

Gene	Forward primer	Reverse primer

U6	5’CTCGCTTCGGCAGCACA3’	5′ AACGCTTCACGAATTTGCGT 3’
CCL2	5’AATAACGCGAGCTATAGAAGAA3’	5’TTATTGTCAGCACAGATCTCCTT3’
IL-6	5’AATAAAACAACCTGAACCTTCCA3’	5’TTATTGATTTTCACCAGGCAAGT3’
α-SMA	5’GAAGAAGAGGACAGCACTG3’	5’TCCCATTCCCACCATCAA3’
CD86	5’CCTTTCTCTATAGGAACCAAC3’	5’GGCTTCATCAGATCTTTCAG3’
CD206	5’AAATTTGAGGGCAGTGAAAG3’	5’GGATTTGGAGTTTATCTGGTAG3’

Table 2: Taqman primers/probes:

Gene	Refseq	Assay ID
CD80	NM_005191.3	Hs00175478_m1
CD163	NM_004244.5, NM_203416.3	Hs00174705_m1
β2-Microglobulin	NM_004048.2	Hs00187842_m1

2.4. Antibodies, small molecule antagonist, and recombinant proteins:

Mouse monoclonal anti α-smooth muscle actin antibody (A2547), horseradish peroxidase-conjugated rabbit anti-mouse IgG (whole molecule)(A9044), and FITC-conjugated mouse anti-α-smooth muscle actin monoclonal antibody (F3777) were obtained from Sigma, UK. Recombinant TGF-β1 (240-B), CCL2 (279-MC), and mouse anti-CCR2 monoclonal PE conjugated antibody (FAB151P) and mouse IgG_{2B} PE isotype control (IC0041P) antibody were from R & D Systems, UK. Mouse monoclonal anti-CD68 antibody (M0814, clone KP1) was from Dako, UK. CCR2 antagonist RS 504393 (ab120813) was from Abcam, UK.

2.5. Isolation of primary normal oral fibroblasts:

Buccal or gingival tissue was obtained from subjects during routine (not malignancy excisions) dental procedures with written, informed consent (ethical approval number Ref: 07/H1309/105). Biopsies of 5-10 mm^3 were collected in sterile tubes of DMEM (Sigma, UK) supplemented with 0.625 µg/ml of amphotericin B, 100 µg/ml of streptomycin, 100 IU/ml of penicillin (all from Sigma, UK) and stored a 4°C.

Primary normal oral fibroblasts (NOF) were then isolated from the connective tissue of the biopsy by mincing it using a surgical scalpel and incubating the tissue in 10 ml

of 0.25% (w/v) collagenase 1A (Thermo Fisher, UK) dissolved in DMEM at 37°C with 5% CO_2 in a humidified incubator for a minimum of 3 h. The tissue was then centrifuged at 384 *g* for 10 min and the cellular pellet was re-suspended in DMEM and supplemented with 10% foetal calf serum (FCS) (Thermo Fisher, UK), 1% amphotericin B and 1% penicillin and streptomycin and seeded in T25 flasks with a vented lids in the same medium, usually reaching confluence at 1.2 x 10^6 cells.

2.6. Cell culture:

Primary NOFs, cancer associated fibroblasts (CAF002, BICR18, BICR69, BICR73, BICR78) and H357 cells - human oral squamous cell carcinoma-derived cell line derived from the tongue (ECACC 06092004) (Sigma, UK) - were cultured in DMEM with 10% (v/v) FCS and 2 mM L-glutamine.

The monocytic cell line; THP-1 derived from peripheral blood of a patient with acute monocytic leukaemia (ECACC 88081201) (Sigma, UK) was cultured in RPMI 1640 (Sigma, UK) supplemented with 5% 100 IU/ml penicillin-streptomycin and 10% (v/v) FCS. The tongue-derived squamous cell carcinoma cell line SCC4 (ECACC 89062002) (Sigma, uk) was cultured in F12 nutrient medium and DMEM (1:1 v/v)

with 10% FCS and 2mM L-glutamine (Sigma, UK). Human monocyte-derived macrophages (refer to section 2.8) were cultured in IMDM (Thermo Fisher, UK) with 2% (v/v) human serum (Thermo Fisher, UK), and 5% (v/v) 100 IU/ml penicillin-streptomycin.

All cell cultures were incubated at 37°C, 100% humidity and 5% CO_2, and routinely tested for mycoplasma infection every 3-4 months.

Table 3: Details of cell type used:

Cell type:	Details:
NOF	Normal oral fibroblast from patients 316, 320, and 343
H357	Squamous cell carcinoma cell line derived from the tongue of a 74 year old male patient, stage I, node negative, with mutant p53, produces high levels of TGF-β1, and undergoes EMT in response to it TGF-β1.
SCC4	Squamous cell carcinoma derived cell line from the tongue of a 55 year old male patient. SCC4 forms colonies in semi-solid medium.
THP-1	Derived from peripheral blood of 1 year old acute monocytic leukaemia patient. THP-1 cells have C3b and Fc receptors but lack surface and cytoplasmic immunoglobulins, produce lysosomes and are phagocytic. They can be differentiated in to macrophage like cells using DMSO.
PBM	Peripheral blood monocytes isolated from buffy coats using Ficoll density gradient method, purified further using monocyte isolation kit (Miltenyibiotec).

CAF002	Cancer associated fibroblasts from oral squamous cell (OSCC) carcinoma patient 002.
BICR18	Cancer associated fibroblasts from genetically unstable OSCC
BICR69	Cancer associated fibroblasts from genetically stable OSCC
BICR73	Cancer associated fibroblasts from genetically stable OSCC
BICR78	Cancer associated fibroblasts from genetically unstable OSCC

2.7. Cell harvesting and passaging:

All fibroblasts, H357 cells, and SCC4 cells were treated with trypsin/EDTA (Sigma, UK) at 80% confluency (5 min for fibroblasts, 15 min for cell lines) at 37°C. The sides of the flask were then struck firmly to physically dislodge cells from the plastic surface. Trypsin was neutralised using DMEM with 10% (v/v) FCS in a 1:3 ratio and centrifuged at 192 *g* for 5 min to form a cell pellet. The supernatant was discarded, the cell pellet re-suspended in appropriate medium for each cell line and seeded at 3 x 10^5 cells in T75 or 5 x 10^5 in T175 tissue culture flasks. Primary oral fibroblasts were not used beyond passage 8, BICRs and CAF002 were not used beyond passage 5, monocytes were used the same day of purification, while macrophages were always used at passage 1.

THP-1 cells were centrifuged at 192 *g* for 5 min and seeded at 1:5 ratio in RPMI medium with 100 IU/ml penicillin-streptomycin and 10% FCS.

2.8. Monocyte isolation and macrophage culture:

Monocytes were isolated from buffy coats from the NHS Blood and Transplant Service (ethical approval reference SMBRER139) using a Ficoll-density gradient in which Hank's buffered salt solution (HBSS) (Thermo Fisher, UK) and blood was mixed (1:1; 30 ml), layered carefully onto 20 ml Ficoll (GE healthcare, UK), and centrifuged at 270 *g* for 40 min with brakes off. The mononuclear cell layer containing monocytes and lymphocytes was visible as a distinct white layer between the upper serum layer and lower Ficoll layer, which was removed using a sterile Pasteur pipette and transferred to a fresh tube. The mononuclear cells were washed by making up to 50 ml with HBSS and centrifuged again for 15 min at 270 *g* with rotor braking on. The supernatant was discarded, the pellet was re-suspended in 50 ml of HBSS, and centrifuged again for 10 min. Cells were re-suspended in HBSS, counted, and washed again for a further 10 min (Eligini et al., 2013, Martinez et al., 2006, Chitra et al.,

2014). Supernatant was discarded, and the cell pellet was used to purify monocytes further for migration assays (section 2.8.1) or re-suspended in IMDM medium with 2% (v/v) human serum, and 5% (v/v) 100 IU/ml penicillin-streptomycin, and either cultured in T75 flasks at $3x10^7$ in 10 ml seeding density for monocyte to macrophage differentiation. Cells were washed twice with PBS following 3 h incubation to remove non-adherent lymphocytes, and fresh medium was added, followed by washes and medium changes every 3 days for a week in total.

2.8.1. Monocyte purification:

Monocytes were purified from lymphocytes using a Pan Monocyte Isolation kit (Miltenyi Biotech, USA) containing antibodies specific for lymphocyte populations to negatively select monocytes; allowing them to pass through a MACs magnetic separation column. Mononuclear cell number was determined, and the reagents from Pan Monocyte Isolation kit were added per 10^7 total cells. Cell pellet from section 2.8 was re-suspended in 30 µl of MACs buffer (appendix 2) followed by addition of 10 µl each of FcR blocking reagent and

Biotin-Antibody cocktail from the kit. The contents of the tube were mixed and incubated at 2-8°C for 5 min. Another 30 µl of MACs buffer was added, followed by 20 µl of anti-biotin Microbeads (included in the kit) which are magnetic, the contents were mixed again and incubated at 2-8°C for 10 min.

Subsequently, a MACs separation column (LS column, Miltenyi Biotech, USA) was placed in a magnetic separator (VarioMACS Separator, Miltenyi Biotech, USA), rinsed with 3 ml MACs buffer, and the cell suspension prepared previously was allowed to run through the column and cells collected after separation. The flow through contained negatively selected monocytes while the lymphocytes were magnetically attached to the column. The column was then washed 3 times with 3 ml MACs buffer to collect any further monocytes sticking within the column, and the resulting purified monocytes were then used for migration assays only. The purity of resulting monocyte culture, tested by flow cytometry for CD14 reported 91.9% pure (fig. 4.4 in section 4.5).

2.8.2. Macrophage polarisation:

From M0 macrophage culture described in section 2.8, the cells were polarised towards 2 states – M1, or M2 using the following methods (Mia et al., 2014, Zhang et al., 2013):

M1 polarisation: Mononuclear cells were seeded and washed as described for M0 macrophages in section 2.8 but with addition of 10 ng/ml granulocyte macrophage colony stimulating factor (GM-CSF) (Peprotech, UK) in the medium. On the 6th day 100 ng/ml lipopolysaccharide ((LPS) *Escherichia coli* O55:B5) (Peprotech, UK), and 20 ng/ml interferon γ (IFNγ) (Peprotech, UK) were added to the medium in addition to 10 ng/ml GM-CSF for 24 h (Zhang et al., 2013).

M2 polarisation: Mononuclear cells were seeded and washed as described for M0 macrophages in section 2.8 but with addition of macrophage colony stimulating factor (M-CSF – 25 ng/ml) (Peprotech, UK) in the medium. On the 6th day 20 ng/ml interleukin 10 (IL-10) (Peprotech, UK) was added to the medium in addition to 25 ng/ml M-CSF for 24 h (Mia et al., 2014).

2.9. Myofibroblast transdifferentiation:

Normal oral fibroblasts from 3 different patients (anonymously coded NOF343, NOF316, NOF320) were cultured in DMEM supplemented with 2mM L-glutamine and 10% (v/v) FCS. At 80-90% confluency cells were trypsinised and 2.5 x 10^5 cells were seeded in 6 well plates in triplicates or 10^6 cells in T75 flask overnight. Cells were serum starved for 24 h prior to treatment with TGF-β1 (R & D Systems, UK).

TGF-β1 (5 ng/ml) made up in serum-free DMEM was added to the wells/flasks and serum-free DMEM was added to the control wells/flasks (Melling, 2015). Cells were exposed to TGF-β1 for 24, 48 and 96 h. After each time point, medium containing TGF-β1 was removed and cells were washed with PBS before 1 ml of serum-free DMEM was added to the culture wells or 5 ml to T75 flask, and collected 24 h later as conditioned medium. Cells were then trypsinised using trypsin/EDTA and harvested in 0.1% (w/v) bovine serum albumin (BSA) (Sigma, UK) in DMEM and used for protein or RNA analyses, as described in sections 2.13 and 2.17.

2.10. Induction of senescence:

Senescence was induced in NOF by treating with cisplatin at a concentration of 10 μM in DMEM for 24 h, followed by culturing in normal DMEM for 14 days (Kabir et al., 2016). Senescence was detected by β-galactosidase detection kit (Abcam, UK) which detects activity of lysosomal β-galactosidase by cleaving X-gal at pH 6, resulting in generation of a blue precipitate, visible by light microscopy. For this assay, cells were trypsinised and re-seeded in a 12 well plate at a concentration of 10,000 cells per well for 24 h. After one wash with PBS, 500 μl of 'Fixative solution' from the kit was added and incubated at room temperature for 20 min. Cells were then washed with PBS twice and 500 μl of staining solution was added to each well. The staining solution was made by adding 25 μl of X-gal (20 mg/ml in dimethyl formamide) to 470 μl of 'Staining solution' and 5 μl of 'Staining supplement', all of which were provided in the kit. The plate was covered in aluminium foil and incubated overnight at 37°C. Photographs were taken at 10 x and 20 x magnification using Nikon Eclipse TS100 microscope. Positively stained cells were counted manually to calculate percentage of positive cells from total number present.

2.11. Preparation of conditioned medium:

Fibroblasts, H357 and SCC4 cells (both OSCC-derived cancer cell lines), and macrophages were washed twice with PBS after the respective treatment and incubated with serum-free DMEM or F12 with DMEM or IMDM for 24 h at 37°C, and 5% CO_2. The conditioned media was collected, passed through 0.22 micron filter (Milipore, UK) and stored at -80°C to be used in migration assays (section 2.12), ELISAs (section 2.20), concentrated for Mass Spectrometry (section 2.22).

2.12. Migration assay:

Monocytic cell line, THP-1 cells were cultured in RPMI with 10% (v/v) FCS and penicillin-streptomycin and allowed to reach 80-90% confluency in preparation for the assay. Cells were then serum starved for 24 h prior to experimentation. Cells were re-suspended in RPMI with 0.1% BSA, and centrifuged at 192 *g* for 5 min to form a pellet. Both THP1 cells and peripheral blood monocytes (after purification described in section 2.81) were counted to obtain 100,000 cells and re-suspended in 200 µl serum-free RPMI, and added to the top chamber of a transwell (Corning, USA) with pore size of 5 µm in a 24 well plate. Conditioned medium (500 µl) was added to the bottom chamber/well of the plate. Serum-free RPMI was used as

negative control and CCL2 (10 ng/ml) (R&D Systems, UK) in RPMI was used as positive control (figure 4.1, section 4.3).

The cells were allowed to migrate at 37°C and 5% CO_2 for 4 h. After incubation, the transwells were moved to a new plate while the conditioned media was gently pipetted to disperse cells evenly in the conditioned media. Cells were counted from 3 randomly selected fields at 20 x magnification using light microscopy.

Remaining cell suspension was removed from the transwells and the upper side of the porous membrane was swabbed with a cotton bud to remove non-migrated cells. PBS (500 µl) was added to upper and lower chamber of the transwell to wash the membrane, followed by addition of cold methanol (Sigma, UK) to fix cells on the lower face of transwell membrane overnight in the fridge.

Methanol was removed and the transwell membrane was washed with PBS, followed by staining of cells using Differential Quik Staining kit according to manufacturer's protocol (Polysciences, UK) and photographs were taken of 3 randomly selected fields at 20 x magnification using Nikon Eclipse TS100 microscope. The cells were counted manually using ImageJ. Relative number of cells migrated was calculated

by averaging counts from 3 random fields of the same well, while absolute number was calculated by normalising to fibroblast

2.12.1. CCR2 inhibition:

To inhibit the CCR2 receptor before migration, peripheral blood monocytes were incubated with 10 μM CCR2 inhibitor in serum free RPMI for 1 h (Carmo et al., 2014). The cells were then centrifuged to form a pellet and re-suspended in fresh serum-free RPMI for migration assay.

2.12.2. Pertussis toxin treatment:

Peripheral blood monocytes were treated with Pertussis toxin (1 μg/ml in serum free RPMI) to inhibit G-protein coupled receptors, which include chemokine receptors, for 30 min prior to migration (Malik et al., 2009).

2.13. Protein extraction:

Cell lysis buffer (radioimmunoprecipitation assay (RIPA) buffer) (Sigma, UK) with Halt Protease and Phosphatase Inhibitor cocktail (1:100) (Thermo Fisher) was added to each well (60 μl) in a 6 well plate to lyse the cells. Cell extracts were kept on ice for 15 min to allow complete cell lysis with minimum effect of proteases. Cells were

scraped and the extract was then centrifuged at 4°C at 8000 *g* for 15 min to separate protein from cell debris, followed by transfer of supernatant containing protein into a new 1.5 ml Eppendorf and stored at -20°C for a maximum of one week before use in western blot (section 2.15).

2.14. Protein concentration:

Protein concentrations were determined by Pierce bicinchoninic acid (BCA) assay (Thermo Fisher, UK) and BSA of known concentrations were used as standards. BCA assay involves reduction of cupric ion (Cu^{2+}) to cuprous ion (Cu^{+}) in an alkaline medium, followed by chelation of 2 molecules of bicinchoninic acid with one cuprous ion; resulting in a purple reaction complex which exhibits strong absorbance at 562 nm wavelength, almost linear with increasing protein concentration in the range of 20-2000 µg/ml. The absorbance was read using BMG POLARstar Galaxy microplate reader at 562 nm, and concentration of protein was determined by interpolating a known standard curve.

2.15. Western blot:

Protein samples (5 µg; from fibroblast lysate) were denatured by addition of 5x Laemmli buffer (appendix 2), vortexed, and heated at 95°C for 5 min. SDS denatures proteins and gives them a negative charge so that they can be separated based on molecular weight rather than charge, while β-mercaptoenthanol reduces disulphide bonds within the protein structure. Glycerol increases the density of the samples so that they settle to the bottom of wells, while bromophenol blue acts as a colouring agent to track movement of samples through the gel. The samples were vortexed again after heating, and a protein ladder (5 µl) (EZ-Run, Fisher) and the samples were loaded into 1.5 mm wells of NuPAGE 3-8% Tris-Acetate gel submerged in running buffer and electrophoresed at 150 V for 1 h followed by 100 V until the dye front reached the end of the gel.

iBlot Dry Blotting System (Invitrogen) was used to transfer proteins from the gel to polyvinylidene fluoride (PVDF) membrane. Success of transfer was observed by soaking the PVDF membrane in Ponceau Red (Sigma, UK) diluted 1:10 in TBS-Tween for 5 min on a rocker and protein bands were observed.

To prevent non-specific binding, the membrane was blocked in 5% (w/v) skimmed milk and 3% (w/v) BSA in TBS (appendix 2) for an hour prior to incubation with primary α-SMA antibody (diluted 1:1000 in 5% skimmed milk and 3% BSA in TBS) for 1 h on a rocker at room temperature. The membrane was washed thrice with TBS-tween and incubated with secondary anti-mouse IgG horseradish peroxidase linked antibody, diluted 1:4000 in 5% skimmed milk and 3% BSA and TBS, for 30 min at room temperature on a rocker. Following two washes with TBS-tween and once with TBS, antibody binding was visualised using the Pierce ECL substrate and autoradiography film (GE Healthcare, UK) developed in a Compact X4 (Xograph healthcare, UK). α-SMA expression was quantified relative to GAPDH (primary antibody – 1:7500, secondary antibody – 1:5000) after stripping the blot with stripping reagent for 1 h on the rocker and reprobing with the anti-GAPDH antibody using the same protocol as described for α-SMA.

Densitometry was carried out using Image J software and band density normalised to GAPDH signals from the same sample.

2.16. Immunocytochemistry:

Normal oral fibroblasts were seeded on coverslips in a 6 well plate for attachment overnight at 37°C and 5% CO_2 in an incubator. The cells were serum starved the next day for 24 h, followed by treatment with 5 ng/ml TGF-β1 for 24 h, 48 h, and 96 h time points with their respective controls cultured in serum-free DMEM.

Upon completion of treatment, the cells were washed twice with PBS for 5 min, and fixed in 100% methanol for 20 min at room temperature. The fixative was removed, and the cells were washed again with PBS for 5 min. The cells were then incubated with 0.5 ml of 4 mM sodium deoxycholate (Sigma, UK) for 10 min. After washing with PBS for 5 min, the non-specific binding sites were blocked with 2.5% BSA in PBS for 30 min. Followed by incubation with 100 µl FITC labelled α-SMA antibody diluted 1:100 in the blocking medium for 1 h at room temperature protected from light. The primary antibody was aspirated, cells were washed twice with PBS for 10 min, and the coverslips were mounted on glass slides using mounting medium containing Dapi (Vector Labs, UK). Images were taken at 20 x magnification using Zeiss Axioplan 2 Imaging microscope.

To quantify fluorescence, ImageJ software was used where the image was converted to grey scale, and corrected total cell fluorescence (CTCF) was calculated using the following formula:

CTCF=Integrated density-(Area of selected cell x mean fluorescence of background readings)

2.17. RNA extraction:

Total RNA was extracted from cell pellets (centrifuged at 438 *g* for 3 min in 0.1% (w/v) BSA) using ISOLATE II RNA mini kit (Bioline, UK) according to manufacturer's protocol, and all buffers are provided in the kit. In brief, for every 5 x 10^6 cells 3.5 µl of β-mercaptoethanol and 350 µl of lysis buffer was added and vortexed vigorously to lyse and homogenise cells. The lysis buffer contains guanidinium thiocynate that immediately deactivates endogenous RNase ensuring purification of intact RNA. The lysate was loaded on to ISOLATE II filter (violet) with their collection tubes, and centrifuged for 1 min at 11,000 *g* to reduce viscosity and clear the lysate. The filters were discarded and 350 µl of 70% ethanol was added to the homogenised lysate, mixed, and loaded on to ISOLATE II RNA mini column (blue). The columns were centrifuged for 30 s at 11,000 *g* and placed in new collection tubes. The silica membrane in the column was desalted by adding 350 µl Membrane Desalting Buffer

and centrifuged for 1 min at 11,000 *g* to enhance DNase I activity. DNase I was diluted 1:10 in Reaction buffer for DNase, and 95 µl of the reaction mixture was applied directly on to the centre of the silica membrane, and incubated for 15 min at room temperature. The silica membrane was then washed with 200 µl of Wash buffer 1 by centrifuging at 11,000 *g* for 30 s. The silica membrane was then washed with 600 µl of Wash buffer 2 at 11,000 *g* for 30 s. Flow through was discarded and the third wash was done by adding 250 µl of Wash buffer 2 to the column and centrifuged at 11,000 *g* for 2 min, ensuring complete drying of the membrane. Elution of RNA was achieved by placing the columns in nuclease free tubes, adding 20 µl of RNase free water and centrifuging at 11,000 *g* for 1 min.

The concentration of extracted RNA was evaluated using a NanoDrop spectrophotometer.

2.18. Complementary DNA preparation:

RNA extracted as described in section 3.19 was used to prepare complimentary DNA (cDNA) for qPCR analysis using High Capacity cDNA Reverse Transcription kit (Thermo Fisher, UK). The following reagents were used for each 20 µl reaction:

Table 4: cDNA preparation reaction:

Component	Volume (µl) per reaction
10X RT Buffer	2.0
25X dNTP Mix (100mM)	0.8
10X RT Random Primers	2.0
MultiScribe Reverse Transcriptase	1.0
Nuclease free water	4.2
RNA	10.0
Total per reaction	**20.0**

The mix was then subjected to different temperatures in a thermal cycler with the following temperature and duration settings:

Table 5: cDNA thermal cycle settings:

Temperature (°C)	Duration (min)
25	10
37	120
85	5
4	∞

The resulting cDNA products were then stored at -20°C for no more than a week before being used for qPCR.

2.19. Quantitative PCR:

SYBR green dye incorporates into double stranded DNA, the resulting complex absorbs blue light (λ_{max} = 497 nm) and emits green light (λ_{max} = 520 nm). As PCR progresses new DNA amplicons are produced and SYBR green dye binds to them increasing fluorescence intensity proportional to the PCR products produced giving an estimate of expression of target gene.

RNU6-1 or U6 was chosen as the endogenous housekeeping gene for SYBR primers. U6 is a highly conserved small nuclear RNA which codes for a component of the spliceosome, and showed least CT cycle deviations (Kabir, 2015).

Taqman probes are composed of a fluorophore attached to the 5' end of an oligonucleotide probe, and a quencher (to quench fluorescence) at the 3' end. These probes anneal to a region of the cDNA, and as long as the probe is intact fluorescence from the excited fluorophore is quenched. However, as Taq polymerase extends the primers of interest, its exonuclease activity degrades the probe, allowing the fluorophore to fluoresce freely. This fluorescence passes through

the detection filters to give an estimate of amount RNA derived from the gene of interest.

Two qPCR systems (ABI 7900HT Fast Real-Time PCR system and Rotor Gene Q) were used to quantitatively detect IL-6, CCL2, α-SMA, CD80, CD86, CD163, and CD206 in the cDNA samples prepared as described in 3.19 with pre-designed SYBR Green and Taqman primers (table 1 & 2).

The reaction mix was prepared according to the manufacturer's instructions:

Table 6: qPCR preparation using SYBR green mix:

Ingredients	Volume (µl)
SYBR Green master mix	5
Forward primer	0.5
Reverse primer	0.5
cDNA	0.5
Nuclease free water	3.5
Total	10

Table 7: qPCR preparation using Taqman mix:

Ingredients	Volume (µl)
Taqman Universal PCR master mix	5
FAM-labelled Primer	0.5
VIC-labelled B2M	0.5
cDNA	0.5
Nuclease free water	3.5
Total	10

For ABI 7900HT Fast Real-Time PCR system, the reaction mix was prepared for triplicates of the endogenous control and target sample in a 96-well plate, which was then centrifuged for a minute at 1000 *g* and loaded onto the thermocycler. SDS 2.4 software was used to set up and run the thermal cycles necessary for qPCR.

For Rotor Gene Q, the reaction mix was prepared in triplicates in PCR tubes. The tubes were then loaded on to the system and following parameters were used for qPCR:

Table 8: qPCR thermal parameters

Temperature (°C)	Duration (s)	Cycle	Purpose
95	20	Hold	AmpliTaq® Fast DNA polymerase, UP activation
95	1	40	Denature
60	20	40	Anneal/Extend

Once the run was complete, RQ manager 1.2.1 software in ABI 7900HT Fast Real-Time PCR system, and Rotor-Gene Q software in the same system were used to extract and analyse raw qPCR data, which measured the cycle number when fluorescence crossed the detection threshold (C_T).

Triplicate C_T values were obtained and accepted only if there was a difference of <1 cycle within each other to ensure a small standard deviation. Target gene values

(ΔC_T) were normalized by calculating the difference between average target gene value and endogenous control gene value as follows:

$$\Delta C_T = C_{T\ endogenous} - C_{T\ target}$$

Relative expression of target gene to endogenous control was determined by the following expression and represented in a bar graph:

$$\text{Relative expression} = 2^{-\Delta\Delta CT}$$

Data are represented as relative to 24 h control as the data set contains a second 15 d control (untreated equivalent for 15 d cisplatin treatment), which when compared to 24 h control highlights changes occurring due to time in culture. Therefore, 24 h control is the least impacted control used for comparison.

2.20. ELISA:

Sandwich Enzyme Linked Immunosorbent Assay was used to detect levels of IL-6, and CCL2 (BD Biosciences, UK) in conditioned media. According to the manufacturer's protocol, the 96-well plate was first coated with 100 µl capture antibody (capture antibodies for both IL-6 and CCL2 diluted 1:250 in 0.1 M sodium carbonate, pH 9.5) and incubated at 4°C overnight; followed by washing three times

with wash buffer (0.05% (v/v) Tween-20 in PBS). Next, the wells were blocked with ≥200 µl assay diluent (PBS with 10% (v/v) FCS) for 1 h at room temperature. The diluent was aspirated and wells were washed as mentioned previously; followed by addition of 100 µl of each standard (from 300 pg/ml to 4.7 pg/ml diluted in assay diluent) and samples (diluted 1:20 in assay diluent) and sealed before incubation at room temperature for 2 h. Samples were aspirated and the wells were washed 5 times. Working detector solution (detection antibody diluted at 1:250 for IL-6, and 1:1000 for CCL2 in assay diluent, while streptavidin-HRP diluted at 1:250 for both in the same working detector solution) was added in volume of 100 µl per well, sealed and incubated at room temperature for 1 h. Working detector was aspirated and the wells washed 7 times, allowing the wells to soak in wash buffer for at least 30-60 s. Substrate solution (BD biosciences, UK) equal volumes of tetramethylbenzidine and hydrogen peroxide from the kit were mixed to make up the substrate solution) was added to each well (100 µl) and incubated in the dark at room temperature without sealing for 30 min. Stop solution (2 N H_2SO_4; 50 µl) was added to each well and the absorbance read at 450 nm and corrected at 570 nm.

2.21. Immunohistochemistry:

Immunohistochemical staining was performed on formalin fixed paraffin embedded tissue sections derived from OSCC patients (10) from Unit of Oral and Maxillofacial Pathology, School of Clinical Dentistry, University of Sheffield archive (year 2000) (ethical approval number: 07/H1309/150). Tissue sections were deparaffinised by immersing sections in xylene (Sigma, UK) twice for 5 min each, followed by immersion in 100% ethanol twice for 5 min each. To quench endogenous peroxidases, the sections were immersed in 3% (v/v) hydrogen peroxide (Thermo Fisher, UK) in methanol for 20 min to reduce background.

For antigen retrieval, the sections were microwaved for 8 min in 0.01 M sodium citrate pH 6, followed by cooling in the same buffer for 30 min. The sections were then blocked with horse serum for 30 min for α-SMA antibody, and 1 h for CD68 antibodies (Dako, UK).

The sections were incubated with primary antibodies diluted in the same serum (α-SMA – 1:200, CD68 – 1:400) overnight at 4°C, and were then washed twice with PBS for 5 min each the following day. Secondary antibody was prepared as 1 drop in

10 ml PBS with 3 drops of horse serum from Vectastain ABC kit (Vector Labs, UK) and incubated with sections for 30 min. ABC reagent from Vectastain kit was prepared 30 min before use as 2 drops of reagent A and B each in 5 ml PBS. The sections were washed twice in PBS before being incubated with ABC reagent for 30 min. Finally, for colour development, NovaRed kit (Vector Labs, UK) was used for α-SMA, and DAB (Vector Labs, UK) for CD68 for 5 mins, followed by a wash in double distilled water. Finally, the sections were counter-stained with haematoxylin and analysed using HistoQuest software.

Positive control for α-SMA (blood vessels in normal tissue) and CD68 (lymph node tissue infiltrated with macrophages confirmed by oral pathologist) stained tissue sections were used to set the threshold for presence or absence of cellular staining for each marker in Histoquest software. This threshold was then used by the software to detect presence or absence of stain in adjacent tumour sections (stained separately for either marker), and calculate a percentage of positively stained cells in region of interest (tumour mass, stroma, tumour invasive front).

2.22. Cytokine array

Human cytokine array C6 (Raybiotech) was used to detect the presence of other cytokines in conditioned media (CM) from 24 h TGF-β1 treated fibroblast, 15 d cisplatin treated fibroblast, and their controls. The membranes were blocked with Blocking Buffer (supplied with the kit) for 30 min at RT. After aspiration, the membranes were incubated with 1 ml CM overnight at 4°C. The CM was aspirated, and membranes were washed thrice with 2 ml of 1X Wash Buffer I (supplied with the kit) for 5 min each, and twice with 2 ml of 1X Wash Buffer II (kit) for 5 min each. The membranes were then incubated with 1 ml of prepared Biotinylated Antibody Cocktail for 2 h at RT. Membranes were washed again as described before. HRP-Streptavidin (1X) in 2 ml volume was added to the membranes, and incubated for 2 h at RT. After aspiration, the membranes were washed again. Detection Buffer C and D (kit) were mixed in 1:1 volumes, and 500 µl was pipetted onto each membrane for 2 min at RT. Autoradiography films were then exposed to the membranes for chemiluminescence and developed as described in section 2.15.

2.23. Concentration and purification of conditioned media:

Conditioned media from NOF, myofibroblasts, senescent fibroblasts, and patient CAF were concentrated, digested, and purified prior to mass spectrometry using the following method:

Protein concentration in the conditioned media was determined using BCA protein assay, following which conditioned media containing 100 µg protein was added to a LoBind microfuge tube containing 10 µl StrataClean resin beads (Agilent Technologies Ltd, UK) (B1). Samples were vortexed for 1 min, centrifuged at 2000 *g* for 2 min, and the supernatant was aspirated and transferred to a second tube (B2) containing 10 µl of resin beads.

The samples and resin in B2 were vortexed for 1 min, and transferred back to B1 with the resin from B2, before centrifuging and discarding the supernatant.

The beads were washed twice with 1 ml of 25 mM ammonium bicarbonate (here after termed as ambic). For on-bead digestion, the beads were re-suspended in 80 µl of 25 mM ambic and 5 µl of 1% (w/v) Rapigest (Waters Limited, UK) in 100 mM ambic. The samples were then heated at 80°C for 10 mins, and reduced by addition

of 5 µl of dithiothreitol (DTT; 9.2 mg/ml in 25 mM ambic), and heated at 60°C for 10 mins. Following cooling, 5 µl of iodoacetamide (33 mg/ml in 25 mM ambic) was added and the samples incubated at RT for 30 mins in the dark. Trypsin (Porcine trypsin, sequencing grade) (1µg) was added and the sample was incubated at 37°C overnight on a rotary mixer. The digests were acidified by the addition of 1 µl of trifluoracetic acid (TFA) and incubated at 37°C for 45 mins. Samples were then centrifuged at 17,000 *g* for 30 mins, and supernatants transferred to 0.5 ml LoBind tubes. The pre and post-acidification digest were analysed by SDS-PAGE to check for the absence of protein and hence complete digestion.

The digested peptides were purified to remove any impurities, and inorganic salts. The filtration column (SUM SS18V, Nest Group Inc., USA) was first conditioned with 200 µl of acetonitrile (ACN) (Sigma, UK), centrifuged at 100 *g* for 30 sec, and discarded. The columns were washed twice with 200 µl HPLC grade water (Sigma, UK). The samples were then added to the loading buffer (3% ACN, 97% H_2O, 0.1% TFA), and loaded on to the columns and centrifuged at 100 *g* for 1 min. The flow through was loaded again, centrifuged, and finally discarded.

The columns were then washed with salt removal buffer (3% ACN, 97% H_2O, 0.1% fluoric acid (FA)) 4 times. The bound protein was eluted in to LoBind microfuge tubes (Sigma, UK) using 200 µl of buffer (3% H_2O, 97% ACN, 0.1% FA) at 100 *g* for 2 min. The filtered samples were then run for QC before being processed for Label-free quantification in Q Exactive HF Orbitrap. Data generated was then analysed using MaxQuant and Perseus softwares.

2.24. Mass Spectrometry

Mass spectrometry procedure was carried out by Dr. Caroline Evans in Chemical and Bioengineering department of University of Sheffield. Mass spectrometry with label-free quantification method was used with the following settings: A 105 minute data dependent acquisition (DDA) method was set up on the QExactive HF. The full MS scan was from 375-1500 m/z was acquired in the Orbitrap at a resolution of 120,000 in profile mode. Subsequent fragmentation was Top 10 in the HCD cell, with detection of ions in the Orbitrap using centroid mode, resolution 30,000. The following MS method parameters were used: MS1, Automatic Gain Control (AGC) target 1e6 with a maximum injection time (IT) of 60 ms. MS2, Automatic Gain Control

(AGC) target 1e5, maximum injection time (IT) of 60 ms and isolation window 2 Da. The intensity threshold was 3.3e4, normalized collision energy 27, charge exclusion was set to unassigned, 1, exclude istopes was on, apex trigger deactivated. The peptide match setting was preferred with dynamic exclusion of 20 seconds.

Raw data obtained was analysed back in Dental School of University of Sheffield using softwares Maxquant and Perseus to generate a list of significantly expressed proteins in the CM analysed. Fold changes were calculated by comparing to secretion by 24 h.

2.25. Statistical analyses:

Graphpad Prism 7 software was used to generate plots and perform statistical analyses. Multiple ANOVAs were used to asses any significant differences between more than 2 conditions, i.e. different time points in TGF-β1 treated, and cisplatin treated, along with their respective controls. When only 2 conditions from the same cells were tested for significance, paired T test was used.

Chapter 3

3. Characterisation of myofibroblast and senescent fibroblast phenotypes in primary normal oral fibroblast

Myofibroblasts are the most studied form of 'activated' fibroblast; normally found at sites of tissue injury, contracting the wound bed and secreting ECM components to repair damaged or lost ECM. This amplified accumulation of collagenous ECM leads to contraction and, sometimes, scarring of the injured tissue (Hinz, 2016). When the repair process is successful and sufficient, myofibroblasts are eliminated via apoptosis, or possibly de-activated (Desmoulière et al., 2005, Yang et al., 2014). Fibroblasts undergo a two-step activation to achieve a myofibroblastic phenotype: (a) the fibroblasts first attain a migratory phenotype by developing contractile fibre bundles made of cytoplasmic actin, but produce smaller traction forces compared to fully activated and contractile myofibroblasts; this early differentiation is known as proto-myofibroblast (Hinz, 2007). b) With continuous remodelling activity in response to mechanical and chemical autocrine and paracrine signals they undergo further differentiation into fully activated myofibroblasts with de novo expression of α-smooth muscle actin (αSMA). This is mainly regulated by the actions of the growth factor

TGF-β1, the ECM protein fibronectin-EDA, and the surrounding mechanical microenvironment (Tomasek et al., 2002). Upon activation myofibroblasts exhibit increased proliferation, migratory ability, production of ECM components and cytokines (Powell, 2000). Myofibroblasts are implicated in most cancers like gastric cancer, colon cancer, colorectal cancer, pancreatic cancer, liver cancer, bladder cancer, and head and neck cancer to promote cancer progression and metastasis via cell proliferation and survival, angiogenesis, immune cell recruitment, ECM re-modelling and cell invasion (Mehner and Radisky, 2013, Serini et al., 1998, Radisky et al., 2007a, Hinz, 2007, Darby et al., 2016, Tomasek et al., 2002, Toullec et al., 2010, Otranto et al., 2012, Evans et al., 2003b, Desmoulière et al., 2005). However, it is becoming increasingly clear that these cancer-associated fibroblasts are not simply myofibroblasts, despite sharing phenotypic similarities, but instead represent a heterogeneous range of fibroblast phenotypes, such as senescence.

Senescence, a state of permanent growth arrest, is induced in cells in response to persistent DNA damage due to smoking/chewing tobacco, anti-cancer treatment such as chemotherapy, and irradiation, as well as oxidative stress from mitochondrial

disorders, overexpression of oncogenes, or shortening of telomeres every replication to a critical length (Di Micco et al., 2006, Crabbe et al., 2004).

Consequent to persistent DNA damage, ataxia-telangiectasia mutated (ATM) gene upregulates p53 which subsequently promotes accumulation of the cyclin dependent kinase inhibitor (CDKi), p21, which inhibits activity of CDK2, a cyclin dependent kinase required for progression from G1 phase to S phase in cell cycle, leading to cell cycle arrest (Herbig et al., 2004). Long-term activation of p21 also leads to mitochondrial dysfunction and elevated ROS, which in turn causes DNA damage, completing the self-inducing loop and maintaining cell cycle arrest (Passos et al., 2010). Unrepairable DNA damage also leads to upregulation of $p16^{INK4A}$, which has a role in maintenance of cell cycle arrest (Robles and Adami, 1998). MicroRNAs such as 26b, 181a, 220 and 424 were found to activate $p16^{INK4A}$ to induce senescence in cells, where microRNA signatures in actively proliferating human mammary epithelial cells (HMECs) and replicative senescent HMECs were established using microRNA array; quenching expression of these microRNAs led to active proliferation of HMECs (Overhoff et al., 2014). As a result of repeated DNA

damage and senescence, fibroblasts stop proliferating but remain metabolically active and develop a senescent associated secretory phenotype (SASP) which up-regulates secretion of many cytokines, one of them being IL-6 (Coppé et al., 2010b).

In cancer, senescent fibroblasts are often overlooked and not differentiated from myofibroblasts as the most common CAF marker used in research is α-SMA, which was recently shown to be expressed by both myofibroblasts and senescent fibroblasts (Mellone et al, 2016). There is evidence of senescent fibroblasts promoting cancer-associated inflammation, cell proliferation, survival, ECM re-modelling and angiogenesis (James et al., 2015, Ohgo et al., 2015, Davalos et al., 2010b, Parkinson et al., 2016, Coppé et al., 2010b, Alspach et al., 2013, Freund et al., 2010, Mellone et al., 2016, Prime et al., 2017, Passos et al., 2010, Burton and Faragher, 2015, Overhoff et al., 2014), but the relative contributions of these different phenotypes to cancer progression is unclear, and their effects on immune cell recruitment and phenotype poorly understood.

Delineating the mechanisms of by which myofibroblasts and senescent fibroblasts influence cancer progression and immune responses will be helpful in devising new therapeutic targets and prognostic biomarkers in the tumour microenvironment.

Based on the literature above and in chapter 1, this chapter sets out to characterise myofibroblastic phenotype and senescent phenotype in normal oral fibroblasts.

3.1. Hypothesis:

Normal fibroblasts transdifferentiate into myofibroblast in response to TGF-β1, while cisplatin – a chemotherapeutic drug - induces senescence in fibroblasts; both myofibroblast and senescent fibroblasts develop a secretory phenotype.

3.2. Aims:

- To determine the optimum duration of TGF-β1 treatment required to transdifferentiate normal oral fibroblast into myofibroblasts; confirm transdifferentiation by validating the expression of the most commonly used myofibroblast marker, α-SMA, over the course of TGF-β1 treatment at mRNA and protein level by qPCR and western blot.

- To induce senescence in normal fibroblasts using cisplatin, and confirm senescence by validating markers $p16^{INK4A}$ and p21 using qPCR, and by senescence associated β-galactosidase assay.
- To compare expression and secretion of the SASP marker, IL-6, between myofibroblasts and senescent fibroblasts using qPCR and ELISA.
- To examine expression levels of ECM components, FNEDA and COL1A1, in myofibroblast and senescent fibroblast.

3.3. Transdifferentiation of normal fibroblast to myofibroblast through TGF-β1 treatment

Normal oral fibroblasts (NOF320, NOF316, NOF343), derived from biopsies taken during routine dental procedures from healthy volunteers, were isolated and treated with 5 ng/ml TGF-β1 for 24, 48, and 96 h (Tamm et al., 1996). Although the optimum time point for TGF-β1 treatment to induce myofibroblast transdifferentiation was previously found in the lab to be 48 h (Melling, 2015), here shorter and longer time points were selected to examine the dynamics of any secretory phenotype detected, and to assess possible desensitisation to TGF-β1 due to long exposure (Baugé et al., 2011, Yamane et al., 2003, Hasan et al., 1997). To determine expression of α-SMA mRNA transcripts in the NOFs, RNA was extracted from these cells, reverse

transcribed and subjected to quantitative PCR normalised to RNU6-1 (U6) as the housekeeping gene. Both NOF316 and NOF320 showed the highest increase in transcription of α-SMA after 24 h TGF-β1 treatment of 11 and 13.5 folds from their 24 h untreated controls, respectively (Fig. 3.1 A and B). The increase was smaller at 48 h (0.5 and 1.3 fold for NOF316 and NOF320, respectively); followed by even smaller increase of 0.14 and 0.1 fold at 97 h in NOF316 and NOF320, respectively. At 24 h, NOF343 showed an increase of 4.5 folds in α-SMA transcripts compared to untreated controls, while the highest increase in transcription was observed after 48 h of TGF-β1 treatment with a fold increase of 14, and dropping down to 4.4 folds at 96 h timepoint (Fig. 3.1 C).

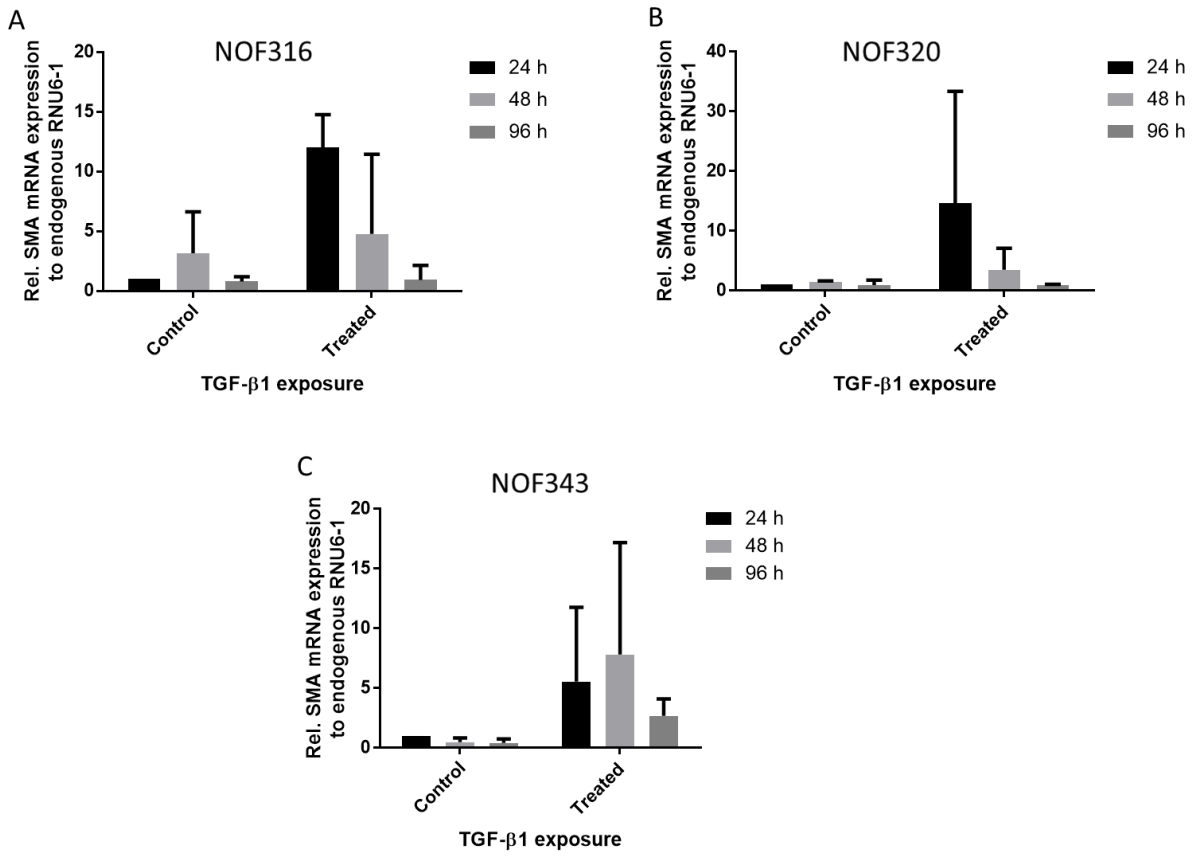

Figure 3.1: Relative mRNA expression of α-SMA in TGF-β1 treated and untreated fibroblasts to 24 h ctrl. Normal oral fibroblasts from 3 patients were treated with 5 ng/ml TGF-β1 for 24, 48, and 96 h duration, with untreated controls cultured in serum-free DMEM. Subsequently, RNA was collected and reverse transcribed from both treated and untreated controls, and α-SMA was validated at mRNA level against RNU6-1 as housekeeping gene through qPCR. A) NOF316 showed a relative increase in α-SMA mRNA transcripts of 11, 0.5, and 0.14 at 24 h, 48 h, and 96 h, respectively. B) NOF320 showed a relative increase of 13.5, 1.3, and 0.1 at 24 h, 48 h, and 96 h, respectively. C) NOF343 showed a relative increase of 4.5, 14, and 4.4 at 24 h, 48 h, and 96 h, respectively. Data +/- SEM, n = 3 biological repeats.

Having identified a trend towards an increase in α-SMA transcript level, albeit of variable magnitude, western blot analysis was carried out next to determine protein expression of α-SMA in the TGF-β1 treated and untreated NOF316, NOF320, NOF343 as shown in fig. 3.2. It was observed that α-SMA mRNA levels decreased with increasing duration of TGF- β1 treatment (fig 3.1 A), yet, NOF316 showed increases in relative expression of α-SMA protein with increasing duration of TGF-β1 treatment; at 24 h, 48 h, and 96 h, the increase in relative expression was 3, 88, and 121-fold, respectively (Fig 3.2 A). Melling made similar observation in the same lab where targeting levels of α-SMA mRNA did not impact translation into α-SMA protein (Melling, 2015). NOF343, following more closely the pattern of mRNA expression (fig. 3.1 C) changes observed, displayed relative increases of 1.9, 3, and 2.3-fold at 24 h, 48 h and 96 h, respectively (Fig. 3.2 C). However, in fig. 3.1. B, NOF320 TGF-β1 treated and untreated cells expressed similar levels of α-SMA (relative expression of 1.2, 1 and 1-fold at 24 h, 48 h, and 96 h, respectively) as seen in Fig. 3.2 B.

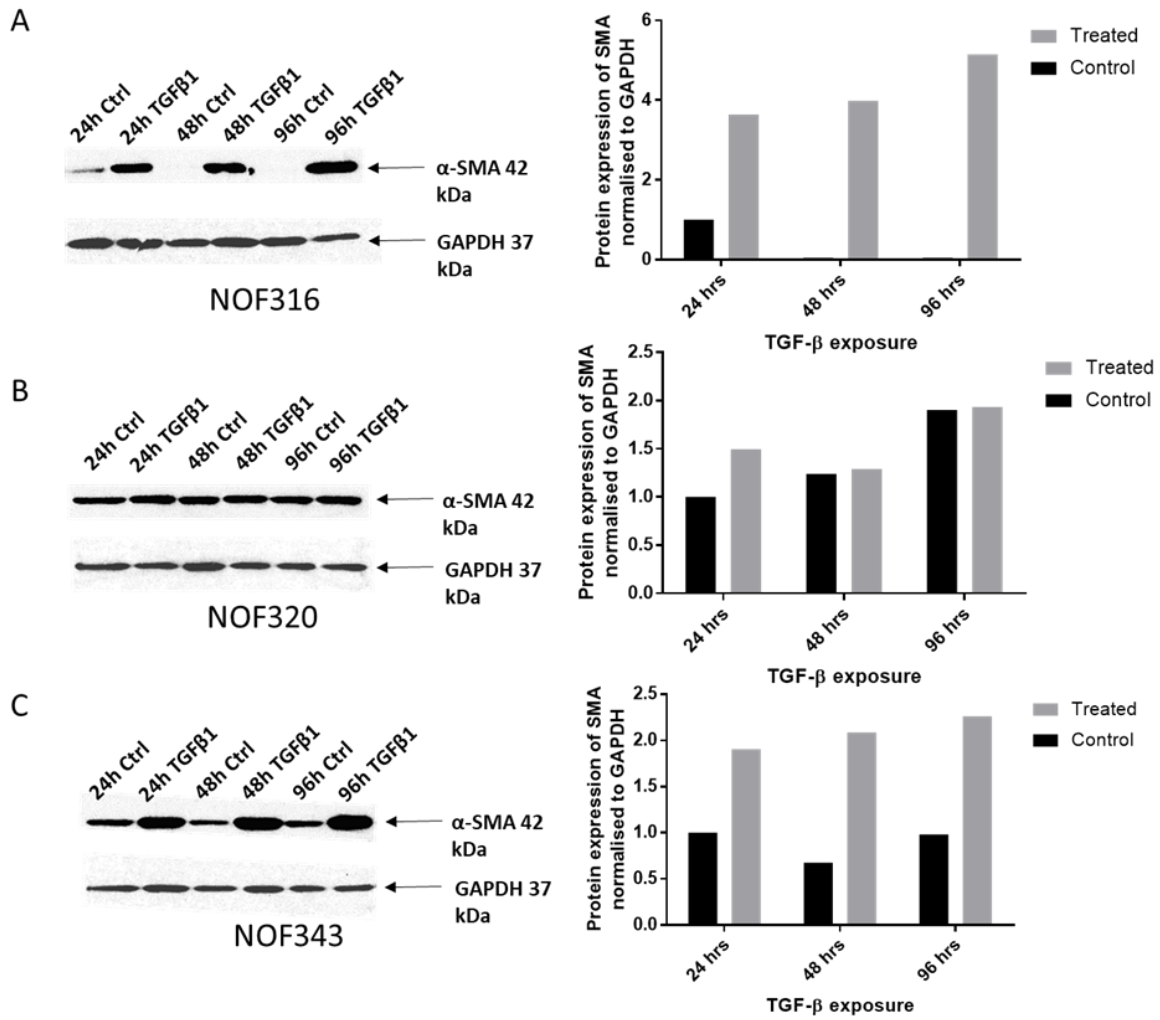

Figure 3.2: Western blot analysis protein expression of α-SMA in TGF-β1 transdifferentiated myofibroblasts. Normal oral fibroblasts were treated with 5 ng/ml TGF-β1 for 24 h, 48 h, and 96 h duration; lysates were collected from treated and untreated fibroblasts and α-SMA and GAPDH proteins were identified using antibodies raised against the same through western blotting. Densitometry was used to quantify expression of α-SMA protein, normalised to GAPDH. A) and C) NOF316 and NOF343 both showed an increase in absolute expression of α-SMA with increasing duration of TGF-β1 treatment B) NOF320 failed show a prominent difference between treated and untreated cells. N = 1 biological repeat.

Out of the three patient samples, NOF343 was selected to continue on with the project due to its robust response to TGF-β1, and availability of low passage cultures.

Having established that TGF-β1 treatment provoked an increase in cellular levels of α-SMA in NOF343 cells, immunofluorescence was next employed whereby a FITC conjugated antibody specific to α-SMA was used to validate and extend the western blot results by allowing visualisation of α-SMA stress fibres following TGF-β1 treatment of fibroblasts using fluorescence microscopy as described in section 2.16 and depicted in Fig 3.3 A. As seen in fig. 3.3 B, the increase in fluorescence of α-SMA stress fibres in TGF-β1 treated NOF343 is significant with respect to their timed untreated controls, with $p<0.0001$ at 24 h and 96 h, and $p<0.007$ at 48 h time points.

A

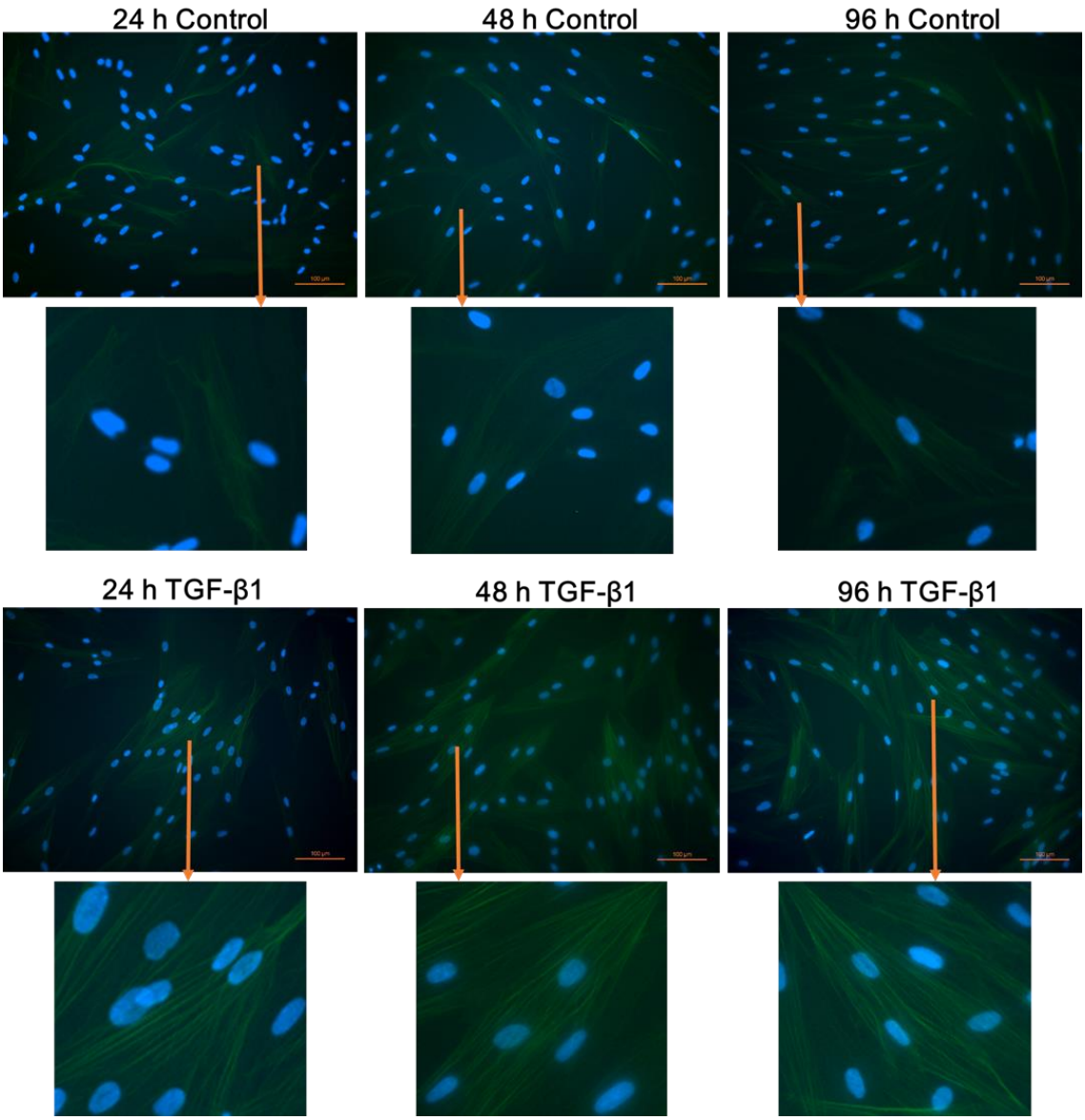
24 h Control
48 h Control
96 h Control
24 h TGF-β1
48 h TGF-β1
96 h TGF-β1

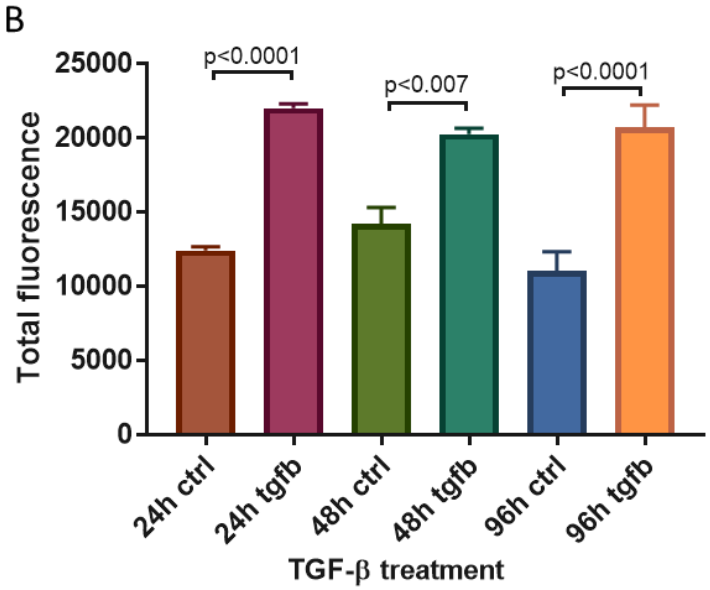

Figure 3.3: Immunofluorescence analysis of α-SMA stress fibres. NOF343 was cultured on coverslips and treated with 5 ng/ml TGF-β1 for 24 h, 48 h, and 96 h, with untreated cells cultured in serum-free DMEM. A) TGF-β1 treated fibroblasts show α-SMA stress fibres clearly at all time points while untreated fibroblasts displayed minimal expression of α-SMA stress fibres. B) Quantification of immunofluorescence shows significantly higher expression of α-SMA with $p<0.0001$ at 24 h and 96 h time point, and $p<0.007$ at 48 h. Statistical analysis – ANOVA, data +/- SEM, n = 3 wells.

3.4. Cisplatin-induced senescence in normal oral fibroblasts

Normal oral fibroblasts NOF343 were treated with a chemotherapeutic drug commonly used in head and neck cancer patients, cisplatin (10 μM) for 24 days, then allowed to senesce over 14 days. These conditions were chosen on the basis of characterisation previously carried out in the lab (Kabir et al., 2016). The acquisition of senescence was indicated by increases in the expression of $p16^{INK4A}$ and p21; cyclin dependent kinase inhibitors regulating cell cycle progression commonly used as indicators of senescence acquisition, as assessed by qPCR. The cisplatin treated fibroblasts exhibited elevated levels of both $p16^{INK4a}$ (1.71 fold increase) and p21 (3.4 fold increase) compared to their untreated counterparts (fig. 3.4), although this did not reach statistical significance due to variation between experiments.

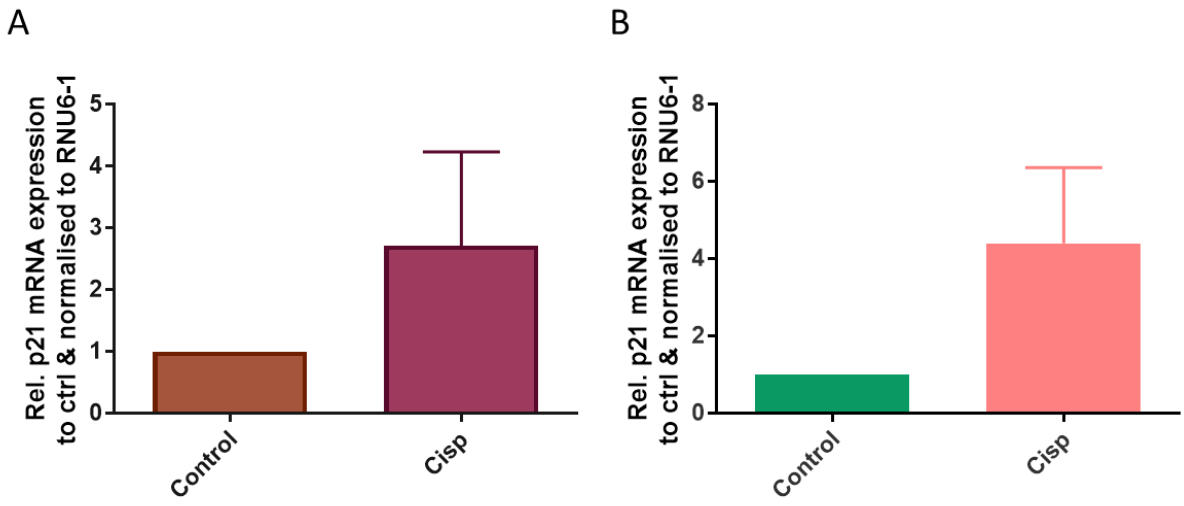

Figure 3.4: Expression of senescence marker transcripts in cisplatin treated and untreated fibroblasts. NOF343 were treated with 10 μM cisplatin for 24 h, then cultured in DMEM over 14 days. RNA was isolated from control and treated NOFs, used to generate cDNA for qPCR using primers for $p16^{INK4A}$, p21, and RNU6-1 (U6) as endogenous control. A) and B) Cisplatin treated senescent fibroblasts expressed elevated levels of both $p16^{INK4a}$ and p21 transcripts, as assessed by qPCR normalised to RNU6-1, compared to untreated control fibroblasts. Statistical analysis – Student paired T test, data are mean +/- SEM, and not significant, n=3 biological repeats.

Senescence associated β-galactosidase assay employs cleavage of a chromogenic substance, X-gal, which upon hydrolysis by β-galactosidase at pH 6 in aged cells forms a blue precipitate, hence it is used as a method of confirming senescence (Dimri et al., 1995) along with elevated $p16^{INK4a}$ and p21 (Ohgo et al., 2015). Cisplatin (10 μM) treated normal oral fibroblasts NOF343 exhibited a blue stain in more than 90% of the cells due to cleavage of X-gal upon accumulation of lysosomal β-galactosidase ($p<0.0009$), while the untreated control was devoid of the blue stain (fig. 3.5 A and B). Senescent fibroblasts were also more flattened and bigger in appearance compared to control fibroblasts (fig. 3.5 A).

A

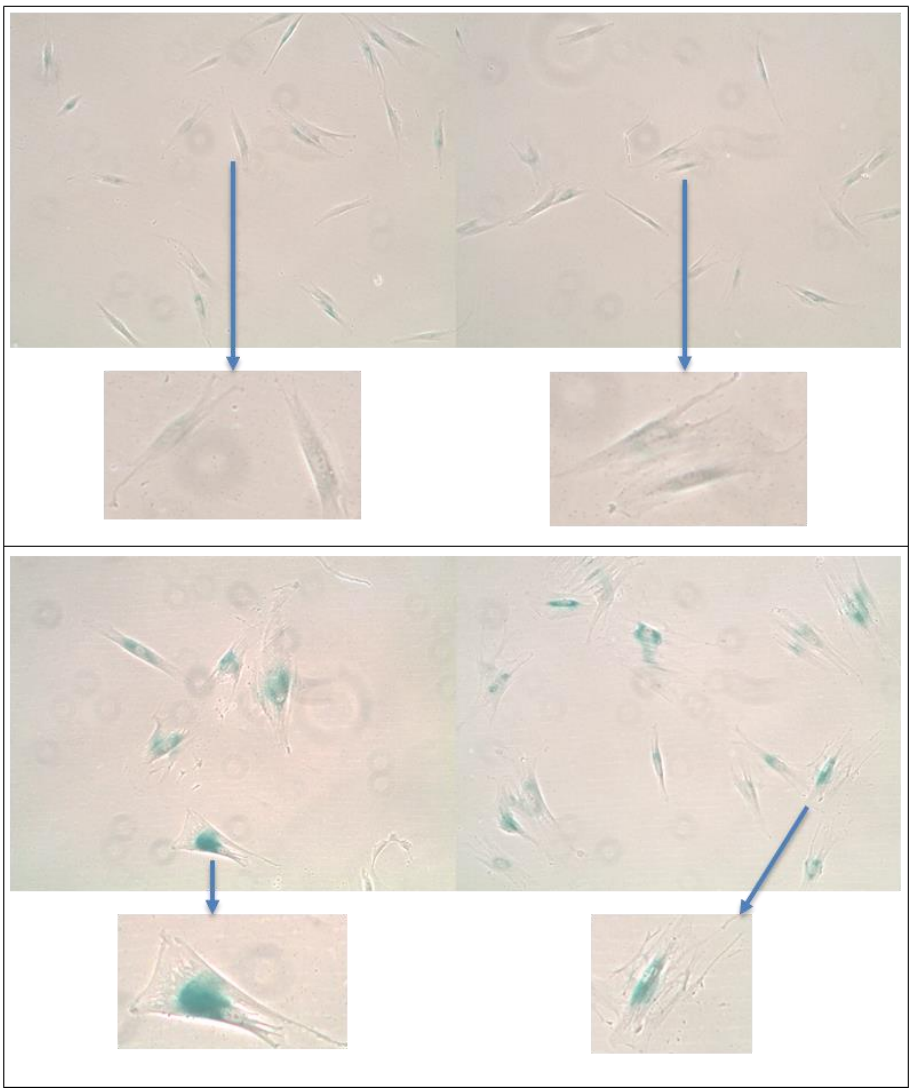
15 day control
(untreated NOF343)
Spindle shaped
and unstained
15 day cisplatin
(treated NOF343)
Flat, broad
and stained

B

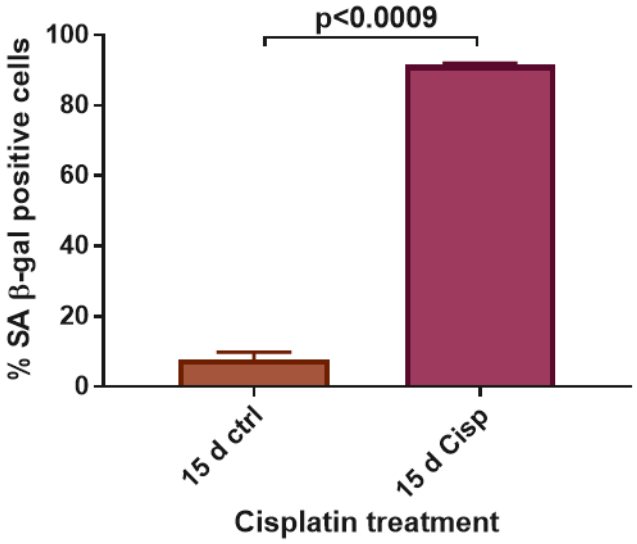
p<0.0009
% SA β-gal positive cells
100
80
60
40
20
0
15 d ctrl
15 d Cisp
Cisplatin treatment

Figure 3.5: Senescence associated β-galactosidase assay (SA β-gal) confirming senescence. Normal oral fibroblast NOF343 were treated with 10 μM cisplatin for 24 h before allowing to senesce for 14 d in DMEM. A) In senescence associated β-galactosidase assay cisplatin treated fibroblasts (>90%) developed a blue precipitate due to cleavage of X-gal at pH 6 because of higher activity of lysosomal β-galactosidase while the control fibroblasts remained free of any precipitate development when subjected to SA β-gal assay. B) The positive precipitate development in cisplatin treated fibroblasts was significant with $p<0.0009$. Statisticaly analysis – Student T test, data +/- SEM, n=3 biological repeats.

IL-6 is a prominent cytokine in the inflammatory environment with evidence in the literature of it being up-regulated in both myofibroblasts and senescent fibroblasts (Zhu et al., 2014, Hendrayani et al., 2016, Ara and Declerck, 2010, Kojima et al., 2013, Rose-John, 2012). In myofibroblasts, IL-6 aids secretion of ECM components during wound healing, promoting angiogenesis, and causing inflammation in the area via recruitment and differentiation of immune cells (Zhu et al., 2014, Rose-John, 2012, Ara and Declerck, 2010, Mueller et al., 2010, Zhu et al., 2016). In senescent fibroblasts, IL-6 helps maintain senescence in an autocrine loop, while promoting senescence in neighbouring fibroblasts by up-regulating production of ROS (Tanaka et al., 2014, Kojima et al., 2013, Burton and Faragher, 2015, Passos et al., 2010, Mellone et al., 2016, Davalos et al., 2010b). Therefore expression and secretion of IL-6 by myofibroblasts and senescent fibroblasts was quantified at mRNA and protein level using qPCR and ELISA, respectively. Surprisingly, at the mRNA level in myofibroblasts at 24 h, 48 h, and 96 h, IL-6 was marginally down-regulated compared to untreated controls (fig. 3.6 A). At the secreted protein level, however, there was a significant increase ($p=0.0123$) in IL-6 secretion after 24 h of treatment with TGF-β1, an increase which declined with increasing duration of TGF-β1

exposure (Fig. 3.6 B). On the other hand, cisplatin induced senescent fibroblasts showed an upregulation in both IL-6 mRNA but not significant (fig. 3.6 A), while there was an upregulation observed at secretory level and significant ($p=0.0125$), compared to proliferating controls (Fig. 3.6 B).

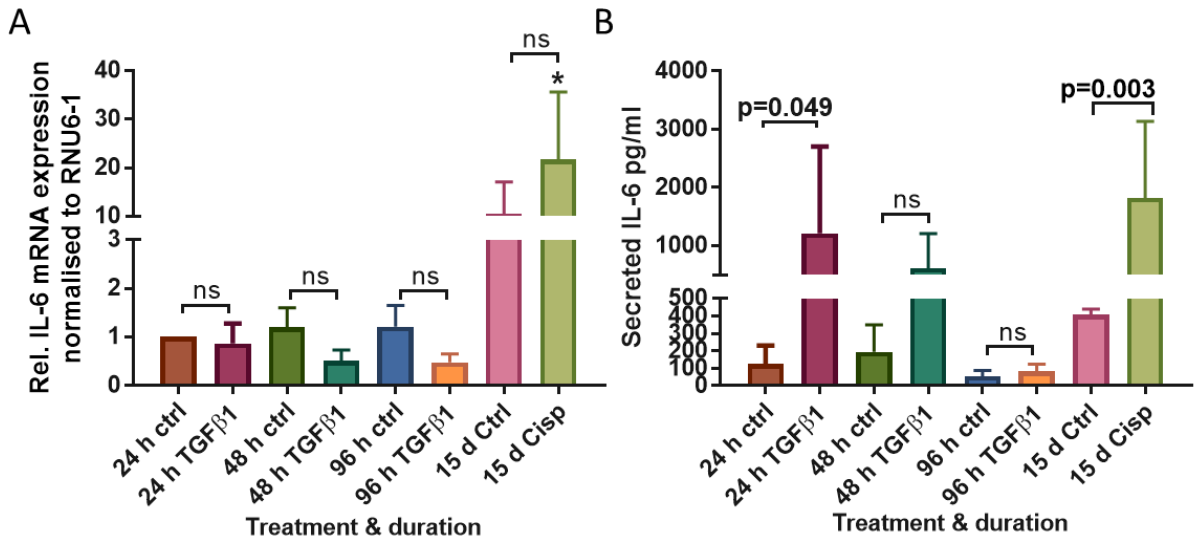

Figure 3.6: IL-6 expression in myofibroblasts and senescent fibroblasts: Normal oral fibroblasts NOF343 were treated with 5 ng/ml TGF-β1 for 24 h, 48 h, and 96 h to induce myofibroblast transdifferentiation. To induce senescence, normal oral fibroblasts NOF343 were treated with cisplatin (10 μM) for 24 h and senesced over 14 d. RNA was extracted from these NOFs to generate cDNA, used in qPCR with IL-6 and RNU6-1 (U6) primers. All bars are relative to 24 h control. A) IL-6 transcripts were down regulated in TGF-β1 treated fibroblasts, and reduced further with increasing duration of treatment. However, IL-6 transcripts were up-regulated in cisplatin induced senescent fibroblasts and significant to control and TGF-β1 treated fibroblast at 24, 48 and 96 h with * = $p<0.002$. B) Secretion of IL-6 was significantly up-regulated at 24 h time point of TGF-β1 treatment (mean 1214 pg/ml) compared to its 24 h control (mean 125.3 pg/ml) with $p=0.0123$. IL-6 secretion down-regulated with increase in duration of TGF-β1 exposure. Cisplatin induced senescent fibroblast showed a significant increase (mean 1824 pg/ml) compared to its control (mean 407.6) with $p=0.0125$. Statistical analysis – ANOVA with Tukey's multiple comparison, data +/- SEM, n=3.

In addition to augmented cytokine and growth factor secretions, CAFs also secrete ECM components, such as fibronectin-EDA (FNEDA), collagen, fibrin, elastin, MMPs and proteoglycans (Tomasek et al., 2002, Ohlund et al., 2014, Erdogan and Webb, 2017).

Levels of transcripts corresponding to the ECM genes fibronectin extradomain A (FNEDA) and collagen α-1 (I) chain (COL1A1) were determined in both myofibroblast and senescent fibroblast phenotypes of NOF343 (Fig. 3.7 A and B), generated as described in sections 3.4 & 3.5. Transcripts of both FNEDA and COL1A1 were found to be up-regulated in TGF-β1 treated fibroblasts (myofibroblasts) (Fig. 3.7 A and B), with FNEDA transcripts significantly elevated at 24 h TGF-β1 treatment time point with $p=0.0169$ (Fig. 3.7 A). In contrast, cisplatin induced senescent fibroblasts showed relatively equal levels of FNEDA (Fig. 3.7 A), and down regulation of COL1A1 (Fig. 3.7 B) compared to their untreated controls. Increase in FNEDA and COL1A1 transcripts in TGF-β1 transdifferentiated myofibroblasts has been observed before in several studies (Melling, 2015, Zeisberg et al., 2007, Torr et al., 2015, Mellone et al., 2017).

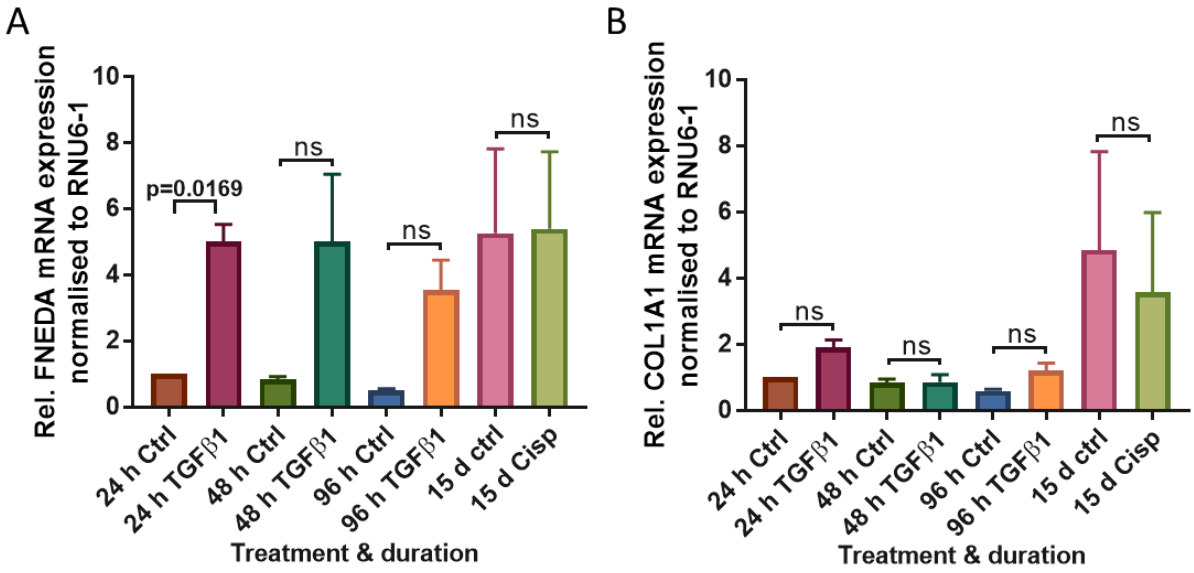

Figure 3.7: Expression of FN-EDA and COL1A1 mRNA transcripts in myofibroblast and senescent fibroblast: Normal oral fibroblast NOF343 was treated with 5 ng/ml TGF-β1 for 24 h, 48 h, and 96 h to transdifferentiate into myofibroblast, while cisplatin (10 μM) was used for 24 h, and 14 d of normal culture to induce senescence. RNA was isolated from control and treated NOFs, used to generate cDNA for qPCR using primers FNEDA, COL1A1, and endogenous control RNU6-1 (U6). All bars are relative to 24 h control. A) Myofibroblast expressed higher mRNA transcripts of FN-EDA compared to their controls, with significance (p=0.0169) after 24 h TGF-β1 treatment. Senescent fibroblast and its untreated control expressed similar level of FN-EDA mRNA transcripts with no significance. B) Col1A1 mRNA was upregulated only in senescent fibroblast and its untreated control, while TGF-β1 treated fibroblasts showed a small increase in expression compared to their controls. Statistical analysis – ANOVA with Tukey's multiple comparison, data are +/- SEM, n=3 biological repeats.

3.5. Summary

This chapter describes characterisation of fibroblast to myofibroblast and senescent fibroblast phenotypes. Normal oral fibroblasts were treated with 5 ng/ml TGF-β1 for three time points – 24 h, 48 h, and 96 h to study the effects of TGF-β1 during both short and long exposures. Senescence was induced in normal oral fibroblasts using cisplatin; treating cells for 24 h and allowing the fibroblasts to senesce over the course of 2 weeks in normal culture.

It was found that upon TGF-β1 treatment, normal oral fibroblasts (NOFs) exhibited increased expression of α-SMA at protein level with appearance of stress fibres, which is also a commonly used identifying marker for myofibroblastic phenotype. The expression of α-SMA increased with increasing duration of TGF-β1 treatment, even though expression at mRNA level differed from protein expression. One of the NOFs, NOF320, used in the study displayed very limited changes in response to TGF-β1 treatment, suggesting desensitisation to TGF-β1. This desensitisation to TGFβ1 and relatively high levels of basal α-SMA expression could be due to possible extraction of these fibroblasts from an already inflamed site; (Hasan et al., 1997, Yamane et al.,

2003) unfortunately this clinical information was not available. A further dose-dependent TGF-β1 treatment compared to untreated control showing no changes in expression of α-SMA would confirm desensitisation but was not completed for this thesis due to time constraints.

Cisplatin induced senescence in NOF343, as indicated by positive staining in SA β-gal assay, broad and flattened cell morphology, and increased expression of $p16^{INK4A}$ and p21 mRNA.

Expression of IL-6 known to be secreted by senescent cells (Kojima et al., 2013). This was confirmed in this study as well, and compared with expression by myofibroblasts where both senescent fibroblasts and myofibroblasts showed significant increases in secretion of IL-6 compared to their respective time controls, with myofibroblasts showing highest secretion at 24 h post TGF-β1 treatment, and declining with increasing duration of treatment.

ECM components FNEDA and COL1A1 are markers of myofibroblast transdifferentiation (Melling, 2015, Zeisberg et al., 2007, Torr et al., 2015, Mellone et

al., 2017). This was then compared with expression by senescent fibroblasts which didn’t show an increase in expression of both FNEDA and COL1A1 mRNA.

With the confirmation of change in phenotype of both TGF-β1 treated fibroblasts and cisplatin treated fibroblasts, capability to recruit monocytes was examined in the next chapter to observe possible differences in the same.

Chapter 4

4. Comparing monocyte recruitment capability of myofibroblast and senescent fibroblastic phenotypes

Monocytes originate in the bone marrow before being released into to bloodstream, where they constitute 3-8% of total circulating leukocytes. Monocytes are further divided in to subsets based on the expression of CD14 and CD16. The most prevalent subset in circulation, the classical monocyte, expresses $CD14^{++}CD16^{-}$ with $CCR2^{hi}CX_3CR1^{low}$ expression and participates in pro-inflammatory and anti-microbial roles (Shi and Pamer, 2011). Other subsets include intermediate and non-classical with $CD14^{++}CD16^{+}$, and $CD14^{-}CD16^{++}$ expression, respectively with roles in inflammation and patrolling (Shi and Pamer, 2011).

Sub-populations of CAFs with varying phenotype present in the TME secrete an array of growth factors, angiogenic factors and numerous cytokines/chemokines (detailed description in chapter 5) which present the capability to recruit these monocytes through promiscuous receptor/ligand axes such as CCR2/CCL2 (Ohgo et al., 2015, Mueller et al., 2010, Wu et al., 2011, Loberg et al., 2007, Min et al., 2015, Li et al., 2014b, Tsuyada et al., 2012b). These monocytes are recruited to the TME

and the tumour mass itself to differentiate and polarise into M1 and M2 macrophages depending on the cytokine environment encountered (Bingle et al., 2002, Mantovani and Sica, 2010, Sica et al., 2006a). The presence of macrophages in most solid tumours, including those of the head and neck, lead to poor prognosis (Li et al., 2002, Marcus et al., 2004, Liu et al., 2008).

The data described in this chapter uses *in vitro* approaches to explore the potentially differential monocyte recruitment capabilities of two recognised subsets of cancer-associated fibroblast phenotypes; myofibroblastic and senescent fibroblasts, and compare this to the recruitment capabilities of tumour-derived CAF. This might provide the mechanistic information required to begin to target subpopulations of CAF more effectively to prevent specific recruitment of immune cells, especially macrophages, to improve prognosis.

4.1 Hypothesis:

Myofibroblasts, senescent fibroblasts and CAFs have distinct secretory phenotypes and have different abilities to recruit monocytes.

4.2 Aims:

- To examine the capability of myofibroblasts, senescent fibroblasts and patient CAFs to recruit THP1 cells and PBMs via secreted factors.
- To measure levels of monocyte chemokine – CCL2 secreted by myofibroblasts, senescent fibroblasts, and patient CAFs.
- To determine expression of CCR2 – receptor for CCL2 on THP1 cells and PBMs.
- To inhibit CCR2 using a small molecule inhibitor or pertussis toxin and study monocyte migration.
- To investigate macrophage polarisation in response to secreted factors from myofibroblasts, and senescent fibroblasts.
- To investigate possible correlation between presence of TAMs and CAFs in tumour sections.

4.3 THP1 cell migration in response to factors secreted by myofibroblast and senescent fibroblast

THP1 cells, a monocytic cell line isolated from the peripheral blood of a patient with acute leukaemia (Tsuchiya et al., 1980), were replicated from the pilot study (Kabir, 2015) to test for suitability for this study. THP-1 were used in a modified Boyden chamber/transwell assay, in which conditioned medium (CM) from myofibroblasts (NOF343 treated with 5 ng/ml TGF-β1), senescent fibroblasts (NOF343 pulsed with 10 μM cisplatin), and their respective untreated controls were placed in the bottom chamber, and the THP1 cells in the upper chamber (Fig. 4.1).

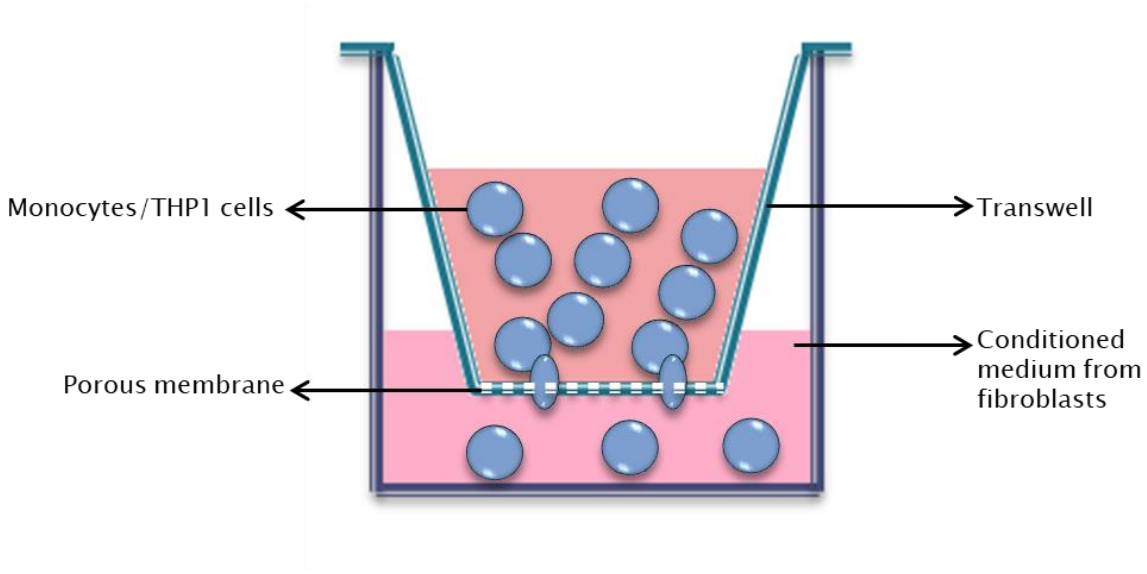

Figure 4.1: Boyden chamber (transwell) setup used for migration assay: THP-1/monocytes were placed in the upper chamber of the transwell in serum free medium, and allowed to migrate through a porous membrane in the transwell to the lower chamber containing conditioned medium (CM) from fibroblasts over 4 h. The number of monocytes in lower chamber and underside of the transwell were counted as migrated and used for statistical analysis comparing migration towards CM from different phenotypes of fibroblasts.

Migrated cells on the underside of the porous membrane were methanol fixed, and stained with DiffQuik (as described in chapter 2, section 2.12), and cells migrated all the way in to the CM were gently agitated; at least three images taken by light microscopy at 20 X magnification. The cells were then counted using ImageJ as described in chapter 2, section 2.12.

At 24 h THP-1 migrated less towards myofibroblast CM compared to 24 h control CM with a fold decrease of 0.14, but at 48 h myofibroblast CM recruited more THP-1 than 48 h control CM with a 2.18 fold increase, although it was not statistically significant (Fig. 4.2). However, at 96 h, both myofibroblast CM and control CM recruited the same number (+/- 1) of THP-1 cells. THP-1 recruitment by senescent fibroblasts showed a 1.6 fold increase from its 15 d control CM. Statistically, recruitment by senescent fibroblast CM was significant compared to recruitment by controls at all time points - 24 h, 48 h, 96 h, and 15 d, as well as recruitment by TGF-β1 treated myofibroblasts at all time points 24 h, 48 h and 96 h, with $p<0.0001$.

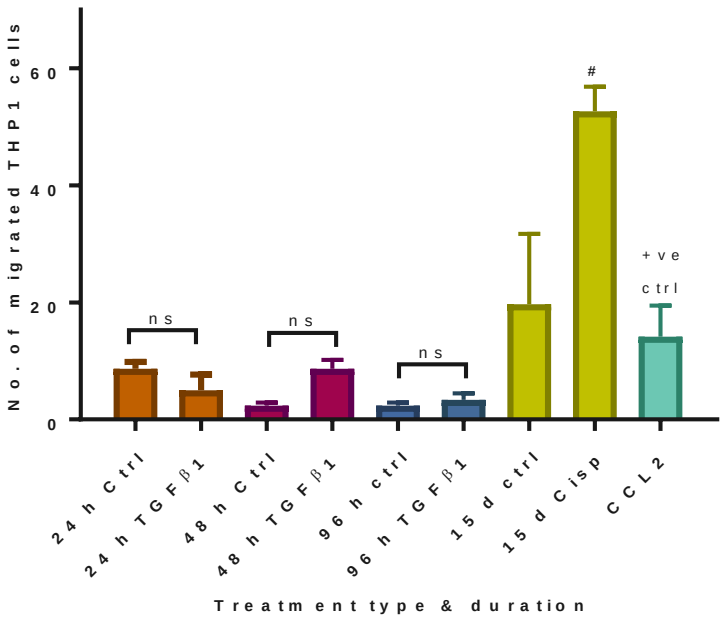

Figure 4.2: THP1 monocyte migration towards CM from myofibroblasts and senescent fibroblasts. NOFs were treated with 5 ng/ml TGF-β1, serum-free medium (SFM) or 10 μM cisplatin for different time durations, and fresh media was conditioned for 24 h before collection and used in migration assay. THP1 cells were allowed to migrate towards CM from myofibroblast, senescent fibroblast, their untreated controls, CCL2 (positive control), and SFM (negative control, later deducted from data as background) in a transwell assay for 4 h, and the number of migrated cells counted. Only 48 h TGF-β1 treated myofibroblast CM showed a 2.18 fold increase from its 48 h control CM, while 24 h and 96 h TGF-β1 treated myofibroblast CM displayed reduced recruitment of THP-1. Senescent fibroblast CM recruited THP-1 cells with a fold increase of 1.6 from its 15 d control CM, and was significant compared to myofibroblast CM at 24 h, 48 h, 96 h, and control CM at 24 h, 48 h, 96 h and 15 d by $p<0.0001$. Statistical analysis - One Way ANOVA where # indicates migration towards 15d cisp treated NOF343 significant to all other conditions (24, 48, 96 h control, and TGF-β1 treated, and 15 d control) with $p<0.0001$; data are mean +/- SEM, n=3 biological repeats.

4.4 Peripheral blood monocyte migration in response to factors secreted by myofibroblast and senescent fibroblast

THP1 is a cell line originating from acute monocytic leukaemia, and therefore results using it can be used to design and optimise conditions of initial experiments but are not directly translatable to primary monocytes. Consequently, monocytes from peripheral blood, isolated from the buffy coats of healthy volunteers (as described in chapter 2, section 2.8) were next used. Migration towards CM from myofibroblasts at 24 h was higher (1.27 fold increase) than 24 h control, but not statistically significantly (Fig. 4.3 A). At 48 h time point, recruitment of PBM by myofibroblast CM showed fold increase of 1.54 from its 48 h control CM (again, this didn't reach significance), while migration at 96 h time point showed a fold increase of 1.48 from its control CM (Fig. 4.3 A).

PBM migration towards CM from senescent fibroblasts exhibited a fold increase of 1.82 from its 15 d control (Fig 4.3 A). However, this increase was not statistically significant compared to recruitment by its control or by the myofibroblasts at any time point (Fig. 4.3 A). This is possibly due to patient-to-patient variability present in the

PBMs isolated from different buffy coat for each biological repeat of the experiment as shown in Fig. 4.3 B.

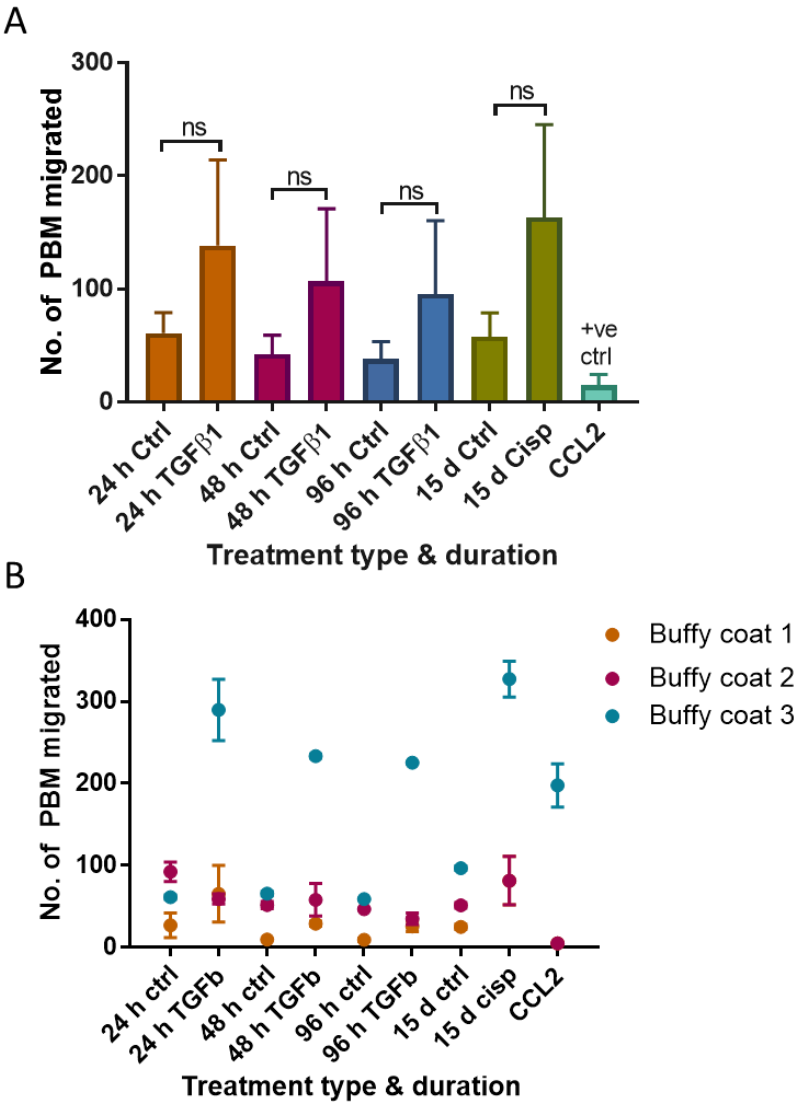

Figure 4.3: Peripheral blood monocyte (PBM) migration towards CM from myofibroblasts and senescent fibroblasts. PBMs were isolated from multi-donor buffy coats, and migrated towards CM from myofibroblast, senescent fibroblast, their untreated controls, CCL2 (positive control), and SFM (negative control, later deducted from data as background) A) Monocytes were recruited by myofibroblasts at 24 h with 1.27 fold increase from its timed untreated control, gradually declining with increase in TGF-β1 treatment duration. Although fold increases at 48 h and 96 h time points were 1.54 and 1.48 from their timed untreated controls, respectively. Senescent fibroblast CM recruited the most number of monocytes and highest fold increase of 1.82. B) Monocyte migration trend from each buffy coat showing variation in number recruited during each biological repeat, resulting in insignificant statistical analysis. Statistical analysis – Two way ANOVA, data are mean+/- SEM with n=3 biological repeats.

4.5 Expression of CCR2 by THP-1 and peripheral blood monocytes

CCR2 is a heptahelical transmembrane, G-protein coupled receptor, and it is the main receptor for chemokine CCL2 but can also bind CCL7, and CCL13 (Li et al., 2002). CCR2 is highly expressed on the classical subset ($CD14^{hi}CD16^{low}$) of monocytes, but can also be found on haematopoietic cells such as macrophages, and on non-haematopoietic cells like fibroblasts, endothelial, and mesenchymal stem cells (Zhang et al., 2010). The CCR2 gene has two splice variants, CCR2A and CCR2B, where CCR2B accounts for 90% of the CCR2 expressed on monocytes, and facilitates monocyte recruitment into sites of inflammation and also facilitates their maturation into tissue macrophages (Van Coillie et al., 1999, Wong et al., 1997).

In order to assess whether the CCL2/CCR2 axis was involved in the observed monocyte responses to fibroblast-derived signals, expression of CCR2 transcript was examined in THP1 cells and PBM using qRT-PCR for both CCR2A and CCR2B isoforms. The CCR2B isoform transcript was readily detectable in both PBM and THP-1, with THP-1 showing higher expression than PBM relative to CCR2A (Fig. 4.4

A). Next, protein expression of CCR2B was investigated using flow cytometry on both THP1 cells and PBMs (Fig. 4.4 B & C). CD14 was used as a classic monocyte marker to confirm that the cells isolated and purified from buffy coats to be used were monocytes (Fig.4.4 D). Flow cytometry showed that only 14.2% of THP1 cells expressed CD14 (Fig. 4.4 B), while a much smaller population of these cells (1.19%) expressed CCR2 (Fig. 4.4 C). Conversely, 91.9% of PBMs expressed CD14 (Fig. 4.4 D), of which 78.6% expressed CCR2 receptor (Fig. 4.4 E).

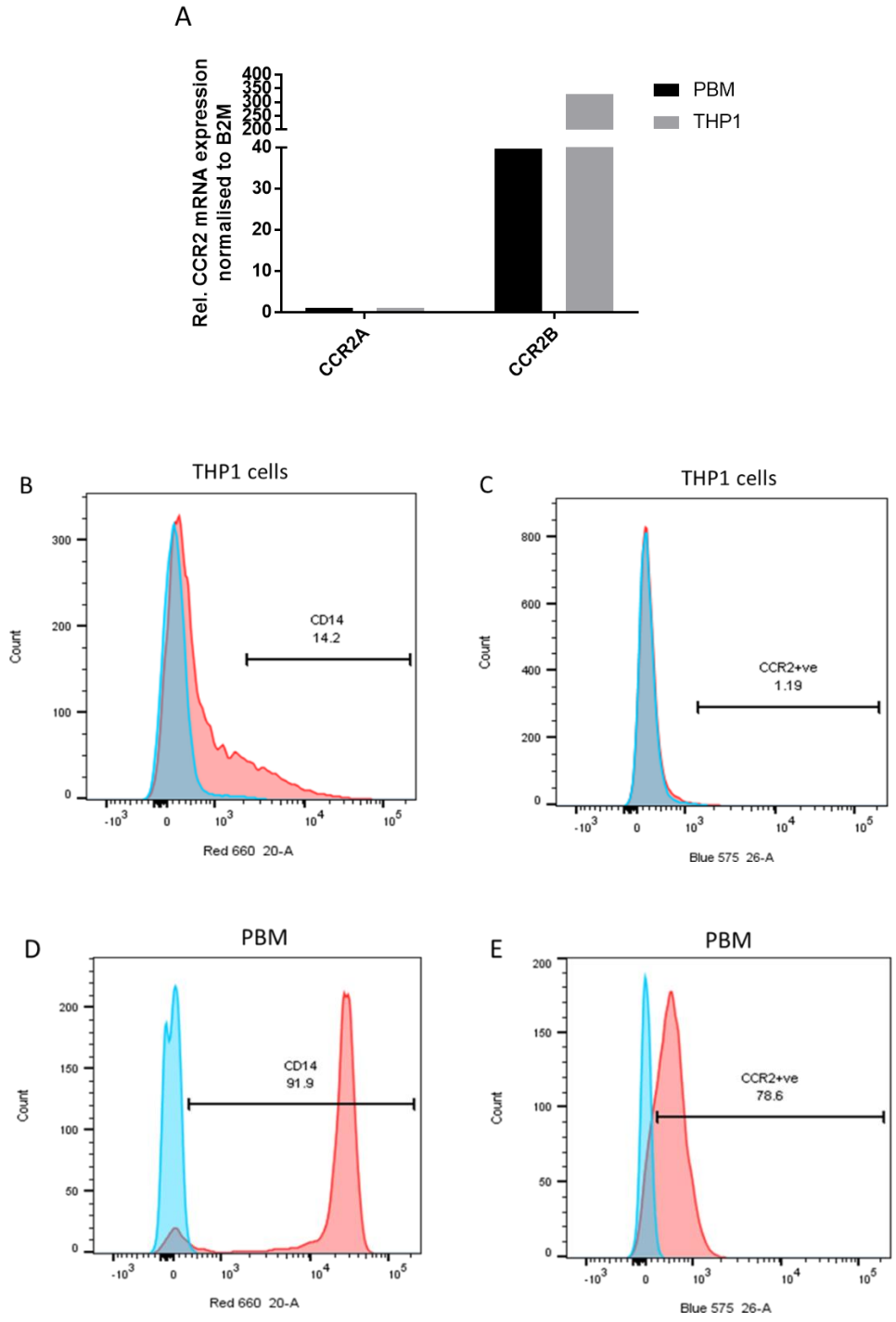

Figure 4.4: CCR2 expression in PBM and THP1 cells. RNA was isolated from both PBM and THP1 cells, followed by generation of cDNA, used in qPCR normalised to β_2 microglobulin (B2M). Flow cytometry was used to validate expression of monocyte marker CD14, and CCR2 on THP1 cells and PBMs, depicted by the red histogram, while blue depicts the isotype control. **A)** PBM and THP1 cells express higher levels of CCR2B variant transcript relative to CCR2A **B)** and **C)** show that only 14.2% and

1.19% of THP1 cells express classic monocyte marker CD14, and CCR2B receptor, respectively. **D)** Red histogram with higher peak shows 91.9% of the monocytes purified expressed CD14, with a smaller peak on the left showing monocyte subset with low CD14 expression. **E)** Of the PBMs positive for CD14 expression, 78.6% of them expressed CCR2 receptor. N = 1.

4.6 CCL2 secretion by myofibroblasts and senescent fibroblasts

Both myofibroblasts and senescent fibroblasts have been reported to develop secretory phenotypes, and produce a gamut of factors, some of which are chemokines that might be responsible for the monocyte migration observed in fig. 4.2 and 4.3. Having confirmed the expression of CCR2 receptor on PBM (Fig. 4.4), the next step was to examine levels of CCL2 in both myofibroblast and senescent fibroblasts by qPCR and ELISA (in conditioned medium) to test the hypothesis that the CCL2/CCR2 axis is the mechanism responsible for the fibroblast-induced migration observed in this study (Fig. 4.5 A and B). The qPCR results from fibroblasts treated with TGF-β1 for 24 h showed almost no change in CCL2 transcript levels compared to its control at 24 h, whereas transcript levels in 48 h and 96 h TGF-β1 treated myofibroblast showed a decrease in expression of CCL2 transcript compared to their respective controls (Fig. 4.5 A). In contrast, at the protein level, TGF-β1 treated fibroblasts showed a 7.4 fold increase in secreted CCL2 at 24 h, a 1.7 fold increase at 48 h, and a 2.7 fold increase at 96 h compared to their timed controls (Fig. 4.5 B). The highest concentration of CCL2 secreted by myofibroblasts was at the 48 h time point (133.1 pg/ml), followed by 129.6 pg/ml at 24 h time point,

finally decreasing to 97.82 pg/ml at 96 h time point. Senescent fibroblasts showed the highest expression of CCL2 transcripts, both in comparison to its control and myofibroblasts and their controls at all time points (Fig. 4.5 A). Surprisingly, the 15 d (untreated) control also expressed higher levels of CCL2 than other controls and TGF-β1 treated fibroblasts. There was no significant difference between CCL2 expressions in the cisplatin treated cells and their respective untreated (15 d) control. In terms of CCL2 secretion, senescent fibroblasts secreted 825.6 pg/ml, a 0.58-fold increase from its 15 d control ($p=0.032$) as shown in Fig. 4.5 B. CCL2 secretion levels were significantly higher from senescent fibroblasts than myofibroblasts and their controls at all time points ($p<0.0001$; Fig. 4.5 B). CCL2 secretion by 15 d untreated control was also higher than TGF-β1 treated NOFs and their untreated controls at all time points with a significance of $p<0.008$ (Fig. 4.5 B).

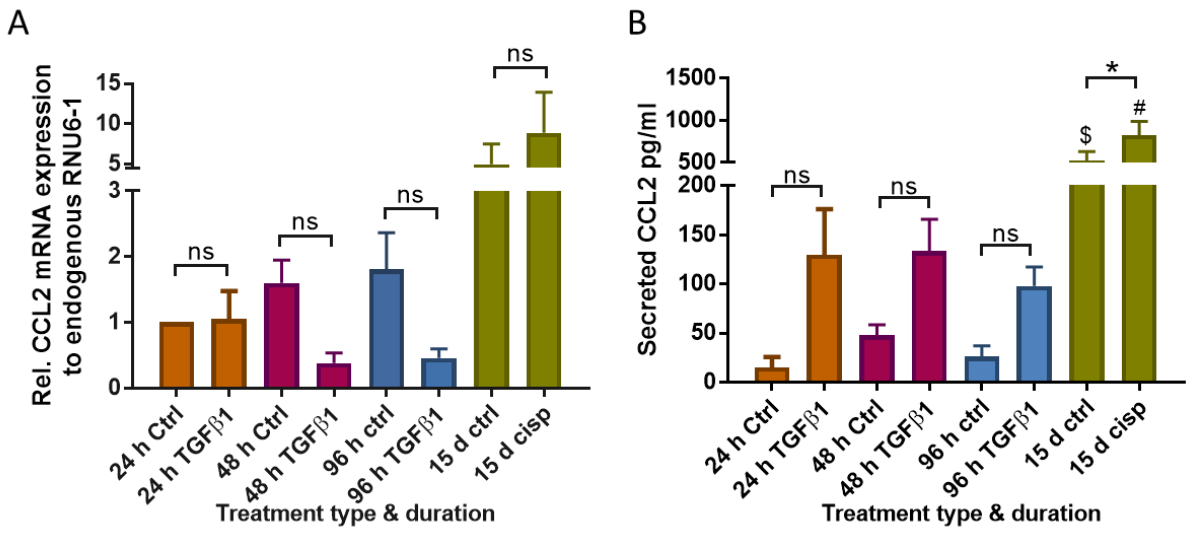

Figure 4.5 Expression of mRNA and secreted levels of CCL2 in myofibroblast and senescent fibroblast. A) Myofibroblast showed a decrease in mRNA expression of CCL2 compared to its untreated controls, while both senescent fibroblast and its control showed an upregulation in comparison. **B)** Myofibroblast initially showed an increase in secretion of CCL2 at 24 h – 7.4 fold, 2.7 fold at 48 h and 2.6 fold at 96 h, declining with increase in duration of TGF-β1, while senescent fibroblast showed a 1.27 fold increase. Statistical analysis – Two way ANOVA, where # is 15 d cisp significant to control & TGF-β1 NOFs at 24, 48, and 96 h with $p<0.0001$, and * is 15 d cisplatin significant to 15 d control with $p=0.032$, and $ is 15 d control significant to TGF-β1 treated NOFs and their controls at 24, 48, and 96 h with $p<0.008$. Data are mean +/- SEM with n=3 biological repeats.

4.7 Targeting CCR2 receptor

Having established the presence of CCR2 on PBM and the ability of both myofibroblasts and senescent fibroblasts to secrete its ligand, CCL2, it was next decided to examine the effect of using a small molecule inhibitor of CCR2, RS 504393, on monocyte migration, to elucidate whether CCL2 was wholly or partly responsible for the observed effects on monocyte recruitment.

PBMs were pre-treated with 10 μM of the CCR2-specific small molecule inhibitor RS 504393 (CCR2i) for one hour; this concentration was based on the study by (Carmo et al., 2014). CCR2i was then removed and PBMs suspended in fresh SFM before migrating towards CM from myofibroblasts or senescent fibroblasts (section 2.12). However, before proceeding with the migration assay, monocyte cell viability was examined at 5, 10, and 20 μM by treating cells with the inhibitor for 1 h (SFM was used as negative control), followed by incubation in SFM for 4 h at 37°C, mimicking the conditions of the transwell migration assay used in this study. This experiment was performed to ensure that the inhibitor did not cause toxicity that might lead to artefactual results in the migration assay. Trypan blue was used to calculate the

percentage of dead cells out of total cells; there was 33% less cell death at 10 μM compared to normal SFM as shown in Fig. 4.6 A. Upon treating PBMs with 10 μM CCR2 inhibitor (+CCR2i), migration towards recombinant CCL2 showed a 0.52 fold decrease with p=0.01 compared to migration by PBMs with uninhibited CCR2 (control; Fig 4.6 B). After treating PBMs with CCR2 inhibitor, they migrated towards CM from myofibroblasts, senescent fibroblasts and their untreated and time controls (Fig. 4.6 C); migration observed to be reduced by 91%, 97.3%, 94.78%, and 92.57% towards CM from 24 h, 48 h, 96 h and 15 d untreated control respectively, while migration towards CM from 24 h, 48 h, and 96 h TGF-β1 treated myofibroblasts was reduced by 79.4%, 83.6%, and 89.8% respectively, and migration towards CM from 15 d cisplatin senesced fibroblasts showed least reduction amongst all with a 76.3% decrease as shown in Fig. 4.6 C.

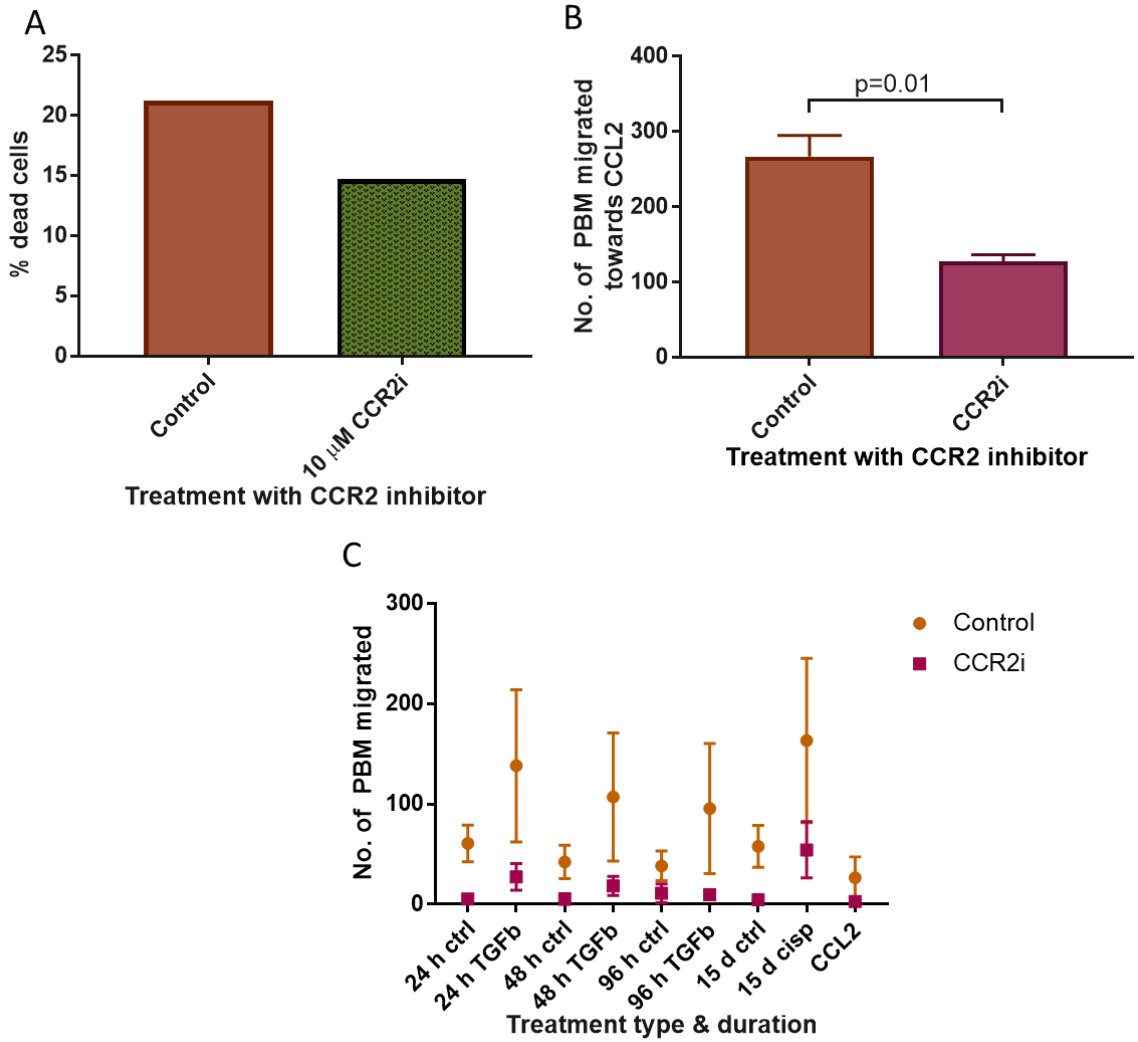

Figure 4.6: Effect of CCR2 inhibition on monocyte migration. PBMs were treated with 10 μM CCR2 inhibitor (CCR2i) RS 504393 for 1 h, followed by 4 h in a transwell assay set up at 37° C and 5% CO_2, n=1. A) Trypan blue exclusion was used to examine cell viability 4 h after treatment with CCR2i for 1 h. CCR2i induced 33% less death at 10 μM concentration compared to serum free media. B) After inhibiting CCR2, migration towards recombinant CCL2 showed a 0.52 decrease with p=0.01 from student t test with n = 3 biological repeats. C) Treatment with CCR2i also decreased migration towards CM from 24 h, 48 h, 96 h and 15 d untreated control fibroblasts by 91%, 97.3%, 94.78%, and 92.57%, respectively, while migration towards CM from 24 h, 48 h, 96 h TGF-β1 treated myofibroblasts, and 15 d cisplatin senesced fibroblasts decreased by 79.4%, 83.6%, 89.8% and 76.3%, respectively. Statistical analsyis – two way ANOVA with no significance with n = 3 biological repeats. All data are mean +/- SEM.

4.8 Inhibition of chemokine receptors on monocytes with pertussis toxin

As presented in fig. 4.6 B, it was observed that PBM migration towards CM from myofibroblast and senescent fibroblasts was not completely abolished upon inhibiting CCR2. Evidence exists suggesting monocytes possess numerous chemokine receptors that are promiscuous in nature and interact with more than one ligand/chemokine (summarised in Table 9), which can compensate for the loss of one receptor to some degree (Anders et al., 2003, Sandblad et al., 2015).

Table 9. Chemokine receptors present on monocytes, and their interacting ligands (Anders et al., 2003, Sandblad et al., 2015).

Receptor	Ligand	Alternative name
CCR1	CCL3,5,7,8,13,14,15,16,23	MIP-1α, Rantes, MCP-3,2,4, HCC-1,2,4, MPIF-1
CCR2	CCL2,7,8,13	MCP-1,3,2,4
CCR3	CCL5,13,24,26	Rantes, MCP-4, Eotaxin-2,3
CCR4	CCL17,22	TARC, MDC
CCR5	CCL3,5,8	MIP-1α, Rantes, MCP-2
CCR6	CCL20	LARC
CCR7	CCL19,21	ELC, SLC/6Ckine
CCR8	CCL1,16	I-309, HCC-4
CCR9	CCL25	TECK
CCR10	CCL27	CTAK/Eskine
CXCR1	CXCL1,4,6,8	Groα, PF4, GCP-2, IL-8
CXCR2	CXCL1,4,5,6,7,8	Groα, PF4, ENA-78, GCP-2, NAP-2, IL-8
CXCR3	CXCL9,10,11	Mig, IP-10, I-TAC
CXCR4	CXCL12	SDF-1
CXCR5	CXCL13	BCA-1
CXCR6	CXCL16	SR-PSOX

CXCR7	CXCL11,12	I-TAC, SDF-1
XCR1	XCL1	Lymphotactin
CX3CR1	CX3CL1	Fractalkine
ChemR23		RARRES2/Chemerin

To investigate whether other chemokine receptors were compensating for the inhibition of CCR2, PBMs were treated with Pertussis toxin (PTX) that inhibits most G-protein coupled receptors by ADP-ribosylation of $G\alpha_{i/o}$ proteins resulting in uncoupling of receptors from G-proteins (Mangmool and Kurose, 2011).

PBMs pre-treated with 1 µg/ml PTX for 30 min where it did not affect cell viability (Malik et al., 2009, Sano et al., 2000), showed a 0.71 fold decrease in migration from untreated PBM with p=0.03 (Fig. 4.7 A). When PTX treated PBMs were migrated towards CM from 24 h, 48 h, 96 h, and 15 d untreated controls, migration decreased by 77%, 19.7%, 47.29%, and 71% compared to untreated PBMs, respectively; while migration towards CM from 24 h, 48 h, and 96 h TGF-β1 treated myofibroblasts, and 15 d cisplatin senesced fibroblasts decreased by 55.5%, 72.4%, 32.4% and 75.85% respectively (Fig 4.7 B).

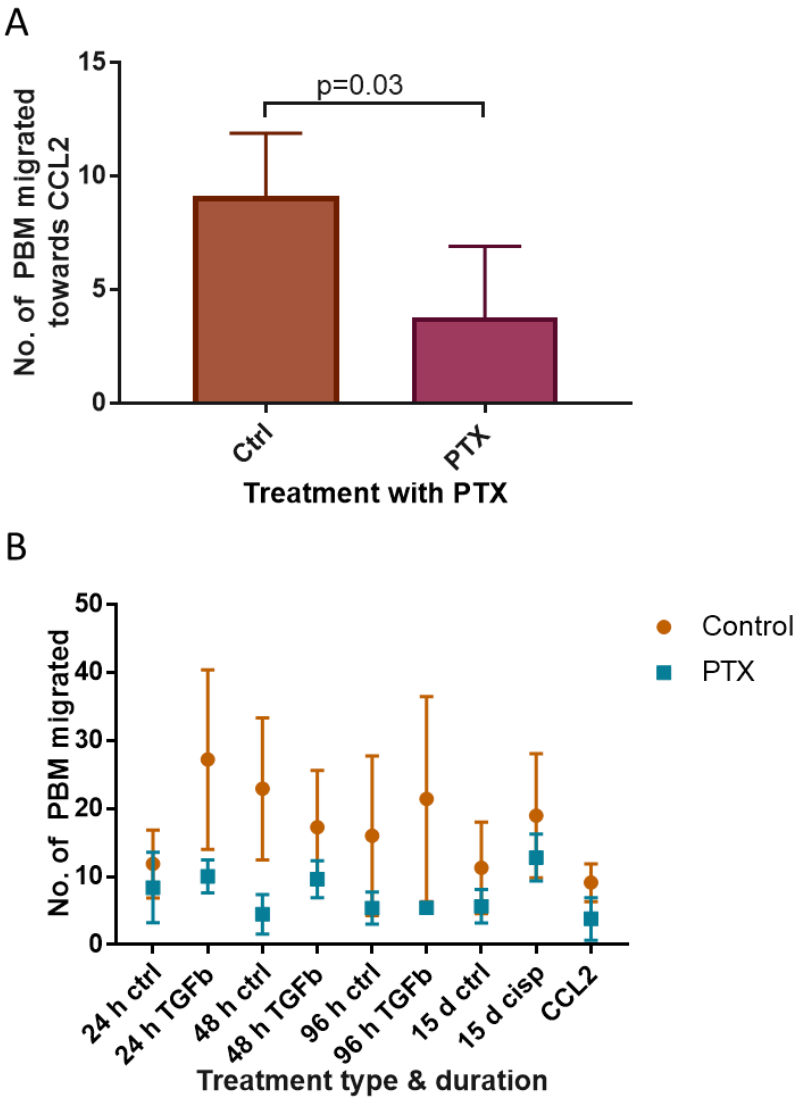

Figure 4.7: Effect of PTX treatment on migration of PBM. PBMs were treated with 1 µg/ml of PTX for 30 min prior to migration towards CM. A) After treatment migration towards recombinant CCL2 decreased with a fold change of 0.71. B) Migration of PTX treated PBMs towards CM from 24 h, 48 h, 96 h, and 15 d untreated controls, decreased by 77%, 19.7%, 47.29%, and 71% compared to untreated PBMs, respectively; while migration towards CM from 24 h, 48 h, and 96 h TGF-β1 treated myofibroblasts, and 15 d cisplatin senesced fibroblasts decreased by 55.5%, 72.4%, 32.4% and 75.85% respectively. Data are mean +/- SEM with n=3.

Between CCR2 inhibition and PTX treatment (Fig. 4.8), CCR2 inhibition reduced overall recruitment of PBMs more efficiently, in response to 24 h myofibroblast CM ($p=0.0349$), 48 h myofibroblast CM ($p=0.0332$) and 24 h control CM with $p= 0.0309$ (Fig. 4.8). The most significant decrease in recruitment was seen by senescent fibroblasts when CCR2 was inhibited, compared to untreated PBMs, with $p=0.008$.

Pertussis toxin is known to be a broad spectrum inhibitor of GPCRs which comprise of most chemokine receptors, surprisingly PTX was not as efficient in preventing PBM migration towards the CM from myofibroblast, but reduced migration towards CM from senescent fibroblast significantly with $p=0.008$ (Fig. 4.8). This is discussed further in section 6.3.

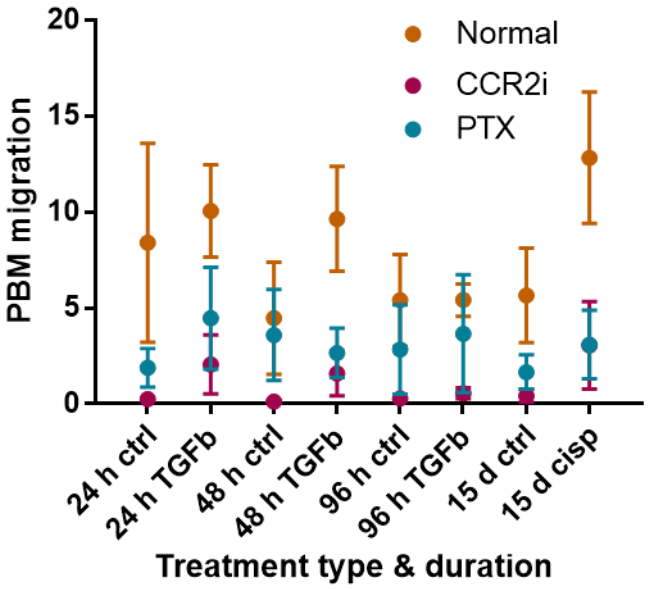

Figure 4.8: Comparison of migration of untreated, CCR2 inhibited (CCR2i), and pertussis toxin (PTX) treated PBMs towards CAF CM. CCR2 inhibitor decreased migration of PBMs the most, with significant decrease by 24 h control CM (p=0.0309), 24 h TGF-β1 CM (p=0.0349), 48 h TGF-β1 CM (p=0.0332), and 15 d cisp (p=0.0008). Decrease in migration by PTX was not as effective as CCR2 inhibition but showed a significant decrease towards 15 d cisp CM with p=0.00083. Statistical analysis – Two way ANOVA, data are mean +/- SEM with n=3.

4.9 Monocyte recruitment by patient CAFs

Next, OSCC patient-derived CAFs were examined to compare similarities and differences between myofibroblasts and senescent fibroblasts in the context of monocyte recruitment. For this study, senescence associated β-galactosidase assay, CCL2 secretion and monocyte recruitment by CAF cultures BICR18, BICR69, BICR73, BICR78, (kindly provided Professor Stephen Prime and Professor Eric Parkinson from the Blizard Institute, QMUL) and CAF002 (generated in Sheffield by Amy Harding, Ref 13/NS/0120, STH17021, approved by Sheffield research ethics committee) were investigated. CAFs BICR18 and BICR78 were isolated from genetically unstable (GU) OSCC, while BICR69 and BICE73 were isolated from genetically stable (GS) OSCC (Hassona et al., 2013b).

Both Hassona *et al* and Kabir *et al* provided evidence that CAFs from GU OSCC are more senescent in comparison to CAFs from GS OSCC (Hassona et al., 2013b, Kabir, 2015). Senescence associated β-galactosidase assay was performed on the CAFs used in this study (Fig. 4.9); CAFs from GS OSCC, BICR69 and BICR73 showed 0% and 4% positively stained cells, respectively. While CAFs from GU OSCC, BICR78 and BICR18 exhibited 100% and 70% positively stained cells, in

agreement with previous evidence. Genetic status of the tumour from which CAF002 was isolated was unknown at the time of this study, but it showed less than 2% positive staining, suggesting lack of presence of senescent fibroblasts.

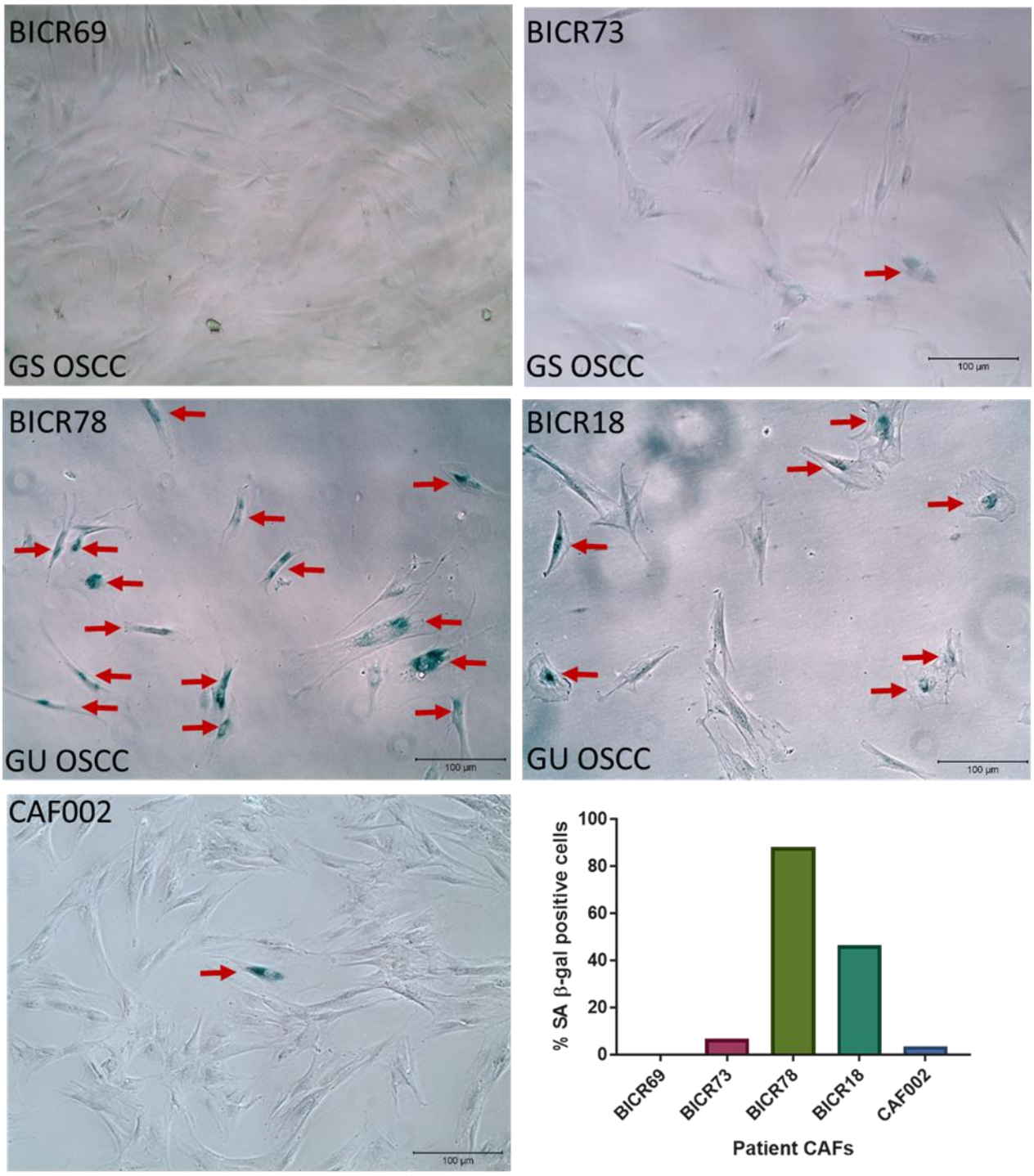

Figure 4.9. Senescence associated β-galactosidase assay on CAFs: CAFs from genetically stable OSCC, BICR69 and BICR73 showed 0% and 4% positively stained cells, respectively. CAFs from genetically unstable OSCC, BICR78 and BICR18 showed 100% and 70% positively stained CAFs. CAF002 exhibited only less than 2% positively stained cells; n=1 biological repeat.

NOF343 produced very little CCL2 (14.67 pg/ml) but CAF002, BICR18, and BICR78 (both from GU OSCC) secreted elevated levels ($p<0.0001$), with slightly lower levels secreted by BICR73 (GS OSCC) ($p<0.0005$) as shown in fig. 4.10 A. Amongst the patient CAFs, BICR69 from GS OSCC produced the lowest levels of CCL2 (20.58 pg/ml), significantly lower than BICR73 with $p<0.0005$ and from BICR78, BICR18, and CAF002 with $p<0.0001$ (Fig. 4.10 A). BICR78 from GU OSCC secreted the highest amount of CCL2 (1054 pg/ml), significantly higher with $p<0.0001$ than NOF343, BICR69, BICR73, BICR18, and CAF002. Genetic status of the tumour from whose stroma CAF002 was isolated is not known, but it still exhibited higher secretion of CCL2 ((435.7 pg/ml) compared to CAFs from GS OSCC – BICR69 and BICR73, as well as NOF343 (Fig 4.10 A).

An important observation to note is that CAFs from GU OSCC are more senescent (Fig. 4.10) and secreted more CCL2 in comparison to CAFs from GS OSCC. This corresponds to result in Fig. 4.5 B which reports senescent fibroblasts generated for this study also secreted more CCL2 than myofibroblasts.

When Pearson's correlation was determined between data from fig. 4.10 A & B, a positive trend was suggested between monocyte recruitment between CCL2 secretion and PBM recruitment by CAFs with r = 0.39 (Fig 4.10 c).

Monocyte recruitment by BICR18 was significantly higher compared to recruitment by NOF343, BICR69, BICR73, BICR78, and CAF002 with $p<0.0001$. NOF343, BICR69, and CAF002 exhibited significantly low monocyte recruitment compared to BICR73 and BICR78 with $p<0.0005$ and $p<0.0001$, respectively. Even though BICR18 secreted less CCL2 than BICR78, it recruited more monocytes, raising the possibility of other chemokines and factors having a role in monocyte recruitment.

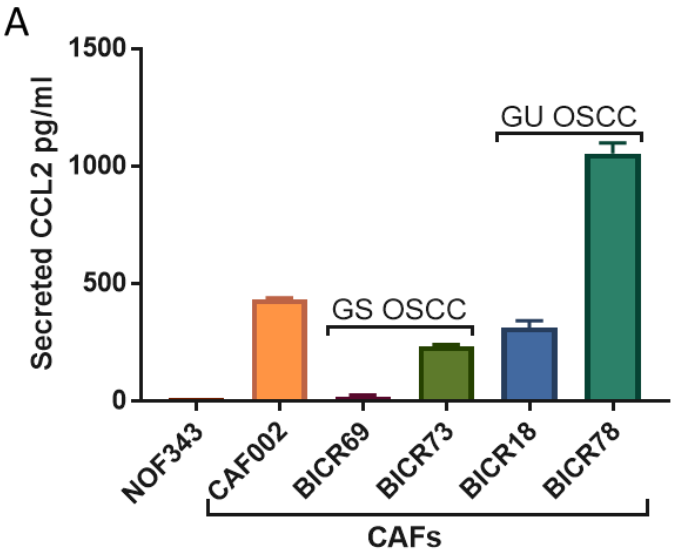
A
Secreted CCL2 pg/ml
1500
1000
500
0
GU OSCC
GS OSCC
NOF343
CAF002
BICR69
BICR73
BICR18
BICR78
CAFs

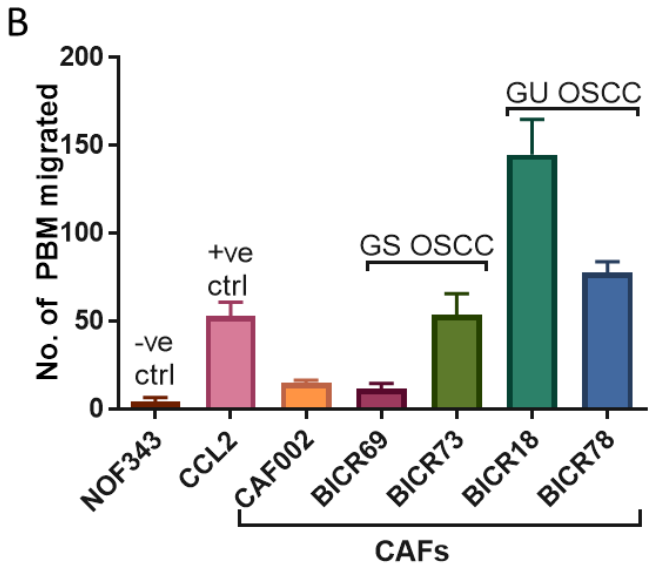
B
No. of PBM migrated
200
150
100
50
0
GU OSCC
GS OSCC
+ve ctrl
-ve ctrl
NOF343
CCL2
CAF002
BICR69
BICR73
BICR18
BICR78
CAFs

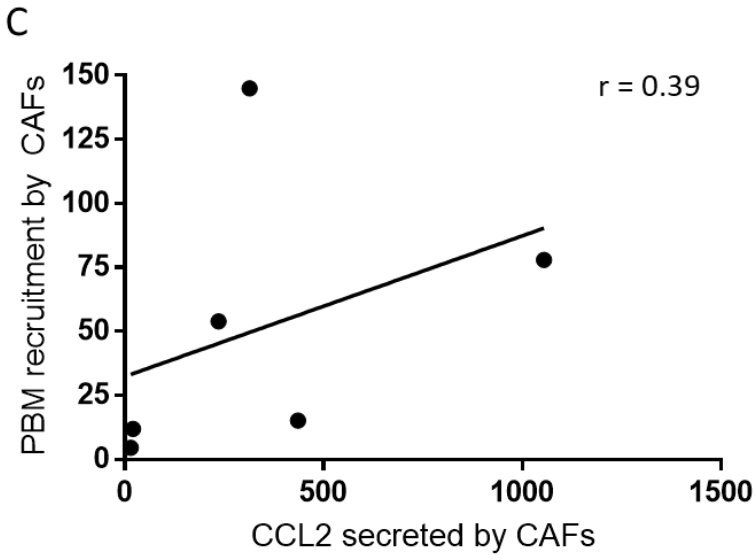
C
PBM recruitment by CAFs
150
125
100
75
50
25
0
r = 0.39
0
500
1000
1500
CCL2 secreted by CAFs

Figure 4.10. Levels of CCL2 secretion and monocyte migration by patient CAFs: CAFs from patients were cultured as described in section 2.6 until 80% confluency, followed by change of medium to serum free medium to be conditioned for 24 h. Levels of CCL2 were measured in the collected CM, and PBMs were migrated towards the same CM. A) Normal oral fibroblast NOF343 (14.67 pg/ml,) and BICR69 (20.58 pg/ml) from genetically stable OSCC (GS OSCC) secreted significantly low amounts of CCL2 compared to BICR73 (235.7 pg/ml, $p<0.04$), BICR78 (1054 pg/ml), BICR18 (314 pg/ml) and CAF002 (435.7 pg/ml) with $p<0.0001$. BICR78 secreted the highest amount of CCL2 with $p<0.0001$ significance to NOF343, BICR69, BICR73, BICR18, and CAF002. Secretion of CCL2 by BICR73 and BICR18 were also significant to secretion by CAF002 with $p<0.0005$, and $p<0.04$, respectively. B) NOF343 and BICR69 recruited significantly fewer number of monocytes with $p<0.0001$ compared to BICR73, BICR78, and BICR18. While BICR18 significantly recruited more monocytes than BICR73, BICR78 and CAF002 with $p<0.0001$ even though it secreted lower levels of CCL2. Recruitment by CAF002 compared to BICR73 and BICR78 was significantly low as well, with $p<0.0005$ and $p<0.0001$, respectively. C) Pearson's correlation coefficient suggests a trend between CCL2 secretion and PBM recruitment with $r = 3.9$. Statistical analysis – ANOVA & Pearson's correlation. Data are mean +/- SEM, n=3 biological repeats.

4.10 Monocyte recruitment by fibroblasts cultured in cancer cell line CM

Normal oral fibroblasts were also cultured for 24 h in CM derived from OSCC cancer cell lines (H357, a non-metastatic line from the tongue with mutant p53, which produces high levels of TGF-β1, and undergoes EMT in response to it TGF-β1. While SCC4 is a metastatic line, also from the tongue.), CM was washed off thoroughly and fresh serum free media was added to the NOF culture to be conditioned by them for 24 h. The resulting CM from NOF was collected and examined for CCL2 and used in migration assays to recruit PBMs to examine whether cancer cells can influence fibroblast secretome in a paracrine manner, in relation to monocyte recruitment (Fig. 4.11 A and B). Both indirect co-cultures, NOF343 with H357 CM (5906 pg/ml) and NOF343 with SCC4 (3357 pg/ml) exhibited a high level of secretion of CCL2 with $p<0.0001$, compared to NOF343 (14.67 pg/ml) on its own. Significantly greater recruitment of monocytes by H357 co-culture ($p=0.0007$) and SCC4 co-culture ($p<0.0001$) was observed compared to NOF343 (Fig. 4.11 A and B). H357 co-culture exhibited significantly higher levels of CCL2 than SCC4 co-culture, but the numbers of monocytes recruited was not statistically different, perhaps suggesting saturation of receptors.

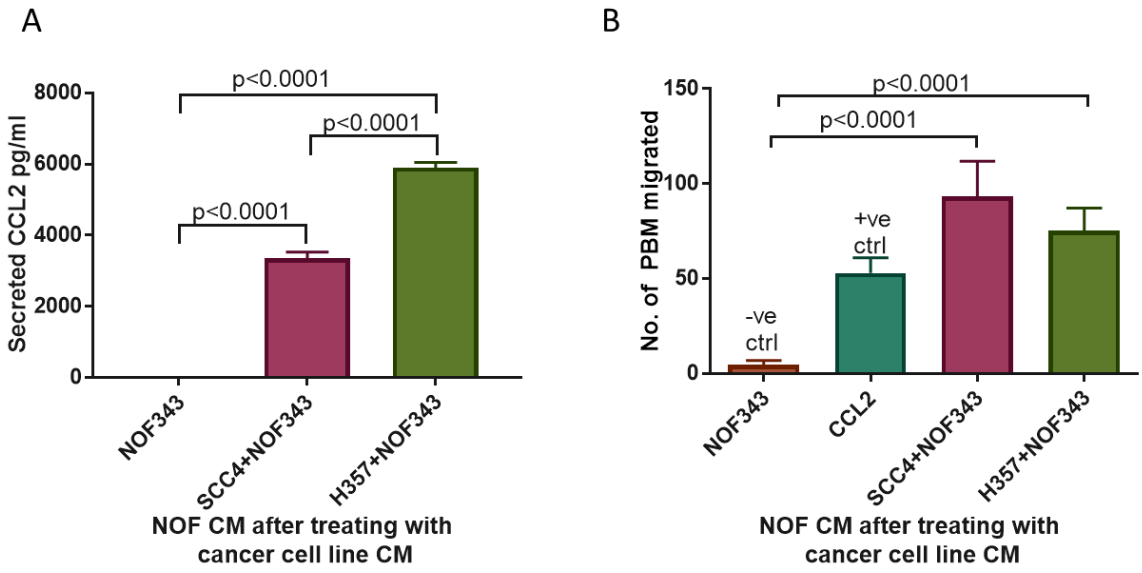

Figure 4.11. Soluble factors from cancer cell line (H357 & SCC4) increased subsequent secretion of CCL2 and monocyte recruitment by resulting NOF CM: NOF343 was cultured with CM from cancer cell line H357 and SCC4 for 24h, washed and changed to fresh SFM to be conditioned. The subsequent media from NOF343 was examined for CCL2 and monocyte recruitment. A) Both indirect co-cultures, H357+NOF343 and SCC4+NOF343 lead to a significant increase, with $p<0.0001$ in secretion of CCL2 compared to NOF343 alone. There was significant difference in effects of H357 and SCC4 on CCL2 secretion after co-culture where secreted factors from H357 caused more CCL2 secretion than SCC4 secretory factors ($p<0.0001$). B) CM from both, H357+NOF343 and SCC4+NOF343 co-culture recruited more monocytes compared to NOF343 alone, but SCC4+NOF343 recruited more monocytes than H357+NOF343. Statistical analysis – ANOVA, data are mean +/- SEM, n=3 biological repeats.

4.11 Effect of soluble factors from polarised macrophages on fibroblast activation:

The TME hosts numerous cells surrounding the malignant cells, including a variety of immune cells, and macrophages being one of the many (section 4.9). Macrophages possess the plasticity to polarise towards an M1 or M2 phenotype in response to cytokines in the surrounding microenvironment (Pollard, 2009). It is important to note that macrophages also secrete cytokines and other factors; therefore after being recruited to TME it was hypothesised here that they may be capable of influencing differentiation of normal fibroblast into developing a CAF-like phenotype before or after their own polarisation. To investigate this possibility, PBMs were differentiated in to M0, M1, and M2 macrophages (as described in section 3.9.2), CM was prepared and collected, and normal oral fibroblast (NOF343) were cultured in macrophage CM for 24 h while TGF-β1 and SFM were used as positive and negative controls, respectively. Immunocytochemistry was then used to examine α-SMA expression as a marker of fibroblast activation/myofibroblast differentiation (Fig. 4.12). Highest SMA expression was induced by M0 CM, followed by M1 and M2 (Fig. 4.12 A-C, F). In comparison to SFM, α-SMA expression showed a trend toward

being induced by M0-derived CM, but this didn’t reach significance ($p<0.065$; Fig. 4.12 F).

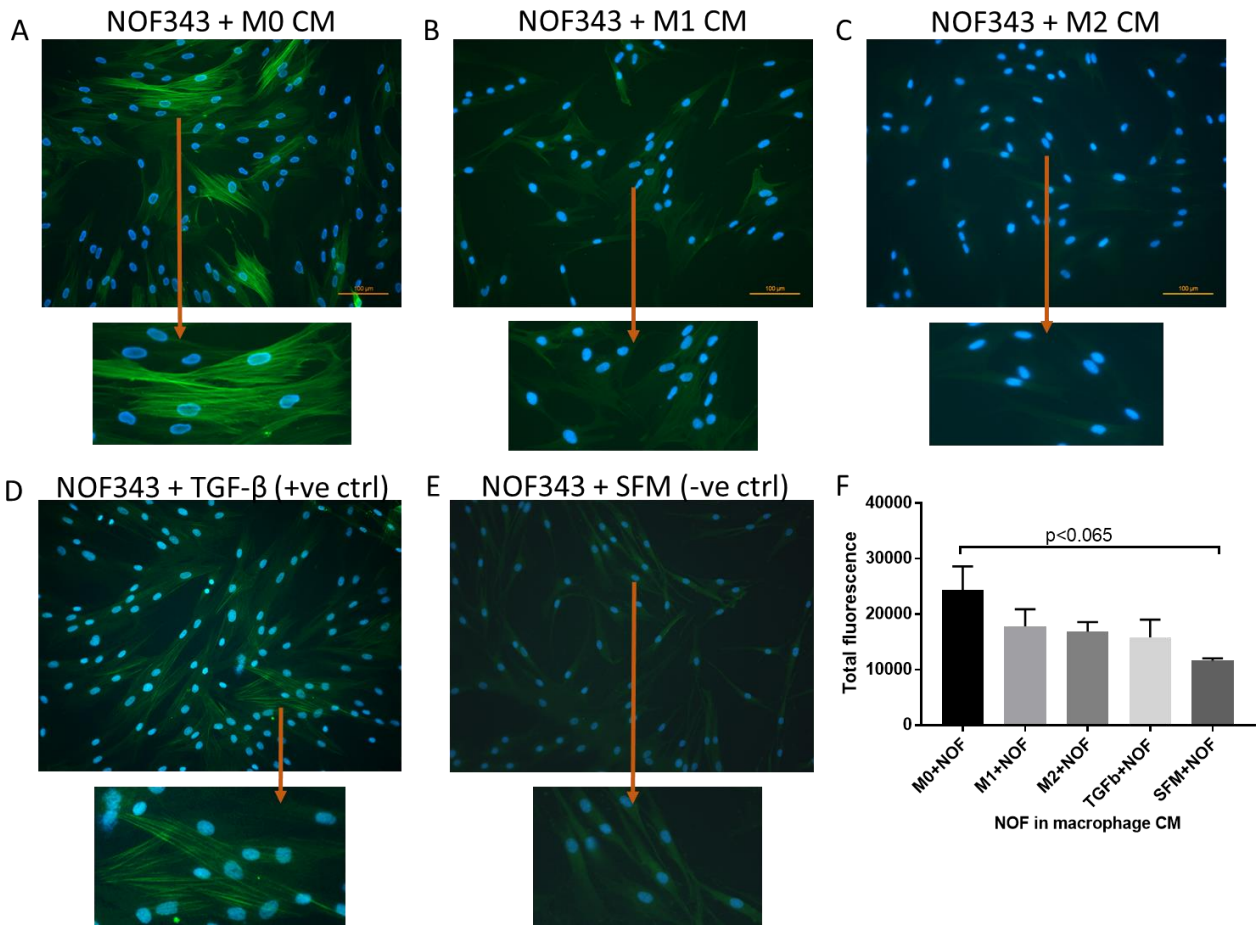

Figure 4.12: Validation of SMA expression in NOF induced by macrophage CM. A) SMA expression in NOF343 after culturing with M0 macrophage CM for 24 h. B) SMA expression in NOF343 after culturing with M1 macrophage CM for 24 h. C) SMA expression in NOF343 after culturing with M2 macrophage CM for 24 h. D) SMA expression in NOF343 after TGF-β1 treatment for 24 h. E) SMA expression in NOF343 after culturing in SFM for 24 h. F) Graph comparing SMA expression between different conditions, with $p<0.065$ between SMA induced by M0 CM and SFM. Statistical analysis performed – ANOVA, error bars indicate SEM, with n = 3 wells.

4.12 Examination of the existence of any correlation between the presence of CAFs and the number of TAMs in tumour tissue *ex vivo*

Based on results from figs. 4.3 A, 4.4, 4.5, 4.10 and 4.11, highlighting monocyte recruitment capabilities displayed by myofibroblasts, senescent fibroblasts, patient CAF, and NOF following cancer cell line co-culture, the next step was to begin to examine the in vivo relevance of these findings by assessing the existence of any correlation between the presence of CAFs and macrophages in tumour and stroma in sections from a cohort of OSCC cases. Using immunohistochemistry on a cohort OSCC tumours (appendix 3), Histoquest software, and CAF marker-α-SMA and macrophage marker-CD68 (as described in section 2.21), to observe a correlation between presence of α-SMA positive CAFs and CD68 positive TAMs, as shown in Fig. 4.13 A. Pearson's correlation coefficient was applied to measure correlation between the presence of α-SMA positive CAFs in TME/stroma (tissue surrounding tumour mass) and at tumour invasive front, and CD68 positive TAMs in TME/stroma and tumour mass. As seen from Fig 4.13 B, presence of CAFs in TME/stroma negatively correlated with presence of TAMs in TME and in tumour mass with r = -0.3461 and r = -0.09594, respectively (Fig. 4.13 B and C). On the other hand, presence of CAFs near the tumour invasive front suggested a positive correlation

with presence of TAMs in TME and in the tumour with r = 0.1192, and r = 0.5666, respectively (Fig. 4.13 D and E).

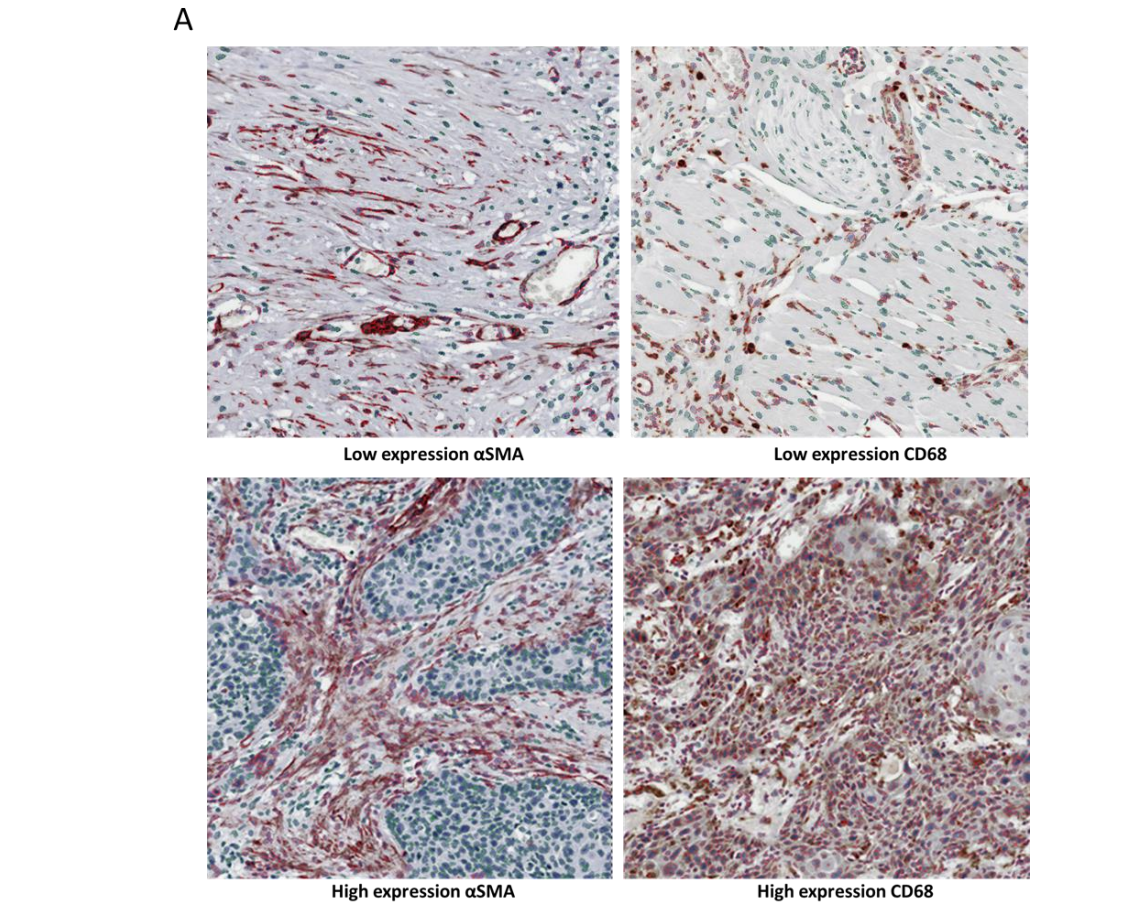
A
Low expression αSMA
Low expression CD68
High expression αSMA
High expression CD68
B
r = -0.3461
% of CD68 stained cells in TME
% of SMA stained cells in TME
C
r = -0.09594
% of CD68 stained cells in tumour
% of SMA stained cells in TME
D
r = 0.1192
% of CD68 stained cells in TME
% of SMA stained cells at tumour invasive front
E
r = 0.5666
% of CD68 stained cells in tumour
% of SMA stained cells at tumour invasive front

Figure 4.13: Immunohistochemical analysis of CAF marker α-SMA and macrophage marker CD68. Adjacent OSCC sections were stained for α-SMA and CD68 immunohistochemically, and percentage (%) of positively stained cells in the tumour, in stroma/tumour microenvironment (TME) and at tumour invasive front were examined for any correlation. A) Both, CAF (α-SMA marker) and tumour associated macrophage (TAM, CD68 marker) antibodies were able to detect their respective protein when sparse or abundant. B) and C) Graphs show a negative Pearson's correlation between CAFs in TME and TAMs in TME (r = -0.3461) as well as CAFs in TME and TAMs in tumour (r = -0.0959). D) Graph shows no correlation between presence of CAFs at the tumour invasive front and presence of TAMs in the tumour, with r = 0.1192 E) Pearson's correlation coefficient showed a trend between presence of CAFs at the tumour invasive front and presence of TAMs in the tumour with r = 0.5556. Statistical analysis – Pearson's correlation coefficient, data are mean +/- SEM, n = 10

4.13 Summary

In this chapter, monocyte recruitment capabilities of senescent fibroblasts, treated with a chemotherapeutic drug-cisplatin, and myofibroblasts, generated by exposure of NOF to TGF-β1 for different durations (24 h, 48 h, and 96 h), was studied. In addition the recruitment capabilities of NOF exposed to cancer cell-derived media and CAF isolated from tumours were analysed. Comparing senescent fibroblasts and myofibroblasts, CM from senescent fibroblasts recruited the most number of THP-1 cells and peripheral blood monocytes (PBM), while 24 h TGF-β1 treated myofibroblasts recruited the most number of THP-1 cells and PBMs between the three time points (24 h, 48 h and 96 h), however, the recruitment by 24 h myofibroblast was still less than by senescent fibroblasts.

It was found that cisplatin treatment induced secretion of high amounts of CCL2 (a well-documented monocyte chemoattractant), in addition 24 h treated TGF-β1 myofibroblast also secreted high levels of CCL2 compared to untreated controls, which again declined with longer TGF-β1 treatment. PBMs also exhibited high expression of CCR2. Therefore, it could be surmised that PBMs were mostly recruited through CCL2/CCR2 axis; this was confirmed by inhibiting CCR2 receptor

(CCR2i) as migration of PBM towards senescent fibroblast CM and 24 h TGF-β1 treated myofibroblast CM was reduced significantly by addition of CCR2i. Migration was not abolished completely after CCR2 inhibition, suggesting other promiscuous chemokine-receptors may compensate and interact with CCL2 and other chemokines present in the CM. Promiscuity of chemokine receptors has been described before (Zlotnik and Yoshie, 2012)

To test this hypothesis, PBMs were then treated with pertussis toxin (PTX) to block G-protein coupled chemokine receptors. Treatment of PBMs with PTX reduced their migration towards CM but not as efficiently as CCR2 inhibition. A possible explanation for this is discussed further in section 6.3.

Patient CAFs were also examined from both genetically stable OSCC (GS OSCC) (BICR69 and BICR73) and genetically unstable OSCC (GU OSCC) (BICR78 and BICR18), and CAF002 from tumour of unknown genetic status at the time of study. It was found that CAFs from GU OSCC were more senescent compared to CAFs from GS OSCC and CAF002, and correspondingly secreted more CCL2. CAFs from GU OSCC also recruited more PBMs compared to CAFs from GS OSCC

and CAF002, however, BICR18 recruited more PBMs in spite of secreting lower levels of CCL2 compared to BICR78, suggesting other secreted factors may be involved; this is investigated further in chapter 5.

NOF were also co-cultured with CM from cancer cell lines – H357 and SCC4, and exhibited high levels of CCL2 and recruitment more PBMs compared CM from NOF alone.

Once recruited, monocytes differentiate in to macrophages and are polarised based on the cytokine environment present around (Qian and Pollard, 2010). The effect of this polarisation on fibroblast phenotype was examined. It was found that unpolarised M0 macrophages activated NOF the most, a surprising finding discussed further in section 6.3.

Immunohistochemical analysis of tumour sections for CAF marker SMA, and TAM marker CD68 revealed no correlation between presence of CAFs in TME and presence of TAM in TME and tumour. However, CAFs present near the tumour invasive front suggested a correlation to presence of TAM in the tumour, further discussed in section 6.3.

Since PBMs migrated towards CM in spite of CCR2 blockage, evidently blocking CCL2/CCR2 axis, and the fact that, BICR18 recruited more PBMs than BICR78 in spite of secreting lower levels of CCL2 suggests secretion of other chemokines by myofibroblast, senescent fibroblast, and a patient CAFs, which lead to further analysis of the same using mass spectrometry.

Chapter 5

5. Secretome of CAF phenotypes

Secreted proteins play an important role in intra- and intercellular communication; therefore they hold a key to understanding cancer progression and metastasis. Some of these secreted proteins are also found in the bloodstream, saliva or lymphatic system, sometimes far from the site of disease and so may serve as a diagnostic biomarker for early cancer diagnosis, or as a measure of cancer progression or response to treatment.

As mentioned in section 1.4, CAFs promote cancer progression by secreting factors that modify the ECM, promote angiogenesis, metabolism, replication, and metastasis of cancer cells. They are also instrumental in recruiting and manipulating immune cells such that cancer cells are able to evade the body's immune system. But CAFs are made up of different sub-populations, therefore it is important to narrow down and identify factors secreted by different CAF phenotypes to examine whether each phenotype has a specific role in cancer progression and may therefore provide therapeutic targets. This chapter sheds light on the secretome of CAF phenotypes using mass spectrometry for further scrunity.

5.1. Hypothesis:

Myofibroblasts and senescent fibroblasts develop distinct secretomes to differentially influence their microenvironment.

5.2. Aims:

- Analyse concentrated and purified conditioned media from myofibroblasts, senescent fibroblasts, and patient CAF by mass spectrometry.
- Compare expression of cytokines in the conditioned media from myofibroblasts, and senescent fibroblasts.
- Examine the effects of conditioned media from myofibroblasts, senescent fibroblasts, and patient CAF on macrophage polarisation through qPCR for CD80, CD86, CD163, and CD206

5.3. Mass spectrometry

A mass spectrometer (MS) is generally composed of three basic components, namely the ioniser, the mass analyser, and the mass detector. The function of the ioniser is to ionise molecules/peptides being tested and imparting a charge to them

with each peptide having a unique mass to charge (m/z) ratio. The mass analyser then evaluates the mass to charge ratio, and the mass detector counts peptides for each m/z ratio reported by the mass analyser; the resulting output is a mass spectra.

For this investigation, conditioned media was concentrated, digested with trypsin, tertiary structures denatured by urea, cysteine residues modified using iodoacetamide, and purified to remove inorganic salts (Wysocki et al., 2005). Subsequently, label-free quantification was selected to expand the range of discovery of peptides. This method also requires lower quantities of samples, which were run with the settings described in section 2.23. The samples tested were: 24 h control (24 h ctrl), 24 h TGF-β1-induced myofibroblast (24 h TGF-β1), 15 d control (15 d ctrl), 15 d cisplatin treated senescent fibroblast (15 d cisp), and tumour-derived CAF002 (CAF).

After the data was processed, principal component analysis revealed the technical repeats clustered together but proteins from CM from different conditions clustering separately (Fig. 5.1). Both 24 h TGF-β1-treated NOF (myofibroblast) and 15 d cisplatin-treated NOF (senescent) cluster away from 24 h control (component 1 axis), and from each other (component 2 axis) highlighting the difference in protein

expression between the three. However, CAF triplicates cluster further along the component 1 axis from 24 h TGF-β1 and 15 d cisp, with a larger difference in protein reads from 15 d cisp on component 2 axis, further validating its non-senescent phenotype from Fig. 4.9.

A remarkable observation in the principal component analysis of CM is the difference between 24 h control and 15 d control. Throughout this study it was observed that 15 d control secreted increased quantities of IL-6 (Fig. 3.6), CCL2 (Fig. 4.5), and exhibited elevated mRNA expression of FNEDA and COL1A1 (Fig. 3.7) and even recruited more monocytes than 24 h control CM as seen in Fig. 4.2 and 4.3. However, 15 d control did not show an increased expression of $p16^{INK4A}$ mRNA, and stained negatively in SA β-gal assay, confirming that these fibroblasts were not senescent; the low levels of p21 mRNA also make quiescence unlikely (Adomako et al., 2015, Sharpless and Sherr)., but further experiments would be required to determine the phenotype of these cells

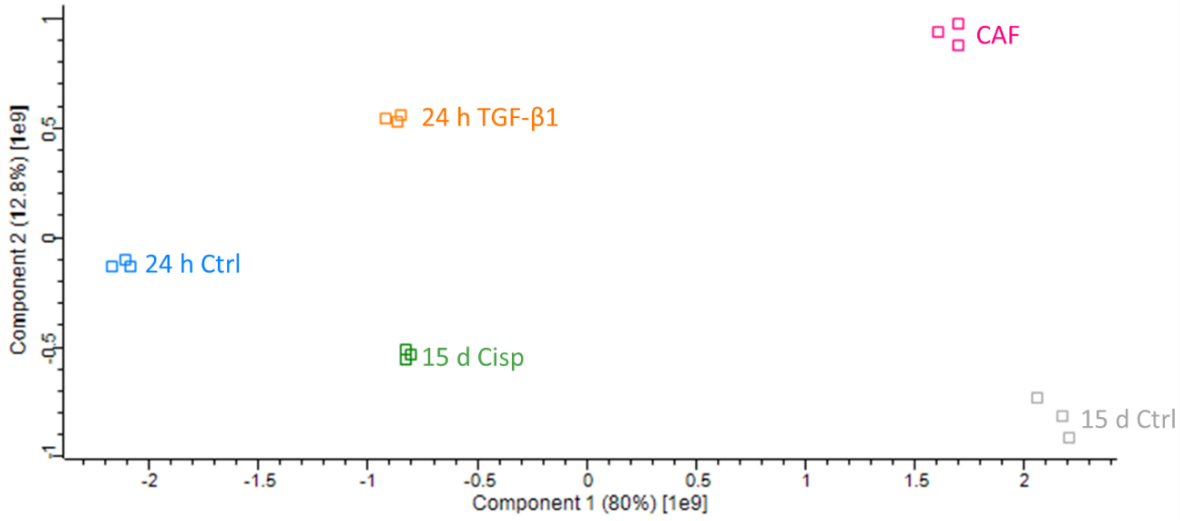

Figure 5.1. Principal component analysis (PCA) of MS analysis: PCA plots variations present within a data set, increasing distance between any two data points denotes increasing variation based on multiple variables (various protein secretions in this case). The graph shows technical repeats (3 boxes) processed in MS clustered together, representing similarity between technical repeats. CM from myofibroblast (24 h TGF-β1) and senescent fibroblast (15 d cisp) showed distinct difference between each other (component 2 axis) and from both 24 h control and CAF on component 1 axis. Proteins expressed by CAFs varied more from 15 d cisp than 24 h TGF-β1 (based on component 2 axis). Another discrete set of proteins were secreted by 15 d control, with most variation compared to 24 h control, followed by CAF, 24 h TGF-β1, and 15 d cisp. N = 3 biological repeats pooled together and then divided in to 3 as technical repeats for MS.

From a list of thousands of protein hits (signal intensities), pairs of fibroblast phenotypes were statistically compared one at a time using T test due to absence of one way ANOVA test in Perseus software; highlighting significantly different proteins expressed between two phenotypes compared (Angi et al., 2016). From the statistical analyses, 193 proteins were identified as significantly expressed between the five samples. Proteins from 24 h TGF-β1 transdifferentiated myofibroblast, 15 d cisplatin induced senescent fibroblast and patient CAF002 were filtered for 5-fold increase from 24 h control secreted protein and putative pathways they may be engaged in analysed using reactome-database for biological pathways (Reactome). The majority of proteins secreted by myofibroblasts were predicted to participate in metabolism (19 proteins; 21% of total), followed 17% (16 proteins) in ECM organisation, and 15% (14 proteins) in signal transduction (Fig. 5.2). Only 8% (7 proteins) of the secreted proteins engaged in the immune system, while the others participate in vesicle transportation of molecules, homeostasis, cell-cell adhesion, cell cycle, gene expression and disease (Fig. 5.2).

About 31% (26 proteins) of the secreted proteins from senescent fibroblasts up-regulated from 24 h control fibroblasts (24 h control fibroblasts were chosen as the comparator to negate effects of 2D culture has on primary cells) participated in ECM organisation, followed by 25% (19 proteins) in metabolism and 16% (13 proteins) as seen in Fig. 5.3. About 9 secreted proteins, making up 11% from senescent fibroblasts engaged in immune system (Fig. 5.3). The majority of CAF secreted proteins with a fold increase from normal 24 h fibroblast are known to participate in ECM organisation (21 proteins making up 29%), followed by 20% (14 proteins) in signal transduction, and 18% (13 proteins) engaged in metabolism as seen in Fig. 5.4. Roughly, 7% (5 proteins) participated in pathway from the immune system (Fig. 5.4).

From this comparison we speculate that there were more variety of proteins secreted from senescent fibroblasts that modulated the ECM compared to the plethora of ECM related proteins from myofibroblast. Senescent fibroblast proteins also engaged heavily in metabolism as well as in pathways involved in the immune system, compared to both patient CAF and myofibroblast.

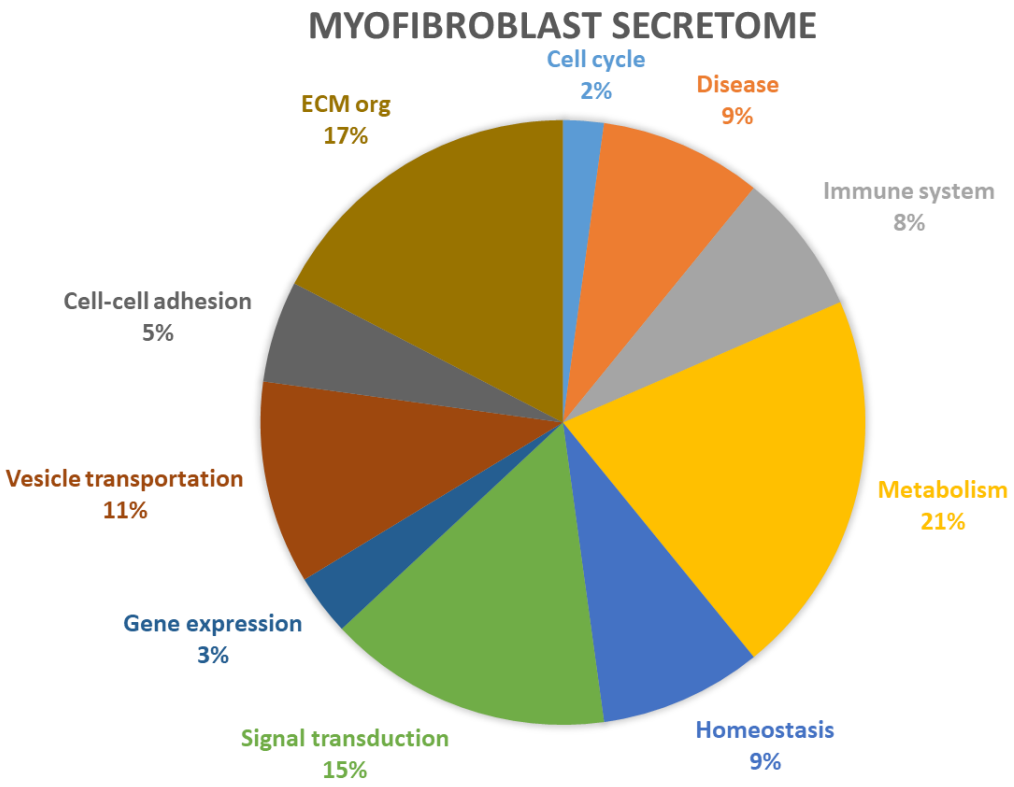

Figure 5.2. Biological pathways myofibroblast secreted proteins have previously been found to engage in: The pie chart represents proteins with fold increase compared to 24 h control CM and the pathways they engage in. A majority of proteins secreted by 24 h TGF-β1 transdifferentiated myofibroblast participate in metabolism (21%), followed by 17% of proteins playing a role in ECM organisation and 15% in signal transduction leading to various other functions. Pathways engaged in vesicle transportation, homeostasis and the immune system included 11%, 9% and 8% of the secreted proteins. N = 3

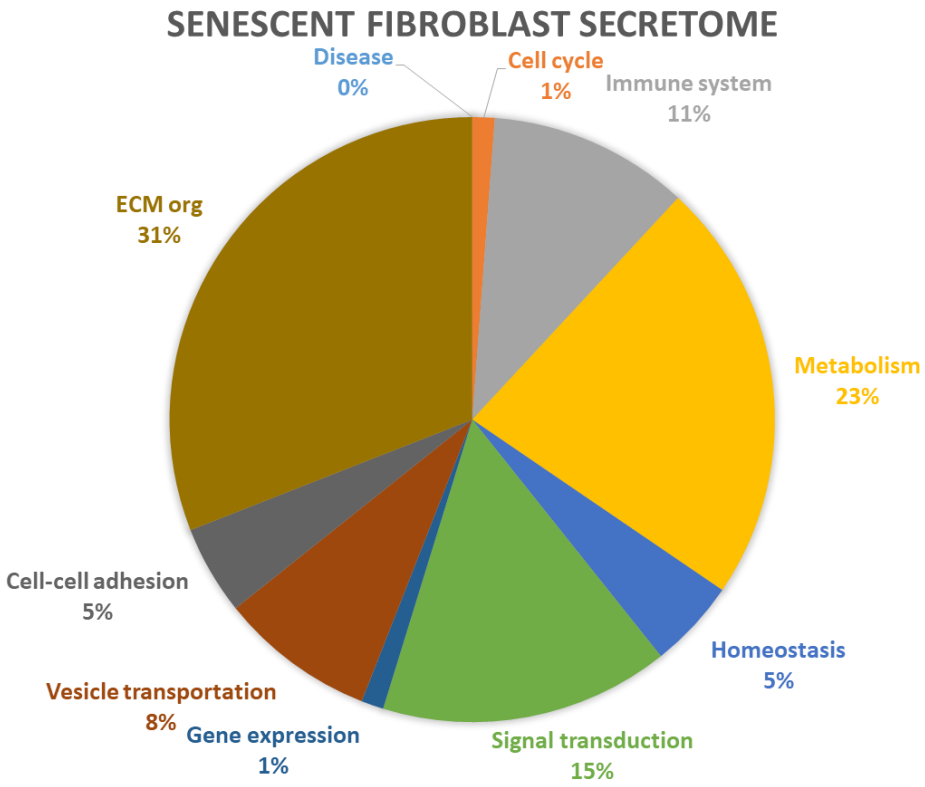

Figure 5.3. Biological pathways senescent fibroblast secreted proteins have previously been found to engage in: The pie chart represents proteins with fold increase compared to 24 h control CM and the pathways they engage in. With a majority of 31%, proteins secreted by senescent fibroblast participate in ECM organisation, followed by 23% of proteins playing a role in metabolism and 16% in signal transduction leading to various other functions. Pathways engaged in immune system, homeostasis and vesicle transportation included 11%, 5% and 8% of the secreted proteins. N=3

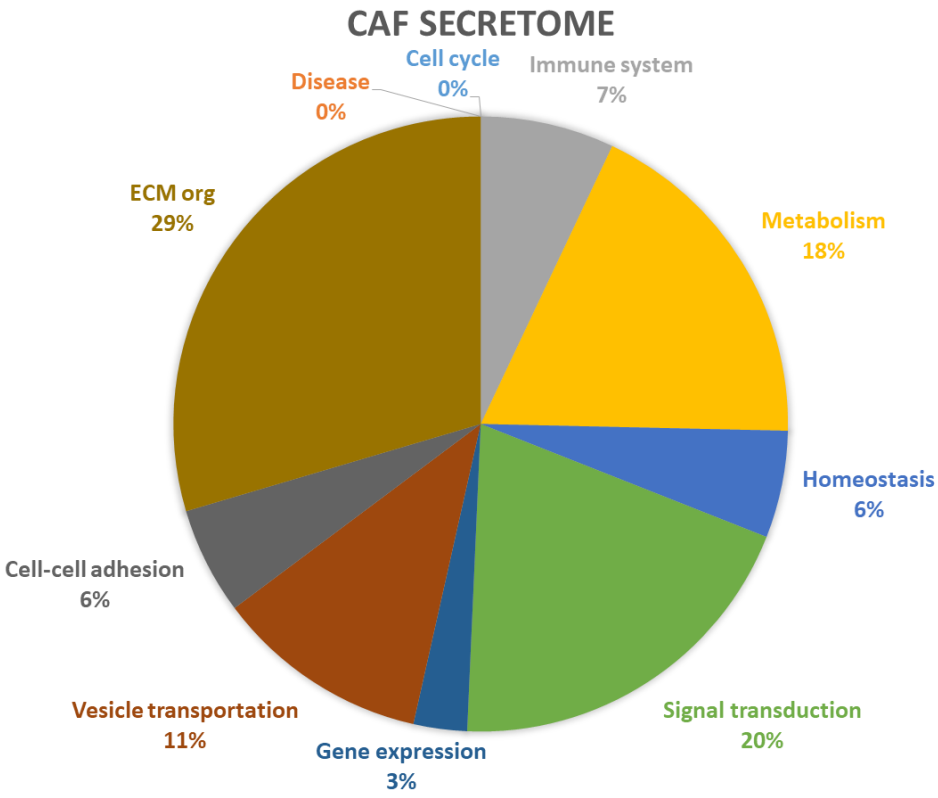

Figure 5.4. Biological pathways patient CAF secreted proteins have previously been found to engage in: The pie chart represents proteins with fold increase compared to 24 h control CM and the pathways they engage in. With a majority of 29%, proteins secreted by patient CAF participate in ECM organisation, followed by 20% of proteins playing a role in signal transduction and 18% in metabolism. Pathways engaged in immune system, homeostasis and vesicle transportation included 7%, 6% and 11% of the secreted proteins. N=3.

Scatterplots were then used to validate differential expression of secreted proteins between patient CAF (CAF002), senescent fibroblasts, myofibroblasts, and controls after 24 h in culture. Comparing NOF (24 h control) vs. patient CAF generated a total of 126 significantly different proteins, highlighting the change in secretome of normal fibroblast compared to the CAF secretome (Fig. 5.5). Comparison between secreted proteins from myofibroblasts and patient CAF (Fig. 5.6) also generated a large number of significantly different proteins (96 in total). Comparison between senescent fibroblasts and CAF, however, highlights only two differentially detected proteins; insulin-like growth factor binding protein (IGFBP) 2 and plectin (PLEC) (Fig. 5.7) suggesting that the two have a very similar secretory profile. A large number of significantly differentially detected proteins were identified when CM from myofibroblasts and senescent fibroblast were compared, 76 in total (Fig. 5.8), indicating profound differences between their secretory profiles.

Figure 5.5. Scatterplot displaying differential expression of proteins between 24 h control fibroblast and patient CAF secretory profiles: Comparison of secretory proteins between 24 h control (normal oral fibroblast) and patient CAF generated the most number of significant proteins – 126, highlighting the effect TME has on fibroblasts and their secretory phenotype. The scatterplots calculate q-value which is p-value adjusted for false discovery rate where a small sample is run for hundreds and thousands of tests (proteins, in this case), therefore q-value of 5% means 5% of total significant results will result in false positives. Statistical analysis performed – Student T test, $q < 0.009$, $n = 3$

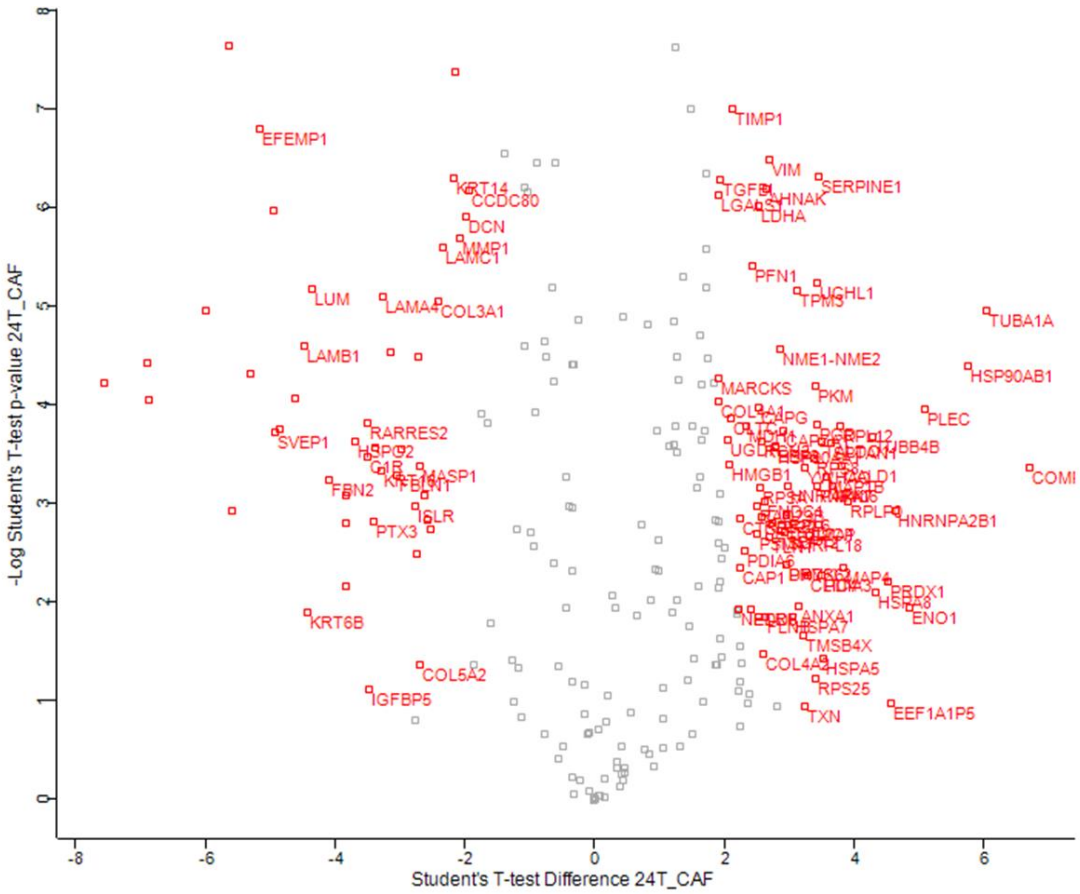

Figure 5.6. Scatterplot displaying differential expression of proteins between myofibroblast and patient CAF secretory profiles: Comparison of secretory proteins between myofibroblasts CM to CAF CM generated 96 significantly differentially expressed proteins, highlighting differences in concentration and variety of proteins secreted. Statistical analysis performed – Student T test, q <0.0097, n = 3.

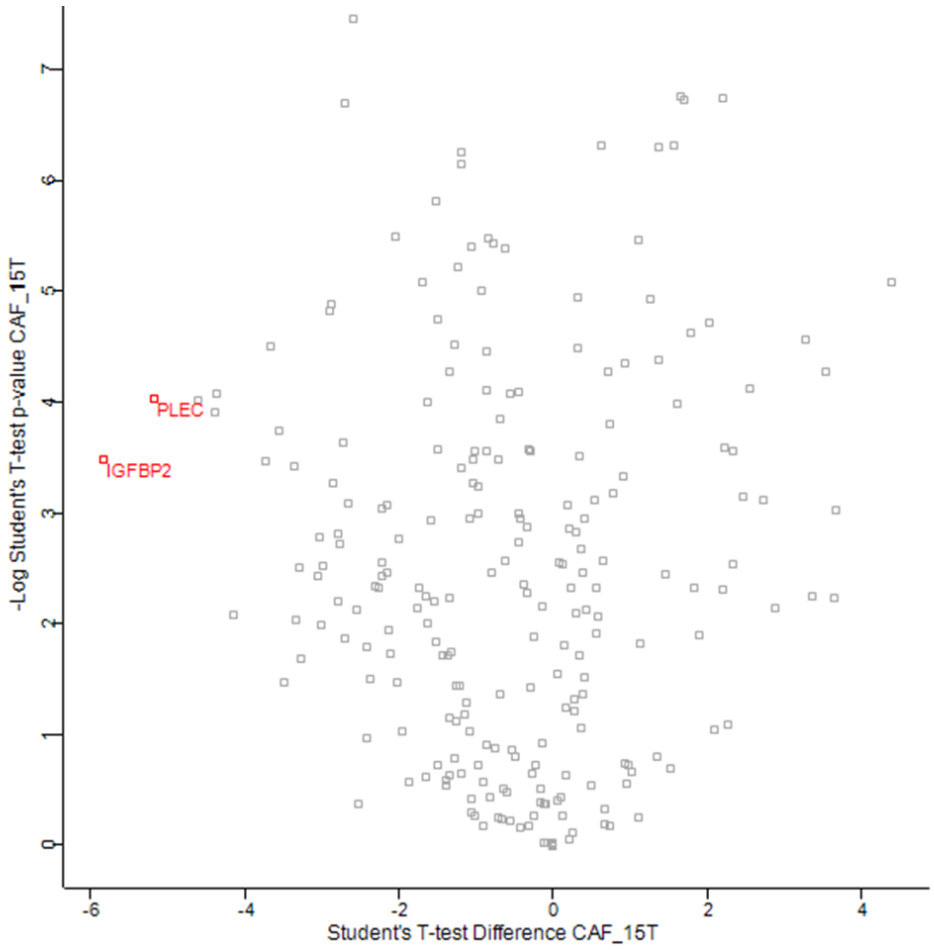

Figure 5.7. Scatterplot displaying differential expression of proteins between senescent fibroblast and patient CAF secretory profiles: Secretory profile of senescent fibroblasts vs. CAF generated only 2 significant proteins, suggesting similarities in variety and concentrations of proteins secreted. Statistical analysis performed – Student T test, q = 0, n = 3.

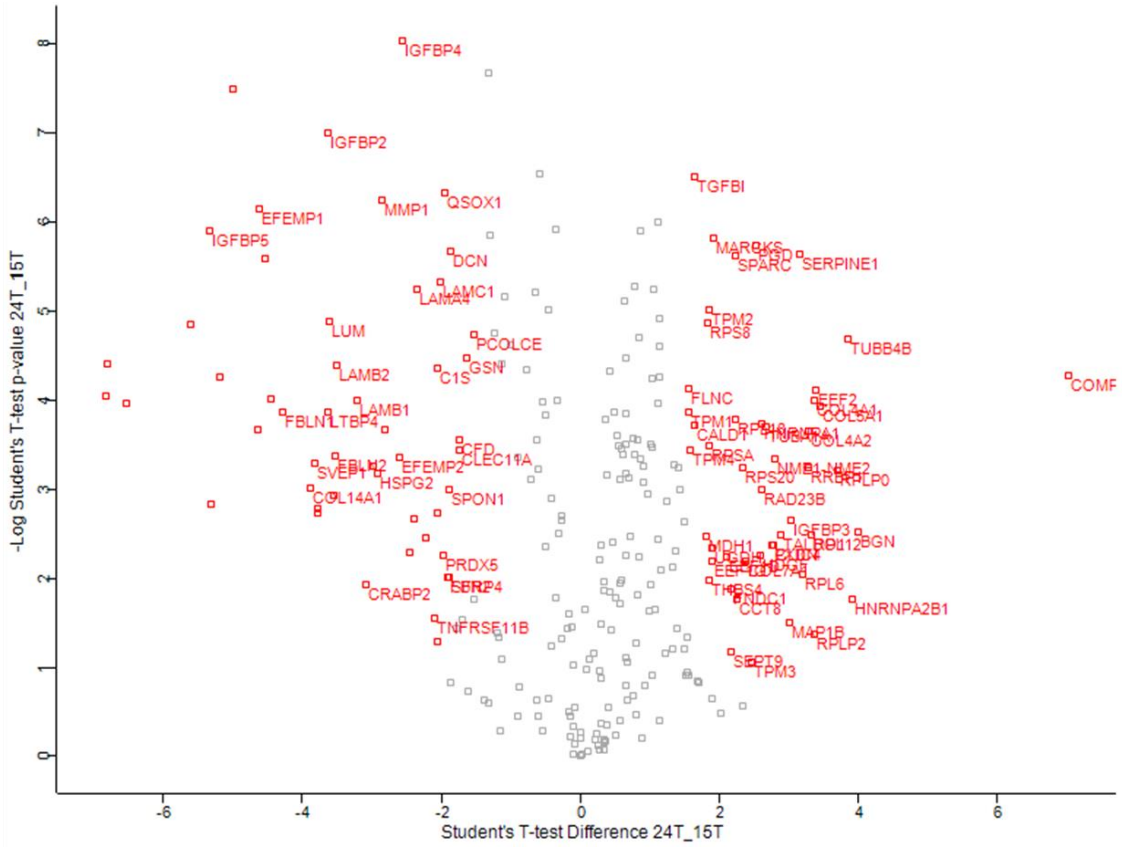

Figure 5.8. Scatterplot displaying differential expression of proteins between myofibroblast and senescent fibroblast secretory profiles: Comparison of CM from myofibroblasts to CM from senescent fibroblast revealed differential expression of 76 significant proteins, accentuating the difference in their secretory proteins. Statistical analysis performed – Student T test, $q < 0.006$, $n = 3$.

A threshold of 5 fold increase from 24 h was applied to reduce the number of proteins sufficiently to interrogate in more detail (summarised in Table 10).

Table 10: Secreted proteins up-regulated more than 5 folds in MF, SF, and CAF

Accession no.	Secretory protein	Up-regulated in (fold increase from 24 h ctrl)	Pathway associated with
P98160	Basement membrane-specific heparan sulfate proteoglycan core protein (HSPG2)	SF (5.15), CAF (7.4)	Metabolism
P21810	Biglycan (BGN)	MF (28.5), CAF (13.11)	Metabolism
P49747	Cartilage oligomeric matrix protein (COMP)	MF ($2.9x10^8$), SF ($6.7x10^5$), CAF ($9.3x10^5$)	ECM
Q76M96	Coiled-coil domain-containing protein 80 (CCDC80)	CAF (5.7)	Cell-cell communication, ECM
P02461	Collagen alpha-1(III) chain (COL3A1)	MF (17.23), SF (7.21), CAF (102.73)	ECM, Immune system, signal transduction, vesicle mediated transport
P02462	Collagen alpha-1(IV) chain (COL4A1)	MF ($4.1x10^7$), CAF ($6.4x10^6$)	ECM, signal transduction, vesicle mediated transport
P20908	Collagen alpha-1(V) chain (COL5A1)	MF (61.42), CAF (18.19)	ECM, signal transduction
Q02388	Collagen alpha-1(VII) chain (COL7A1)	MF ($1.9x10^7$)	ECM, protein metabolism, vesicle mediated transport
Q05707	Collagen alpha-1(XIV) chain (COL14A1)	SF ($4.4x10^7$), CAF ($9.4x10^5$)	ECM
P08572	Collagen alpha-2(IV) chain (COL4A2)	MF (61), CAF (10.3)	ECM, signal transduction, vesicle mediated transport
P05997	Collagen alpha-2(V) chain (COL5A2)	MF (19.97), CAF (54.94)	ECM
P00736	Complement C1r component (C1R)	SF (7.57), CAF (18.04)	Immune system

P00746	Complement factor D (CFD)	SF ($8.6x10^6$)	Immune system
Q12805	EGF-containing fibulin-like extracellular matrix protein 1 (EFEMP1)	SF ($4.7x10^7$), CAF ($8.1x10^7$)	ECM
Q4ZHG4	Fibronectin type III domain-containing protein 1 (FNDC1)	MF (5)	Signal transduction
P17936	Insulin-like growth factor binding protein 3 (IGFBP3)	MF ($2.1x10^7$), CAF ($3.9x10^7$)	Gene expression, protein metabolism
P24593	Insulin-like growth factor binding protein 5 (IGFBP5)	SF (10.4)	Protein metabolism
Q16363	Laminin subunit alpha-4 (LAMA4)	SF (18.79), CAF (44.79)	ECM, signal transduction
P55268	Laminin subunit beta-2 (LAMB2)	SF (39.87)	ECM, signal transduction
Q15063	Periostin (POSTN)	MF ($8.8x10^6$), SF ($1.4x10^6$), CAF ($4.1x10^6$)	ECM, signal transduction, response to external stimuli
Q92626	Peroxidasin homolog (PXDN)	MF ($4.3x10^7$), SF ($3.2x10^6$), CAF ($1.5x10^7$)	ECM
P05121	Plasminogen activator inhibitor 1 (SERPINE1)	MF (12.82)	ECM
O14818	Proteasome subunit alpha type-7 (PSMA7)	MF (5.8)	Cell cycle, response to external stimuli, DNA replication, disease, gene expression, immune system, metabolism, signal transduction, molecule transport
Q99969	Retinoic acid receptor responder protein 2 (RARRES2)	SF ($3.3x10^6$), CAF ($2.8x10^7$)	Signal transduction, metabolism
Q6FHJ7	Secreted frizzled-related protein 4 (SFRP4)	SF ($8.5x10^6$), CAF ($4.4x10^6$)	Cell cycle, signal transduction
P09486	SPARC	MF (7.5)	Signal transduction, ECM
Q9HCB6	Spondin 1 (SPON1)	SF ($1.1x10^7$)	Protein metabolism
Q15582	Transforming growth factor-	MF (9.23)	Protein metabolism

	beta-induced protein ig-h3 (TGFBI)		
P06753	Tropomyosin alpha-3 chain (TPM3)	MF ($3.4x10^6$)	Cell movement

The proteins highlighted in blue in table 10 were found to not be expressed at all in the untreated normal oral fibroblasts but were present in TGF-β1 and cisplatin treated counterparts, suggesting these secreted proteins might be unique to the phenotype. Table 11 presents evidence from the literature of how these unique proteins might participate in cancer progression.

Table 11. List of proteins from current MS data showing association with cancer progression previously

Protein	Function
COMP/TSP5	Protects cells against apoptosis (Gagarina et al., 2008), promotes breast cancer development & metastasis by boosting metabolism & cell survival (Englund et al., 2016)
COL7A1	Modifies ECM. Correlates with tumour and lymphatic invasion in esophageal SCC (ESCC) (Kita et al., 2009).
COL14A1	Modifies ECM. High methylation of COL14A1 gene correlation with tumour stage in ESCC (Li et al., 2014c).
EFEMP1	Binds to EGF receptor, plays a role in invasion of osteosarcoma via NF-κB signaling pathway (Wang et al., 2015c), ovarian cancer (Yin et al., 2016), and cervical cancer (En-lin et al., 2010).
POSTN	Aids incorporation of BMP1 in fibronectin matrix, and activates lysyl oxidase to modify ECM to promote cell migration (Gillan et al., 2002). Associated with colon cancer (Xiao et al., 2015), esophageal adenocarcinoma (Underwood et al., 2015), pancreatic cancer (Liu and Du, 2015), and prostate cancer (Tian et al., 2015).
PXDN	Metabolises H_2O_2 (Cheng et al., 2008), and modifies ECM produced by

	myofibroblasts (Peterfi et al., 2009).
RARRES2	Recruits M1 macrophages possessing receptor CMKLR1 (Herova et al., 2015), and stimulates angiogenesis (Bozaoglu et al., 2010) and adipogenesis (Roh et al., 2007)
SFRP4	Wnt-signalling antagonist (Pohl et al., 2015)
SPON1	Cell adhesion protein, and upregulated in osteosarcoma and correlates expression of MMP9 to promote cell migration and invasion (Chang et al., 2015b)

A noteworthy observation is that even after applying 5 fold increase threshold the patient CAF had 11 highly expressed proteins (biglycan, cartilage oligomeric matrix protein, COL3A1, COL4A1, COL5A1, COL4A2, COL5A2) in common with myofibroblast, while compared to senescent fibroblast there were 13 proteins (basement membrane specific heparin sulphate proteoglycan core protein, cartilage oligomeric matrix protein, COL3A1, COL4A1, COL5A1, COL14A1, complement C1r component, EGF-containing fibulin like extracellular matrix protein1, lamini α4, periostin, retinoic acid receptor responder protein 2, secreted frizzled related protein 4) in common suggesting some similarities between in secretory profiles of lab-generated CAF phenotypes (myofibroblast and senescent fibroblast) and CAFs obtained from cancer patients.

5.4. Cytokine array

As described in this chapter in section 5.3, most of the protein hits by MS played a major role in metabolism, ECM organisation and the immune system, however not many cytokines were detected using MS. The reason for this could be that cytokines are low molecular weight proteins, and potentially lost during concentration and processing of CM, also observed previously (Chevallet et al., 2007). The data presented in chapter 3 (Fig. 3.6) and chapter 4 (Fig. 4.5) confirmed robust secretion by fibroblasts of two cytokines, IL-6 and CCL2, which has been established in literature previously (Kabir et al., 2016). In light of this discrepancy between the MS data and the apparent abundance of these cytokines detected using other methods, a cytokine array panel was carried out to identify differences in cytokines present in the CM from myofibroblast and senescent fibroblast. Cytokines detected using the array are detailed in table 12, where CM from myofibroblast (24 h TGF-β1) (Fig. 5.9) exhibited a wider range of cytokines compared to CM from senescent fibroblasts (Fig. 5.10). The panel also detected the following chemokines: Eotaxin-1, 2, 3, GCP-2, I-309, CCL2, Rantes, CCL13, SCF, SDF-1α, and TARC, which serve as chemoattractants for monocytes, eosinophils, neutrophils, mast cells, B cells and T

cells secreted by myofibroblasts (Fig. 5.9 B) (Moore et al., 2015). While Eotaxin 2/3, chemoattractants for eosinophils, neutrophils, and basophils, fibroblast growth factor 6/7 in CM from senescent fibroblast were down-regulated (Fig. 5.10 F).

The cytokine array also reported a down-regulation of anti-inflammatory cytokines like IL-10 and IL-13 by myofibroblast (Fig. 5.9 C).

The cytokine array also indicates elevated secretion of both IL-6 and CCL2 from both myofibroblasts and senescent fibroblasts, in keeping with the ELISA data presented in sections 3.1.2 and 4.5.

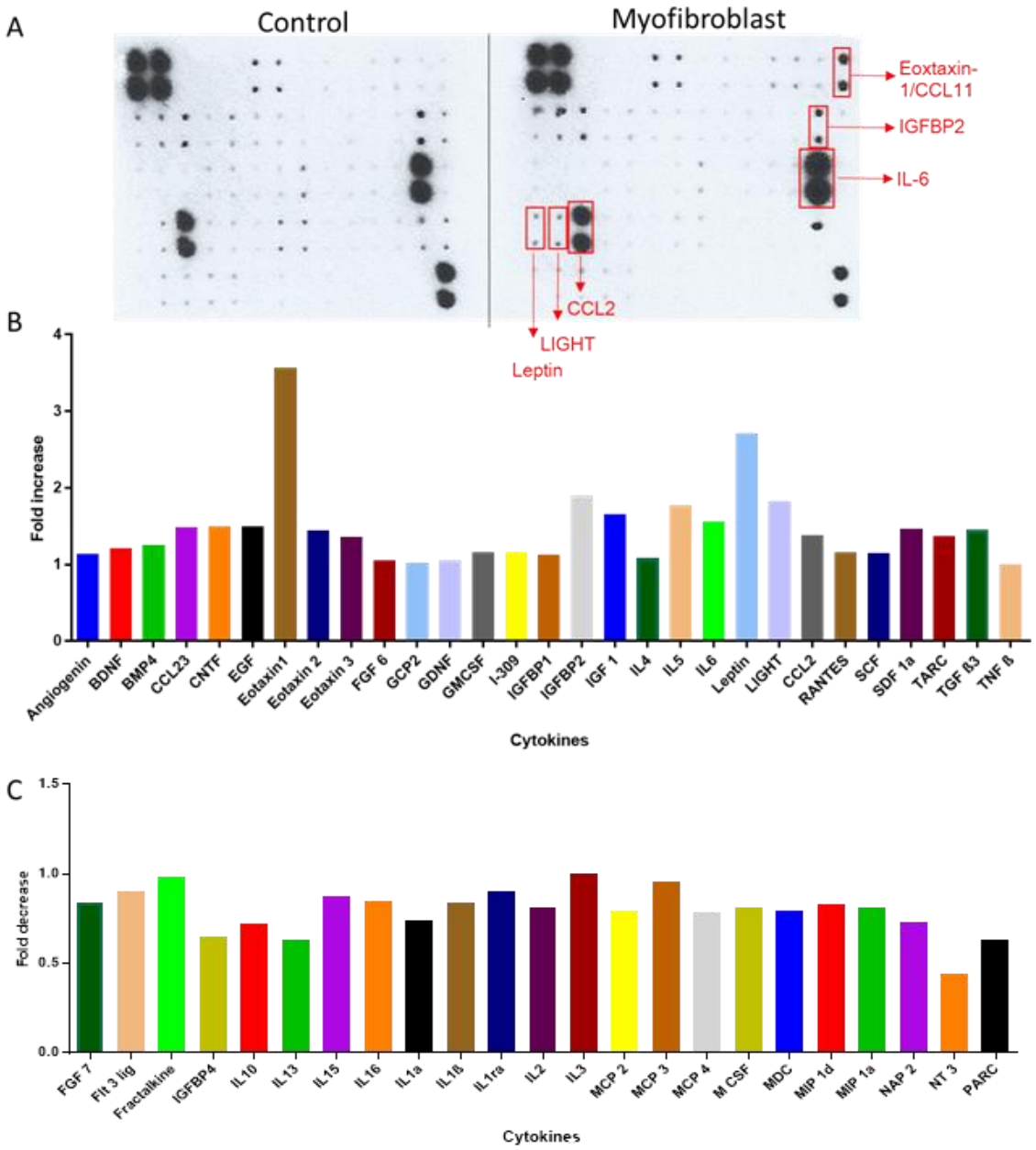

Figure 5.9. Cytokine array analysis of CM from myofibroblast: NOFs were treated with TGF-β1 for 24 h, and serum free media was conditioned by the resulting myofibroblast and its untreated control for 24 h, which was incubated on a cytokine array. A) Radiographic film depicting change in cytokine expression after 24 h TGF-β 1 treatment via chemiluminescence. B) Thirty cytokines up-regulated in 24 h TGF-β1 treated myofibroblast compared to its control, out of which 9 are chemokines responsible for macrophage recruitment and others promote inflammation, angiogenesis, matrix remodelling, and cell proliferation. C) Anti-inflammatory cytokines like IL-10 and IL-13 were downregulated, and so were other chemoattractants like MCP 2/3/4 (CCL8/7/13).

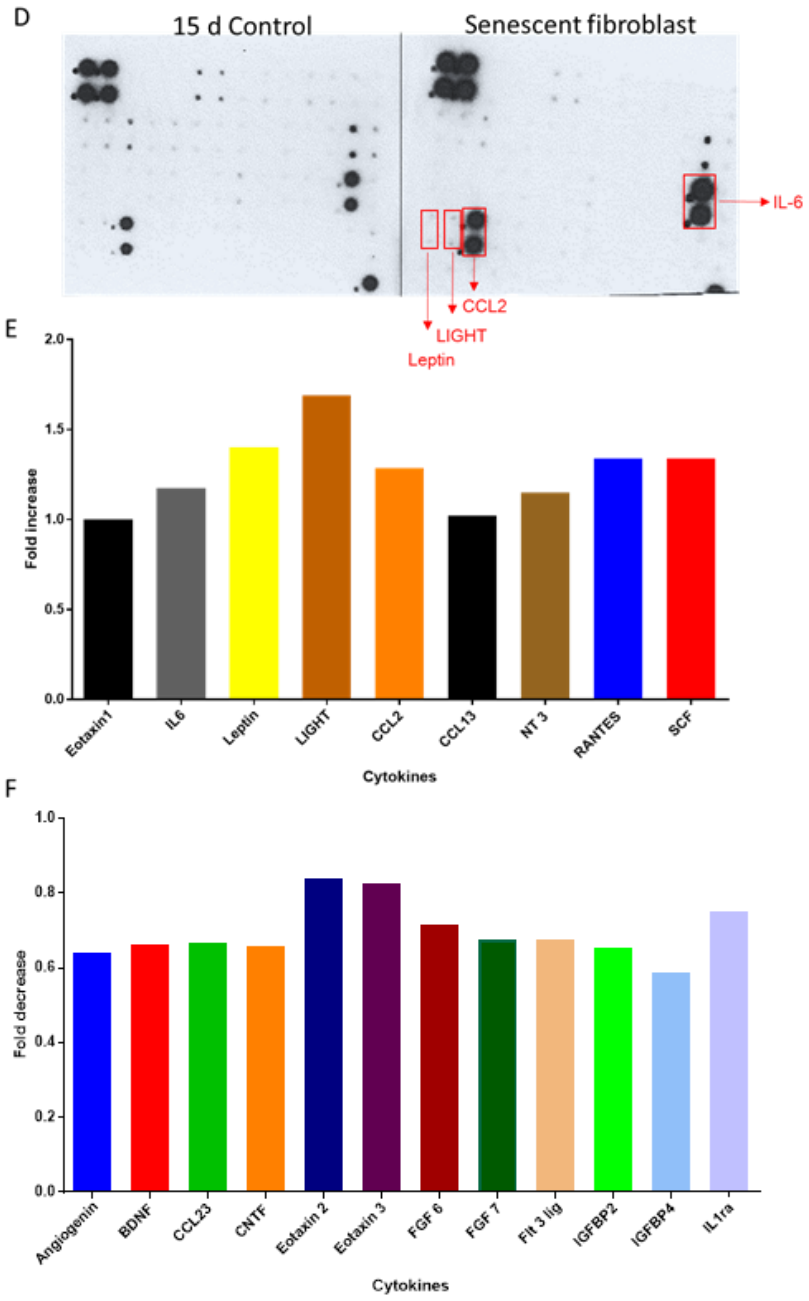

Figure 5.10. Cytokine array analysis of CM from senescent fibroblast: NOFs were senesced with cisplatin over 15 d, and serum free media was conditioned by the resulting senescent fibroblast and its untreated control for 24 h, which was incubated on a cytokine array. A) Radiographic film depicting change in cytokine expression after 15 d cisp treatment via chemiluminescence. B) Four chemokines (CCL2, CCL13, Rantes, Eotaxin-1) for macrophage migration were up-regulated compared to its control, while others were responsible for angiogenesis, inflammation, matrix remodelling, and cell proliferation. C) While other chemo-attractants like eotaxin 2/3

for eosinophils, neutrophils, and basophils, and fibroblast growth factors 6/7 were down-regulated.

Table 12. Cytokines from array panel in cancer progression

Accession no.	Cytokine	Function
P03950	ANG	Promotes angiogenesis, cell proliferation, ECM remodelling malignant tissues (Barcena et al., 2015, He et al., 2015, Kishimoto et al., 2014, Shu et al., 2015)
P23560	BDNF	Promotes cell survival and angiogenesis (Lin et al., 2014, Vanhecke et al., 2011, Yang et al., 2012)
P12644	BMP4	Implicated as both pro-tumorigenic (Ivanova et al., 2013, Kim et al., 2015) and anti-tumorigenic (Li et al., 2014a, Tsuchida et al., 2014)
P01133	EGF	Promotes cell growth, and implicated in cell invasion in ovarian, prostate, colorectal cancer and HNC (Bae et al., 2014, Bhat et al., 2014, Chang et al., 2015c, Qiu et al., 2014)
P10767	FGF6	Promotes cell growth, differentiation, angiogenesis. Responsible for cell proliferation in prostate cancer (Ropiquet et al., 2000)
P80162	GCP2	Chemoattractant for neutrophils and implicated in cell invasion and angiogenesis (Otomo et al., 2014, Tian et al., 2014)
P39905	GDNF	Implicated in cell invasion and conferring chemoresistance in cancers (Chuang et al., 2013, Ding et al., 2014a, Ferranti et al., 2012, Huang et al., 2014, Liu et al., 2012, Ng et al., 2009)
P04141	GM-CSF	Stimulates growth and differentiation of macrophage. Promotes tumour inflammation (Bayne et al., 2012, Mueller et al., 1999)
P05112	IL-4	Supports metastasis, metabolism, and inflammation in TME (Bankaitis and Fingleton, 2015, Venmar et al., 2014, Venmar et al., 2015)
P05231	IL-6	Facilitates monocyte to macrophage differentiation, angiogenesis, inflammation in TME (Caetano et al., 2016, Nowak et al., 2015, Patel and Gooderham, 2015, Pinciroli et al., 2013, Zou et al., 2016, Castellana et al., 2015, Eligini et al., 2013, Kojima et al., 2013, Mia et al., 2014, Nguyen et al., 2014)
P41159	LEP	Maintains body weight and fat. Promotes growth, ECM remodelling, EMT, inflammation, cell migration (Alshaker et al., 2015, Catalano et al., 2015, Chang et al., 2015a, Kato et al., 2015, Lee et al., 2014b, Newman and Gonzalez-Perez,

		2014, Wang et al., 2015a)
P21583	SCF	Promotes cell proliferation, stemness, and metastasis in cancers (Chen et al., 2015, Krasagakis et al., 2011, Kuonen et al., 2012, Park et al., 2013b, Perumal et al., 2014)
P10600	TGF-β3	Involved in cancer metastasis (Petrella et al., 2012, Qin et al., 2016, Tang et al., 2015)
P01374	TNF-β	Associated with tumour proliferation, invasion, and inflammation in TME (Bauer et al., 2012, Bjordahl et al., 2013, Lau et al., 2014, Villanueva et al., 2009)

5.5. Effects of CAF secretome on macrophage polarisation

Keeping in line with the hypothesis that CAFs have capability to recruit immune cells, specifically monocytes, the CAF secretome (fig. 5.9 and 5.10) also demonstrated expression of IL-4 and IL-6 which are known to promote macrophage polarisation towards M2 (Mauer et al., 2014, Casella et al., 2016, Sanmarco et al., 2017). This observation led to the hypothesis that fibroblast-derived secretions, as well as recruiting monocytes, might influence the macrophage phenotype. To examine this, monocytes were isolated and differentiated into unpolarised M0 macrophages (as described in section 2.8) and cultured in CM from myofibroblast, senescent fibroblast and a patient-derived CAF (as used for MS) for 24 h. Polarisation markers CD80 and CD86 for M1 macrophage, and CD163 and CD206 for M2 macrophage, were examined at the mRNA level by RT qPCR (Fig. 5.11) (Bertani et al., 2017).

Macrophages cultured with CM from 24 h TGF-β1 treated NOF (myofibroblast), 15 d cisplatin treated NOF (senescent fibroblast), and CAF002 (patient CAF) exhibited higher level of M2 marker CD206 (in blue boxes) transcripts compared to the 24 h and 15 d control (Fig. 5.11), but this did not reach significance due to variation in results obtained using the different cultures. CD86 (in orange boxes), an M1 marker, was elevated at the transcript level in indirect co-cultures of macrophages with either 24 h TGF-β1 treated (myofibroblast), 15 d cisplatin treated (senescent fibroblast), and CAF002 (patient CAF) compared to 24 h and 15 d controls, but this change was lower than observed for CD206 transcripts (Fig. 5.11).

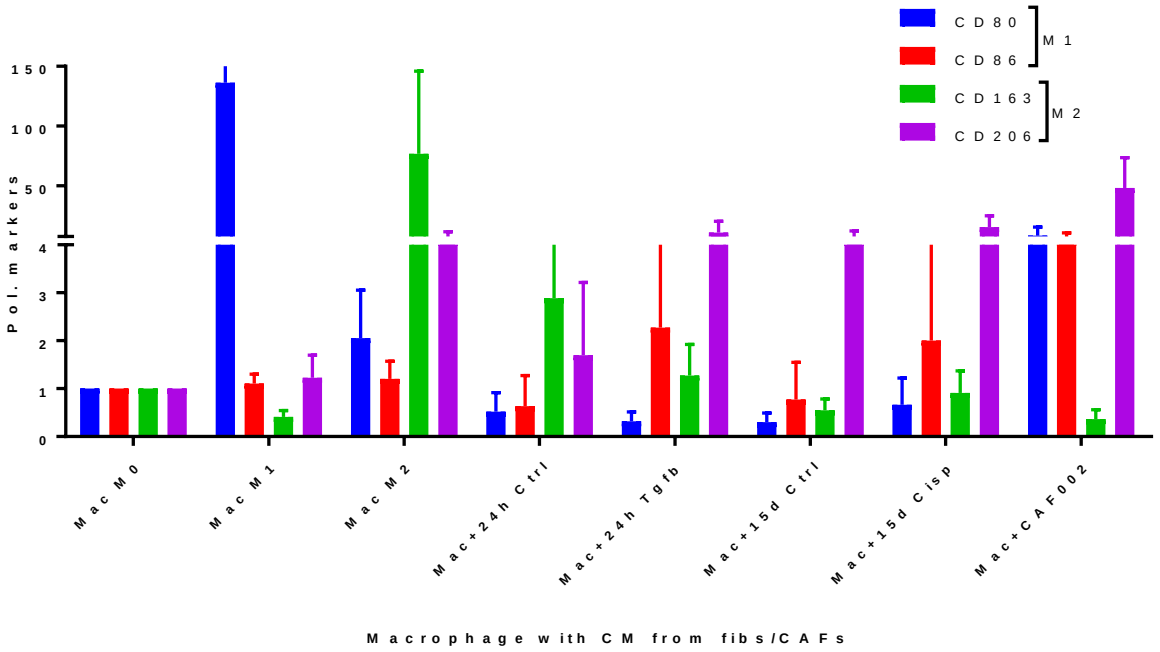

Figure 5.11. Effect of macrophage incubation with CAF CM on macrophage polarisation: Macrophages were incubated for 24 h with CM from lab generated myofibroblast, senescent fibroblast, their untreated controls, and a patient CAF. RNA from these macrophages was isolated to generate cDNA which was used in qPCR, normalised to B2M, to look at polarisation markers (CD80, CD86, CD163 and CD206). M2 marker CD206 transcript was expressed in higher quantity when macrophages were cultured in CM from myofibroblast, senescent fibroblast, and patient CAF compared to their respective controls. Amongst the 3, incubation with patient CAF CM expressed the highest level of CD206 transcript followed by CM from senescent fibroblast. Statistical analysis – not significant, TWO way ANOVA, data are mean with +/- SEM, n = 3 biological repeats.

5.6. Summary

To conclude, MS technique was used in this project to examine differences as well as similarities between the secretomes of lab-generated CAF phenotypes, myofibroblasts and senescent fibroblasts, and a tumour-derived CAF. Principal component analysis validated that each control, phenotype, and one patient CAF was different from the other and spread out, yet technical repeats of each condition clustered together.

Out of the thousands of protein hits in the CM tested, the analysis revealed a total of 193 significant proteins hits, out of which most (26%) proteins; HSPG2, BGN, COMP, COL7A1, IGFBP3 & 5, MDH1, PSMA7, RARRES2, SPON1, TGFBI, ALDOA, TKT, EEF2 were highly upregulated and are observed previously to participate in metabolism in other studies based on Reactome database. Possible signal transduction proteins involved COL3A1, COL4A1, 5A1, 4A2, FNDC1, LAMA4, LAMB2, POSTN, PSMA7, RARRES2, SFRP4, SPARC which were highly expressed, especially in myofibroblast CM.

Only few highly expressed proteins participated in the immune system; COL3A1, C1r, CFD and PSMA7, most of these proteins were expressed by senescent fibroblast according to reactome database.

A well-known characteristic of fibroblast is to modify the ECM; COMP, CCDC80, COL3A1, COL4A1, COL5A1, COL7A1, COL14A1, COL4A2, COL5A2, EFEMP1, LAMA4, LAMB2, POSTN, PXDN, SERPINE1, SPARC were found to upregulated above the 5 fold threshold applied, and again most of these proteins were expressed by myofibroblast.

Even though MS analysis exhibited some uncommon, it didn't show any cytokines. MS requires higher concentration of proteins to achieve hits, and literature shows evidence of cytokines like IL-6, IL-8, CCL2, and the like being secreted from CAFs. And the cytokine array validated secretion of cytokines by both myofibroblast and senescent fibroblast.

Similar to MS analysis, myofibroblast CM displayed a wider range of cytokine cocktail secreted compared to senescent fibroblast. However, not all cytokines secreted by the myofibroblasts maybe of biologically effective concentration as some of the antibodies on the panel detect protein levels at pg/ml range.

Many of the upregulated cytokines were responsible for promoting angiogenesis, cell proliferation, survival, cell invasion and most importantly maintaining inflammatory environment, yet providing immune evasion; namely ANG, BDNF, BMP4, EGF, FGF6, GCP2, GDNF, GMCSF, IL-4, IL-6, LEP, SCF, TGF-β, TNF-β (Ivanova et al., 2013, Owens et al., 2013, Kim et al., 2015, Vanhecke et al., 2011, Yang et al., 2012, Lin et al., 2014, Pozzi and Weiser, 1992, Riedel et al., 2005, Lin et al., 2007, Duffy et al., 2008, Sullivan et al., 2009, Ara and Declerck, 2010, Rose-John, 2012).

As seen in chapter 4, CM from both myofibroblast and senescent fibroblast recruited monocytes, the cytokine array also showed other chemokines like eotaxin-1, 2, 3, GCP-2, I-309, CCL2, Rantes, CCL13, SCF, SDF-1α, and TARC which recruit monocytes, eosinophils, mast cells, neutrophils, T cells, and B cells. With proof in hand that CAFs are able to recruit monocytes, effects of co-culture with CAF CM with macrophage on polarisation were observed.

qPCR results from the co-culture showed that CM from myofibroblast, senescent fibroblast, and patient CAF up-regulated transcripts of M2 macrophage marker CD206 compared to their controls. However, the same macrophages also showed a slightly higher transcription of CD86 compared to the controls, which is an M1

marker suggesting that M1 and M2 phenotypes are not rigid phenotypes, but the expression of the markers (M1 – CD80 and CD86, M2 – CD163 and CD206) lie on a spectrum and their expression is influenced by the cytokine environment around them. Therefore can express varying levels of each polarisation marker across the span of the tumour to serve varying purposes.

Chapter 6

6. Discussion

6.1 Introduction

Cancer associated fibroblasts (CAFs) found in tumour microenvironment (TME) are commonly the most prominent cell type in solid tumours and secrete a multitude of soluble factors promoting ECM changes, angiogenesis, tumour growth, invasion, and immune cell infiltrate (Lim et al., 2011a). CAFs are thought to comprise a heterogeneous mix of activated fibroblasts arising from local fibroblasts, epithelial/tumour cell through EMT, pericytes, endothelial cells, adipocytes, bone-marrow derived mesenchymal stem cells in response to the local paracrine environment; this may differ depending on the tissue in which the tumour grows (Augsten, 2014a).

With the existence of different sub-populations of CAFs, one of the questions that arise is whether there is any difference in their role of tumour progression. Two of the many sub-populations of CAFs identified are myofibroblastic CAF and senescent CAF, both of which are α-SMA positive (Routray et al., 2014b, Davalos et al., 2010b, Mellone et al., 2017). α-SMA is the most common marker used in CAF studies, but it

fails to recognise distinguish between sub-populations, and differences/similarities between those sub-populations. Perhaps certain sub-populations are more tumour promoting than another, when identified can serve as a prognostic marker, and as a possible treatment target. This study was designed to examine and compare the secretome of myofibroblasts and senescent fibroblasts, and their capabilities to recruit monocytes. Monocytes which differentiate in to macrophages were chosen as the immune cell of interest as there is evidence of monocyte chemoattractants being secreted by CAFs (Mueller et al., 2010, Wu et al., 2011, Ohgo et al., 2015, Li et al., 2014b, Tsuyada et al., 2012b), and evidence suggests the presence of these tumour associated marcophages often leads to poor prognosis in most solid tumours, including oral cancers (Gajewski et al., 2013, Bingle et al., 2002, Chen et al., 2005, Ryder et al., 2008, Zhu et al., 2008).

6.2 Generation of CAF like phenotype

This study used normal oral fibroblasts (NOFs) isolated from buccal or gingival tissue extracted during routine oral surgeries. NOFs were treated with TGF-β1, a very prominent soluble factor present in TME, to induce myofibroblast transdifferentiation as previously reported (Melling, 2015, Elmusrati et al, 2017), and cisplatin was used

to induce senescence in the same NOFs (Melling, 2015, Kabir et al., 2016). CAFs isolated from OSCC patients were also used to compare their phenotypes with the lab-generated myofibroblasts and senescent fibroblasts. Myofibroblastic transdifferentiation from NOFs was confirmed by up-regulation of myofibroblastic markers like α-SMA, FNEDA, COL1A1, as previously reported (Melling, 2015, Dugina et al., 2001, Desmouliere et al., 1993).

During initial stages of the project, three separate NOF cultures (NOF316, NOF320, and NOF343) were treated with TGF-β1 (5 ng/ml) for 24 h, 48 h, and 96 h. The ideal duration of TGF-β1 for myofibroblastic transdifferentiation had previously been reported in the lab to be 48 h (Melling, 2015) but two more time points were selected – half and double the ideal duration - to examine effects of TGF-β1 on secretory factors, especially cytokines.

All three NOFs showed an increase in α-SMA transcripts at 24 and 48 h post treatment but this declined with longer treatment duration, suggesting that continuous production of α-SMA mRNA is not required for protein production as seen in NOF316 and NOF343 showed an increasing expression of α-SMA protein with longer treatment of TGF-β1. Both the control and TGF-β1 treated NOF320, however,

exhibited similar expression of α-SMA protein, indicating a lack of responsiveness to TGF-β1. This could be due to extraction of NOF320 from an inflamed site which is usually rich in TGF-β1, desensitizing cells including fibroblasts in the vicinity (Hasan et al., 1997). Finally, NOF343 was selected for further experimentation due to its clear response to TGF-β1 and availability in the lab. Immunocytochemistry of NOF343 after TGF-β1 treatment also confirmed the expression of α-SMA stress fibers as seen previously in other studies (Melling, 2015, Mellone et al., 2017).

Senescence was induced in fibroblasts (NOF343) using cisplatin. These cells displayed an enlarged and flattened cell morphology; showed an up-regulation of p16INK4a, p21 mRNA, and stained positive in senescence associated β-galactosidase assay in agreement with previous studies (Kabir et al., 2016, Dimri et al., 1995, Ben-Porath and Weinberg, 2004, Sedelnikova et al., 2004, Passos et al., 2010, Overhoff et al., 2014). CAFs are also reported to display increased secretion of ECM components; here myofibroblasts displayed a significant increase in transcript levels of FNEDA, and a non-significant trend towards an increase in COL1A1 transcripts. Senescent fibroblasts, however, did not show an increase in either FNEDA or COL1A1 transcripts; this is in agreement with similar data reported

in a study by (Mellone et al., 2017). This suggests that perhaps myofibroblasts are more responsible than senescent fibroblasts for modifying the ECM in the TME.

The next secreted factor examined was IL-6, known to be a notorious cytokine; it has been linked to chronic inflammation initiating cancer, and subsequent progression and metastasis. IL-6 signalling promotes survival and proliferation of immune cells such macrophages and Th17 cells, and in neighbouring cancer cells activates transcription of cell cycle regulator cyclin D1, proto-oncogene c-myc, JAK/STAT3/PI3AK, angiogenic factors – VEGF & FGF, anti-apoptotic proteins like survivin, bcl2 and bcl-XL (Yao et al., 2014, Middleton et al., 2014, Ara and Declerck, 2010, Rose-John, 2012, Tanaka et al., 2014, Fisher et al., 2014). Previously, senescent fibroblasts have been reported to exhibit secretion of IL-6 in our lab (Kabir et al., 2016), and this finding was extended in this study, with both 24 h TGF-β1 treated myofibroblast and senescent fibroblasts shown to secrete significant amounts of IL-6, with latter secreting more than the former. This suggests that CAF with a myofibroblastic phenotype, as well as senescent fibroblasts, may contribute to an inflammatory TME.

In the literature, IL-6 shows conflicting roles in relation to CAFs, on one hand it down-regulated p16INK4a, p21, and p53 in normal fibroblasts through paracrine signalling, and increased expression of α-SMA, SDF-1, and TGF-β1 after 24 h (Hendrayani et al., 2014), while another study (Kojima et al., 2013) provided evidence of IL-6 inducing senescence in fibroblast by activating STAT3, inducing expression of IGFBP5 which in turn produces ROS. When this axis is constantly activated, ROS induced senescence as a DNA damage response leading to further secretion of IL-6, subsequently senescing neighbouring fibroblasts.

It was also observed that IL-6 secretion reduced with increasing duration of TGF-β1, suggesting that myofibroblasts produce IL-6 in short bursts, which along with a previous study showing short exposure (24 h) to IL-6 induced myofibroblastic activation (Hendrayani et al., 2014) indicates that myofibroblasts may form segregated clusters where neighbouring normal fibroblasts maybe activated to myofibroblasts farther away from other sources of IL-6.

Senescent fibroblasts, in contrast, are capable of maintaining secretion of IL-6 suggesting that they can overpower myofibroblasts, along with other cancer cells,

and macrophages (which also produce IL-6) and senesce them through the IL-6/STAT3/IGFBP5 loop.

6.3 Monocyte/macrophage recruitment by myofibroblasts and senescent fibroblasts

Once the myofibroblastic and senescent fibroblastic phenotypes were characterised, the next aim of the study was to examine their capability to recruit monocytes. A monocytic cell line, THP-1 was migrated towards secreted factors from both myofibroblasts and senescent fibroblasts. Significant migration was observed towards conditioned media (CM) from senescent fibroblasts compared to minimal migration towards myofibroblast CM. THP-1 migration towards CM from cisplatin induced senescent fibroblasts corroborates and extends preliminary data from (Kabir, 2015).

Since THP-1 is a monocytic cell line, and does not accurately represent the phenotype or functions of primary cells, monocytes from peripheral blood were isolated (confirmed by expression of CD14) and migrated towards CM from myofibroblasts and senescent fibroblasts. Secreted factors by senescent fibroblasts again showed the highest recruitment of peripheral blood monocytes (PBM), but myofibroblasts showed recruitment of PBMs too, especially 24 h TGF-β1 treated

myofibroblasts, and declining towards CM from myofibroblasts treated with TGF-β1 longer, unlike THP-1 cells. However, the results from PBM migration were not statistically significant, most likely due to patient to patient variability as each biological repeat used PBMs from a different buffy coat.

In the case of both THP-1 cells and PBMs, senescent fibroblasts recruited the highest number of monocytes, but only PBMs (not THP-1) migrated towards myofibroblast CM. In light of this finding the presence and function of the most common chemokine/receptor axis for monocytes, CCL2/CCR2, was investigated to examine the underlying mechanisms.

CCR2 is found to have two isoforms, CCR2A and CCR2B, where the latter is the most commonly found isoform biologically. Levels of the transcripts of both isoforms were examined in THP-1 and PBMs; both showed high expression of CCR2B which was higher in THP-1. However, at protein level, only PBMs exhibited expression of CCR2B, which agrees with the study by (Tanaka et al., 2002), suggesting that perhaps migrating THP-1 cells use a different chemokine or express another variant of CCR2 that the antibody used in this study does not bind to.

Next, expression of CCL2 was investigated in both myofibroblasts and senescent fibroblasts. At transcript level, 24 h TGF-β1 treated myofibroblasts showed a small increase, only to decline with longer TGF-β1 treatment, but senescent fibroblasts expressed very high levels of CCL2 transcripts compared to control cells. ELISA showed that myofibroblasts secreted increased levels of CCL2 after 24 h of TGF-β1 treatment but slowly declined with time suggesting that CCL2 mRNA is transcribed and translated swiftly after a short exposure to TGF-β1, but senescent fibroblasts expressed high levels of CCL2 transcripts, as well as significantly high levels of secreted CCL2 protein as observed in (Kabir et al., 2016) suggesting that production of CCL2 is a sustained activity, similar to IL-6 production as described in section 6.2. Subsequently, CCR2 (the CCL2 receptor) was inhibited on PBMs to investigate whether this discouraged migration in response CCL2 from CM. Although it did not abolish migration, it did decrease migration towards CM 24 h TGF-β1 treated myofibroblasts and senescent fibroblast significantly as shown by the use of same CCR2 antagonist in a different context ((Carmo et al., 2014). Nonetheless, monocytes express a variety of chemokine receptors as described in (Sandblad et

al., 2015), which could possibly compensate for the inhibition of CCR2, permitting the residual minimal migration observed in this study.

To further inhibit these remaining chemokine receptors, Pertussis toxin (PTX) was employed which is known to inhibit most G-protein coupled receptors, in this case chemokine receptors, and suppress monocyte migration as verified by various studies (Ogawa et al., 1983, Malik et al., 2009, Syrovets et al., 1997, Kang et al., 2014). Compared to untreated monocytes, the migration of PTX treated monocytes was reduced but surprisingly, migration was still higher compared to migration of monocytes with CCR2 inhibited. The reason for this anomaly could be explained by the activation of proline rich tyrosine kinase 2 (Pyk2), which is a non-receptor tyrosine kinase known to be activated by chemokines, GPCR ligands, and growth factors (Dikic et al., 1996, Dikic and Schlessinger, 1998). It is also one of the signalling mediators of GPCRs including CCR5 and CXCR4 leading to activation of MAPK, calcium induced regulation of ion channels and c-Jun N-terminal kinase, and is known to participate in cell motility and migration (Del Corno et al., 2001, Ganju et al., 1998, Avraham et al., 2000). A group studying activation of Pyk2 in primary macrophages by HIV-1 gp120 and chemokines found that Pyk2 was activated by

CCL4 (MIP-1β) binding to CCR5 in spite of treatment with PTX (100 ng/ml for 18 h), suggesting migration through activation of CCR5 is either only partially or not G-protein ($G\alpha_i$) mediated (Del Corno et al., 2001). Even though CCR2 is the most prominent chemokine receptor on monocytes and there aren't any studies looking at Pyk2 subsequent to CCR2 activation, it could be possible that CCR2 migration is not fully G-protein mediated either, hence complete inhibition of CCR2 had more of an impact on migration than PTX treated inhibition of GPCR component of CCR2. It is also possible that the dose of PTX used here was not sufficiently high to completely inhibit receptor function.

Next, CCL2 secretion and monocyte recruitment by patient CAFs were examined. A study by (Hassona et al., 2013a) suggested that genetically unstable OSCC first activates, then senesces CAFs through TGF-β1 and ROS dependent pathways. This senescence was not observed in CAF isolated from genetically stable tumours. Four CAFs from the same study were used in this study; BICR18 and BICR78 are derived from genetically unstable (GU) OSCC, and BICR69 and BICR73 from genetically stable (GS) OSCC. Senescent associated β-galactosidase assay on these CAFs showed BICR18 and BICR78 from GU OSCC staining positively, while BICR69 and

BICR73 developed little to no staining; similar results using BICR18 and BICR69 were obtained in the same lab (Kabir, 2015). In accordance with the results reported earlier in this thesis with senescent fibroblasts generated in the lab, the naturally senescent BICR18 and BICR78 from GU OSCC also secreted high levels of CCL2 with high levels of monocyte recruitment, compared to BICR69 and BICR73 which secreted low levels of CCL2 and recruited fewer monocytes.

However, a peculiarity was observed in this case; BICR78 produced very strong staining in SA β-gal assay, and secreted the highest level of CCL2, yet it recruited fewer monocytes than BICR18; both CAFs are from GU OSCC. It is possible that BICR18, along with senescent fibroblasts contains myofibroblasts or a 3rd sub population of CAF that secreted other chemokines responsible for monocyte recruitment. Due to lack of time further characterisation of BICR18 was not pursued. Another CAF, CAF002, which was isolated recently in the same Sheffield lab where this study took place, didn't show positive staining for senescence, and recruited fewer monocytes compared to the more senescent fibroblasts CAFs in the group – BICR78 and BICR18. Except for BICR69, all the other CAFs examined – BICR73, BICR78, BICR18, and CAF002, irrespective of the type of tumour they were isolated

from displayed higher secretion of CCL2 and recruitment of monocytes compared to normal oral fibroblast NOF343 confirming that both activated/senescent CAF are capable of recruiting monocytes.

Subsequently, NOF343 was co-cultured with CM from cancer cell lines: H357 and SCC4 for 24 h to examine whether cancer cells can influence the secretome of fibroblasts in a paracrine manner. CM from NOF343 after the co-culture resulted in higher secretion of CCL2 and recruitment of monocytes. An experiment similar to this was conducted previously in the same lab, where the NOFs were co-cultured with cancer cell line for 48 h in an attempt to generate a myofibroblast phenotype in keeping with previous findings (Lewis et al., 2004, Marsh et al., 2011). Only a very small increase in α-SMA expression at both mRNA and protein level was identified, suggesting perhaps a longer incubation period with cancer cell line CM or co-culturing with cancer cells directly is required to generate a myofibroblastic phenotype (Melling, 2015). Here, however, novel evidence is provided that indirect coculture of fibroblasts with cancer cells generates a rapid secretion of pro-inflammatory cytokines, which recruit monoctes. Melling's suggestion of longer incubation is justified as α-SMA protein expression increased with longer incubation

with TGF-β1 in this study, however, high expression of α-SMA may not necessarily equate to an active secretome; IL-6 and CCL2 secretion was highest after 24 h incubation with TGF-β1.

At this stage, it was evident from this study that CAF phenotypes: myofibroblasts and senescent fibroblasts are capable of recruiting monocytes. Immunohistochemical analysis of OSCC tissue sections were therefore undertaken to validate the existence of any correlation between the presence of α-SMA^{+} CAFs and CD68^{+} TAMs as previously been reported (Marsh et al., 2011, Lewis et al., 2004, Takahashi et al., 2017). A trend was found between presence of CAFs close to the invasive tumour front, and presence of tumour associated macrophages (TAMs) in the tumour but not in the stroma. There was no trend or correlation seen between presence of CAFs and TAMs in the stroma. However, this could be due to a small sample size of only 10 sections being analysed, while other studies which found correlation between their presences used a much larger sample size (Marsh et al., 2011, Lewis et al., 2004, Takahashi et al., 2017).

Macrophages are known to be secretory in nature, and influence inflammation by both causing and resolving it. This power to cause and resolve inflammation also

exists in the TME and depends on their polarised phenotypes – M1 and M2, which is attained after differentiation from monocyte to M0 macrophage in tissue, and subsequent polarisation based on the cytokine environment around them. (Sica et al., 2006a, Bayne et al., 2012, Chen et al., 2005, Ueno et al., 2000, Zhang et al., 2013, Mantovani and Locati, 2013, Bingle et al., 2002, Shi and Pamer, 2011, Biswas and Mantovani, 2010, Sanmarco et al., 2017). After confirming paracrine activation of fibroblasts by cancer cells, effect of polarised macrophages on fibroblast activation was examined. Surprisingly, the study showed that CM from unpolarised M0 macrophages activated the fibroblasts to the greatest extent compared to CM from M1 and M2. This result requires further validation, however, by examination of other markers of the myofibroblast phenotype. Unfortunately, there are not many studies on M0 phenotype and its secretome, however, a transcriptome profiling study (Gabrusiewicz et al., 2016, Liu et al., 2016) showed that M0 macrophages from glioblastoma patients express markers CD163 and CD206, similar to M2, and CD204 hinting at an active secretome. They also overexpressed miR-223 which can activate NF-κB signalling in M0 macrophages resulting in inflammatory secretions (Haneklaus et al., 2013). Another study found that M0/M2 macrophages respond in

similar ways to M1 macrophages when Rho pathway was inhibited suggesting that M0 may have subtle similarities to M2 (Liu et al., 2016). Based on these limited evidences and suggestions, it is possible M0 macrophages secrete factors to activate fibroblasts, but further analysis of M0 secretome and the fibroblast phenotype in co-culture is required to validate this.

6.4 Differential expression of proteins in myofibroblast, senescent fibroblast and CAF secretome.

The importance TME in tumour progression and metastasis has been widely accepted, however, the molecules involved in crosstalk between cancer and stromal cells is still far from fully understood. With a diverse selection of stromal cells; fibroblasts, adipocytes, endothelial cells, lymphocytes, inflammatory cells including macrophages communicate through a network of signalling molecules (Yang and Lin, 2017, Kise et al., 2016, Scharping and Delgoffe, 2016, Raffaghello and Dazzi, 2015, Lyssiotis and Kimmelman, 2017). Amongst these stromal cells cancer associated fibroblasts remain a poorly characterised heterogeneous population. In order to shed more light on their phenotypes and function, this study examined the secretome of two previously described sub-populations of CAFs, myofibroblasts and

senescent fibroblasts using mass spectrometry and a cytokine array. Previously, Mellone *et al* compared the transcriptome of myofibroblasts and senescent fibroblasts, giving us a preliminary insight in to genetic differences between the two sub-populations of CAFs from OSCC (Mellone et al., 2017).

In this thesis, principal component analysis (PCA) revealed the degree of variation in the types and levels of proteins secreted by 24 h control NOF, 24 h TGF-β1 myofibroblast, 15 d control NOF, 15 d cisplatin induced senescent fibroblast, and patient CAF-CAF002.

The largest variation was seen between 24 h control NOF and CAF002, as expected, highlighting the active secretory phenotype CAFs possess. A difference was observed between the secretome of myofibroblasts and senescent fibroblasts on PCA, a finding in meeting one of the aims of this study, that is to examine differences between the secretomes of these two phenotypes. Differences between myofibroblast and senescent fibroblasts were also observed by (Mellone et al., 2017) at a whole cell transcriptional level. Out of 193 significantly expressed proteins reported in this thesis, changes in transcripts encoding 63 of those proteins were found in the study by (Mellone et al., 2017), where 45 proteins expressed by

myofibroblasts were consistent with their gene expression, while 18 weren't. In case of senescent fibroblasts, 29 proteins were consistent with their gene expression, and 34 were not (Mellone et al., 2017). Table 13 compares protein regulation with gene regulation data from the study conducted by Mellone *et al* (Mellone et al., 2017).

Table 13: Comparison between gene regulation and protein regulation in myofibroblast (MF) and senescent fibroblast (SF) compared to their controls.

Protein	Protein regulation in MF compared to NOF	Gene regulation in MF compared to NOF	Protein regulation in SF compared to NOF	Gene regulation in SF compared to NOF
COL1A1	Up-regulated	Up-regulated	Up-regulated	Down-regulated
COL1A2	Up-regulated	Up-regulated	Up-regulated	Down-regulated
COL3A1	Up-regulated	Up-regulated	Up-regulated	Down-regulated
COL5A1	Up-regulated	Up-regulated	No change	Down-regulated
COL5A2	Up-regulated	Up-regulated	Up-regulated	Down-regulated
COL6A3	Up-regulated	Up-regulated	Up-regulated	Up-regulated
COL4A1	Up-regulated	Up-regulated	No change	Down-regulated
COL4A2	Up-regulated	Up-regulated	Down-regulated	Down-regulated
COL7A1	Up-regulated	Up-regulated	No change	Down-regulated

COL11A1	Down-regulated	Up-regulated	Up-regulated	Up-regulated
COL14A1	No change	Up-regulated	Up-regulated	Up-regulated
HSPG2	No change	Up-regulated	Up-regulated	Up-regulated
BGN	Up-regulated	Up-regulated	Up-regulated	Up-regulated
COMP	Up-regulated	Up-regulated	Up-regulated	Up-regulated
CTSB	Down-regulated	Down-regulated	Up-regulated	Up-regulated
CRABP2	Down-regulated	Up-regulated	Up-regulated	Down-regulated
CCDC80	Up-regulated	Down-regulated	Down-regulated	Up-regulated
C1R	Down-regulated	Down-regulated	Up-regulated	Down-regulated
C1S	Down-regulated	Down-regulated	Up-regulated	Down-regulated
CFD	No change	Down-regulated	Up-regulated	Down-regulated
DCN	Down-regulated	Down-regulated	Up-regulated	Down-regulated
EFEMP1	No change	Down-regulated	Up-regulated	Down-regulated
EFEMP2	Down-regulated	Up-regulated	Up-regulated	Up-regulated
FNDC1	Up-regulated	Up-regulated	Down-regulated	Down-regulated
FBN1	Down-regulated	Up-regulated	Up-regulated	Down-regulated

FBN2	Down-regulated	Up-regulated	Up-regulated	Up-regulated
FSTL1	Up-regulated	Up-regulated	Up-regulated	Up-regulated
ISLR	Up-regulated	Up-regulated	Up-regulated	Down-regulated
IGFBP2	Down-regulated	Down-regulated	Up-regulated	Up-regulated
IGFBP3	Up-regulated	Up-regulated	No change	Up-regulated
IGFBP4	Down-regulated	Down-regulated	Up-regulated	Down-regulated
IGFBP5	Down-regulated	Down-regulated	Up-regulated	Down-regulated
ITGBL1	Up-regulated	Down-regulated	Up-regulated	Up-regulated
MMP1	Down-regulated	Up-regulated	Up-regulated	Up-regulated
LAMA4	Down-regulated	Down-regulated	Up-regulated	Up-regulated
LAMB1	Down-regulated	Down-regulated	Up-regulated	Up-regulated
LAMB2	Down-regulated	Up-regulated	Up-regulated	Up-regulated
LAMC1	Down-regulated	Down-regulated	Up-regulated	Up-regulated
LTBP4	Down-regulated	Down-regulated	Up-regulated	Up-regulated
LUM	Down-regulated	Down-regulated	Up-regulated	Down-regulated
MDH2	Up-regulated	Up-regulated	Down-regulated	Up-regulated

TIMP1	Down-regulated	Up-regulated	Down-regulated	Up-regulated
YBX1	Up-regulated	Up-regulated	Down-regulated	Down-regulated
NME1	Up-regulated	Up-regulated	Down-regulated	Up-regulated
POSTN	Up-regulated	Up-regulated	Up-regulated	Down-regulated
PXDN	Up-regulated	Up-regulated	Up-regulated	Up-regulated
SERPINE 1	Up-regulated	Up-regulated	Down-regulated	Up-regulated
PCOLCE	Down-regulated	Up-regulated	Up-regulated	Down-regulated
PSMA7	Up-regulated	Up-regulated	Up-regulated	Up-regulated
RARRES 2	No change	Up-regulated	Up-regulated	Down-regulated
PRSS23	Up-regulated	Up-regulated	Up-regulated	Up-regulated
SPARC	Up-regulated	Up-regulated	Up-regulated	Up-regulated
SPON1	No change	Down-regulated	Up-regulated	Down-regulated
QSOX1	Down-regulated	Down-regulated	Up-regulated	Up-regulated
SVEP1	Up-regulated	Up-regulated	Up-regulated	Up-regulated

THSB1	Up-regulated	Up-regulated	Up-regulated	Down-regulated
THSB2	Up-regulated	Up-regulated	Up-regulated	Down-regulated
TGFBI	Up-regulated	Up-regulated	Up-regulated	Down-regulated
TAGLN	Up-regulated	Up-regulated	Down-regulated	Up-regulated
TPM1	Up-regulated	Up-regulated	Down-regulated	Up-regulated
TPM3	Up-regulated	Down-regulated	No change	Up-regulated
TPM4	Up-regulated	Up-regulated	Down-regulated	Down-regulated
VCAN	Up-regulated	Up-regulated	Down-regulated	Down-regulated

From table 13, it is clear that more proteins correlate with their cellular gene expression (as determined by RNA-seq) in myofibroblasts than senescent fibroblasts. From their Gene Set Enrichment Analysis of the transcriptomes, Mellone *et al* also suggested that myofibroblasts have genes associated with ECM deposition upregulated which correlates with the protein data from this study showing over-expression of COL1A1, COLA1A2, COL3A1, COL4A1, COL4A2, COL5A1, COL5A2, COL6A3, and COL7A1. According to Mellone *et al*, the same genes were observed to be down-regulated in senescent fibroblasts in comparison (Mellone et al., 2017),

however, the data in this thesis identified confounding protein results where fold increases were observed in expression of COL1A1, COLA1A2, COL3A1, COL4A2, COL5A1, COL5A2, COL6A3, COL11A1, and COL14A1 showing a negative correlation with their gene expression. COL6A3, also known as endotrophin, was found to be over-expressed in both myofibroblast and senescent fibroblasts, and has been implicated in several cancers like melanoma, ovarian cancer, lung cancer, oesophageal cancer, breast cancer, pancreatic cancer and colon cancer (Arafat et al., 2011, Sherman-Baust et al., 2003, Nanda et al., 2004, Motrescu et al., 2008, Iyengar et al., 2005, Park and Scherer, 2012). COL6A3 is also known to promote fibrosis, endothelial cell migration, alternate activation of macrophages with high expression of M2c marker – CD150, IL-10, IL-12 and TGF-β, and impart chemoresistance to tumour cells (Park et al., 2013a, Park and Scherer, 2012, Spencer et al., 2010). As mentioned previously, COL6A3 not only activates macrophages alternatively, it also serves as a chemoattractant for macrophages, and is actively secreted by M2 macrophages as well (Park and Scherer, 2012, Schnoor et al., 2008). Therefore, it could be hypothesised that both myofibroblasts and senescent fibroblasts recruit macrophages via COL6A3, as well as by the

cytokines identified functionally earlier in this thesis, and reported by others. Similar to COL6A3, type I collagen has also been reported to prevent monocytes differentiation in to M1 macrophage (Kaplan, 1983).

Other types of collagen secreted by both myofibroblasts and senescent fibroblasts, such as, collagen type V has shown to promote malignant behaviour of pancreatic ductal adenocarcinoma (Berchtold et al., 2015), collagen type IV feeds proliferative, migratory and survival behaviour of pancreatic cancer cells in an autocrine loop (Ohlund et al., 2013); collagen type VII, especially COL7A1 increased PI3K and MAPK resulting in cell migration and invasion in cutaneous SCC (Pourreyron et al., 2014), COL7A1 mRNA expression was also found to be up-regulated in malignant esophageal tissue.

COL11A, secreted by senescent fibroblasts but not by myofibroblasts, promoted tumour cell migration and invasion in ovarian cancer, correlated with metastasis in invasive carcinomas, and promoted HNSCC growth and invasion (Sok et al., 2013, Cheon et al., 2014, Vazquez-Villa et al., 2015).

Several proteins and glycoproteins known to interact with collagen fibres, such as DCN, HSPG2, EFEMP1, EFEMP2, FBN1, FBN2, LAMA4, LAMB1, LAMB2, LAMC1,

LTBP4, LUM were over-expressed in senescent fibroblasts compared to myofibroblasts (also correlating their gene expression with (Mellone et al., 2017), while some ECM interacting proteins like BGN, THBS1, and THBS2 were over-expressed by both myofibroblasts and senescent fibroblasts. Many of these proteins have been implicated in cancer, although some have shown conflicting roles, for example, decorin modulates endothelial cell motility on type 1 collagen through activation of IGF1 receptor (Fiedler et al., 2008), but it also interferes with angiogenic activities of THBS1 and VEGFA to attenuate angiogenesis in several cancers including OSCC (Grant et al., 2002, de Lange Davies et al., 2001). However, decorin often associates with HNC positively (Stylianou et al., 2008, Dil and Banerjee, 2011, Wu et al., 2010, Nayak et al., 2013, Dil and Banerjee, 2012, Skandalis et al., 2006, Kasamatsu et al., 2015, Banerjee et al., 2003). Thus, targeting decorin or its source could have a positive impact on prognosis in HNC.

Another heavily researched ECM component is perlecan (HSPG2), shown in this study to be secreted by senescent fibroblasts but not by myofibroblasts, and has been positively associated with cancers of the head and neck, and promotes invasion of HNC cells and its knockdown reduces cell migration (Maruyama et al.,

2014, Kimura et al., 2000, Mishra et al., 2011, Tilakaratne et al., 2009, Ikarashi et al., 2004, Hasegawa et al., 2016, Ahsan et al., 2011, Kawahara et al., 2014, Chen et al., 2006). Targeting senescent fibroblasts, thus eliminating an important source of perlecan in the TME, might therefore be beneficial to treating cancers of the head and neck.

An interesting protein secreted by senescent fibroblasts but not myofibroblasts is quiescin sulfhydryl oxidase 1 (QSOX1). It has shown tumour promoting functions in breast and pancreatic cancer, by preventing oxidative stress induced apoptosis, activates MMP2/9 promoting invasion, and is overexpressed in both cancers serving as a potential biomarker (Katchman et al., 2011, Poillet et al., 2014, Morel et al., 2007, Sobral et al., 2015, Shi et al., 2013, Lake and Faigel, 2014, Hanavan et al., 2015). The expression and function of QSOX1 has not been examined in HNC; this is worth further analysis as it has a potential role which could be abolished by targeting senescent fibroblasts.

The final protein to mention secreted only by senescent fibroblasts, and not myofibroblasts, is retinoic acid receptor responder protein 2 (RARRES2) RARRES2, also known as chemerin, is a chemokine for ChemR23 receptor expressed on

dendritic cells and macrophages (Samson et al., 1998). Chemerin promotes angiogenesis through activation of MAPK, Akt and MMP2/9 supporting endothelial cell proliferation, migration and new capillary formation (Bozaoglu et al., 2010). M1 macrophages lose their expression of ChemR23 upon polarisation via TLR ligands, and cytokines (IFN-γ and TNF-α), while M2 macrophages up-regulate their expression of ChemR23 after polarisation by TGF-β, suggesting chemerin may facilitate further movement of M2 macrophages within the TME (Zabel et al., 2006), which could also go towards explaining the IHC results reported here; α-SMA positive CAFs (especially senescent fibroblasts) at the tumour margin and tumour cells could themselves secrete chemerin to recruit M2 macrophages within the tumour but further confirmation with senescent fibroblast markers and M2 markers are required. Chemerin has also shown evidence of recruiting other immune cells like dendritic cells and neutrophils via ChemR23 receptor, suggesting an influential role in tailoring the inflammatory environment of the tumour stroma (Parolini et al., 2007). This again suggests senescent fibroblasts, a potential source of chemerin in the TME, may be a good target to reduce recruitment of macrophages.

6.5 Limitations of the study

The majority of the study has been conducted using one particular NOF culture, NOF343, due to its distinct response to TGF-β1, and time constraints; it is possible that other NOFs may give different results, as initially seen in NOF316 and NOF320, therefore. These experiments need to be conducted with more normal fibroblast samples, perhaps even from different locations (dermal, liver, pancreas) of the body to reinforce the data gathered from this study.

CAFs arise from many sources which might include bone marrow derived mesenchymal stem cells from a distant location, or resident fibroblasts, pericytes, or even cancer cells themselves via EMT. Perhaps as a result of these variable origins, CAFs display numerous markers, such as, α-SMA, FNEDA, COL1A1, podoplanin, FAP, and FSP1 (Augsten, 2014a, Paulsson and Micke, 2014). This study only used α-SMA as a marker for myofibroblast activation at protein level, and FNEDA and COL1A1 at mRNA level. Other markers, could be be examined to further interrogate the myofibroblast and senescent CAF like phenotypes.

The migration assays were conducted using monocytes from different buffy coats each time, increasing patient to patient variability with each repeat leading to non-

significant result. However, a migratory trend was suggested from the results which could prove significant with more biological repeats.

The immunohistochemical staining sample size contained sections from 10 patients due to time and tissue availablility constraints. A trend was observed between presence of CAFs near the tumour invasive front and presence of macrophages in the tumour, however a larger cohort needs to be analysed to reach a significant conclusive result.

6.6 Future work

The data gathered in this study has raised many new questions for which extra experimentation might provide answers. First of all, further characterisation of the patient CAF (CAF002) used in mass spectrometry is needed, as it had some similarities to myofibroblast (8 secreted proteins in common above the applied threshold), and some to senescent fibroblasts (10 secreted proteins in common above the applied threshold), and yet, not staining positively in SA β-gal assay. The patient CAF used could possibly be a third sub-population, and characterising it would open doors to new questions and theories. Increasing the number of CAF cultures analysed would also increase confidence in the results obtained.

It would also be interesting to investigate whether normal fibroblasts from other parts of the body, such as dermal, liver, and pancreatic fibroblasts, when activated to myofibroblastic or senescent phenotype attract macrophages in similar manner, and other secretory differences between them, as resident fibroblasts have a different genetic profile based on their location in the body suited specifically the homing tissue.

With limited literature existing on M0 macrophages, a cytokine array on the secretome comparing CM from M0, M1, and M2 macrophages could possible give us a hint on why secretory factors from M0 macrophages activated NOF the most, expressing α-SMA. Having said that, when NOFs were cultured in CM from cancer cell lines, they secreted more CCL2 and recruited more macrophages compared to NOFs cultured in normal medium, suggesting activation of the said NOFs. Further investigation is required to characterise the phenotypical changes those NOFs underwent in response to secretory factors from cancer cell lines, which in turn needs analysis as well, to give us a picture of the secretome of the cancer cell lines and what activated the fibroblasts. Subsequently, the effect on secretory factors from myofibroblasts, senescent fibroblasts and CAF002 (patient CAF) on M0

macrophages indicated polarisation towards an M2 phenotype (up-regulation of CD206), but this was examined at mRNA level. Macrophage polarisation markers could also be examined at protein level, perhaps using flow cytometry to examine CD80, CD86, CD163, and CD206.

Finally, phenotypes of normal, myofibroblasts and senescent fibroblasts should be examined in 3D models to see how a 3D environment, more akin to that encountered in the body, affects these cells and their secretome.

6.7 Conclusion

The data described in this thesis identifies differences between the secretome of myofibroblasts and senescent fibroblasts, and their capabilities to recruit macrophages based on those differences. Senescent fibroblasts secreted the main chemokine responsible for macrophage recruitment – CCL2, in greater quantities than myofibroblasts along with other factors responsible for macrophage chemotaxis, such as CCL5, CCL13 IL-6, and chemerin/RARRES2. An important observation to note is that myofibroblasts also secreted CCL2 and IL-6, however the highest secretion was seen 24 h post TGF-β1 treatment, and these secretions declined with increase in treatment duration, even though expression of α-SMA kept increasing

with time and treatment suggesting perhaps, maintenance of TGF-β1 exposure by additional administration may attenuate the secretion of cytokines from myofibroblast.

The recruitment of macrophages mostly occurred via the CCL2/CCR2 axis, which was confirmed by a substantial reduction in migration of monocytes when CCR2 on their surfaces were antagonised. However, due to the presence of other chemokines in the CM and expression of numerous other promiscuous chemokine receptor, low levels of migration was still observed in the presence of inhibitor. Nonetheless, targeting the CCR2 receptor might reduce infiltration of macrophages, improving prognosis as well.

Through mass spectrometry, it was also found that both myofibrobasts and senescent fibroblasts secrete collagen of various types, implicated in several cancers but myofibroblasts secreted higher levels than senescent fibroblasts. However, senescent fibroblast secreted a plethora of factors (proteoglycans and laminins) that interact with collagen fibres, therefore suggesting that both phenotypes work in synchronisation to create an ECM which might be permissible for tumour cell survival, proliferation, growth of new capillaries, chemo-resistance, and modulating

immune cell polarisation towards immune-suppression. Hence, targeting either fibroblast phenotype or collagen or the proteins that interact with it would disrupt the ECM, possibly directly impacting upon tumour viability or invasive ability, or increasing bioavailability of cancer-targeting drugs in the TME.

Finally, this study found the hypothesis that CAFs of different phenotypes have different macrophage recruitment capability holds true to a great extent, with senescent fibroblasts secreting and recruiting more macrophages via chemokines than myofibroblasts in head and neck cancer.

Appendix 1: Lab equipment

Equipment	Manufacturer
Applied Biosystems 7900HT Fast Real-Time PCR System	Life Technologies
Applied Biosystems 2720 Thermal Cycler	Life Technologies
3 – 18k SciQuip centrifuge	Sigma Aldrich
Class II Safety Cabinets	Walker
Compact X4 Automatic X-ray Film Processor	Xograph
Dri-Block Heater	Techne
Electromagnetic Stirrer	FALC
Galaxy CO_2 Incubators	Eppendorf
Inverted Tissue Culture Microscope	AmScope
Microplate Reader	BMG POLARstar Galaxy
Microplate Reader	Tecan infinite M200
Microtube Centrifuge	Sigma Aldrich

NanoDrop 1000	Thermo-Fisher
PureLab Option Water De-ioniser	Elga
SteriMate Autoclave	Astell
Rotor Gene Q	Qiagen

Appendix 2: Buffers and solutions:

Buffer/Solution	Contents
Laemmli buffer	4% Sodium dodecyl sulphate, 20% glycerol, 10% β-mercaptoethanol, 0.004% bromophenol blue, 0.125 M Tris HCl
Running buffer	25 mM Tris base, 190 mM glycine, 0.1% SDS, pH – 8.3
TBS	2.423 g Trizma HCL, 8.006 g NaCl, 800 ml ultra-pure water, pH to 7.6 using HCL
TBS-Tween	TBS + 1 ml Tween
Macs buffer	0.5% BSA and 2 mM EDTA in PBS, pH 7.2

Appendix 3: Stages of tumour section:

Tumour sections	Stage
10/46 B2 C5P	T1
07/1996 A18 A3P	T3
12/0016 B1	T4
07/1396 B7 A2P	T1
12/0763 A1	T2
06/2300 A2 C4P	T1
12/1009 D2	T2
12/1911 C3	T1
12/0641 D2	T1
12/0763 E2	T2

Reactome [Online]. Available: https://reactome.org/ [Accessed 17.12.2017].
ACERBI, I., CASSEREAU, L., DEAN, I., SHI, Q., AU, A., PARK, C., CHEN, Y. Y., LIPHARDT, J., HWANG, E. S. & WEAVER, V. M. 2015. Human breast cancer invasion and aggression correlates with ECM stiffening and immune cell infiltration. *Integr Biol (Camb),* 7**,** 1120-34.
ADOMAKO, A., CALVO, V., BIRAN, N., OSMAN, K., CHARI, A., PATON, J. C., PATON, A. W., MOORE, K., SCHEWE, D. M. & AGUIRRE-GHISO, J. A. 2015. Identification of markers that functionally define a quiescent multiple myeloma cell sub-population surviving bortezomib treatment. *BMC Cancer,* 15**,** 444.
AERTS, H. J., VELAZQUEZ, E. R., LEIJENAAR, R. T., PARMAR, C., GROSSMANN, P., CARVALHO, S., CAVALHO, S., BUSSINK, J., MONSHOUWER, R., HAIBE-KAINS, B., RIETVELD, D., HOEBERS, F., RIETBERGEN, M. M., LEEMANS, C. R., DEKKER, A., QUACKENBUSH, J., GILLIES, R. J. & LAMBIN, P. 2014. Decoding tumour phenotype by noninvasive imaging using a quantitative radiomics approach. *Nat Commun,* 5**,** 4006.
AHMED, S. T. & DARNELL, J. E. 2009. Serpin B3/B4, activated by STAT3, promote survival of squamous carcinoma cells. *Biochem Biophys Res Commun,* 378**,** 821-5.
AHSAN, M. S., YAMAZAKI, M., MARUYAMA, S., KOBAYASHI, T., IDA-YONEMOCHI, H., HASEGAWA, M., HENRY ADEMOLA, A., CHENG, J. & SAKU, T. 2011. Differential expression of perlecan receptors, alpha-dystroglycan and integrin beta1, before and after invasion of oral squamous cell carcinoma. *J Oral Pathol Med,* 40**,** 552-9.
ALBERS, A. E., FERRIS, R. L., KIM, G. G., CHIKAMATSU, K., DELEO, A. B. & WHITESIDE, T. L. 2005. Immune responses to p53 in patients with cancer: enrichment in tetramer+ p53 peptide-specific T cells and regulatory T cells at tumor sites. *Cancer Immunol Immunother,* 54**,** 1072-81.
ALBINI, A., TOSETTI, F., BENELLI, R. & NOONAN, D. M. 2005. Tumor inflammatory angiogenesis and its chemoprevention. *Cancer Res,* 65**,** 10637-41.
ALSHAKER, H., SACCO, K., ALFRAIDI, A., MUHAMMAD, A., WINKLER, M. & PCHEJETSKI, D. 2015. Leptin signalling, obesity and prostate cancer: molecular and clinical perspective on the old dilemma. *Oncotarget,* 6**,** 35556-63.
ALSPACH, E., FU, Y. & STEWART, S. A. 2013. Senescence and the pro-tumorigenic stroma. *Crit Rev Oncog,* 18**,** 549-58.
ANDERS, H. J., VIELHAUER, V. & SCHLONDORFF, D. 2003. Chemokines and chemokine receptors are involved in the resolution or progression of renal disease. *Kidney Int,* 63**,** 401-15.
ANGI, M., KALIRAI, H., PRENDERGAST, S., SIMPSON, D., HAMMOND, D. E., MADIGAN, M. C., BEYNON, R. J. & COUPLAND, S. E. 2016. In-depth proteomic profiling of the uveal melanoma secretome. *Oncotarget,* 7**,** 49623-49635.
ARA, T. & DECLERCK, Y. A. 2010. Interleukin-6 in bone metastasis and cancer progression. *Eur J Cancer,* 46**,** 1223-31.
ARAFAT, H., LAZAR, M., SALEM, K., CHIPITSYNA, G., GONG, Q., PAN, T. C., ZHANG, R. Z., YEO, C. J. & CHU, M. L. 2011. Tumor-specific expression and alternative splicing of the COL6A3 gene in pancreatic cancer. *Surgery,* 150**,** 306-15.
AUGSTEN, M. 2014a. Cancer-associated fibroblasts as another polarized cell type of the tumor microenvironment. *Front Oncol,* 4**,** 62.
AUGSTEN, M. 2014b. Cancer-associated fibroblasts as another polarized cell type of the tumor microenvironment. *Frontiers in Oncology,* 4.
AVRAHAM, H., PARK, S. Y., SCHINKMANN, K. & AVRAHAM, S. 2000. RAFTK/Pyk2-mediated cellular signalling. *Cell Signal,* 12**,** 123-33.
BABA, M., IMAI, T., NISHIMURA, M., KAKIZAKI, M., TAKAGI, S., HIESHIMA, K., NOMIYAMA, H. & YOSHIE, O. 1997. Identification of CCR6, the Specific Receptor for a Novel Lymphocyte-directed CC Chemokine LARC. *Journal of Biological Chemistry,* 272**,** 14893-14898.
BAE, J. A., YOON, S., PARK, S. Y., LEE, J. H., HWANG, J. E., KIM, H., SEO, Y. W., CHA, Y. J., HONG, S. P., CHUNG, I. J. & KIM, K. K. 2014. An unconventional KITENIN/ErbB4-mediated downstream

signal of EGF upregulates c-Jun and the invasiveness of colorectal cancer cells. *Clin Cancer Res,* 20**,** 4115-28.

BAKER, A. M., BIRD, D., LANG, G., COX, T. R. & ERLER, J. T. 2013. Lysyl oxidase enzymatic function increases stiffness to drive colorectal cancer progression through FAK. *Oncogene,* 32**,** 1863-8.

BANERJEE, A. G., BHATTACHARYYA, I., LYDIATT, W. M. & VISHWANATHA, J. K. 2003. Aberrant expression and localization of decorin in human oral dysplasia and squamous cell carcinoma. *Cancer Res,* 63**,** 7769-76.

BANKAITIS, K. V. & FINGLETON, B. 2015. Targeting IL4/IL4R for the treatment of epithelial cancer metastasis. *Clin Exp Metastasis,* 32**,** 847-56.

BAO, C. H., WANG, X. T., MA, W., WANG, N. N., UN NESA, E., WANG, J. B., WANG, C., JIA, Y. B., WANG, K., TIAN, H. & CHENG, Y. F. 2015. Irradiated fibroblasts promote epithelial-mesenchymal transition and HDGF expression of esophageal squamous cell carcinoma. *Biochem Biophys Res Commun,* 458**,** 441-7.

BARCENA, C., STEFANOVIC, M., TUTUSAUS, A., MARTINEZ-NIETO, G. A., MARTINEZ, L., GARCIA-RUIZ, C., DE MINGO, A., CABALLERIA, J., FERNANDEZ-CHECA, J. C., MARI, M. & MORALES, A. 2015. Angiogenin secretion from hepatoma cells activates hepatic stellate cells to amplify a self-sustained cycle promoting liver cancer. *Sci Rep,* 5**,** 7916.

BAUER, J., NAMINENI, S., REISINGER, F., ZOLLER, J., YUAN, D. & HEIKENWALDER, M. 2012. Lymphotoxin, NF-kB, and cancer: the dark side of cytokines. *Dig Dis,* 30**,** 453-68.

BAUGÉ, C., CAUVARD, O., LECLERCQ, S., GALÉRA, P. & BOUMÉDIENE, K. 2011. Modulation of transforming growth factor beta signalling pathway genes by transforming growth factor beta in human osteoarthritic chondrocytes: involvement of Sp1 in both early and late response cells to transforming growth factor beta. *Arthritis Res Ther.*

BAUML, J., SEIWERT, T. Y., PFISTER, D. G., WORDEN, F., LIU, S. V., GILBERT, J., SABA, N. F., WEISS, J., WIRTH, L., SUKARI, A., KANG, H., GIBSON, M. K., MASSARELLI, E., POWELL, S., MEISTER, A., SHU, X., CHENG, J. D. & HADDAD, R. 2017. Pembrolizumab for Platinum- and Cetuximab-Refractory Head and Neck Cancer: Results From a Single-Arm, Phase II Study. *J Clin Oncol,* 35**,** 1542-1549.

BAYNE, L. J., BEATTY, G. L., JHALA, N., CLARK, C. E., RHIM, A. D., STANGER, B. Z. & VONDERHEIDE, R. H. 2012. Tumor-derived granulocyte-macrophage colony-stimulating factor regulates myeloid inflammation and T cell immunity in pancreatic cancer. *Cancer Cell,* 21**,** 822-35.

BECK, S. 2013. Acute and chronis inflammation. *http://www.hopkinsmedicine.org/mcp/Education/300.713%20Lectures/300.713%202013/Beck_08.26.2013.pdf*.

BEN-PORATH, I. & WEINBERG, R. A. 2004. When cells get stressed: an integrative view of cellular senescence. *J Clin Invest,* 113**,** 8-13.

BENOY, I. H., SALGADO, R., VAN DAM, P., GEBOERS, K., VAN MARCK, E., SCHARPE, S., VERMEULEN, P. B. & DIRIX, L. Y. 2004. Increased serum interleukin-8 in patients with early and metastatic breast cancer correlates with early dissemination and survival. *Clin Cancer Res,* 10**,** 7157-62.

BERCHTOLD, S., GRUNWALD, B., KRUGER, A., REITHMEIER, A., HAHL, T., CHENG, T., FEUCHTINGER, A., BORN, D., ERKAN, M., KLEEFF, J. & ESPOSITO, I. 2015. Collagen type V promotes the malignant phenotype of pancreatic ductal adenocarcinoma. *Cancer Lett,* 356**,** 721-32.

BERTANI, F. R., MOZETIC, P., FIORAMONTI, M., IULIANI, M., RIBELLI, G., PANTANO, F., SANTINI, D., TONINI, G., TROMBETTA, M., BUSINARO, L., SELCI, S. & RAINER, A. 2017. Classification of M1/M2-polarized human macrophages by label-free hyperspectral reflectance confocal microscopy and multivariate analysis. *Sci Rep,* 7**,** 8965.

BHAT, F. A., SHARMILA, G., BALAKRISHNAN, S., ARUNKUMAR, R., ELUMALAI, P., SUGANYA, S., RAJA SINGH, P., SRINIVASAN, N. & ARUNAKARAN, J. 2014. Quercetin reverses EGF-induced epithelial to mesenchymal transition and invasiveness in prostate cancer (PC-3) cell line via EGFR/PI3K/Akt pathway. *J Nutr Biochem,* 25**,** 1132-1139.

BIERIE, B. & MOSES, H. L. 2006. TGF-β and cancer. *Cytokine & Growth Factor Reviews,* 17**,** 29-40.
BINGLE, L., BROWN, N. J. & LEWIS, C. E. 2002. The role of tumour-associated macrophages in tumour progression: implications for new anticancer therapies. *J Pathol,* 196**,** 254-65.
BISWAS, S. K. & MANTOVANI, A. 2010. Macrophage plasticity and interaction with lymphocyte subsets: cancer as a paradigm. *Nat Immunol,* 11**,** 889-96.
BJORDAHL, R. L., STEIDL, C., GASCOYNE, R. D. & WARE, C. F. 2013. Lymphotoxin network pathways shape the tumor microenvironment. *Curr Opin Immunol,* 25**,** 222-9.
BLOBEL, C. P. 2005. ADAMs: key components in EGFR signalling and development. *Nat Rev Mol Cell Biol,* 6**,** 32-43.
BOCHET, L., LEHUÉDÉ, C., DAUVILLIER, S., WANG, Y. Y., DIRAT, B., LAURENT, V., DRAY, C., GUIET, R., MARIDONNEAU-PARINI, I., LE GONIDEC, S., COUDERC, B., ESCOURROU, G., VALET, P. & MULLER, C. 2013. Adipocyte-derived fibroblasts promote tumor progression and contribute to the desmoplastic reaction in breast cancer. *Cancer Res,* 73**,** 5657-68.
BONNER, J. A., HARARI, P. M., GIRALT, J., AZARNIA, N., SHIN, D. M., COHEN, R. B., JONES, C. U., SUR, R., RABEN, D., JASSEM, J., OVE, R., KIES, M. S., BASELGA, J., YOUSSOUFIAN, H., AMELLAL, N., ROWINSKY, E. K. & ANG, K. K. 2006. Radiotherapy plus cetuximab for squamous-cell carcinoma of the head and neck. *N Engl J Med,* 354**,** 567-78.
BOYLE, P. L., B. 2008. World cancer report. International Agency for Research on Cancer.
BOZAOGLU, K., CURRAN, J. E., STOCKER, C. J., ZAIBI, M. S., SEGAL, D., KONSTANTOPOULOS, N., MORRISON, S., CARLESS, M., DYER, T. D., COLE, S. A., GORING, H. H., MOSES, E. K., WALDER, K., CAWTHORNE, M. A., BLANGERO, J. & JOWETT, J. B. 2010. Chemerin, a novel adipokine in the regulation of angiogenesis. *J Clin Endocrinol Metab,* 95**,** 2476-85.
BURTON, D. G. & FARAGHER, R. G. 2015. Cellular senescence: from growth arrest to immunogenic conversion. *Age (Dordr),* 37**,** 27.
CAETANO, M. S., ZHANG, H., CUMPIAN, A. M., GONG, L., UNVER, N., OSTRIN, E. J., DALIRI, S., CHANG, S. H., OCHOA, C. E., HANASH, S., BEHRENS, C., WISTUBA, II, STERNBERG, C., KADARA, H., FERREIRA, C. G., WATOWICH, S. S. & MOGHADDAM, S. J. 2016. IL6 Blockade Reprograms the Lung Tumor Microenvironment to Limit the Development and Progression of K-ras-Mutant Lung Cancer. *Cancer Res,* 76**,** 3189-99.
CAI, J., TANG, H., XU, L., WANG, X., YANG, C., RUAN, S., GUO, J., HU, S. & WANG, Z. 2012. Fibroblasts in omentum activated by tumor cells promote ovarian cancer growth, adhesion and invasiveness. *Carcinogenesis,* 33**,** 20-29.
CALLE, E. E. & KAAKS, R. 2004. Overweight, obesity and cancer: epidemiological evidence and proposed mechanisms. *Nat Rev Cancer,* 4**,** 579-91.
CALON, A., TAURIELLO, D. V. F. & BATLLE, E. 2014. TGF-beta in CAF-mediated tumor growth and metastasis. *Seminars in Cancer Biology,* 25**,** 15-22.
CANALS, F., COLOMÉ, N., FERRER, C., PLAZA-CALONGE, M. E. C. & RODRÍGUEZ-MANZANEQUE, J. C. 2006. Identification of substrates of the extracellular protease ADAMTS1 by DIGE proteomic analysis. *Proteomics,* 6 Suppl 1**,** S28-35.
CARMO, A. A., COSTA, B. R., VAGO, J. P., DE OLIVEIRA, L. C., TAVARES, L. P., NOGUEIRA, C. R., RIBEIRO, A. L., GARCIA, C. C., BARBOSA, A. S., BRASIL, B. S., DUSSE, L. M., BARCELOS, L. S., BONJARDIM, C. A., TEIXEIRA, M. M. & SOUSA, L. P. 2014. Plasmin induces in vivo monocyte recruitment through protease-activated receptor-1-, MEK/ERK-, and CCR2-mediated signaling. *J Immunol,* 193**,** 3654-63.
CASELLA, G., GARZETTI, L., GATTA, A. T., FINARDI, A., MAIORINO, C., RUFFINI, F., MARTINO, G., MUZIO, L. & FURLAN, R. 2016. IL4 induces IL6-producing M2 macrophages associated to inhibition of neuroinflammation in vitro and in vivo. *J Neuroinflammation.* London.
CASTELLANA, B., AASEN, T., MORENO-BUENO, G., DUNN, S. E. & RAMON Y CAJAL, S. 2015. Interplay between YB-1 and IL-6 promotes the metastatic phenotype in breast cancer cells. *Oncotarget,* 6**,** 38239-56.

CATALANO, S., LEGGIO, A., BARONE, I., DE MARCO, R., GELSOMINO, L., CAMPANA, A., MALIVINDI, R., PANZA, S., GIORDANO, C., LIGUORI, A., BONOFIGLIO, D. & ANDO, S. 2015. A novel leptin antagonist peptide inhibits breast cancer growth in vitro and in vivo. *J Cell Mol Med,* 19**,** 1122-32.

CHANG, C. C., WU, M. J., YANG, J. Y., CAMARILLO, I. G. & CHANG, C. J. 2015a. Leptin-STAT3-G9a Signaling Promotes Obesity-Mediated Breast Cancer Progression. *Cancer Res,* 75**,** 2375-2386.

CHANG, H., DONG, T., MA, X., ZHANG, T., CHEN, Z., YANG, Z. & ZHANG, Y. 2015b. Spondin 1 promotes metastatic progression through Fak and Src dependent pathway in human osteosarcoma. *Biochem Biophys Res Commun,* 464**,** 45-50.

CHANG, W. C., WU, S. L., HUANG, W. C., HSU, J. Y., CHAN, S. H., WANG, J. M., TSAI, J. P. & CHEN, B. K. 2015c. PTX3 gene activation in EGF-induced head and neck cancer cell metastasis. *Oncotarget,* 6**,** 7741-57.

CHAUDHURI, O., KOSHY, S. T., BRANCO DA CUNHA, C., SHIN, J. W., VERBEKE, C. S., ALLISON, K. H. & MOONEY, D. J. 2014. Extracellular matrix stiffness and composition jointly regulate the induction of malignant phenotypes in mammary epithelium. *Nat Mater,* 13**,** 970-8.

CHEN, E. C., KARL, T. A., KALISKY, T., GUPTA, S. K., O'BRIEN, C. A., LONGACRE, T. A., VAN DE RIJN, M., QUAKE, S. R., CLARKE, M. F. & ROTHENBERG, M. E. 2015. KIT Signaling Promotes Growth of Colon Xenograft Tumors in Mice and Is Up-Regulated in a Subset of Human Colon Cancers. *Gastroenterology,* 149**,** 705-17.e2.

CHEN, G., DING, J., LUO, L., LIU, Y., YAN, K., CHEN, P., SONG, P., FU, Y., WANG, J. & GONG, S. 2006. [Expression of perlecan in laryngeal carcinoma cell and its significance]. *Lin Chuang Er Bi Yan Hou Ke Za Zhi,* 20**,** 78-80.

CHEN, J. J., LIN, Y. C., YAO, P. L., YUAN, A., CHEN, H. Y., SHUN, C. T., TSAI, M. F., CHEN, C. H. & YANG, P. C. 2005. Tumor-associated macrophages: the double-edged sword in cancer progression. *J Clin Oncol,* 23**,** 953-64.

CHEN, S. F., NIEH, S., JAO, S. W., WU, M. Z., LIU, C. L., CHANG, Y. C. & LIN, Y. S. 2013. The paracrine effect of cancer-associated fibroblast-induced interleukin-33 regulates the invasiveness of head and neck squamous cell carcinoma. *J Pathol,* 231**,** 180-9.

CHEN, W., JIN, W., HARDEGEN, N., LEI, K. J., LI, L., MARINOS, N., MCGRADY, G. & WAHL, S. M. 2003. Conversion of peripheral CD4+CD25- naive T cells to CD4+CD25+ regulatory T cells by TGF-beta induction of transcription factor Foxp3. *J Exp Med,* 198**,** 1875-86.

CHEN, Z., MALHOTRA, P. S., THOMAS, G. R., ONDREY, F. G., DUFFEY, D. C., SMITH, C. W., ENAMORADO, I., YEH, N. T., KROOG, G. S., RUDY, S., MCCULLAGH, L., MOUSA, S., QUEZADO, M., HERSCHER, L. L. & VAN WAES, C. 1999. Expression of proinflammatory and proangiogenic cytokines in patients with head and neck cancer. *Clin Cancer Res,* 5**,** 1369-79.

CHENG, G., SALERNO, J. C., CAO, Z., PAGANO, P. J. & LAMBETH, J. D. 2008. Identification and characterization of VPO1, a new animal heme-containing peroxidase. *Free Radic Biol Med,* 45**,** 1682-94.

CHEON, D. J., TONG, Y., SIM, M. S., DERING, J., BEREL, D., CUI, X., LESTER, J., BEACH, J. A., TIGHIOUART, M., WALTS, A. E., KARLAN, B. Y. & ORSULIC, S. 2014. A collagen-remodeling gene signature regulated by TGF-beta signaling is associated with metastasis and poor survival in serous ovarian cancer. *Clin Cancer Res,* 20**,** 711-23.

CHEVALLET, M., DIEMER, H., VAN DORSSEALER, A., VILLIERS, C. & RABILLOUD, T. 2007. Toward a better analysis of secreted proteins: the example of the myeloid cells secretome. *Proteomics,* 7**,** 1757-70.

CHIN, D., BOYLE, G. M., WILLIAMS, R. M., FERGUSON, K., PANDEYA, N., PEDLEY, J., CAMPBELL, C. M., THEILE, D. R., PARSONS, P. G. & COMAN, W. B. 2005. Novel markers for poor prognosis in head and neck cancer. *International Journal of Cancer,* 113**,** 789-797.

CHUANG, J. Y., TSAI, C. F., CHANG, S. W., CHIANG, I. P., HUANG, S. M., LIN, H. Y., YEH, W. L. & LU, D. Y. 2013. Glial cell line-derived neurotrophic factor induces cell migration in human oral squamous cell carcinoma. *Oral Oncol,* 49**,** 1103-12.

COHEN, A. J. & POPE, C. A., 3RD 1995. Lung cancer and air pollution. *Environ Health Perspect,* 103 Suppl 8**,** 219-24.
COHEN, E. E. 2017. 1135O Phase 1b/2 Study (SCORES) assessing safety, tolerability, and preliminary anti-tumor activity of durvalumab plus AZD9150 or AZD 5069 in patients with advanced solid malignancies and squamous cell carcinoma of the head and neck (SCCHN). Annals of Oncology.
CONWAY, D. I., PETTICREW, M., MARLBOROUGH, H., BERTHILLER, J., HASHIBE, M. & MACPHERSON, L. M. 2008. Socioeconomic inequalities and oral cancer risk: a systematic review and meta-analysis of case-control studies. *Int J Cancer,* 122**,** 2811-9.
COPPE, J. P., BOYSEN, M., SUN, C. H., WONG, B. J., KANG, M. K., PARK, N. H., DESPREZ, P. Y., CAMPISI, J. & KRTOLICA, A. 2008. A role for fibroblasts in mediating the effects of tobacco-induced epithelial cell growth and invasion. *Mol Cancer Res,* 6**,** 1085-98.
COPPÉ, J.-P., DESPREZ, P.-Y., KRTOLICA, A. & CAMPISI, J. 2010a. The Senescence-Associated Secretory Phenotype: The Dark Side of Tumor Suppression. *Annual Review of Pathology: Mechanisms of Disease,* 5**,** 99-118.
COPPÉ, J. P., DESPREZ, P. Y., KRTOLICA, A. & CAMPISI, J. 2010b. The senescence-associated secretory phenotype: the dark side of tumor suppression. *Annu Rev Pathol,* 5**,** 99-118.
CRABBE, L., VERDUN, R. E., HAGGBLOM, C. I. & KARLSEDER, J. 2004. Defective telomere lagging strand synthesis in cells lacking WRN helicase activity. *Science,* 306**,** 1951-3.
CUI, J., HU, Y. F., FENG, X. M., TIAN, T., GUO, Y. H., MA, J. W., NAN, K. J. & ZHANG, H. Y. 2014. EGFR inhibitors and autophagy in cancer treatment. *Tumour Biol,* 35**,** 11701-9.
CURIEL, T. J., COUKOS, G., ZOU, L., ALVAREZ, X., CHENG, P., MOTTRAM, P., EVDEMON-HOGAN, M., CONEJO-GARCIA, J. R., ZHANG, L., BUROW, M., ZHU, Y., WEI, S., KRYCZEK, I., DANIEL, B., GORDON, A., MYERS, L., LACKNER, A., DISIS, M. L., KNUTSON, K. L., CHEN, L. & ZOU, W. 2004. Specific recruitment of regulatory T cells in ovarian carcinoma fosters immune privilege and predicts reduced survival. *Nat Med,* 10**,** 942-9.
CURRY, J. M., SPRANDIO, J., COGNETTI, D., LUGINBUHL, A., BAR-AD, V., PRIBITKIN, E. & TULUC, M. 2014. Tumor microenvironment in head and neck squamous cell carcinoma. *Semin Oncol,* 41**,** 217-34.
DARBY, I. A., ZAKUAN, N., BILLET, F. & DESMOULIERE, A. 2016. The myofibroblast, a key cell in normal and pathological tissue repair. *Cell Mol Life Sci,* 73**,** 1145-57.
DAVALOS, A., COPPE, J.-P., CAMPISI, J. & DESPREZ, P.-Y. 2010a. Senescent cells as a source of inflammatory factors for tumor progression. *Cancer and Metastasis Reviews,* 29**,** 273-283.
DAVALOS, A. R., COPPE, J. P., CAMPISI, J. & DESPREZ, P. Y. 2010b. Senescent cells as a source of inflammatory factors for tumor progression. *Cancer Metastasis Rev,* 29**,** 273-83.
DE FALCO, M., LUCARIELLO, A., IAQUINTO, S., ESPOSITO, V., GUERRA, G. & DE LUCA, A. 2015. Molecular Mechanisms of Helicobacter pylori Pathogenesis. *J Cell Physiol,* 230**,** 1702-7.
DE LANGE DAVIES, C., ENGESAETER, B. O., HAUG, I., ORMBERG, I. W., HALGUNSET, J. & BREKKEN, C. 2001. Uptake of IgG in osteosarcoma correlates inversely with interstitial fluid pressure, but not with interstitial constituents. *Br J Cancer,* 85**,** 1968-77.
DEL CORNO, M., LIU, Q., SCHOLS, D., DE CLERECQ, E., GESSANI, S., FREEDMAN, B. & COLLMAN, R. 2001. HIV-1 gp120 and chemokine activation of Pyk2 and mitogen-activated protein kinases in primary macrophages mediated by calcium-dependent, pertussis toxin -insensitive chemokine receptor signaling. *Blood,* 98**,** 2909-16.
DESHMANE, S. L., KREMLEV, S., AMINI, S. & SAWAYA, B. E. 2009. Monocyte chemoattractant protein-1 (MCP-1): an overview. *J Interferon Cytokine Res,* 29**,** 313-26.
DESMOULIERE, A., GEINOZ, A., GABBIANI, F. & GABBIANI, G. 1993. Transforming growth factor-beta 1 induces alpha-smooth muscle actin expression in granulation tissue myofibroblasts and in quiescent and growing cultured fibroblasts. *J Cell Biol,* 122**,** 103-11.
DESMOULIÈRE, A., CHAPONNIER, C. & GABBIANI, G. 2005. Tissue repair, contraction, and the myofibroblast. *Wound Repair Regen,* 13**,** 7-12.

DI MICCO, R., FUMAGALLI, M., CICALESE, A., PICCININ, S., GASPARINI, P., LUISE, C., SCHURRA, C., GARRE', M., NUCIFORO, P. G., BENSIMON, A., MAESTRO, R., PELICCI, P. G. & D'ADDA DI FAGAGNA, F. 2006. Oncogene-induced senescence is a DNA damage response triggered by DNA hyper-replication. *Nature,* 444**,** 638-42.

DIKIC, I. & SCHLESSINGER, J. 1998. Identification of a new Pyk2 isoform implicated in chemokine and antigen receptor signaling. *J Biol Chem,* 273**,** 14301-8.

DIKIC, I., TOKIWA, G., LEV, S., COURTNEIDGE, S. A. & SCHLESSINGER, J. 1996. A role for Pyk2 and Src in linking G-protein-coupled receptors with MAP kinase activation. *Nature,* 383**,** 547-50.

DIL, N. & BANERJEE, A. G. 2011. A role for aberrantly expressed nuclear localized decorin in migration and invasion of dysplastic and malignant oral epithelial cells. *Head Neck Oncol,* 3**,** 44.

DIL, N. & BANERJEE, A. G. 2012. Knockdown of aberrantly expressed nuclear localized decorin attenuates tumour angiogenesis related mediators in oral cancer progression model in vitro. *Head Neck Oncol,* 4**,** 11.

DIMRI, G. P., LEE, X., BASILE, G., ACOSTA, M., SCOTT, G., ROSKELLEY, C., MEDRANO, E. E., LINSKENS, M., RUBELJ, I. & PEREIRA-SMITH, O. 1995. A biomarker that identifies senescent human cells in culture and in aging skin in vivo. *Proc Natl Acad Sci U S A,* 92**,** 9363-7.

DING, K., BANERJEE, A., TAN, S., ZHAO, J., ZHUANG, Q., LI, R., QIAN, P., LIU, S., WU, Z. S., LOBIE, P. E. & ZHU, T. 2014a. Artemin, a member of the glial cell line-derived neurotrophic factor family of ligands, is HER2-regulated and mediates acquired trastuzumab resistance by promoting cancer stem cell-like behavior in mammary carcinoma cells. *J Biol Chem,* 289**,** 16057-71.

DING, L., LI, B., ZHAO, Y., FU, Y. F., HU, E. L., HU, Q. G., NI, Y. H. & HOU, Y. Y. 2014b. Serum CCL2 and CCL3 as potential biomarkers for the diagnosis of oral squamous cell carcinoma. *Tumour Biol,* 35**,** 10539-46.

DIREKZE, N. C., HODIVALA-DILKE, K., JEFFERY, R., HUNT, T., POULSOM, R., OUKRIF, D., ALISON, M. R. & WRIGHT, N. A. 2004. Bone marrow contribution to tumor-associated myofibroblasts and fibroblasts. *Cancer Res,* 64**,** 8492-5.

DOLL, R. & PETO, R. 1981. The causes of cancer: quantitative estimates of avoidable risks of cancer in the United States today. *J Natl Cancer Inst,* 66**,** 1191-308.

DUFFY, S. A., TAYLOR, J. M., TERRELL, J. E., ISLAM, M., LI, Y., FOWLER, K. E., WOLF, G. T. & TEKNOS, T. N. 2008. Interleukin-6 predicts recurrence and survival among head and neck cancer patients. *Cancer,* 113**,** 750-7.

DUGINA, V., FONTAO, L., CHAPONNIER, C., VASILIEV, J. & GABBIANI, G. 2001. Focal adhesion features during myofibroblastic differentiation are controlled by intracellular and extracellular factors. *J Cell Sci,* 114**,** 3285-96.

DVORANKOVA, B., SMETANA, K., JR., RIHOVA, B., KUCERA, J., MATEU, R. & SZABO, P. 2015. Cancer-associated fibroblasts are not formed from cancer cells by epithelial-to-mesenchymal transition in nu/nu mice. *Histochem Cell Biol,* 143**,** 463-9.

DÖBRÓSSY, L. 2005. Epidemiology of head and neck cancer: Magnitude of the problem. *Cancer and Metastasis Reviews,* 24**,** 9-17.

ELIGINI, S., CRISCI, M., BONO, E., SONGIA, P., TREMOLI, E., COLOMBO, G. I. & COLLI, S. 2013. Human monocyte-derived macrophages spontaneously differentiated in vitro show distinct phenotypes. *J Cell Physiol,* 228**,** 1464-72.

EN-LIN, S., SHENG-GUO, C. & HUA-QIAO, W. 2010. The expression of EFEMP1 in cervical carcinoma and its relationship with prognosis. *Gynecol Oncol,* 117**,** 417-22.

ENGLUND, E., BARTOSCHEK, M., REITSMA, B., JACOBSSON, L., ESCUDERO-ESPARZA, A., ORIMO, A., LEANDERSSON, K., HAGERLING, C., ASPBERG, A., STORM, P., OKROJ, M., MULDER, H., JIRSTROM, K., PIETRAS, K. & BLOM, A. M. 2016. Cartilage oligomeric matrix protein contributes to the development and metastasis of breast cancer. *Oncogene,* 35**,** 5585-5596.

ERDOGAN, B. & WEBB, D. J. 2017. Cancer-associated fibroblasts modulate growth factor signaling and extracellular matrix remodeling to regulate tumor metastasis. *Biochem Soc Trans,* 45**,** 229-236.

EVANS, R. A., TIAN, Y. A. C., STEADMAN, R. & PHILLIPS, A. O. 2003a. TGF-β1-mediated fibroblast–myofibroblast terminal differentiation—the role of smad proteins. *Experimental Cell Research,* 282**,** 90-100.

EVANS, R. A., TIAN, Y. C., STEADMAN, R. & PHILLIPS, A. O. 2003b. TGF-beta1-mediated fibroblast-myofibroblast terminal differentiation-the role of Smad proteins. *Exp Cell Res,* 282**,** 90-100.

FANG, W. B., JOKAR, I., ZOU, A., LAMBERT, D., DENDUKURI, P. & CHENG, N. 2012. CCL2/CCR2 chemokine signaling coordinates survival and motility of breast cancer cells through Smad3 protein- and p42/44 mitogen-activated protein kinase (MAPK)-dependent mechanisms. *J Biol Chem,* 287**,** 36593-608.

FERRANTI, F., MUCIACCIA, B., RICCI, G., DOVERE, L., CANIPARI, R., MAGLIOCCA, F., STEFANINI, M., CATIZONE, A. & VICINI, E. 2012. Glial cell line-derived neurotrophic factor promotes invasive behaviour in testicular seminoma cells. *Int J Androl,* 35**,** 758-68.

FERRARA, N. & DAVIS-SMYTH, T. 1997. The biology of vascular endothelial growth factor. *Endocr Rev,* 18**,** 4-25.

FERRIS, R. L., BLUMENSCHEIN, G., FAYETTE, J., GUIGAY, J., COLEVAS, A. D., LICITRA, L., HARRINGTON, K., KASPER, S., VOKES, E. E., EVEN, C., WORDEN, F., SABA, N. F., IGLESIAS DOCAMPO, L. C., HADDAD, R., RORDORF, T., KIYOTA, N., TAHARA, M., MONGA, M., LYNCH, M., GEESE, W. J., KOPIT, J., SHAW, J. W. & GILLISON, M. L. 2016. Nivolumab for Recurrent Squamous-Cell Carcinoma of the Head and Neck. *N Engl J Med,* 375**,** 1856-1867.

FIEDLER, L. R., SCHONHERR, E., WADDINGTON, R., NILAND, S., SEIDLER, D. G., AESCHLIMANN, D. & EBLE, J. A. 2008. Decorin regulates endothelial cell motility on collagen I through activation of insulin-like growth factor I receptor and modulation of alpha2beta1 integrin activity. *J Biol Chem,* 283**,** 17406-15.

FISHER, D. T., APPENHEIMER, M. M. & EVANS, S. S. 2014. The Two Faces of IL-6 in the Tumor Microenvironment. *Semin Immunol,* 26**,** 38-47.

FORAN, E., GARRITY-PARK, M. M., MUREAU, C., NEWELL, J., SMYRK, T. C., LIMBURG, P. J. & EGAN, L. J. 2010. Upregulation of DNA methyltransferase-mediated gene silencing, anchorage-independent growth, and migration of colon cancer cells by interleukin-6. *Mol Cancer Res,* 8**,** 471-81.

FRANCESCONE, R., HOU, V. & GRIVENNIKOV, S. I. 2015. Cytokines, IBD, and colitis-associated cancer. *Inflamm Bowel Dis,* 21**,** 409-18.

FREUND, A., ORJALO, A. V., DESPREZ, P. Y. & CAMPISI, J. 2010. Inflammatory networks during cellular senescence: causes and consequences. *Trends Mol Med,* 16**,** 238-46.

FRIDLENDER, Z. G., SUN, J., MISHALIAN, I., SINGHAL, S., CHENG, G., KAPOOR, V., HORNG, W., FRIDLENDER, G., BAYUH, R., WORTHEN, G. S. & ALBELDA, S. M. 2012. Transcriptomic analysis comparing tumor-associated neutrophils with granulocytic myeloid-derived suppressor cells and normal neutrophils. *PLoS One,* 7**,** e31524.

FRIDMAN, W. H., PAGÈS, F., SAUTÈS-FRIDMAN, C. & GALON, J. 2012. The immune contexture in human tumours: impact on clinical outcome. *Nat Rev Cancer,* 12**,** 298-306.

GABRUSIEWICZ, K., RODRIGUEZ, B., WEI, J., HASHIMOTO, Y., HEALY, L. M., MAITI, S. N., THOMAS, G., ZHOU, S., WANG, Q., ELAKKAD, A., LIEBELT, B. D., YAGHI, N. K., EZHILARASAN, R., HUANG, N., WEINBERG, J. S., PRABHU, S. S., RAO, G., SAWAYA, R., LANGFORD, L. A., BRUNER, J. M., FULLER, G. N., BAR-OR, A., LI, W., COLEN, R. R., CURRAN, M. A., BHAT, K. P., ANTEL, J. P., COOPER, L. J., SULMAN, E. P. & HEIMBERGER, A. B. 2016. Glioblastoma-infiltrated innate immune cells resemble M0 macrophage phenotype. *JCI Insight,* 1.

GAGARINA, V., CARLBERG, A. L., PEREIRA-MOURIES, L. & HALL, D. J. 2008. Cartilage oligomeric matrix protein protects cells against death by elevating members of the IAP family of survival proteins. *J Biol Chem,* 283**,** 648-59.

GAGGIOLI, C., HOOPER, S., HIDALGO-CARCEDO, C., GROSSE, R., MARSHALL, J. F., HARRINGTON, K. & SAHAI, E. 2007. Fibroblast-led collective invasion of carcinoma cells with differing roles for RhoGTPases in leading and following cells. *Nat Cell Biol,* 9**,** 1392-400.

GAJEWSKI, T. F., SCHREIBER, H. & FU, Y. X. 2013. Innate and adaptive immune cells in the tumor microenvironment. *Nat Immunol,* 14**,** 1014-22.

GANJU, R. K., DUTT, P., WU, L., NEWMAN, W., AVRAHAM, H., AVRAHAM, S. & GROOPMAN, J. E. 1998. Beta-chemokine receptor CCR5 signals via the novel tyrosine kinase RAFTK. *Blood,* 91**,** 791-7.

GAO, L., WANG, F. Q., LI, H. M., YANG, J. G., REN, J. G., HE, K. F., LIU, B., ZHANG, W. & ZHAO, Y. F. 2016. CCL2/EGF positive feedback loop between cancer cells and macrophages promotes cell migration and invasion in head and neck squamous cell carcinoma. *Oncotarget,* 7**,** 87037-87051.

GAO, M. Q., KIM, B. G., KANG, S., CHOI, Y. P., YOON, J. H. & CHO, N. H. 2013. Human breast cancer-associated fibroblasts enhance cancer cell proliferation through increased TGF-alpha cleavage by ADAM17. *Cancer Lett,* 336**,** 240-6.

GASCHE, J. A., HOFFMANN, J., BOLAND, C. R. & GOEL, A. 2011. Interleukin-6 promotes tumorigenesis by altering DNA methylation in oral cancer cells. *Int J Cancer,* 129**,** 1053-63.

GIANNONI, E., BIANCHINI, F., MASIERI, L., SERNI, S., TORRE, E., CALORINI, L. & CHIARUGI, P. 2010. Reciprocal Activation of Prostate Cancer Cells and Cancer-Associated Fibroblasts Stimulates Epithelial-Mesenchymal Transition and Cancer Stemness. *Cancer Research,* 70**,** 6945-6956.

GILES, K. M., ROSS, K., ROSSI, A. G., HOTCHIN, N. A., HASLETT, C. & DRANSFIELD, I. 2001. Glucocorticoid augmentation of macrophage capacity for phagocytosis of apoptotic cells is associated with reduced p130Cas expression, loss of paxillin/pyk2 phosphorylation, and high levels of active Rac. *J Immunol,* 167**,** 976-86.

GILLAN, L., MATEI, D., FISHMAN, D. A., GERBIN, C. S., KARLAN, B. Y. & CHANG, D. D. 2002. Periostin secreted by epithelial ovarian carcinoma is a ligand for alpha(V)beta(3) and alpha(V)beta(5) integrins and promotes cell motility. *Cancer Res,* 62**,** 5358-64.

GILROY, D. & DE MAEYER, R. 2015. New insights into the resolution of inflammation. *Semin Immunol,* 27**,** 161-8.

GILROY, D. W., COLVILLE-NASH, P. R., MCMASTER, S., SAWATZKY, D. A., WILLOUGHBY, D. A. & LAWRENCE, T. 2003. Inducible cyclooxygenase-derived 15-deoxy(Delta)12-14PGJ2 brings about acute inflammatory resolution in rat pleurisy by inducing neutrophil and macrophage apoptosis. *Faseb j,* 17**,** 2269-71.

GRANT, D. S., YENISEY, C., ROSE, R. W., TOOTELL, M., SANTRA, M. & IOZZO, R. V. 2002. Decorin suppresses tumor cell-mediated angiogenesis. *Oncogene,* 21**,** 4765-77.

GUHA, N., BOFFETTA, P., WÜNSCH FILHO, V., ELUF NETO, J., SHANGINA, O., ZARIDZE, D., CURADO, M. P., KOIFMAN, S., MATOS, E., MENEZES, A., SZESZENIA-DABROWSKA, N., FERNANDEZ, L., MATES, D., DAUDT, A. W., LISSOWSKA, J., DIKSHIT, R. & BRENNAN, P. 2007. Oral health and risk of squamous cell carcinoma of the head and neck and esophagus: results of two multicentric case-control studies. *Am J Epidemiol,* 166**,** 1159-73.

GUO, Y., XU, F., LU, T., DUAN, Z. & ZHANG, Z. 2012. Interleukin-6 signaling pathway in targeted therapy for cancer. *Cancer Treat Rev,* 38**,** 904-10.

HADDAD, R. I. & SHIN, D. M. 2008. Recent Advances in Head and Neck Cancer. *New England Journal of Medicine,* 359**,** 1143-1154.

HANAVAN, P. D., BORGES, C. R., KATCHMAN, B. A., FAIGEL, D. O., HO, T. H., MA, C. T., SERGIENKO, E. A., MEURICE, N., PETIT, J. L. & LAKE, D. F. 2015. Ebselen inhibits QSOX1 enzymatic activity and suppresses invasion of pancreatic and renal cancer cell lines. *Oncotarget,* 6**,** 18418-28.

HANEKLAUS, M., GERLIC, M., O'NEILL, L. A. & MASTERS, S. L. 2013. miR-223: infection, inflammation and cancer. *J Intern Med,* 274**,** 215-26.

HASAN, A., MURATA, H., FALABELLA, A., OCHOA, S., ZHOU, L., BADIAVAS, E. & FALANGA, V. 1997. Dermal fibroblasts from venous ulcers are unresponsive to the action of transforming growth factor-beta 1. *J Dermatol Sci,* 16**,** 59-66.

HASEGAWA, M., CHENG, J., MARUYAMA, S., YAMAZAKI, M., ABE, T., BABKAIR, H., SAITO, C. & SAKU, T. 2016. Differential immunohistochemical expression profiles of perlecan-binding growth factors in epithelial dysplasia, carcinoma in situ, and squamous cell carcinoma of the oral mucosa. *Pathol Res Pract,* 212**,** 426-36.

HASSONA, Y., CIRILLO, N., HEESOM, K., PARKINSON, E. K. & PRIME, S. S. 2014. Senescent cancer-associated fibroblasts secrete active MMP-2 that promotes keratinocyte dis-cohesion and invasion. *Br J Cancer,* 111**,** 1230-7.

HASSONA, Y., CIRILLO, N., LIM, K. P., HERMAN, A., MELLONE, M., THOMAS, G. J., PITIYAGE, G. N., PARKINSON, E. K. & PRIME, S. S. 2013a. Progression of genotype-specific oral cancer leads to senescence of cancer-associated fibroblasts and is mediated by oxidative stress and TGF-beta. *Carcinogenesis,* 34**,** 1286-95.

HASSONA, Y., CIRILLO, N., LIM, K. P., HERMAN, A., MELLONE, M., THOMAS, G. J., PITIYAGE, G. N., PARKINSON, E. K. & PRIME, S. S. 2013b. Progression of genotype-specific oral cancer leads to senescence of cancer-associated fibroblasts and is mediated by oxidative stress and TGF-β. *Carcinogenesis,* 34**,** 1286-1295.

HE, T., QI, F., JIA, L., WANG, S., WANG, C., SONG, N., FU, Y., LI, L. & LUO, Y. 2015. Tumor cell-secreted angiogenin induces angiogenic activity of endothelial cells by suppressing miR-542-3p. *Cancer Lett,* 368**,** 115-25.

HEMBRUFF, S. L., JOKAR, I., YANG, L. & CHENG, N. 2010. Loss of transforming growth factor-beta signaling in mammary fibroblasts enhances CCL2 secretion to promote mammary tumor progression through macrophage-dependent and -independent mechanisms. *Neoplasia,* 12**,** 425-33.

HENDRAYANI, S. F., AL-HARBI, B., AL-ANSARI, M. M., SILVA, G. & ABOUSSEKHRA, A. 2016. The inflammatory/cancer-related IL-6/STAT3/NF-kappaB positive feedback loop includes AUF1 and maintains the active state of breast myofibroblasts. *Oncotarget,* 7**,** 41974-41985.

HENDRAYANI, S. F., AL-KHALAF, H. H. & ABOUSSEKHRA, A. 2014. The cytokine IL-6 reactivates breast stromal fibroblasts through transcription factor STAT3-dependent up-regulation of the RNA-binding protein AUF1. *J Biol Chem,* 289**,** 30962-76.

HERBIG, U., JOBLING, W. A., CHEN, B. P., CHEN, D. J. & SEDIVY, J. M. 2004. Telomere shortening triggers senescence of human cells through a pathway involving ATM, p53, and p21(CIP1), but not p16(INK4a). *Mol Cell,* 14**,** 501-13.

HEROVA, M., SCHMID, M., GEMPERLE, C. & HERSBERGER, M. 2015. ChemR23, the receptor for chemerin and resolvin E1, is expressed and functional on M1 but not on M2 macrophages. *J Immunol,* 194**,** 2330-7.

HINSLEY, E. E., HUNT, S., HUNTER, K. D., WHAWELL, S. A. & LAMBERT, D. W. 2012. Endothelin-1 stimulates motility of head and neck squamous carcinoma cells by promoting stromal-epithelial interactions. *Int J Cancer,* 130**,** 40-7.

HINZ, B. 2007. Formation and function of the myofibroblast during tissue repair. *J Invest Dermatol,* 127**,** 526-37.

HINZ, B. 2016. Myofibroblasts. *Exp Eye Res,* 142**,** 56-70.

HLATKY, L., TSIONOU, C., HAHNFELDT, P. & COLEMAN, C. N. 1994. Mammary fibroblasts may influence breast tumor angiogenesis via hypoxia-induced vascular endothelial growth factor up-regulation and protein expression. *Cancer Res,* 54**,** 6083-6.

HOV, H., TIAN, E., HOLIEN, T., HOLT, R. U., VATSVEEN, T. K., FAGERLI, U. M., WAAGE, A., BORSET, M. & SUNDAN, A. 2009. c-Met signaling promotes IL-6-induced myeloma cell proliferation. *Eur J Haematol,* 82**,** 277-87.

HUANG, C., YANG, G., JIANG, T., ZHU, G., LI, H. & QIU, Z. 2011. The effects and mechanisms of blockage of STAT3 signaling pathway on IL-6 inducing EMT in human pancreatic cancer cells in vitro. *Neoplasma,* 58**,** 396-405.

HUANG, S. M., CHEN, T. S., CHIU, C. M., CHANG, L. K., LIAO, K. F., TAN, H. M., YEH, W. L., CHANG, G. R., WANG, M. Y. & LU, D. Y. 2014. GDNF increases cell motility in human colon cancer through VEGF-VEGFR1 interaction. *Endocr Relat Cancer,* 21**,** 73-84.

HUGHES, J. P., ALUSI, G. & WANG, Y. 2015a. Viral gene therapy for head and neck cancer. *J Laryngol Otol,* 129**,** 314-20.

HUGHES, R., QIAN, B. Z., ROWAN, C., MUTHANA, M., KEKLIKOGLOU, I., OLSON, O. C., TAZZYMAN, S., DANSON, S., ADDISON, C., CLEMONS, M., GONZALEZ-ANGULO, A. M., JOYCE, J. A., DE PALMA, M., POLLARD, J. W. & LEWIS, C. E. 2015b. Perivascular M2 Macrophages Stimulate Tumor Relapse after Chemotherapy. *Cancer Res,* 75**,** 3479-91.

HUYNH, M. L., FADOK, V. A. & HENSON, P. M. 2002. Phosphatidylserine-dependent ingestion of apoptotic cells promotes TGF-beta1 secretion and the resolution of inflammation. *J Clin Invest,* 109**,** 41-50.

IKARASHI, T., IDA-YONEMOCHI, H., OHSHIRO, K., CHENG, J. & SAKU, T. 2004. Intraepithelial expression of perlecan, a basement membrane-type heparan sulfate proteoglycan reflects dysplastic changes of the oral mucosal epithelium. *J Oral Pathol Med,* 33**,** 87-95.

IRVING, S. G., ZIPFEL, P. F., BALKE, J., MCBRIDE, O. W., MORTON, C. C., BURD, P. R., SIEBENLIST, U. & KELLY, K. 1990. Two inflammatory mediator cytokine genes are closely linked and variably amplified on chromosome 17q. *Nucleic Acids Research,* 18**,** 3261.

ISHII, G., SANGAI, T., ODA, T., AOYAGI, Y., HASEBE, T., KANOMATA, N., ENDOH, Y., OKUMURA, C., OKUHARA, Y., MAGAE, J., EMURA, M., OCHIYA, T. & OCHIAI, A. 2003. Bone-marrow-derived myofibroblasts contribute to the cancer-induced stromal reaction. *Biochem Biophys Res Commun,* 309**,** 232-40.

IVANOVA, T., ZOURIDIS, H., WU, Y., CHENG, L. L., TAN, I. B., GOPALAKRISHNAN, V., OOI, C. H., LEE, J., QIN, L., WU, J., LEE, M., RHA, S. Y., HUANG, D., LIEM, N., YEOH, K. G., YONG, W. P., TEH, B. T. & TAN, P. 2013. Integrated epigenomics identifies BMP4 as a modulator of cisplatin sensitivity in gastric cancer. *Gut,* 62**,** 22-33.

IYENGAR, P., ESPINA, V., WILLIAMS, T. W., LIN, Y., BERRY, D., JELICKS, L. A., LEE, H., TEMPLE, K., GRAVES, R., POLLARD, J., CHOPRA, N., RUSSELL, R. G., SASISEKHARAN, R., TROCK, B. J., LIPPMAN, M., CALVERT, V. S., PETRICOIN, E. F., 3RD, LIOTTA, L., DADACHOVA, E., PESTELL, R. G., LISANTI, M. P., BONALDO, P. & SCHERER, P. E. 2005. Adipocyte-derived collagen VI affects early mammary tumor progression in vivo, demonstrating a critical interaction in the tumor/stroma microenvironment. *J Clin Invest,* 115**,** 1163-76.

JAMES, E. L., MICHALEK, R. D., PITIYAGE, G. N., DE CASTRO, A. M., VIGNOLA, K. S., JONES, J., MOHNEY, R. P., KAROLY, E. D., PRIME, S. S. & PARKINSON, E. K. 2015. Senescent human fibroblasts show increased glycolysis and redox homeostasis with extracellular metabolomes that overlap with those of irreparable DNA damage, aging, and disease. *J Proteome Res,* 14**,** 1854-71.

JI, W. T., CHEN, H. R., LIN, C. H., LEE, J. W. & LEE, C. C. 2014. Monocyte chemotactic protein 1 (MCP-1) modulates pro-survival signaling to promote progression of head and neck squamous cell carcinoma. *PLoS One,* 9**,** e88952.

JIA, C. C., WANG, T. T., LIU, W., FU, B. S., HUA, X., WANG, G. Y., LI, T. J., LI, X., WU, X. Y., TAI, Y., ZHOU, J., CHEN, G. H. & ZHANG, Q. 2013. Cancer-associated fibroblasts from hepatocellular carcinoma promote malignant cell proliferation by HGF secretion. *PLoS One,* 8**,** e63243.

JIAO, J., ZHAO, X., LIANG, Y., TANG, D. & PAN, C. 2015. FGF1-FGFR1 axis promotes tongue squamous cell carcinoma (TSCC) metastasis through epithelial-mesenchymal transition (EMT). *Biochem Biophys Res Commun,* 466**,** 327-32.

JIE, H. B., SCHULER, P. J., LEE, S. C., SRIVASTAVA, R. M., ARGIRIS, A., FERRONE, S., WHITESIDE, T. L. & FERRIS, R. L. 2015. CTLA-4^{+} Regulatory T Cells Increased in Cetuximab-Treated Head and

Neck Cancer Patients Suppress NK Cell Cytotoxicity and Correlate with Poor Prognosis. *Cancer Res,* 75**,** 2200-10.

JOHNSON, N. W., WARNAKULASURIYA, S., GUPTA, P. C., DIMBA, E., CHINDIA, M., OTOH, E. C., SANKARANARAYANAN, R., CALIFANO, J. & KOWALSKI, L. 2011. Global oral health inequalities in incidence and outcomes for oral cancer: causes and solutions. *Adv Dent Res,* 23**,** 237-46.

JONIETZ, E. 2012. Mechanics: The forces of cancer. *Nature,* 491**,** S56-7.

JUN, J.-I. & LAU, L. F. 2010. The Matricellular Protein CCN1/CYR61 Induces Fibroblast Senescence and Restricts Fibrosis in Cutaneous Wound Healing. *Nature cell biology,* 12**,** 676-685.

JUNTTILA, M. R. & DE SAUVAGE, F. J. 2013. Influence of tumour micro-environment heterogeneity on therapeutic response. *Nature,* 501**,** 346-54.

KABIR, T. D. 2015. *Micro-managing senescence: the role of small non-coding RNA in senescence associated secretory phenotype.* PhD, University of Sheffield.

KABIR, T. D., LEIGH, R. J., TASENA, H., MELLONE, M., COLETTA, R. D., PARKINSON, E. K., PRIME, S. S., THOMAS, G. J., PATERSON, I. C., ZHOU, D., MCCALL, J., SPEIGHT, P. M. & LAMBERT, D. W. 2016. A miR-335/COX-2/PTEN axis regulates the secretory phenotype of senescent cancer-associated fibroblasts. *Aging (Albany NY),* 8**,** 1608-35.

KANG, B. H., SHIM, Y. J., TAE, Y. K., SONG, J. A., CHOI, B. K., PARK, I. S. & MIN, B. H. 2014. Clusterin stimulates the chemotactic migration of macrophages through a pertussis toxin sensitive G-protein-coupled receptor and Gbetagamma-dependent pathways. *Biochem Biophys Res Commun,* 445**,** 645-50.

KAPLAN, G. 1983. In vitro differentiation of human monocytes. Monocytes cultured on glass are cytotoxic to tumor cells but monocytes cultured on collagen are not. *J Exp Med,* 157**,** 2061-72.

KASAMATSU, A., UZAWA, K., MINAKAWA, Y., ISHIGE, S., KASAMA, H., ENDO-SAKAMOTO, Y., OGAWARA, K., SHIIBA, M., TAKIGUCHI, Y. & TANZAWA, H. 2015. Decorin in human oral cancer: a promising predictive biomarker of S-1 neoadjuvant chemosensitivity. *Biochem Biophys Res Commun,* 457**,** 71-6.

KATCHMAN, B. A., ANTWI, K., HOSTETTER, G., DEMEURE, M. J., WATANABE, A., DECKER, G. A., MILLER, L. J., VON HOFF, D. D. & LAKE, D. F. 2011. Quiescin sulfhydryl oxidase 1 promotes invasion of pancreatic tumor cells mediated by matrix metalloproteinases. *Mol Cancer Res,* 9**,** 1621-31.

KATO, S., ABARZUA-CATALAN, L., TRIGO, C., DELPIANO, A., SANHUEZA, C., GARCIA, K., IBANEZ, C., HORMAZABAL, K., DIAZ, D., BRANES, J., CASTELLON, E., BRAVO, E., OWEN, G. & CUELLO, M. A. 2015. Leptin stimulates migration and invasion and maintains cancer stem-like properties in ovarian cancer cells: an explanation for poor outcomes in obese women. *Oncotarget,* 6**,** 21100-19.

KAWAHARA, R., GRANATO, D. C., CARNIELLI, C. M., CERVIGNE, N. K., OLIVERIA, C. E., RIVERA, C., YOKOO, S., FONSECA, F. P., LOPES, M., SANTOS-SILVA, A. R., GRANER, E., COLETTA, R. D. & PAES LEME, A. F. 2014. Agrin and perlecan mediate tumorigenic processes in oral squamous cell carcinoma. *PLoS One,* 9**,** e115004.

KELLERMANN, M. G., SOBRAL, L. M., DA SILVA, S. D., ZECCHIN, K. G., GRANER, E., LOPES, M. A., KOWALSKI, L. P. & COLETTA, R. D. 2008. Mutual paracrine effects of oral squamous cell carcinoma cells and normal oral fibroblasts: Induction of fibroblast to myofibroblast transdifferentiation and modulation of tumor cell proliferation. *Oral Oncology,* 44**,** 509-517.

KIM, D. W., MIN, H. S., LEE, K. H., KIM, Y. J., OH, D. Y., JEON, Y. K., LEE, S. H., IM, S. A., CHUNG, D. H., KIM, Y. T., KIM, T. Y., BANG, Y. J., SUNG, S. W., KIM, J. H. & HEO, D. S. 2008. High tumour islet macrophage infiltration correlates with improved patient survival but not with EGFR mutations, gene copy number or protein expression in resected non-small cell lung cancer. *Br J Cancer,* 98**,** 1118-24.

KIM, J. M., RASMUSSEN, J. P. & RUDENSKY, A. Y. 2007. Regulatory T cells prevent catastrophic autoimmunity throughout the lifespan of mice. *Nat Immunol,* 8**,** 191-7.

KIM, J. S., KURIE, J. M. & AHN, Y. H. 2015. BMP4 depletion by miR-200 inhibits tumorigenesis and metastasis of lung adenocarcinoma cells. *Mol Cancer,* 14**,** 173.

KIMURA, S., CHENG, J., IDA, H., HAO, N., FUJIMORI, Y. & SAKU, T. 2000. Perlecan (heparan sulfate proteoglycan) gene expression reflected in the characteristic histological architecture of salivary adenoid cystic carcinoma. *Virchows Arch,* 437**,** 122-8.

KISE, K., KINUGASA-KATAYAMA, Y. & TAKAKURA, N. 2016. Tumor microenvironment for cancer stem cells. *Adv Drug Deliv Rev,* 99**,** 197-205.

KISHIMOTO, K., YOSHIDA, S., IBARAGI, S., YOSHIOKA, N., HU, G. F. & SASAKI, A. 2014. Neamine inhibits oral cancer progression by suppressing angiogenin-mediated angiogenesis and cancer cell proliferation. *Anticancer Res,* 34**,** 2113-21.

KITA, Y., MIMORI, K., TANAKA, F., MATSUMOTO, T., HARAGUCHI, N., ISHIKAWA, K., MATSUZAKI, S., FUKUYOSHI, Y., INOUE, H., NATSUGOE, S., AIKOU, T. & MORI, M. 2009. Clinical significance of LAMB3 and COL7A1 mRNA in esophageal squamous cell carcinoma. *Eur J Surg Oncol,* 35**,** 52-8.

KOJIMA, H., INOUE, T., KUNIMOTO, H. & NAKAJIMA, K. 2013. IL-6-STAT3 signaling and premature senescence. *JAKSTAT,* 2**,** e25763.

KOJIMA, Y., ACAR, A., EATON, E. N., MELLODY, K. T., SCHEEL, C., BEN-PORATH, I., ONDER, T. T., WANG, Z. C., RICHARDSON, A. L., WEINBERG, R. A. & ORIMO, A. 2010. Autocrine TGF-beta and stromal cell-derived factor-1 (SDF-1) signaling drives the evolution of tumor-promoting mammary stromal myofibroblasts. *Proc Natl Acad Sci U S A,* 107**,** 20009-14.

KOONTONGKAEW, S., AMORNPHIMOLTHAM, P., MONTHANPISUT, P., SAENSUK, T. & LEELAKRIANGSAK, M. 2012. Fibroblasts and extracellular matrix differently modulate MMP activation by primary and metastatic head and neck cancer cells. *Med Oncol,* 29**,** 690-703.

KRASAGAKIS, K., FRAGIADAKI, I., METAXARI, M., KRUGER-KRASAGAKIS, S., TZANAKAKIS, G. N., STATHOPOULOS, E. N., EBERLE, J., TAVERNARAKIS, N. & TOSCA, A. D. 2011. KIT receptor activation by autocrine and paracrine stem cell factor stimulates growth of merkel cell carcinoma in vitro. *J Cell Physiol,* 226**,** 1099-109.

KRIZHANOVSKY, V., YON, M., DICKINS, R. A., HEARN, S., SIMON, J., MIETHING, C., YEE, H., ZENDER, L. & LOWE, S. W. 2008a. Senescence of activated stellate cells limits liver fibrosis. *Cell,* 134**,** 657-667.

KRIZHANOVSKY, V., YON, M., DICKINS, R. A., HEARN, S., SIMON, J., MIETHING, C., YEE, H., ZENDER, L. & LOWE, S. W. 2008b. Senescence of activated stellate cells limits liver fibrosis. *Cell,* 134**,** 657-67.

KUDO-SAITO, C., SHIRAKO, H., OHIKE, M., TSUKAMOTO, N. & KAWAKAMI, Y. 2013. CCL2 is critical for immunosuppression to promote cancer metastasis. *Clin Exp Metastasis,* 30**,** 393-405.

KUMAR, D., KANDL, C., HAMILTON, C. D., SHNAYDER, Y., TSUE, T. T., KAKARALA, K., LEDGERWOOD, L., SUN, X. S., HUANG, H. J., GIROD, D. & THOMAS, S. M. 2015. Mitigation of Tumor-Associated Fibroblast-Facilitated Head and Neck Cancer Progression With Anti-Hepatocyte Growth Factor Antibody Ficlatuzumab. *JAMA Otolaryngol Head Neck Surg,* 141**,** 1133-9.

KUMAR, J. D., KANDOLA, S., TISZLAVICZ, L., REISZ, Z., DOCKRAY, G. J. & VARRO, A. 2016. The role of chemerin and ChemR23 in stimulating the invasion of squamous oesophageal cancer cells. *Br J Cancer,* 114**,** 1152-9.

KUNDU, J. S., YJ. 2008. Inflammation: gearing the journey to cancer. *Mutation research***,** 15-30.

KUNO, K., OKADA, Y., KAWASHIMA, H., NAKAMURA, H., MIYASAKA, M., OHNO, H. & MATSUSHIMA, K. 2000. ADAMTS-1 cleaves a cartilage proteoglycan, aggrecan. *FEBS Lett,* 478**,** 241-5.

KUONEN, F., LAURENT, J., SECONDINI, C., LORUSSO, G., STEHLE, J. C., RAUSCH, T., FAES-VAN'T HULL, E., BIELER, G., ALGHISI, G. C., SCHWENDENER, R., ANDREJEVIC-BLANT, S., MIRIMANOFF, R. O. & RUEGG, C. 2012. Inhibition of the Kit ligand/c-Kit axis attenuates metastasis in a mouse model mimicking local breast cancer relapse after radiotherapy. *Clin Cancer Res,* 18**,** 4365-74.

KUPER, H., ADAMI, H. O. & TRICHOPOULOS, D. 2000. Infections as a major preventable cause of human cancer. *J Intern Med,* 248**,** 171-83.
LAKE, D. F. & FAIGEL, D. O. 2014. The emerging role of QSOX1 in cancer. *Antioxid Redox Signal,* 21**,** 485-96.
LARKIN, J., HODI, F. S. & WOLCHOK, J. D. 2015. Combined Nivolumab and Ipilimumab or Monotherapy in Untreated Melanoma. *N Engl J Med,* 373**,** 1270-1.
LAU, T. S., CHUNG, T. K., CHEUNG, T. H., CHAN, L. K., CHEUNG, L. W., YIM, S. F., SIU, N. S., LO, K. W., YU, M. M., KULBE, H., BALKWILL, F. R. & KWONG, J. 2014. Cancer cell-derived lymphotoxin mediates reciprocal tumour-stromal interactions in human ovarian cancer by inducing CXCL11 in fibroblasts. *J Pathol,* 232**,** 43-56.
LEDERLE, W., DEPNER, S., SCHNUR, S., OBERMUELLER, E., CATONE, N., JUST, A., FUSENIG, N. E. & MUELLER, M. M. 2011. IL-6 promotes malignant growth of skin SCCs by regulating a network of autocrine and paracrine cytokines. *Int J Cancer,* 128**,** 2803-14.
LEE, C. C., HO, H. C., SU, Y. C., LEE, M. S., HUNG, S. K. & LIN, C. H. 2015. MCP1-Induced Epithelial-Mesenchymal Transition in Head and Neck Cancer by AKT Activation. *Anticancer Res,* 35**,** 3299-306.
LEE, C. C., SHIAO, H. Y., WANG, W. C. & HSIEH, H. P. 2014a. Small-molecule EGFR tyrosine kinase inhibitors for the treatment of cancer. *Expert Opin Investig Drugs,* 23**,** 1333-48.
LEE, K. N., CHOI, H. S., YANG, S. Y., PARK, H. K., LEE, Y. Y., LEE, O. Y., YOON, B. C., HAHM, J. S. & PAIK, S. S. 2014b. The role of leptin in gastric cancer: clinicopathologic features and molecular mechanisms. *Biochem Biophys Res Commun,* 446**,** 822-9.
LEWIS, M. P., LYGOE, K. A., NYSTROM, M. L., ANDERSON, W. P., SPEIGHT, P. M., MARSHALL, J. F. & THOMAS, G. J. 2004. Tumour-derived TGF-beta1 modulates myofibroblast differentiation and promotes HGF/SF-dependent invasion of squamous carcinoma cells. *Br J Cancer,* 90**,** 822-32.
LI, C., SHINTANI, S., TERAKADO, N., NAKASHIRO, K. & HAMAKAWA, H. 2002. Infiltration of tumor-associated macrophages in human oral squamous cell carcinoma. *Oncol Rep,* 9**,** 1219-23.
LI, H., ZHANG, J., CHEN, S. W., LIU, L. L., LI, L., GAO, F., ZHUANG, S. M., WANG, L. P., LI, Y. & SONG, M. 2015. Cancer-associated fibroblasts provide a suitable microenvironment for tumor development and progression in oral tongue squamous cancer. *J Transl Med,* 13**,** 198.
LI, J., GUAN, J., LONG, X., WANG, Y. & XIANG, X. 2016a. mir-1-mediated paracrine effect of cancer-associated fibroblasts on lung cancer cell proliferation and chemoresistance. *Oncol Rep,* 35**,** 3523-31.
LI, J., JIA, Z., KONG, J., ZHANG, F., FANG, S., LI, X., LI, W., YANG, X., LUO, Y., LIN, B. & LIU, T. 2016b. Carcinoma-Associated Fibroblasts Lead the Invasion of Salivary Gland Adenoid Cystic Carcinoma Cells by Creating an Invasive Track. *PLoS One,* 11**,** e0150247.
LI, Q., WIJESEKERA, O., SALAS, S. J., WANG, J. Y., ZHU, M., APRHYS, C., CHAICHANA, K. L., CHESLER, D. A., ZHANG, H., SMITH, C. L., GUERRERO-CAZARES, H., LEVCHENKO, A. & QUINONES-HINOJOSA, A. 2014a. Mesenchymal stem cells from human fat engineered to secrete BMP4 are nononcogenic, suppress brain cancer, and prolong survival. *Clin Cancer Res,* 20**,** 2375-87.
LI, X., XU, Q., WU, Y., LI, J., TANG, D., HAN, L. & FAN, Q. 2014b. A CCL2/ROS autoregulation loop is critical for cancer-associated fibroblasts-enhanced tumor growth of oral squamous cell carcinoma. *Carcinogenesis,* 35**,** 1362-70.
LI, X., ZHOU, F., JIANG, C., WANG, Y., LU, Y., YANG, F., WANG, N., YANG, H., ZHENG, Y. & ZHANG, J. 2014c. Identification of a DNA methylome profile of esophageal squamous cell carcinoma and potential plasma epigenetic biomarkers for early diagnosis. *PLoS One,* 9**,** e103162.
LIM, K. P., CIRILLO, N., HASSONA, Y., WEI, W., THURLOW, J. K., CHEONG, S. C., PITIYAGE, G., PARKINSON, E. K. & PRIME, S. S. 2011a. Fibroblast gene expression profile reflects the stage of tumour progression in oral squamous cell carcinoma. *J Pathol,* 223**,** 459-69.
LIM, K. P., CIRILLO, N., HASSONA, Y., WEI, W., THURLOW, J. K., CHEONG, S. C., PITIYAGE, G., PARKINSON, E. K. & PRIME, S. S. 2011b. Fibroblast gene expression profile reflects the stage

of tumour progression in oral squamous cell carcinoma. *The Journal of Pathology,* 223**,** 459-469.
LIM, S. Y., YUZHALIN, A. E., GORDON-WEEKS, A. N. & MUSCHEL, R. J. 2016. Targeting the CCL2-CCR2 signaling axis in cancer metastasis. *Oncotarget,* 7**,** 28697-710.
LIN, C. Y., HUNG, S. Y., CHEN, H. T., TSOU, H. K., FONG, Y. C., WANG, S. W. & TANG, C. H. 2014. Brain-derived neurotrophic factor increases vascular endothelial growth factor expression and enhances angiogenesis in human chondrosarcoma cells. *Biochem Pharmacol,* 91**,** 522-33.
LIN, E. Y., NGUYEN, A. V., RUSSELL, R. G. & POLLARD, J. W. 2001. Colony-stimulating factor 1 promotes progression of mammary tumors to malignancy. *J Exp Med,* 193**,** 727-40.
LIN, J., LIU, C., GE, L., GAO, Q., HE, X., LIU, Y., LI, S., ZHOU, M., CHEN, Q. & ZHOU, H. 2011. Carcinoma-associated fibroblasts promotes the proliferation of a lingual carcinoma cell line by secreting keratinocyte growth factor. *Tumour Biol,* 32**,** 597-602.
LIN, M. T., LIN, B. R., CHANG, C. C., CHU, C. Y., SU, H. J., CHEN, S. T., JENG, Y. M. & KUO, M. L. 2007. IL-6 induces AGS gastric cancer cell invasion via activation of the c-Src/RhoA/ROCK signaling pathway. *Int J Cancer,* 120**,** 2600-8.
LINGEN, M. W., KALMAR, J. R., KARRISON, T. & SPEIGHT, P. M. 2008. Critical evaluation of diagnostic aids for the detection of oral cancer. *Oral Oncol,* 44**,** 10-22.
LITTMAN, D. R. & RUDENSKY, A. Y. 2010. Th17 and regulatory T cells in mediating and restraining inflammation. *Cell,* 140**,** 845-58.
LIU, H., LI, X., XU, Q., LV, S., LI, J. & MA, Q. 2012. Role of glial cell line-derived neurotrophic factor in perineural invasion of pancreatic cancer. *Biochim Biophys Acta,* 1826**,** 112-20.
LIU, S. Y., CHANG, L. C., PAN, L. F., HUNG, Y. J., LEE, C. H. & SHIEH, Y. S. 2008. Clinicopathologic significance of tumor cell-lined vessel and microenvironment in oral squamous cell carcinoma. *Oral Oncol,* 44**,** 277-85.
LIU, Y., CHEN, W., MINZE, L. J., KUBIAK, J. Z., LI, X. C., GHOBRIAL, R. M. & KLOC, M. 2016. Dissonant response of M0/M2 and M1 bone-marrow-derived macrophages to RhoA pathway interference. *Cell Tissue Res,* 366**,** 707-720.
LIU, Y. & DU, L. 2015. Role of pancreatic stellate cells and periostin in pancreatic cancer progression. *Tumour Biol,* 36**,** 3171-7.
LOBERG, R. D., DAY, L. L., HARWOOD, J., YING, C., ST JOHN, L. N., GILES, R., NEELEY, C. K. & PIENTA, K. J. 2006. CCL2 is a potent regulator of prostate cancer cell migration and proliferation. *Neoplasia,* 8**,** 578-86.
LOBERG, R. D., YING, C., CRAIG, M., DAY, L. L., SARGENT, E., NEELEY, C., WOJNO, K., SNYDER, L. A., YAN, L. & PIENTA, K. J. 2007. Targeting CCL2 with systemic delivery of neutralizing antibodies induces prostate cancer tumor regression in vivo. *Cancer Res,* 67**,** 9417-24.
LU, X. & KANG, Y. 2009. Chemokine (C-C motif) ligand 2 engages CCR2+ stromal cells of monocytic origin to promote breast cancer metastasis to lung and bone. *J Biol Chem,* 284**,** 29087-96.
LU, Y., CHEN, Q., COREY, E., XIE, W., FAN, J., MIZOKAMI, A. & ZHANG, J. 2009. Activation of MCP-1/CCR2 axis promotes prostate cancer growth in bone. *Clin Exp Metastasis,* 26**,** 161-9.
LUI, V. W., YAU, D. M., CHEUNG, C. S., WONG, S. C., CHAN, A. K., ZHOU, Q., WONG, E. Y., LAU, C. P., LAM, E. K., HUI, E. P., HONG, B., HUI, C. W., CHAN, A. S., NG, P. K., NG, Y. K., LO, K. W., TSANG, C. M., TSUI, S. K., TSAO, S. W. & CHAN, A. T. 2011. FGF8b oncogene mediates proliferation and invasion of Epstein-Barr virus-associated nasopharyngeal carcinoma cells: implication for viral-mediated FGF8b upregulation. *Oncogene,* 30**,** 1518-30.
LYSSIOTIS, C. A. & KIMMELMAN, A. C. 2017. Metabolic Interactions in the Tumor Microenvironment. *Trends Cell Biol,* 27**,** 863-875.
MALIK, R. K., GHURYE, R. R., LAWRENCE-WATT, D. J. & STEWART, H. J. 2009. Galectin-1 stimulates monocyte chemotaxis via the p44/42 MAP kinase pathway and a pertussis toxin-sensitive pathway. *Glycobiology,* 19**,** 1402-7.
MANGMOOL, S. & KUROSE, H. 2011. G(i/o) protein-dependent and -independent actions of Pertussis Toxin (PTX). *Toxins (Basel),* 3**,** 884-99.

MANTOVANI, A. & LOCATI, M. 2013. Tumor-associated macrophages as a paradigm of macrophage plasticity, diversity, and polarization: lessons and open questions. *Arterioscler Thromb Vasc Biol,* 33**,** 1478-83.

MANTOVANI, A. & SICA, A. 2010. Macrophages, innate immunity and cancer: balance, tolerance, and diversity. *Curr Opin Immunol,* 22**,** 231-7.

MARCU, L. G. & YEOH, E. 2009. A review of risk factors and genetic alterations in head and neck carcinogenesis and implications for current and future approaches to treatment. *J Cancer Res Clin Oncol,* 135**,** 1303-14.

MARCUS, B., ARENBERG, D., LEE, J., KLEER, C., CHEPEHA, D. B., SCHMALBACH, C. E., ISLAM, M., PAUL, S., PAN, Q., HANASH, S., KUICK, R., MERAJVER, S. D. & TEKNOS, T. N. 2004. Prognostic factors in oral cavity and oropharyngeal squamous cell carcinoma. *Cancer,* 101**,** 2779-87.

MARSH, D., SUCHAK, K., MOUTASIM, K. A., VALLATH, S., HOPPER, C., JERJES, W., UPILE, T., KALAVREZOS, N., VIOLETTE, S. M., WEINREB, P. H., CHESTER, K. A., CHANA, J. S., MARSHALL, J. F., HART, I. R., HACKSHAW, A. K., PIPER, K. & THOMAS, G. J. 2011. Stromal features are predictive of disease mortality in oral cancer patients. *J Pathol,* 223**,** 470-81.

MARTIN, L. J. & BOYD, N. F. 2008. Mammographic density. Potential mechanisms of breast cancer risk associated with mammographic density: hypotheses based on epidemiological evidence. *Breast Cancer Res,* 10**,** 201.

MARTINEZ-OUTSCHOORN, U. E., LISANTI, M. P. & SOTGIA, F. 2014. Catabolic cancer-associated fibroblasts transfer energy and biomass to anabolic cancer cells, fueling tumor growth. *Semin Cancer Biol,* 25**,** 47-60.

MARUYAMA, S., SHIMAZU, Y., KUDO, T., SATO, K., YAMAZAKI, M., ABE, T., BABKAIR, H., CHENG, J., AOBA, T. & SAKU, T. 2014. Three-dimensional visualization of perlecan-rich neoplastic stroma induced concurrently with the invasion of oral squamous cell carcinoma. *J Oral Pathol Med,* 43**,** 627-36.

MATHERS, C. D. L., D. 2006. Projections of global mortality and burden of disease from 2002 to 2030. *PLoS Med,* 3:e442

MATSUMOTO, K. & EMA, M. 2014. Roles of VEGF-A signalling in development, regeneration, and tumours. *J Biochem,* 156**,** 1-10.

MATSUMOTO, K. & NAKAMURA, T. 2006. Hepatocyte growth factor and the Met system as a mediator of tumor–stromal interactions. *International Journal of Cancer,* 119**,** 477-483.

MAUER, J., CHAURASIA, B., GOLDAU, J., VOGT, M. C., RUUD, J., NGUYEN, K. D., THEURICH, S., HAUSEN, A. C., SCHMITZ, J., BRONNEKE, H. S., ESTEVEZ, E., ALLEN, T. L., MESAROS, A., PARTRIDGE, L., FEBBRAIO, M. A., CHAWLA, A., WUNDERLICH, F. T. & BRUNING, J. C. 2014. Signaling by IL-6 promotes alternative activation of macrophages to limit endotoxemia and obesity-associated resistance to insulin. *Nat Immunol,* 15**,** 423-30.

MCGUIRE, S. 2016. World Cancer Report 2014. Geneva, Switzerland: World Health Organization, International Agency for Research on Cancer, WHO Press, 2015. *Adv Nutr,* 7**,** 418-9.

MEHNER, C. & RADISKY, D. C. 2013. Triggering the landslide: The tumor-promotional effects of myofibroblasts. *Exp Cell Res,* 319**,** 1657-62.

MELLING, G. 2015. *The role of microRNA-145 in tumour microenvironment.* PhD, University of Sheffield.

MELLONE, M., HANLEY, C. J., THIRDBOROUGH, S., MELLOWS, T., GARCIA, E., WOO, J., TOD, J., FRAMPTON, S., JENEI, V., MOUTASIM, K. A., KABIR, T. D., BRENNAN, P. A., VENTURI, G., FORD, K., HERRANZ, N., LIM, K. P., CLARKE, J., LAMBERT, D. W., PRIME, S. S., UNDERWOOD, T. J., VIJAYANAND, P., ELICEIRI, K. W., WOELK, C., KING, E. V., GIL, J., OTTENSMEIER, C. H. & THOMAS, G. J. 2016. Induction of fibroblast senescence generates a non-fibrogenic myofibroblast phenotype that differentially impacts on cancer prognosis. *Aging (Albany NY),* 9**,** 114-132.

MELLONE, M., HANLEY, C. J., THIRDBOROUGH, S., MELLOWS, T., GARCIA, E., WOO, J., TOD, J., FRAMPTON, S., JENEI, V., MOUTASIM, K. A., KABIR, T. D., BRENNAN, P. A., VENTURI, G.,

FORD, K., HERRANZ, N., LIM, K. P., CLARKE, J., LAMBERT, D. W., PRIME, S. S., UNDERWOOD, T. J., VIJAYANAND, P., ELICEIRI, K. W., WOELK, C., KING, E. V., GIL, J., OTTENSMEIER, C. H. & THOMAS, G. J. 2017. Induction of fibroblast senescence generates a non-fibrogenic myofibroblast phenotype that differentially impacts on cancer prognosis. *Aging (Albany NY).*

MIA, S., WARNECKE, A., ZHANG, X. M., MALMSTRÖM, V. & HARRIS, R. A. 2014. An optimized protocol for human M2 macrophages using M-CSF and IL-4/IL-10/TGF-β yields a dominant immunosuppressive phenotype. *Scand J Immunol,* 79**,** 305-14.

MIDDLETON, K., JONES, J., LWIN, Z. & COWARD, J. I. 2014. Interleukin-6: an angiogenic target in solid tumours. *Crit Rev Oncol Hematol,* 89**,** 129-39.

MILLS, C. D. 2012. M1 and M2 Macrophages: Oracles of Health and Disease. *Crit Rev Immunol,* 32**,** 463-88.

MIN, A., ZHU, C., WANG, J., PENG, S., SHUAI, C., GAO, S., TANG, Z. & SU, T. 2015. Focal adhesion kinase knockdown in carcinoma-associated fibroblasts inhibits oral squamous cell carcinoma metastasis via downregulating MCP-1/CCL2 expression. *J Biochem Mol Toxicol,* 29**,** 70-6.

MISHRA, M., NAIK, V. V., KALE, A. D., ANKOLA, A. V. & PILLI, G. S. 2011. Perlecan (basement membrane heparan sulfate proteoglycan) and its role in oral malignancies: an overview. *Indian J Dent Res,* 22**,** 823-6.

MITRA, A. K., ZILLHARDT, M., HUA, Y., TIWARI, P., MURMANN, A. E., PETER, M. E. & LENGYEL, E. 2012. MicroRNAs reprogram normal fibroblasts into cancer-associated fibroblasts in ovarian cancer. *Cancer Discov,* 2**,** 1100-8.

MOISAN, F., FRANCISCO, E. B., BROZOVIC, A., DURAN, G. E., WANG, Y. C., CHATURVEDI, S., SEETHARAM, S., SNYDER, L. A., DOSHI, P. & SIKIC, B. I. 2014. Enhancement of paclitaxel and carboplatin therapies by CCL2 blockade in ovarian cancers. *Mol Oncol,* 8**,** 1231-9.

MOJTAHEDI, Z., KHADEMI, B., HASHEMI, S. B., ABTAHI, S. M., GHASEMI, M. A., FATTAHI, M. J. & GHADERI, A. 2011. Serum interleukine-6 concentration, but not interleukine-18, is associated with head and neck squamous cell carcinoma progression. *Pathol Oncol Res,* 17**,** 7-10.

MOLLOY, A. P., MARTIN, F. T., DWYER, R. M., GRIFFIN, T. P., MURPHY, M., BARRY, F. P., O'BRIEN, T. & KERIN, M. J. 2009. Mesenchymal stem cell secretion of chemokines during differentiation into osteoblasts, and their potential role in mediating interactions with breast cancer cells. *Int J Cancer,* 124**,** 326-32.

MOORE, M. C., PANDOLFI, V. & MCFETRIDGE, P. S. 2015. Novel human-derived extracellular matrix induces in vitro and in vivo vascularization and inhibits fibrosis. *Biomaterials,* 49**,** 37-46.

MOREL, C., ADAMI, P., MUSARD, J. F., DUVAL, D., RADOM, J. & JOUVENOT, M. 2007. Involvement of sulfhydryl oxidase QSOX1 in the protection of cells against oxidative stress-induced apoptosis. *Exp Cell Res,* 313**,** 3971-82.

MOTRESCU, E. R., BLAISE, S., ETIQUE, N., MESSADDEQ, N., CHENARD, M. P., STOLL, I., TOMASETTO, C. & RIO, M. C. 2008. Matrix metalloproteinase-11/stromelysin-3 exhibits collagenolytic function against collagen VI under normal and malignant conditions. *Oncogene,* 27**,** 6347-55.

MUELLER, L., VON SEGGERN, L., SCHUMACHER, J., GOUMAS, F., WILMS, C., BRAUN, F. & BROERING, D. C. 2010. TNF-alpha similarly induces IL-6 and MCP-1 in fibroblasts from colorectal liver metastases and normal liver fibroblasts. *Biochem Biophys Res Commun,* 397**,** 586-91.

MUELLER, M. M., HEROLD-MENDE, C. C., RIEDE, D., LANGE, M., STEINER, H. H. & FUSENIG, N. E. 1999. Autocrine growth regulation by granulocyte colony-stimulating factor and granulocyte macrophage colony-stimulating factor in human gliomas with tumor progression. *Am J Pathol,* 155**,** 1557-67.

MURDOCH, C., MUTHANA, M., COFFELT, S. B. & LEWIS, C. E. 2008. The role of myeloid cells in the promotion of tumour angiogenesis. *Nat Rev Cancer,* 8**,** 618-31.

MUTHANA, M., RODRIGUES, S., CHEN, Y. Y., WELFORD, A., HUGHES, R., TAZZYMAN, S., ESSAND, M., MORROW, F. & LEWIS, C. E. 2013. Macrophage delivery of an oncolytic virus abolishes tumor regrowth and metastasis after chemotherapy or irradiation. *Cancer Res,* 73**,** 490-5.

NANDA, A., CARSON-WALTER, E. B., SEAMAN, S., BARBER, T. D., STAMPFL, J., SINGH, S., VOGELSTEIN, B., KINZLER, K. W. & ST CROIX, B. 2004. TEM8 interacts with the cleaved C5 domain of collagen alpha 3(VI). *Cancer Res,* 64**,** 817-20.

NAVEGANTES, K. C., DE SOUZA GOMES, R., PEREIRA, P. A. T., CZAIKOSKI, P. G., AZEVEDO, C. H. M. & MONTEIRO, M. C. 2017. Immune modulation of some autoimmune diseases: the critical role of macrophages and neutrophils in the innate and adaptive immunity. *J Transl Med,* 15**,** 36.

NAYAK, S., GOEL, M. M., BHATIA, V., CHANDRA, S., MAKKER, A., KUMAR, S., AGRAWAL, S. P., MEHROTRA, D. & RATH, S. K. 2013. Molecular and phenotypic expression of decorin as modulator of angiogenesis in human potentially malignant oral lesions and oral squamous cell carcinomas. *Indian J Pathol Microbiol,* 56**,** 204-10.

NETEA, M. G., KULLBERG, B. J., VERSCHUEREN, I. & VAN DER MEER, J. W. 2000. Interleukin-18 induces production of proinflammatory cytokines in mice: no intermediate role for the cytokines of the tumor necrosis factor family and interleukin-1beta. *Eur J Immunol,* 30**,** 3057-60.

NEWMAN, G. & GONZALEZ-PEREZ, R. R. 2014. Leptin-cytokine crosstalk in breast cancer. *Mol Cell Endocrinol,* 382**,** 570-82.

NG, W. H., WAN, G. Q., PENG, Z. N. & TOO, H. P. 2009. Glial cell-line derived neurotrophic factor (GDNF) family of ligands confer chemoresistance in a ligand-specific fashion in malignant gliomas. *J Clin Neurosci,* 16**,** 427-36.

NGUYEN, D. P., LI, J. & TEWARI, A. K. 2014. Inflammation and prostate cancer: the role of interleukin 6 (IL-6). *BJU Int,* 113**,** 986-92.

NIGHTINGALE, J., PATEL, S., SUZUKI, N., BUXTON, R., TAKAGI, K. I., SUZUKI, J., SUMI, Y., IMAIZUMI, A., MASON, R. M. & ZHANG, Z. 2004. Oncostatin M, a cytokine released by activated mononuclear cells, induces epithelial cell-myofibroblast transdifferentiation via Jak/Stat pathway activation. *J Am Soc Nephrol,* 15**,** 21-32.

NOWAK, D. G., CHO, H., HERZKA, T., WATRUD, K., DEMARCO, D. V., WANG, V. M., SENTURK, S., FELLMANN, C., DING, D., BEINORTAS, T., KLEINMAN, D., CHEN, M., SORDELLA, R., WILKINSON, J. E., CASTILLO-MARTIN, M., CORDON-CARDO, C., ROBINSON, B. D. & TROTMAN, L. C. 2015. MYC Drives Pten/Trp53-Deficient Proliferation and Metastasis due to IL6 Secretion and AKT Suppression via PHLPP2. *Cancer Discov,* 5**,** 636-51.

NYUNOYA, T., MONICK, M. M., KLINGELHUTZ, A., YAROVINSKY, T. O., CAGLEY, J. R. & HUNNINGHAKE, G. W. 2006. Cigarette smoke induces cellular senescence. *Am J Respir Cell Mol Biol,* 35**,** 681-8.

O'BYRNE, K. J. & DALGLEISH, A. G. 2001. Chronic immune activation and inflammation as the cause of malignancy. *Br J Cancer,* 85**,** 473-483.

OGAWA, T., TAKADA, H., KOTANI, S., SATO, H. & SATO, Y. 1983. Novel biological property of pertussis toxin: chemotactic activity on human monocytes. *Infect Immun,* 41**,** 420-2.

OHGO, S., HASEGAWA, S., HASEBE, Y., MIZUTANI, H., NAKATA, S. & AKAMATSU, H. 2015. Senescent dermal fibroblasts enhance stem cell migration through CCL2/CCR2 axis. *Exp Dermatol,* 24**,** 552-4.

OHLUND, D., ELYADA, E. & TUVESON, D. 2014. Fibroblast heterogeneity in the cancer wound. *J Exp Med,* 211**,** 1503-23.

OHLUND, D., FRANKLIN, O., LUNDBERG, E., LUNDIN, C. & SUND, M. 2013. Type IV collagen stimulates pancreatic cancer cell proliferation, migration, and inhibits apoptosis through an autocrine loop. *BMC Cancer,* 13**,** 154.

OHNISHI, S., MA, N., THANAN, R., PINLAOR, S., HAMMAM, O., MURATA, M. & KAWANISHI, S. 2013. DNA damage in inflammation-related carcinogenesis and cancer stem cells. *Oxid Med Cell Longev,* 2013**,** 387014.

ONG, S. M., TAN, Y. C., BERETTA, O., JIANG, D., YEAP, W. H., TAI, J. J., WONG, W. C., YANG, H., SCHWARZ, H., LIM, K. H., KOH, P. K., LING, K. L. & WONG, S. C. 2012. Macrophages in human

colorectal cancer are pro-inflammatory and prime T cells towards an anti-tumour type-1 inflammatory response. *Eur J Immunol,* 42**,** 89-100.

OSAKI, T., HASHIMOTO, W., GAMBOTTO, A., OKAMURA, H., ROBBINS, P. D., KURIMOTO, M., LOTZE, M. T. & TAHARA, H. 1999. Potent antitumor effects mediated by local expression of the mature form of the interferon-gamma inducing factor, interleukin-18 (IL-18). *Gene Ther,* 6**,** 808-15.

OTOMO, R., OTSUBO, C., MATSUSHIMA-HIBIYA, Y., MIYAZAKI, M., TASHIRO, F., ICHIKAWA, H., KOHNO, T., OCHIYA, T., YOKOTA, J., NAKAGAMA, H., TAYA, Y. & ENARI, M. 2014. TSPAN12 is a critical factor for cancer-fibroblast cell contact-mediated cancer invasion. *Proc Natl Acad Sci U S A,* 111**,** 18691-6.

OTRANTO, M., SARRAZY, V., BONTE, F., HINZ, B., GABBIANI, G. & DESMOULIERE, A. 2012. The role of the myofibroblast in tumor stroma remodeling. *Cell Adh Migr,* 6**,** 203-19.

OVERHOFF, M. G., GARBE, J. C., KOH, J., STAMPFER, M. R., BEACH, D. H. & BISHOP, C. L. 2014. Cellular senescence mediated by p16INK4A-coupled miRNA pathways. *Nucleic Acids Res,* 42**,** 1606-18.

OWENS, P., POLIKOWSKY, H., PICKUP, M. W., GORSKA, A. E., JOVANOVIC, B., SHAW, A. K., NOVITSKIY, S. V., HONG, C. C. & MOSES, H. L. 2013. Bone Morphogenetic Proteins stimulate mammary fibroblasts to promote mammary carcinoma cell invasion. *PLoS One,* 8**,** e67533.

PARDOLL, D. M. 2012. The blockade of immune checkpoints in cancer immunotherapy. *Nat Rev Cancer,* 12**,** 252-64.

PARK, J., MORLEY, T. S. & SCHERER, P. E. 2013a. Inhibition of endotrophin, a cleavage product of collagen VI, confers cisplatin sensitivity to tumours. *EMBO Mol Med,* 5**,** 935-48.

PARK, J. & SCHERER, P. E. 2012. Adipocyte-derived endotrophin promotes malignant tumor progression. *J Clin Invest,* 122**,** 4243-56.

PARK, M., KIM, W. K., SONG, M., KIM, H., NAM, H. J. & BAEK, S. H. 2013b. Protein kinase C-delta-mediated recycling of active KIT in colon cancer. *Clin Cancer Res,* 19**,** 4961-71.

PARKINSON, E. K., JAMES, E. L. & PRIME, S. S. 2016. Senescence-Derived Extracellular Molecules as Modulators of Oral Cancer Development: A Mini-Review. *Gerontology,* 62**,** 417-24.

PAROLINI, S., SANTORO, A., MARCENARO, E., LUINI, W., MASSARDI, L., FACCHETTI, F., COMMUNI, D., PARMENTIER, M., MAJORANA, A., SIRONI, M., TABELLINI, G., MORETTA, A. & SOZZANI, S. 2007. The role of chemerin in the colocalization of NK and dendritic cell subsets into inflamed tissues. *Blood,* 109**,** 3625-32.

PASSOS, J. F., NELSON, G., WANG, C., RICHTER, T., SIMILLION, C., PROCTOR, C. J., MIWA, S., OLIJSLAGERS, S., HALLINAN, J., WIPAT, A., SARETZKI, G., RUDOLPH, K. L., KIRKWOOD, T. B. & VON ZGLINICKI, T. 2010. Feedback between p21 and reactive oxygen production is necessary for cell senescence. *Mol Syst Biol,* 6**,** 347.

PASZEK, M. J., ZAHIR, N., JOHNSON, K. R., LAKINS, J. N., ROZENBERG, G. I., GEFEN, A., REINHART-KING, C. A., MARGULIES, S. S., DEMBO, M., BOETTIGER, D., HAMMER, D. A. & WEAVER, V. M. 2005. Tensional homeostasis and the malignant phenotype. *Cancer Cell,* 8**,** 241-54.

PATEL, S. A. & GOODERHAM, N. J. 2015. IL6 Mediates Immune and Colorectal Cancer Cell Cross-talk via miR-21 and miR-29b. *Mol Cancer Res,* 13**,** 1502-8.

PAULSSON, J. & MICKE, P. 2014. Prognostic relevance of cancer-associated fibroblasts in human cancer. *Semin Cancer Biol,* 25**,** 61-8.

PEARSON, S., JIA, H. & KANDACHI, K. China approves first gene therapy.

PENG, Y., LI, Z. & LI, Z. 2013. GRP78 secreted by tumor cells stimulates differentiation of bone marrow mesenchymal stem cells to cancer-associated fibroblasts. *Biochemical and Biophysical Research Communications,* 440**,** 558-563.

PENG, Z. 2005. Current status of gendicine in China: recombinant human Ad-p53 agent for treatment of cancers. *Hum Gene Ther,* 16**,** 1016-27.

PERROTTA, C., CERVIA, D., DI RENZO, I., MOSCHENI, C., BASSI, M. T., CAMPANA, L., MARTELLI, C., CATALANI, E., GIOVARELLI, M., ZECCHINI, S., COAZZOLI, M., CAPOBIANCO, A., OTTOBRINI, L.,

LUCIGNANI, G., ROSA, P., ROVERE-QUERINI, P., DE PALMA, C. & CLEMENTI, E. 2018. Nitric Oxide Generated by Tumor-Associated Macrophages Is Responsible for Cancer Resistance to Cisplatin and Correlated With Syntaxin 4 and Acid Sphingomyelinase Inhibition. *Front Immunol,* 9**,** 1186.

PERUMAL, D., PILLAI, S., NGUYEN, J., SCHAAL, C., COPPOLA, D. & CHELLAPPAN, S. P. 2014. Nicotinic acetylcholine receptors induce c-Kit ligand/Stem Cell Factor and promote stemness in an ARRB1/ beta-arrestin-1 dependent manner in NSCLC. *Oncotarget,* 5**,** 10486-502.

PETERFI, Z., DONKO, A., ORIENT, A., SUM, A., PROKAI, A., MOLNAR, B., VEREB, Z., RAJNAVOLGYI, E., KOVACS, K. J., MULLER, V., SZABO, A. J. & GEISZT, M. 2009. Peroxidasin is secreted and incorporated into the extracellular matrix of myofibroblasts and fibrotic kidney. *Am J Pathol,* 175**,** 725-35.

PETRELLA, B. L., ARMSTRONG, D. A. & VINCENTI, M. P. 2012. Interleukin-1 beta and transforming growth factor-beta 3 cooperate to activate matrix metalloproteinase expression and invasiveness in A549 lung adenocarcinoma cells. *Cancer Lett,* 325**,** 220-6.

PEÑA, C., CÉSPEDES, M. V., LINDH, M. B., KIFLEMARIAM, S., MEZHEYEUSKI, A., EDQVIST, P.-H., HÄGGLÖF, C., BIRGISSON, H., BOJMAR, L., JIRSTRÖM, K., SANDSTRÖM, P., OLSSON, E., VEERLA, S., GALLARDO, A., SJÖBLOM, T., CHANG, A. C.-M., REDDEL, R. R., MANGUES, R., AUGSTEN, M. & ÖSTMAN, A. 2013. STC1 Expression By Cancer-Associated Fibroblasts Drives Metastasis of Colorectal Cancer. *Cancer Research,* 73**,** 1287-1297.

PHILIPPIDIS, P., MASON, J. C., EVANS, B. J., NADRA, I., TAYLOR, K. M., HASKARD, D. O. & LANDIS, R. C. 2004. Hemoglobin scavenger receptor CD163 mediates interleukin-10 release and heme oxygenase-1 synthesis: antiinflammatory monocyte-macrophage responses in vitro, in resolving skin blisters in vivo, and after cardiopulmonary bypass surgery. *Circ Res,* 94**,** 119-26.

PINCIROLI, P., ALBERTI, C., SENSI, M., CANEVARI, S. & TOMASSETTI, A. 2013. An IL6-correlated signature in serous epithelial ovarian cancer associates with growth factor response. *BMC Genomics,* 14**,** 508.

PITIYAGE, G. N., SLIJEPCEVIC, P., GABRANI, A., CHIANEA, Y. G., LIM, K. P., PRIME, S. S., TILAKARATNE, W. M., FORTUNE, F. & PARKINSON, E. K. 2011. Senescent mesenchymal cells accumulate in human fibrosis by a telomere-independent mechanism and ameliorate fibrosis through matrix metalloproteinases. *The Journal of Pathology,* 223**,** 604-617.

POH, A. R. & ERNST, M. 2018. Targeting Macrophages in Cancer: From Bench to Bedside. *Front Oncol,* 8**,** 49.

POHL, S., SCOTT, R., ARFUSO, F., PERUMAL, V. & DHARMARAJAN, A. 2015. Secreted frizzled-related protein 4 and its implications in cancer and apoptosis. *Tumour Biol,* 36**,** 143-52.

POILLET, L., PERNODET, N., BOYER-GUITTAUT, M., ADAMI, P., BORG, C., JOUVENOT, M., DELAGE-MOURROUX, R. & DESPOUY, G. 2014. QSOX1 inhibits autophagic flux in breast cancer cells. *PLoS One,* 9**,** e86641.

POLLARD, J. W. 2009. Trophic macrophages in development and disease. *Nat Rev Immunol,* 9**,** 259-70.

PONCET, N., GUILLAUME, J. & MOUCHIROUD, G. 2011. Epidermal growth factor receptor transactivation is implicated in IL-6-induced proliferation and ERK1/2 activation in non-transformed prostate epithelial cells. *Cell Signal,* 23**,** 572-8.

POURREYRON, C., CHEN, M., MCGRATH, J. A., SALAS-ALANIS, J. C., SOUTH, A. P. & LEIGH, I. M. 2014. High levels of type VII collagen expression in recessive dystrophic epidermolysis bullosa cutaneous squamous cell carcinoma keratinocytes increases PI3K and MAPK signalling, cell migration and invasion. *Br J Dermatol,* 170**,** 1256-65.

POWELL, D. W. 2000. Myofibroblasts: paracrine cells important in health and disease. *Trans Am Clin Climatol Assoc,* 111**,** 271-92; discussion 292-3.

POZZI, L. A. & WEISER, W. Y. 1992. Human recombinant migration inhibitory factor activates human macrophages to kill tumor cells. *Cell Immunol,* 145**,** 372-9.

PRIME, S. S., CIRILLO, N., HASSONA, Y., LAMBERT, D. W., PATERSON, I. C., MELLONE, M., THOMAS, G. J., JAMES, E. N. & PARKINSON, E. K. 2017. Fibroblast activation and senescence in oral cancer. *J Oral Pathol Med,* 46**,** 82-88.

PROVENZANO, P. P., INMAN, D. R., ELICEIRI, K. W. & KEELY, P. J. 2009. Matrix density-induced mechanoregulation of breast cell phenotype, signaling and gene expression through a FAK-ERK linkage. *Oncogene,* 28**,** 4326-43.

PYONTECK, S. M., GADEA, B. B., WANG, H. W., GOCHEVA, V., HUNTER, K. E., TANG, L. H. & JOYCE, J. A. 2012. Deficiency of the macrophage growth factor CSF-1 disrupts pancreatic neuroendocrine tumor development. *Oncogene,* 31**,** 1459-67.

QIAN, B. Z., LI, J., ZHANG, H., KITAMURA, T., ZHANG, J., CAMPION, L. R., KAISER, E. A., SNYDER, L. A. & POLLARD, J. W. 2011. CCL2 recruits inflammatory monocytes to facilitate breast-tumour metastasis. *Nature,* 475**,** 222-5.

QIAN, B. Z. & POLLARD, J. W. 2010. Macrophage diversity enhances tumor progression and metastasis. *Cell,* 141**,** 39-51.

QIN, X., YAN, M., ZHANG, J., WANG, X., SHEN, Z., LV, Z., LI, Z., WEI, W. & CHEN, W. 2016. TGFbeta3-mediated induction of Periostin facilitates head and neck cancer growth and is associated with metastasis. *Sci Rep,* 6**,** 20587.

QIU, X., CHENG, J. C., CHANG, H. M. & LEUNG, P. C. 2014. COX2 and PGE2 mediate EGF-induced E-cadherin-independent human ovarian cancer cell invasion. *Endocr Relat Cancer,* 21**,** 533-43.

QUAIL, D. F. & JOYCE, J. A. 2013. Microenvironmental regulation of tumor progression and metastasis. *Nat Med,* 19**,** 1423-37.

RADISKY, D. C., KENNY, P. A. & BISSELL, M. J. 2007a. Fibrosis and cancer: do myofibroblasts come also from epithelial cells via EMT? *J Cell Biochem,* 101**,** 830-9.

RADISKY, D. C., KENNY, P. A. & BISSELL, M. J. 2007b. Fibrosis and cancer: Do myofibroblasts come also from epithelial cells via EMT? *Journal of Cellular Biochemistry,* 101**,** 830-839.

RADISKY, D. C., LEVY, D. D., LITTLEPAGE, L. E., LIU, H., NELSON, C. M., FATA, J. E., LEAKE, D., GODDEN, E. L., ALBERTSON, D. G., NIETO, M. A., WERB, Z. & BISSELL, M. J. 2005. Rac1b and reactive oxygen species mediate MMP-3-induced EMT and genomic instability. *Nature,* 436**,** 123-127.

RAFFAGHELLO, L. & DAZZI, F. 2015. Classification and biology of tumour associated stromal cells. *Immunol Lett,* 168**,** 175-82.

REACTOME. Available: https://reactome.org/ [Accessed 17.12.2017].

REHMAN, A., ALI, S., LONE, M. A., ATIF, M., HASSONA, Y., PRIME, S. S., PITIYAGE, G. N., JAMES, E. L. & PARKINSON, E. K. 2016. Areca nut alkaloids induce irreparable DNA damage and senescence in fibroblasts and may create a favourable environment for tumour progression. *J Oral Pathol Med,* 45**,** 365-72.

RESTIFO, N. P., DUDLEY, M. E. & ROSENBERG, S. A. 2012. Adoptive immunotherapy for cancer: harnessing the T cell response. *Nat Rev Immunol,* 12**,** 269-81.

RHYU, D. Y., YANG, Y., HA, H., LEE, G. T., SONG, J. S., UH, S.-T. & LEE, H. B. 2005. Role of Reactive Oxygen Species in TGF-β1-Induced Mitogen-Activated Protein Kinase Activation and Epithelial-Mesenchymal Transition in Renal Tubular Epithelial Cells. *Journal of the American Society of Nephrology,* 16**,** 667-675.

RIEDEL, F., ZAISS, I., HERZOG, D., GÖTTE, K., NAIM, R. & HÖRMANN, K. 2005. Serum levels of interleukin-6 in patients with primary head and neck squamous cell carcinoma. *Anticancer Res,* 25**,** 2761-5.

ROBLES, S. J. & ADAMI, G. R. 1998. Agents that cause DNA double strand breaks lead to p16INK4a enrichment and the premature senescence of normal fibroblasts. *Oncogene,* 16**,** 1113-23.

ROCKS, N., PAULISSEN, G., QUESADA-CALVO, F., MUNAUT, C., GONZALEZ, M. L., GUEDERS, M., HACHA, J., GILLES, C., FOIDART, J. M., NOEL, A. & CATALDO, D. D. 2008. ADAMTS-1 metalloproteinase promotes tumor development through the induction of a stromal reaction in vivo. *Cancer Res,* 68**,** 9541-50.

ROH, S. G., SONG, S. H., CHOI, K. C., KATOH, K., WITTAMER, V., PARMENTIER, M. & SASAKI, S. 2007. Chemerin--a new adipokine that modulates adipogenesis via its own receptor. *Biochem Biophys Res Commun,* 362**,** 1013-8.

ROPIQUET, F., GIRI, D., KWABI-ADDO, B., MANSUKHANI, A. & ITTMANN, M. 2000. Increased expression of fibroblast growth factor 6 in human prostatic intraepithelial neoplasia and prostate cancer. *Cancer Res,* 60**,** 4245-50.

ROSE-JOHN, S. 2012. IL-6 trans-signaling via the soluble IL-6 receptor: importance for the pro-inflammatory activities of IL-6. *Int J Biol Sci,* 8**,** 1237-47.

ROSENQUIST, K. 2005. Risk factors in oral and oropharyngeal squamous cell carcinoma: a population based case control study in southern Sweden. *Swedish Dental Journal Supplement,* 179**,** 1-66.

ROUTRAY, S., SUNKAVALI, A. & BARI, K. A. 2014a. Carcinoma-associated fibroblasts, its implication in head and neck squamous cell carcinoma: a mini review. *Oral Diseases,* 20**,** 246-253.

ROUTRAY, S., SUNKAVALI, A. & BARI, K. A. 2014b. Carcinoma-associated fibroblasts, its implication in head and neck squamous cell carcinoma: a mini review. *Oral Dis,* 20**,** 246-53.

RYDER, M., GHOSSEIN, R. A., RICARTE-FILHO, J. C., KNAUF, J. A. & FAGIN, J. A. 2008. Increased density of tumor-associated macrophages is associated with decreased survival in advanced thyroid cancer. *Endocr Relat Cancer,* 15**,** 1069-74.

RŐSZER, T. 2015. Understanding the Mysterious M2 Macrophage through Activation Markers and Effector Mechanisms. *Mediators Inflamm,* 2015**,** 816460.

SAGIV, A., BURTON, D. G., MOSHAYEV, Z., VADAI, E., WENSVEEN, F., BEN-DOR, S., GOLANI, O., POLIC, B. & KRIZHANOVSKY, V. 2016. NKG2D ligands mediate immunosurveillance of senescent cells. *Aging (Albany NY),* 8**,** 328-44.

SAKURAI, T. & KUDO, M. 2011. Signaling pathways governing tumor angiogenesis. *Oncology,* 81 Suppl 1**,** 24-9.

SAMSON, M., EDINGER, A. L., STORDEUR, P., RUCKER, J., VERHASSELT, V., SHARRON, M., GOVAERTS, C., MOLLEREAU, C., VASSART, G., DOMS, R. W. & PARMENTIER, M. 1998. ChemR23, a putative chemoattractant receptor, is expressed in monocyte-derived dendritic cells and macrophages and is a coreceptor for SIV and some primary HIV-1 strains. *Eur J Immunol,* 28**,** 1689-700.

SANDBLAD, K. G., JONES, P., KOSTALLA, M. J., LINTON, L., GLISE, H. & WINQVIST, O. 2015. Chemokine receptor expression on monocytes from healthy individuals. *Clin Immunol,* 161**,** 348-53.

SANDY, J. D., WESTLING, J., KENAGY, R. D., IRUELA-ARISPE, M. L., VERSCHAREN, C., RODRIGUEZ-MAZANEQUE, J. C., ZIMMERMANN, D. R., LEMIRE, J. M., FISCHER, J. W., WIGHT, T. N. & CLOWES, A. W. 2001. Versican V1 proteolysis in human aorta in vivo occurs at the Glu441-Ala442 bond, a site that is cleaved by recombinant ADAMTS-1 and ADAMTS-4. *J Biol Chem,* 276**,** 13372-8.

SANKARANARAYANAN, R., MASUYER, E., SWAMINATHAN, R., FERLAY, J. & WHELAN, S. 1998. Head and neck cancer: a global perspective on epidemiology and prognosis. *Anticancer Res,* 18**,** 4779-86.

SANMARCO, L. M., PONCE, N. E., VISCONTI, L. M., EBERHARDT, N., THEUMER, M. G., MINGUEZ, A. R. & AOKI, M. P. 2017. IL-6 promotes M2 macrophage polarization by modulating purinergic signaling and regulates the lethal release of nitric oxide during Trypanosoma cruzi infection. *Biochim Biophys Acta,* 1863**,** 857-869.

SANO, H., HSU, D. K., YU, L., APGAR, J. R., KUWABARA, I., YAMANAKA, T., HIRASHIMA, M. & LIU, F. T. 2000. Human galectin-3 is a novel chemoattractant for monocytes and macrophages. *J Immunol,* 165**,** 2156-64.

SANTURAY, R. T., JOHNSON, D. E. & GRANDIS, J. R. 2018. New Therapies in Head and Neck Cancer. *Trends Cancer,* 4**,** 385-396.

SCHARPING, N. E. & DELGOFFE, G. M. 2016. Tumor Microenvironment Metabolism: A New Checkpoint for Anti-Tumor Immunity. *Vaccines (Basel),* 4.

SCHERZAD, A., STEBER, M., GEHRKE, T., RAK, K., FROELICH, K., SCHENDZIELORZ, P., HAGEN, R., KLEINSASSER, N. & HACKENBERG, S. 2015. Human mesenchymal stem cells enhance cancer cell proliferation via IL-6 secretion and activation of ERK1/2. *Int J Oncol,* 47**,** 391-7.

SCHMITZ, S., BINDEA, G., ALBU, R. I., MLECNIK, B. & MACHIELS, J. P. 2015. Cetuximab promotes epithelial to mesenchymal transition and cancer associated fibroblasts in patients with head and neck cancer. *Oncotarget,* 6**,** 34288-99.

SCHNOOR, M., CULLEN, P., LORKOWSKI, J., STOLLE, K., ROBENEK, H., TROYER, D., RAUTERBERG, J. & LORKOWSKI, S. 2008. Production of type VI collagen by human macrophages: a new dimension in macrophage functional heterogeneity. *J Immunol,* 180**,** 5707-19.

SECRETAN, B., STRAIF, K., BAAN, R., GROSSE, Y., EL GHISSASSI, F., BOUVARD, V., BENBRAHIM-TALLAA, L., GUHA, N., FREEMAN, C., GALICHET, L., COGLIANO, V. & GROUP, W. I. A. F. R. O. C. M. W. 2009. A review of human carcinogens--Part E: tobacco, areca nut, alcohol, coal smoke, and salted fish. *Lancet Oncol,* 10**,** 1033-4.

SEDELNIKOVA, O. A., HORIKAWA, I., ZIMONJIC, D. B., POPESCU, N. C., BONNER, W. M. & BARRETT, J. C. 2004. Senescing human cells and ageing mice accumulate DNA lesions with unrepairable double-strand breaks. *Nat Cell Biol,* 6**,** 168-70.

SERINI, G., BOCHATON-PIALLAT, M. L., ROPRAZ, P., GEINOZ, A., BORSI, L., ZARDI, L. & GABBIANI, G. 1998. The fibronectin domain ED-A is crucial for myofibroblastic phenotype induction by transforming growth factor-beta1. *J Cell Biol,* 142**,** 873-81.

SHANLEY, C. J., GHARAEE-KERMANI, M., SARKAR, R., WELLING, T. H., KRIEGEL, A., FORD, J. W., STANLEY, J. C. & PHAN, S. H. 1997. Transforming growth factor-beta 1 increases lysyl oxidase enzyme activity and mRNA in rat aortic smooth muscle cells. *J Vasc Surg,* 25**,** 446-52.

SHARPLESS, N. E. & SHERR, C. J. Forging a signature of in vivo senescence.

SHERMAN-BAUST, C. A., WEERARATNA, A. T., RANGEL, L. B., PIZER, E. S., CHO, K. R., SCHWARTZ, D. R., SHOCK, T. & MORIN, P. J. 2003. Remodeling of the extracellular matrix through overexpression of collagen VI contributes to cisplatin resistance in ovarian cancer cells. *Cancer Cell,* 3**,** 377-86.

SHI, C. & PAMER, E. G. 2011. Monocyte recruitment during infection and inflammation. *Nat Rev Immunol,* 11**,** 762-74.

SHI, C. Y., FAN, Y., LIU, B. & LOU, W. H. 2013. HIF1 contributes to hypoxia-induced pancreatic cancer cells invasion via promoting QSOX1 expression. *Cell Physiol Biochem,* 32**,** 561-8.

SHIBUYA, M. & CLAESSON-WELSH, L. 2006. Signal transduction by VEGF receptors in regulation of angiogenesis and lymphangiogenesis. *Exp Cell Res,* 312**,** 549-60.

SHINRIKI, S., JONO, H., UEDA, M., OTA, K., OTA, T., SUEYOSHI, T., OIKE, Y., IBUSUKI, M., HIRAKI, A., NAKAYAMA, H., SHINOHARA, M. & ANDO, Y. 2011. Interleukin-6 signalling regulates vascular endothelial growth factor-C synthesis and lymphangiogenesis in human oral squamous cell carcinoma. *J Pathol,* 225**,** 142-50.

SHOSTAK, K. & CHARIOT, A. 2015. EGFR and NF-kappaB: partners in cancer. *Trends Mol Med,* 21**,** 385-93.

SHU, J., HUANG, M., TIAN, Q., SHUI, Q., ZHOU, Y. & CHEN, J. 2015. Downregulation of angiogenin inhibits the growth and induces apoptosis in human bladder cancer cells through regulating AKT/mTOR signaling pathway. *J Mol Histol,* 46**,** 157-71.

SICA, A., SCHIOPPA, T., MANTOVANI, A. & ALLAVENA, P. 2006a. Tumour-associated macrophages are a distinct M2 polarised population promoting tumour progression: potential targets of anti-cancer therapy. *Eur J Cancer,* 42**,** 717-27.

SICA, A., SCHIOPPA, T., MANTOVANI, A. & ALLAVENA, P. 2006b. Tumour-associated macrophages are a distinct M2 polarised population promoting tumour progression: Potential targets of anti-cancer therapy. *European Journal of Cancer,* 42**,** 717-727.

SIERRA-FILARDI, E., NIETO, C., DOMÍNGUEZ-SOTO, A., BARROSO, R., SÁNCHEZ-MATEOS, P., PUIG-KROGER, A., LÓPEZ-BRAVO, M., JOVEN, J., ARDAVÍN, C., RODRÍGUEZ-FERNÁNDEZ, J. L., SÁNCHEZ-TORRES, C., MELLADO, M. & CORBÍ, A. L. 2014. CCL2 shapes macrophage

polarization by GM-CSF and M-CSF: identification of CCL2/CCR2-dependent gene expression profile. *J Immunol,* 192**,** 3858-67.

SINGH, B., BERRY, J. A., VINCENT, L. E. & LUCCI, A. 2006. Involvement of IL-8 in COX-2-mediated bone metastases from breast cancer. *J Surg Res,* 134**,** 44-51.

SINGH, J. K., SIMOES, B. M., HOWELL, S. J., FARNIE, G. & CLARKE, R. B. 2013. Recent advances reveal IL-8 signaling as a potential key to targeting breast cancer stem cells. *Breast Cancer Res,* 15**,** 210.

SKANDALIS, S. S., THEOCHARIS, A. D., PAPAGEORGAKOPOULOU, N., VYNIOS, D. H. & THEOCHARIS, D. A. 2006. The increased accumulation of structurally modified versican and decorin is related with the progression of laryngeal cancer. *Biochimie,* 88**,** 1135-43.

SOBRAL, A. C., NETO, V. M., TRAIANO, G., PERCICOTE, A. P., GUGELMIN, E. S., DE SOUZA, C. M., NAKAO, L., TORRES, L. F. & DE NORONHA, L. 2015. Immunohistochemical expression of sulfhydryl oxidase (QSOX1) in pediatric medulloblastomas. *Diagn Pathol,* 10**,** 37.

SOK, J. C., LEE, J. A., DASARI, S., JOYCE, S., CONTRUCCI, S. C., EGLOFF, A. M., TREVELLINE, B. K., JOSHI, R., KUMARI, N., GRANDIS, J. R. & THOMAS, S. M. 2013. Collagen type XI alpha1 facilitates head and neck squamous cell cancer growth and invasion. *Br J Cancer,* 109**,** 3049-56.

SPENCER, M., YAO-BORENGASSER, A., UNAL, R., RASOULI, N., GURLEY, C. M., ZHU, B., PETERSON, C. A. & KERN, P. A. 2010. Adipose tissue macrophages in insulin-resistant subjects are associated with collagen VI and fibrosis and demonstrate alternative activation. *Am J Physiol Endocrinol Metab,* 299**,** E1016-27.

STANAM, A., LOVE-HOMAN, L., JOSEPH, T. S., ESPINOSA-COTTON, M. & SIMONS, A. L. 2015. Upregulated interleukin-6 expression contributes to erlotinib resistance in head and neck squamous cell carcinoma. *Mol Oncol,* 9**,** 1371-83.

STYLIANOU, M., SKANDALIS, S. S., PAPADAS, T. A., MASTRONIKOLIS, N. S., THEOCHARIS, D. A., PAPAGEORGAKOPOULOU, N. & VYNIOS, D. H. 2008. Stage-related decorin and versican expression in human laryngeal cancer. *Anticancer Res,* 28**,** 245-51.

SU, Y. W., XIE, T. X., SANO, D. & MYERS, J. N. 2011. IL-6 stabilizes Twist and enhances tumor cell motility in head and neck cancer cells through activation of casein kinase 2. *PLoS One,* 6**,** e19412.

SUBRAMANIAM, K. S., THAM, S. T., MOHAMED, Z., WOO, Y. L., MAT ADENAN, N. A. & CHUNG, I. 2013. Cancer-associated fibroblasts promote proliferation of endometrial cancer cells. *PLoS One,* 8**,** e68923.

SULLIVAN, N. J., SASSER, A. K., AXEL, A. E., VESUNA, F., RAMAN, V., RAMIREZ, N., OBERYSZYN, T. M. & HALL, B. M. 2009. Interleukin-6 induces an epithelial-mesenchymal transition phenotype in human breast cancer cells. *Oncogene,* 28**,** 2940-7.

SUN, W., LI, W. J., WEI, F. Q., WONG, T. S., LEI, W. B., ZHU, X. L., LI, J. & WEN, W. P. 2016. Blockade of MCP-1/CCR4 signaling-induced recruitment of activated regulatory cells evokes an antitumor immune response in head and neck squamous cell carcinoma. *Oncotarget,* 7**,** 37714-37727.

SYN, N. L., TENG, M. W. L., MOK, T. S. K. & SOO, R. A. 2017. De-novo and acquired resistance to immune checkpoint targeting. *Lancet Oncol,* 18**,** e731-e741.

SYRJÄNEN, S., LODI, G., VON BÜLTZINGSLÖWEN, I., ALIKO, A., ARDUINO, P., CAMPISI, G., CHALLACOMBE, S., FICARRA, G., FLAITZ, C., ZHOU, H. M., MAEDA, H., MILLER, C. & JONTELL, M. 2011. Human papillomaviruses in oral carcinoma and oral potentially malignant disorders: a systematic review. *Oral Dis,* 17 Suppl 1**,** 58-72.

SYROVETS, T., TIPPLER, B., RIEKS, M. & SIMMET, T. 1997. Plasmin is a potent and specific chemoattractant for human peripheral monocytes acting via a cyclic guanosine monophosphate-dependent pathway. *Blood,* 89**,** 4574-83.

TAKAHASHI, H., SAKAKURA, K., KUDO, T., TOYODA, M., KAIRA, K., OYAMA, T. & CHIKAMATSU, K. 2017. Cancer-associated fibroblasts promote an immunosuppressive microenvironment through the induction and accumulation of protumoral macrophages. *Oncotarget.*

TAMM, E. R., SIEGNER, A., BAUR, A. & LUTJEN-DRECOLL, E. 1996. Transforming growth factor-beta 1 induces alpha-smooth muscle-actin expression in cultured human and monkey trabecular meshwork. *Exp Eye Res,* 62**,** 389-97.

TANAKA, S., GREEN, S. R. & QUEHENBERGER, O. 2002. Differential expression of the isoforms for the monocyte chemoattractant protein-1 receptor, CCR2, in monocytes. *Biochem Biophys Res Commun,* 290**,** 73-80.

TANAKA, T., NARAZAKI, M. & KISHIMOTO, T. 2014. IL-6 in inflammation, immunity, and disease. *Cold Spring Harb Perspect Biol,* 6**,** a016295.

TANG, C. H. & TSAI, C. C. 2012. CCL2 increases MMP-9 expression and cell motility in human chondrosarcoma cells via the Ras/Raf/MEK/ERK/NF-kappaB signaling pathway. *Biochem Pharmacol,* 83**,** 335-44.

TANG, M. R., WANG, Y. X., GUO, S., HAN, S. Y., LI, H. H. & JIN, S. F. 2015. Prognostic significance of in situ and plasma levels of transforming growth factor beta1, -2 and -3 in cutaneous melanoma. *Mol Med Rep,* 11**,** 4508-12.

TAYLOR, C., LOOMANS, H. A., LE BRAS, G. F., KOUMANGOYE, R. B., ROMERO-MORALES, A. I., QUAST, L. L., ZAIKA, A. I., EL-RIFAI, W., ANDL, T. & ANDL, C. D. 2015. Activin a signaling regulates cell invasion and proliferation in esophageal adenocarcinoma. *Oncotarget,* 6**,** 34228-44.

THIERY, J. P. & SLEEMAN, J. P. 2006. Complex networks orchestrate epithelial-mesenchymal transitions. *Nat Rev Mol Cell Biol,* 7**,** 131-142.

TIAN, H., HUANG, P., ZHAO, Z., TANG, W. & XIA, J. 2014. HIF-1alpha plays a role in the chemotactic migration of hepatocarcinoma cells through the modulation of CXCL6 expression. *Cell Physiol Biochem,* 34**,** 1536-46.

TIAN, Y., CHOI, C. H., LI, Q. K., RAHMATPANAH, F. B., CHEN, X., KIM, S. R., VELTRI, R., CHIA, D., ZHANG, Z., MERCOLA, D. & ZHANG, H. 2015. Overexpression of periostin in stroma positively associated with aggressive prostate cancer. *PLoS One,* 10**,** e0121502.

TILAKARATNE, W. M., KOBAYASHI, T., IDA-YONEMOCHI, H., SWELAM, W., YAMAZAKI, M., MIKAMI, T., ALVARADO, C. G., SHAHIDUL, A. M., MARUYAMA, S., CHENG, J. & SAKU, T. 2009. Matrix metalloproteinase 7 and perlecan in oral epithelial dysplasia and carcinoma in situ: an aid for histopathologic recognition of their cell proliferation centers. *J Oral Pathol Med,* 38**,** 348-55.

TOMASEK, J. J., GABBIANI, G., HINZ, B., CHAPONNIER, C. & BROWN, R. A. 2002. Myofibroblasts and mechano-regulation of connective tissue remodelling. *Nat Rev Mol Cell Biol,* 3**,** 349-63.

TORR, E. E., NGAM, C. R., BERNAU, K., TOMASINI-JOHANSSON, B., ACTON, B. & SANDBO, N. 2015. Myofibroblasts exhibit enhanced fibronectin assembly that is intrinsic to their contractile phenotype. *J Biol Chem,* 290**,** 6951-61.

TOULLEC, A., GERALD, D., DESPOUY, G., BOURACHOT, B., CARDON, M., LEFORT, S., RICHARDSON, M., RIGAILL, G., PARRINI, M. C., LUCCHESI, C., BELLANGER, D., STERN, M. H., DUBOIS, T., SASTRE-GARAU, X., DELATTRE, O., VINCENT-SALOMON, A. & MECHTA-GRIGORIOU, F. 2010. Oxidative stress promotes myofibroblast differentiation and tumour spreading. *EMBO Mol Med,* 2**,** 211-30.

TSUCHIDA, R., OSAWA, T., WANG, F., NISHII, R., DAS, B., TSUCHIDA, S., MURAMATSU, M., TAKAHASHI, T., INOUE, T., WADA, Y., MINAMI, T., YUASA, Y. & SHIBUYA, M. 2014. BMP4/Thrombospondin-1 loop paracrinically inhibits tumor angiogenesis and suppresses the growth of solid tumors. *Oncogene,* 33**,** 3803-11.

TSUCHIYA, S., YAMABE, M., YAMAGUCHI, Y., KOBAYASHI, Y., KONNO, T. & TADA, K. 1980. Establishment and characterization of a human acute monocytic leukemia cell line (THP-1). *Int J Cancer,* 26**,** 171-6.

TSUYADA, A., CHOW, A., WU, J., SOMLO, G., CHU, P., LOERA, S., LUU, T., LI, A. X., WU, X., YE, W., CHEN, S., ZHOU, W., YU, Y., WANG, Y.-Z., REN, X., LI, H., SCHERLE, P., KUROKI, Y. & WANG, S. E. 2012a. CCL2 Mediates Cross-talk between Cancer Cells and Stromal Fibroblasts That Regulates Breast Cancer Stem Cells. *Cancer Research,* 72**,** 2768-2779.

TSUYADA, A., CHOW, A., WU, J., SOMLO, G., CHU, P., LOERA, S., LUU, T., LI, A. X., WU, X., YE, W., CHEN, S., ZHOU, W., YU, Y., WANG, Y. Z., REN, X., LI, H., SCHERLE, P., KUROKI, Y. & WANG, S. E. 2012b. CCL2 mediates cross-talk between cancer cells and stromal fibroblasts that regulates breast cancer stem cells. *Cancer Res,* 72**,** 2768-79.

TUXHORN, J. A., AYALA, G., SMITH, M., SMITH, V. & ROWLEY, D. 2002. Reactive stroma in human prostate cancer: induction of myofibroblast phenotype and extracellular matrix remodelling. Clinical Cancer Research.

TYAN, S.-W., HSU, C.-H., PENG, K.-L., CHEN, C.-C., KUO, W.-H., LEE, E. Y. H. P., SHEW, J.-Y., CHANG, K.-J., JUAN, L.-J. & LEE, W.-H. 2012. Breast Cancer Cells Induce Stromal Fibroblasts to Secrete ADAMTS1 for Cancer Invasion through an Epigenetic Change. *PLoS ONE,* 7**,** e35128.

UENO, T., TOI, M., SAJI, H., MUTA, M., BANDO, H., KUROI, K., KOIKE, M., INADERA, H. & MATSUSHIMA, K. 2000. Significance of macrophage chemoattractant protein-1 in macrophage recruitment, angiogenesis, and survival in human breast cancer. *Clin Cancer Res,* 6**,** 3282-9.

UNDERWOOD, T. J., HAYDEN, A. L., DEROUET, M., GARCIA, E., NOBLE, F., WHITE, M. J., THIRDBOROUGH, S., MEAD, A., CLEMONS, N., MELLONE, M., UZOHO, C., PRIMROSE, J. N., BLAYDES, J. P. & THOMAS, G. J. 2015. Cancer-associated fibroblasts predict poor outcome and promote periostin-dependent invasion in oesophageal adenocarcinoma. *J Pathol,* 235**,** 466-77.

VAN COILLIE, E., VAN DAMME, J. & OPDENAKKER, G. 1999. The MCP/eotaxin subfamily of CC chemokines. *Cytokine Growth Factor Rev,* 10**,** 61-86.

VANHECKE, E., ADRIAENSSENS, E., VERBEKE, S., MEIGNAN, S., GERMAIN, E., BERTEAUX, N., NURCOMBE, V., LE BOURHIS, X. & HONDERMARCK, H. 2011. Brain-derived neurotrophic factor and neurotrophin-4/5 are expressed in breast cancer and can be targeted to inhibit tumor cell survival. *Clin Cancer Res,* 17**,** 1741-52.

VAZQUEZ-VILLA, F., GARCIA-OCANA, M., GALVAN, J. A., GARCIA-MARTINEZ, J., GARCIA-PRAVIA, C., MENENDEZ-RODRIGUEZ, P., GONZALEZ-DEL REY, C., BARNEO-SERRA, L. & DE LOS TOYOS, J. R. 2015. COL11A1/(pro)collagen 11A1 expression is a remarkable biomarker of human invasive carcinoma-associated stromal cells and carcinoma progression. *Tumour Biol,* 36**,** 2213-22.

VENMAR, K. T., CARTER, K. J., HWANG, D. G., DOZIER, E. A. & FINGLETON, B. 2014. IL4 receptor ILR4alpha regulates metastatic colonization by mammary tumors through multiple signaling pathways. *Cancer Res,* 74**,** 4329-40.

VENMAR, K. T., KIMMEL, D. W., CLIFFEL, D. E. & FINGLETON, B. 2015. IL4 receptor alpha mediates enhanced glucose and glutamine metabolism to support breast cancer growth. *Biochim Biophys Acta,* 1853**,** 1219-28.

VERED, M., DAYAN, D., YAHALOM, R., DOBRIYAN, A., BARSHACK, I., BELLO, I. O., KANTOLA, S. & SALO, T. 2010. Cancer-associated fibroblasts and epithelial-mesenchymal transition in metastatic oral tongue squamous cell carcinoma. *Int J Cancer,* 127**,** 1356-62.

VERMORKEN, J. B., MESIA, R., RIVERA, F., REMENAR, E., KAWECKI, A., ROTTEY, S., ERFAN, J., ZABOLOTNYY, D., KIENZER, H. R., CUPISSOL, D., PEYRADE, F., BENASSO, M., VYNNYCHENKO, I., DE RAUCOURT, D., BOKEMEYER, C., SCHUELER, A., AMELLAL, N. & HITT, R. 2008. Platinum-based chemotherapy plus cetuximab in head and neck cancer. *N Engl J Med,* 359**,** 1116-27.

VIKRAM, B., STRONG, E. W., SHAH, J. P. & SPIRO, R. 1984. Failure at distant sites following multimodality treatment for advanced head and neck cancer. *Head Neck Surg,* 6**,** 730-3.

VILLANUEVA, A., SAVIC, R. & LLOVET, J. M. 2009. Lymphotoxins: new targets for hepatocellular carcinoma. *Cancer Cell,* 16**,** 272-3.

WALTER, M., LIANG, S., GHOSH, S., HORNSBY, P. J. & LI, R. 2009. Interleukin 6 secreted from adipose stromal cells promotes migration and invasion of breast cancer cells. *Oncogene,* 28**,** 2745-55.

WANG, L., TANG, C., CAO, H., LI, K., PANG, X., ZHONG, L., DANG, W., TANG, H., HUANG, Y., WEI, L., SU, M. & CHEN, T. 2015a. Activation of IL-8 via PI3K/Akt-dependent pathway is involved in

leptin-mediated epithelial-mesenchymal transition in human breast cancer cells. *Cancer Biol Ther,* 16**,** 1220-30.

WANG, M., WU, C. P., PAN, J. Y., ZHENG, W. W., CAO, X. J. & FAN, G. K. 2015b. Correction: Cancer-Associated Fibroblasts in a Human HEp-2 Established Laryngeal Xenografted Tumor Are Not Derived from Cancer Cells through Epithelial-Mesenchymal Transition, Phenotypically Activated but Karyotypically Normal. *PLoS One.* United States.

WANG, T., GE, Y., XIAO, M., LOPEZ-CORAL, A., AZUMA, R., SOMASUNDARAM, R., ZHANG, G., WEI, Z., XU, X., RAUSCHER, F. J., HERLYN, M. & KAUFMAN, R. E. 2012. Melanoma-derived conditioned media efficiently induce the differentiation of monocytes to macrophages that display a highly invasive gene signature. *Pigment Cell Melanoma Res,* 25**,** 493-505.

WANG, Z., CAO, C. J., HUANG, L. L., KE, Z. F., LUO, C. J., LIN, Z. W., WANG, F., ZHANG, Y. Q. & WANG, L. T. 2015c. EFEMP1 promotes the migration and invasion of osteosarcoma via MMP-2 with induction by AEG-1 via NF-kappaB signaling pathway. *Oncotarget,* 6**,** 14191-208.

WARNAKULASURIYA, S. 2009. Global epidemiology of oral and oropharyngeal cancer. *Oral Oncol,* 45**,** 309-16.

WAUGH, D. J. & WILSON, C. 2008. The interleukin-8 pathway in cancer. *Clin Cancer Res,* 14**,** 6735-41.

WEBER, C. E., KOTHARI, A. N., WAI, P. Y., LI, N. Y., DRIVER, J., ZAPF, M. A. C., FRANZEN, C. A., GUPTA, G. N., OSIPO, C., ZLOBIN, A., SYN, W. K., ZHANG, J., KUO, P. C. & MI, Z. 2015. Osteopontin mediates an MZF1-TGF-[beta]1-dependent transformation of mesenchymal stem cells into cancer-associated fibroblasts in breast cancer.

WHEELER, S. E., SHI, H., LIN, F., DASARI, S., BEDNASH, J., THORNE, S., WATKINS, S., JOSHI, R. & THOMAS, S. M. 2014. Enhancement of head and neck squamous cell carcinoma proliferation, invasion, and metastasis by tumor-associated fibroblasts in preclinical models. *Head Neck,* 36**,** 385-92.

WIEGAND, S., ZIMMERMANN, A., WILHELM, T. & WERNER, J. A. 2015. Survival After Distant Metastasis in Head and Neck Cancer. *Anticancer Res,* 35**,** 5499-502.

WONG, L. M., MYERS, S. J., TSOU, C. L., GOSLING, J., ARAI, H. & CHARO, I. F. 1997. Organization and differential expression of the human monocyte chemoattractant protein 1 receptor gene. Evidence for the role of the carboxyl-terminal tail in receptor trafficking. *J Biol Chem,* 272**,** 1038-45.

WU, I. C., WU, D. C., HUANG, C. C., LIN, H. S., CHEN, Y. K., TSAI, H. J., LU, C. Y., CHOU, S. H., CHOU, Y. P., LI, L. H., TAI, S. Y. & WU, M. T. 2010. Plasma decorin predicts the presence of esophageal squamous cell carcinoma. *Int J Cancer,* 127**,** 2138-46.

WU, M. H., HONG, H. C., HONG, T. M., CHIANG, W. F., JIN, Y. T. & CHEN, Y. L. 2011. Targeting galectin-1 in carcinoma-associated fibroblasts inhibits oral squamous cell carcinoma metastasis by downregulating MCP-1/CCL2 expression. *Clin Cancer Res,* 17**,** 1306-16.

WU, T. T. & ZHOU, S. H. 2015. Nanoparticle-based targeted therapeutics in head-and-neck cancer. *Int J Med Sci,* 12**,** 187-200.

WU, X., CAI, M., JI, F. & LOU, L. M. 2014. The impact of COX-2 on invasion of osteosarcoma cell and its mechanism of regulation. *Cancer Cell Int,* 14**,** 27.

WYSOCKI, V. H., RESING, K. A., ZHANG, Q. & CHENG, G. 2005. Mass spectrometry of peptides and proteins. *Methods,* 35**,** 211-22.

XIA, Z. J., CHANG, J. H., ZHANG, L., JIANG, W. Q., GUAN, Z. Z., LIU, J. W., ZHANG, Y., HU, X. H., WU, G. H., WANG, H. Q., CHEN, Z. C., CHEN, J. C., ZHOU, Q. H., LU, J. W., FAN, Q. X., HUANG, J. J. & ZHENG, X. 2004. [Phase III randomized clinical trial of intratumoral injection of E1B gene-deleted adenovirus (H101) combined with cisplatin-based chemotherapy in treating squamous cell cancer of head and neck or esophagus]. *Ai Zheng,* 23**,** 1666-70.

XIAO, Z. M., WANG, X. Y. & WANG, A. M. 2015. Periostin induces chemoresistance in colon cancer cells through activation of the PI3K/Akt/survivin pathway. *Biotechnol Appl Biochem,* 62**,** 401-6.

XU, J., LU, Y., QIU, S., CHEN, Z.-N. & FAN, Z. 2013. A novel role of EMMPRIN/CD147 in transformation of quiescent fibroblasts to cancer-associated fibroblasts by breast cancer cells. *Cancer Letters,* 335**,** 380-386.

XU, L., DENG, Q., PAN, Y., PENG, M., WANG, X., SONG, L., XIAO, M., & WANG, Z. 2014. Cancer-associated fibroblasts enhance the migration ability of ovarian cancer cells by increasing EZH2 expression. *International Journal of Molecular Medicine,* 33**,** 91-96.

XU, Q., BRIGGS, J., PARK, S., NIU, G., KORTYLEWSKI, M., ZHANG, S., GRITSKO, T., TURKSON, J., KAY, H., SEMENZA, G. L., CHENG, J. Q., JOVE, R. & YU, H. 2005. Targeting Stat3 blocks both HIF-1 and VEGF expression induced by multiple oncogenic growth signaling pathways. *Oncogene,* 24**,** 5552-60.

YADAV, A., KUMAR, B., DATTA, J., TEKNOS, T. N. & KUMAR, P. 2011. IL-6 promotes head and neck tumor metastasis by inducing epithelial-mesenchymal transition via the JAK-STAT3-SNAIL signaling pathway. *Mol Cancer Res,* 9**,** 1658-67.

YAMANE, K., IHN, H., ASANO, Y., JINNIN, M. & TAMAKI, K. 2003. Antagonistic effects of TNF-alpha on TGF-beta signaling through down-regulation of TGF-beta receptor type II in human dermal fibroblasts. *J Immunol,* 171**,** 3855-62.

YANG, G. Y., ZHANG, C. L., LIU, X. C., QIAN, G. & DENG, D. Q. 2013a. Effects of cigarette smoke extracts on the growth and senescence of skin fibroblasts in vitro. *Int J Biol Sci,* 9**,** 613-23.

YANG, L. & LIN, P. C. 2017. Mechanisms that drive inflammatory tumor microenvironment, tumor heterogeneity, and metastatic progression. *Semin Cancer Biol*.

YANG, N., MOSHER, R., SEO, S., BEEBE, D. & FRIEDL, A. 2011. Syndecan-1 in breast cancer stroma fibroblasts regulates extracellular matrix fiber organization and carcinoma cell motility. *Am J Pathol,* 178**,** 325-35.

YANG, S., CUI, H., XIE, N., ICYUZ, M., BANERJEE, S., ANTONY, V. B., ABRAHAM, E., THANNICKAL, V. J. & LIU, G. 2013b. miR-145 regulates myofibroblast differentiation and lung fibrosis. *Faseb j,* 27**,** 2382-91.

YANG, X., CHEN, B., LIU, T. & CHEN, X. 2014. Reversal of myofibroblast differentiation: a review. *Eur J Pharmacol,* 734**,** 83-90.

YANG, X., MARTIN, T. A. & JIANG, W. G. 2012. Biological influence of brain-derived neurotrophic factor on breast cancer cells. *Int J Oncol,* 41**,** 1541-6.

YAO, X., HUANG, J., ZHONG, H., SHEN, N., FAGGIONI, R., FUNG, M. & YAO, Y. 2014. Targeting interleukin-6 in inflammatory autoimmune diseases and cancers. *Pharmacol Ther,* 141**,** 125-39.

YIN, X., FANG, S., WANG, M., WANG, Q., FANG, R. & CHEN, J. 2016. EFEMP1 promotes ovarian cancer cell growth, invasion and metastasis via activated the AKT pathway. *Oncotarget,* 7**,** 47938-47953.

ZABEL, B. A., OHYAMA, T., ZUNIGA, L., KIM, J. Y., JOHNSTON, B., ALLEN, S. J., GUIDO, D. G., HANDEL, T. M. & BUTCHER, E. C. 2006. Chemokine-like receptor 1 expression by macrophages in vivo: regulation by TGF-beta and TLR ligands. *Exp Hematol,* 34**,** 1106-14.

ZEISBERG, E. M., POTENTA, S., XIE, L., ZEISBERG, M. & KALLURI, R. 2007. Discovery of Endothelial to Mesenchymal Transition as a Source for Carcinoma-Associated Fibroblasts. *Cancer Research,* 67**,** 10123-10128.

ZHANG, J., PATEL, L. & PIENTA, K. J. 2010. Targeting chemokine (C-C motif) ligand 2 (CCL2) as an example of translation of cancer molecular biology to the clinic. *Prog Mol Biol Transl Sci,* 95**,** 31-53.

ZHANG, Y., CHOKSI, S., CHEN, K., POBEZINSKAYA, Y., LINNOILA, I. & LIU, Z. G. 2013. ROS play a critical role in the differentiation of alternatively activated macrophages and the occurrence of tumor-associated macrophages. *Cell Res,* 23**,** 898-914.

ZHOU, B., CHEN, W. L., WANG, Y. Y., LIN, Z. Y., ZHANG, D. M., FAN, S. & LI, J. S. 2014. A role for cancer-associated fibroblasts in inducing the epithelial-to-mesenchymal transition in human tongue squamous cell carcinoma. *J Oral Pathol Med,* 43**,** 585-92.

ZHU, L., CHENG, X., DING, Y., SHI, J., JIN, H., WANG, H., WU, Y., YE, J., LU, Y., WANG, T. C., YANG, C. S. & TU, S. P. 2014. Bone marrow-derived myofibroblasts promote colon tumorigenesis through the IL-6/JAK2/STAT3 pathway. *Cancer Lett,* 343**,** 80-9.

ZHU, L., CHENG, X., SHI, J., JIACHENG, L., CHEN, G., JIN, H., LIU, A. B., PYO, H., YE, J., ZHU, Y., WANG, H., CHEN, H., FANG, J., CAI, L., WANG, T. C., YANG, C. S. & TU, S. P. 2016. Crosstalk between bone marrow-derived myofibroblasts and gastric cancer cells regulates cancer stemness and promotes tumorigenesis. *Oncogene,* 35**,** 5388-5399.

ZHU, X. D., ZHANG, J. B., ZHUANG, P. Y., ZHU, H. G., ZHANG, W., XIONG, Y. Q., WU, W. Z., WANG, L., TANG, Z. Y. & SUN, H. C. 2008. High expression of macrophage colony-stimulating factor in peritumoral liver tissue is associated with poor survival after curative resection of hepatocellular carcinoma. *J Clin Oncol,* 26**,** 2707-16.

ZIGRINO, P., LÖFFEK, S. & MAUCH, C. 2005. Tumor–stroma interactions: their role in the control of tumor cell invasion. *Biochimie,* 87**,** 321-328.

ZLOTNIK, A. & YOSHIE, O. 2012. The chemokine superfamily revisited. *Immunity,* 36**,** 705-16.

ZOU, M., ZHANG, X. & XU, C. 2016. IL6-induced metastasis modulators p-STAT3, MMP-2 and MMP-9 are targets of 3,3'-diindolylmethane in ovarian cancer cells. *Cell Oncol (Dordr),* 39**,** 47-57.